
Sedimentology, stratigraphy and reservoir quality of the Paleozoic Wajid Sandstone in SW Saudi Arabia

PhD Thesis of

MSc Hussain Al Ajmi, (POB Riyadh, Saudi Arabia)

Institut für Angewandte Geowissenschaften

Darmstadt, February 2013, D17

Vom Fachbereich Material- und Geowissenschaften genehmigte
Dissertation

Examiners:

Prof. Matthias Hinderer

Prof. Christoph Schüth

Prof. Stephan Kempe

Prof. Wilhelm Urban



TECHNISCHE
UNIVERSITÄT
DARMSTADT

Date of submission: 15.02.2013

Date of exam: 15.03.2013

Declaration of Authorship

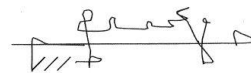
I hereby certify that the complete work to this PhD thesis

“Sedimentology, stratigraphy and reservoir quality of the Paleozoic Wajid Sandstone in SW Saudi Arabia”

was done by me and only with the use of the referenced literature and the described methods.

Darmstadt, 06.02.2013

.....
Place, date



(Hussain Al Ajmi)

.....
Signature

Table of content

Abstract

Zusammenfassung

1. Introduction.....	- 1 -
1.1. Context.....	- 1 -
1.2. Aims.....	- 1 -
1.3. Concept.....	- 1 -
1.4. Study area.....	- 2 -
2. Geological background.....	- 4 -
2.1. Evolution of the Arabian Plate.....	- 4 -
2.2. Tectonic framework.....	- 5 -
3. Former research and state of the art.....	- 7 -
3.1. Sedimentology and stratigraphy.....	- 7 -
3.2. Reservoir quality.....	- 14 -
3.3. Hydrogeology.....	- 15 -
4. Methods and material.....	- 16 -
4.1. Field work.....	- 16 -
4.1.1. Sedimentological logging.....	- 16 -
4.1.2. Gamma-ray logging.....	- 18 -
4.2. Laboratory work.....	- 18 -
4.2.1. Thin sections.....	- 18 -
4.2.1. Palynology.....	- 19 -
4.2.2. Porosity and permeability.....	- 19 -
5. Sedimentology and stratigraphy.....	- 24 -
5.1. Lithostratigraphy.....	- 24 -
5.1.1. Dibsiyah Formation.....	- 24 -
5.1.2. Qalibah Formation.....	- 26 -
5.1.3. Khusayyayn Formation.....	- 26 -
5.1.4. Juwayl Formation.....	- 26 -
5.2. Lithofacies types.....	- 27 -
5.3. Facies associations and depositional environments.....	- 37 -
5.4. Sediment logs and depositional models.....	- 45 -
5.4.1. Dibsiyah Formation.....	- 45 -
5.4.2. Sanamah Formation.....	- 48 -
5.4.3. Qalibah Formation.....	- 50 -
5.4.4. Khusayyayn Formation.....	- 50 -
5.4.5. Juwayl Formation.....	- 52 -
5.5. A new standard log for the Wajid Sandstone Group.....	- 54 -
5.6. Palynology.....	- 55 -
5.7. Discussion.....	- 56 -
5.7.1. Biostratigraphical evidences for the age of the Wajid formations.....	- 56 -
5.7.2. Estimation of the time involved in deposition of the Wajid Group.....	- 57 -
5.7.3. Geotectonic setting of the Wajid Basin.....	- 58 -
5.7.4. Provenance of the Wajid Sandstone Group.....	- 59 -
6. Glacial depositional environments.....	- 61 -
6.1. Glacial deposits in the Wajid Group.....	- 61 -
6.2. Facies associations, glaciogenic processes and depositional model.....	- 61 -
6.3. Analysis and evaluation of selected structures as evidence of ancient glaciations.....	- 72 -
6.3.1. Striations.....	- 72 -
6.3.2. Fluted surfaces.....	- 74 -

6.3.3.	Dropstones and boulder pavements	- 74 -
6.3.4.	Local post-depositional sedimentary deformation	- 74 -
6.3.5.	Origin and possible significance of the large valleys	- 74 -
6.3.6.	Large-scale soft-sediment deformation by glacier push	- 74 -
6.3.7.	Palaeozoic glaciological models for SW Saudi Arabia	- 75 -
6.4.	Palaeozoic glaciations of Gondwana	- 75 -
7.	Gamma ray logging.....	- 77 -
7.1.	Theoretical background.....	- 77 -
7.2.	Natural gamma-ray of sections	- 78 -
7.3.	Natural gamma-ray and the standard Wajid log	- 82 -
8.	Reservoir characteristics	- 84 -
8.1.	Theoretical background.....	- 84 -
8.2.	Porosity and permeability	- 85 -
8.2.1.	Statistics	- 85 -
8.2.2.	Anisotropy.....	- 86 -
8.2.3.	Total and intrinsic permeability	- 87 -
8.2.4.	Crossplots porosity and permeability.....	- 88 -
8.2.5.	Hydraulic permeability	- 89 -
8.3.	Reservoir characterisation.....	- 91 -
8.3.1.	Poroperm and sedimentary facies	- 91 -
8.3.2.	Poroperm and petrology.....	- 92 -
9.	Discussion and conclusion.....	98
9.1.	Sedimentary facies and stratigraphy	98
9.2.	Glacial depositional environments.....	99
9.3.	Natural gamma-ray	99
9.4.	Reservoir quality	100
9.5.	Implications for hydrogeology.....	101
	Acknowledgement	103
	References.....	106
	Annex	
	Curriculum vitae	

Figures:

- Figure 1: Geologic map of the main outcrop area of the Wajid Sandstone in southwestern Saudi Arabia. - 3 -
- Figure 2: Palaeogeographic configuration and terranes of northwestern Gondwana during the Cambrian centered on Arabia. - 5 -
- Figure 3: Lithostratigraphic subdivision of the Wajid Group (“Wajid Sandstone”) in SW Saudi Arabia after Kellogg et al. (1986). - 9 -
- Figure 4: Evolution of the stratigraphic framework of the Wajid Group through time and proposed in this thesis. - 13 -
- Figure 5: Descriptive nomenclature of bedforms (ripples and subaqueous dunes) and their internal structures as applied in this study. - 17 -
- Figure 6: Sample preparation for palynological studies at TU Darmstadt. - 19 -
- Figure 7: AccupycII 1330 (left) and 1360 (right) Pycnometer at the Institute for Applied Geosciences, Darmstadt. - 20 -
- Figure 8: a Principle of mini permeameter measurements of cube-shaped or cylindrical samples (after Greb, 2006). b Drilling core plugs for Poroperm measurements. - 21 -
- Figure 9: Gas permeameter at the Institute of Applied Geosciences, Darmstadt and principle of measurement after Bär (2008). - 22 -
- Figure 10: Set-up of water permeability equipment as developed for this project (from Ngole, 2012). - 23 -
- Figure 11: Sample chamber with connecting pipes to the hydraulic cylinders (from Ngole, 2012). - 23 -
- Figure 12: Meter-scale facies changes between piperock and tabular sandstones without *Skolithos*, outer part of sand sheet complex b *Monocraterion* city in medium-grained sandstone. Note concentric layers on wall, what might indicate that these tubes are actually *Rosselia* c Strongly segmented tubes of unknown origin d *Skolithos* piperock. In the lower part, individual beds are preserved and individual *Skolithos* pipes do not cross bedding surfaces. In the upper part, *Skolithos* burrowing has obliterated bedding and burrows cross bedding surfaces e *Cruziana* sp f Various types of *Skolithoturbation*: basal layers show individual *Skolithos* burrows, cross bedding is still visible. Above is a succession, in which *Skolithoturbation* has obliterated most of the primary structures. Reactivation within this package is recognized through burrows that stop at former bedding planes and others that cross them. Upper part is separated by a bedding plane indicating a major break in sedimentation. - 25 -
- Figure 13: Fine-grained lithofacies of the Wajid Group. a Massive green shale (LF 1), Juwayl Formation, Section. b Shale-siltstone alternation (LF-2) strongly silicified, Juwayl Formation, Section. The rhythmic alternation of light and dark layers is typical of varve sediments. c Shale-siltstone alternations with conglomerate layers represent lake sediments with ice-rafted debris. d

Siltstones with ripples (LF-3.2), Juwayl Formation Section e Variegated siltstones in the upper part of the Juwayl Formation f Wave ripples in fine sandstone (LF-5) g Thin-bedded sandstone with flaser bedding (LF-6), Juwayl Formation h White sandstone with horizontal bedding (LF-7.1), Juwayl Formation. - 28 -

Figure 14: Soft- sediment deformation in the Wajid Group a Large, almost recumbant folds in coarse sandstones (LF-8.2) of the Khusayyayn Formation, Section , b Slumping in sandstones of the Khusayyayn Formation, Section , c Slumping in the sandstones of the Dibsiyah Formation, Jibal Al Qahr d Dewatering (flame) structures in sandstones of the Dibsiyah Formation, Jibal Al Qahr e Sliding and bed-internal folding in rapidly deposited sandstones, Juwayl Formation, Jabal Blehan f Sliding with bed-internal folding in a single sandstone layer of the Juwayl Formation, Jabal Blehan g Massive siltstones strongly deformed by grounding icebergs, Juwayl Formation, Bani Khatmah h Total destruction of primary sedimentary structures in lake sediments of Bani Khatmah, Juwayl Formation. - 30 -

Figure 15: Aspects of bioturbation in the Dibsiyah Formation at Jabal Nafla a Bedding plane surface with *Monocraterion* b Sandstones and siltstones, lower bed is strongly bioturbated, no bioturbation in overlying siltstones c Well-developed longitudinal cross section of *Monocraterion sp.* d Conglomeratic piperock, Bioturbation Index 4 to 5 e *Skolithos* tubes in micro-scale cross bedded tabular sandstones f Piperock with various generations and penetration depths of *Skolithos* erosionally overlain by 2D dune sandstone g *Monocraterion?* tubes and small interspersed *Skolithos* tubes. *Monocraterion* tubes are up to 5 cm in diameter h similar to g but with longitudinal sections through *Monocraterion*. Some of them might actually represent *Rosselia sp.* - 33 -

Figure 16: Steeply dipping, slightly curved, graded foresets of a package of micro-scale bedforms of 2D dunes (LF-8.1.2), Dibsiyah Formation, Jabal Dibsiyah b meso-scale angular cross beds. Each of the cross beds is graded from fine pebble to coarse sand (LF-8.3.1), Dibsiyah Formation, Jabal Nafla c 2D cross bed is a cross section through 3D dune (LF-9.2), Dibsiyah Formation, Jabal Nafla d Set of 2D cross beds in white sandstones. Each of the individual sets has a basal layer of siltstone intraclasts, Section , Juwayl Formation e Micro-scale stack of 2D cross beds in the core of the sand sheet complex of the Dibsiyah Formation, Jabal Nafla f Meso-scale to macro-scale 2D trough cross beds in the Khusayyayn Formation (LF-10.1) g 3D through cross bedded conglomeratic sandstones (LF-11.1) of glacio-fluvial origin, Sanamah Formation, Jabal Sanamah g Channel fill sandstone, in which almost all foresets are graded from fine pebbles to coarse or medium sand (LF-11.2). - 35 -

Figure 17: Composite lithostratigraphic masterlog and succession of lithofacies associations for the Wajid Group, mainly based on outcrops in the northern study area. - 38 -

Figure 18: Sedimentary successions of the Wajid Group a Alternation (LF-A2) of sandstones with tangential basal contact (LF-8.1.2) and purely tabular sandstones (LF-8.2), Dibsiyah Formation, Jabal Nafla b Piperock, Bioturbation Index 4 to 5, sharply overlain by 2D trough cross-bedded sandstones, Dibsiyah Formation, Jabal Nafla c Remnant of red siltstones (LF-3.2) within tabular sandstones of LF-8.1.2. Migration of 2D dunes over interdune areas led to erosion of the siltstones d Set of tabular sandstones (LF-8) erosionally cover piperock with a Bioturbation Index of 5 to 6. e Sedimentary succession of the upper Sanamah Formation (LF-A6) with micro-scale to medium-scale sandstones and siltstones. Massive beds on top of outcrop are unconformable Khusayyayn Formation, Jibal Al Qahr f Outcrop of Qalibah Formation (LF-A7) with alternation of fine-grained siliciclastic rocks, roadcut south of Hima g Qalibah Formation with variegated fine-grained siliciclastics overlain by white calcareous sandstone.

Massive tabular cross beds are base of unconformable Khusayyayn Formation. Roadcut south of Hima. h Detail of g, calcareous sandstone with a few undetermined shells. - 39 -

Figure 19: Sedimentary successions of the Wajid Group a Qalibah Formation with thick-bedded sandstones and unconformable Khusayyayn Formation, Hima b Typical outcrop of Khusayyayn Formation with macro-scale to giant bedforms and rocks of LF-A2. Section approximately 15 m high, Jabal Khusayyayn c Very uniformly dipping meso-scale tabular cross beds of the Dibsiyah Formation (LF-A2). Beds are part of outer sand sheet complex, Jabal Dibsiyah d Light-coloured sandstones and siltstones with conglomerate layer (LF-A6) in the Juwayl Formation, Bani Ruhayyah e The glacial lake succession at Bani Khatmah. Section is approximately 40 m thick and consists of fine-grained siliciclastics and matrix-supported conglomerates (LF-A9). - 41 -

Figure 20: Massive sandstones and conglomerates of the Wajid Group a Massive “Tigillites” or piperock of the Dibsiyah Formation (LF-12.4). The entire primary structure is destroyed by bioturbation, individual pipes are more than one meter long, Jabal Nafla b Massive sandstone of the Juwayl Formation (“Sorbet Facies”, LF-12.1). The outcrop is approximately 25 m high, Jabal Overheat c Basal conglomerate of the Sanamah Formation overlying Dibsiyah piperock. The conglomerate (LF-13.1) is poorly sorted and mainly consists of quartz pebbles d Massive to 3D cross bedded conglomerates, poorly sorted (LF-12.1 to LF-11). The quartz pebbles show glacial striations and shatter marks, Sanamah Formation, Jabal Dibsiyah e Almost pure quartz pebble conglomerate with clasts of low sphericity and long a-axis (LF-13.1.1), Sanamah Formation, Jabal Sanamah f Sanamah conglomerate (LF-13-1) with large siltstone slabs eroded from the underlying Dibsiyah Formation, Section g Matrix-supported conglomerate with large basement boulder (LF-13.2.2) interpreted as dropstone. The varves and the dropstone have been deformed by a later glacier advance, Jabal , Juwayl Formation h Matrix-supported conglomerate of siltstone and shale with abundant pebbles of basement origin (LF-13.2.3). The pebbles are interpreted as rainout from icebergs, the fine-grained sediments are glacial-lake sediments, Juwayl Formation, Bani Khatmah. - 43 -

Figure 21: Lithostratigraphic logs of the Dibsiyah Formation and the basal overlying strata of the Sanamah Formation. - 47 -

Figure 22: Spatial architecture of the Wajid Group and approximate paleogeographic position of the lithologs used for the construction of the masterlog of Figure 19. - 48 -

Figure 23: Lithostratigraphic logs of the Sanamah Formation. - 49 -

Figure 24: Lithostratigraphic correlation of the Khusayyayn Formation. - 51 -

Figure 25: Lithostratigraphic logs of the Juwayl Formation. - 53 -

Figure 26: a, b, c: Flimsy and decomposed organic bodies, possible acritarch (sample Wuh-1 9, Juwayl Formation). d: Needle-shaped translucent phytoclast (plant debris, sample WKh-T 5, Khusayyayn Formation). e: Decomposed fragment of a bissacate gymnosperm pollen (sample Fard C, Juwayl Formation). - 56 -

Figure 27: Schematic model of the sedimentary architecture of the fill of tunnel valleys and onlapping glacial to postglacial successions for the Late Ordovician (a, b) and the Permo-Carboniferous (c, d) glaciations in SW Saudi Arabia (Wajid Sandstone). - 62 -

Figure 28: a: Erosional unconformity of a palaeovalley incised into the shallow-marine Dibsiyah Formation and filled with glacial to proglacial deposits of the Sanamah Formation. b: Sedimentary architecture of an Upper Ordovician palaeovalley fill showing low-angle prograding sediments of the basal conglomeratic unit S1. They are overlain by steeply downlapping clinoforms of the sandy unit S2. Clinoforms dip towards the south. c: Low-angle cross-bedded lobes of conglomeratic unit S1 with erosional base (Sanamah Formation). d: Low-angle cross-bedded medium- to coarse-grained sandstones with nests of pebbles in unit S2 (Sanamah Formation). - 63 -

Figure 29: Sketch of a kettle hole in S2 at Jabal Maaleeq. - 64 -

Figure 30: Glacial model for the Late Ordovician (A) and Permo-Carboniferous (B) glaciation based on sedimentary facies and glacial signatures in the outcrop area of the Wajid sandstone in SW Saudi Arabia. - 67 -

Figure 31: a: Downbending of clayey varve beds of unit J1 at the rim of a Permo-Carboniferous tunnel valley. b: Silicified shales interpreted as varves (unit J1). c: Slumped varve deposits with intercalated sandstone bed (unit J1). d: Angular granitic block deposited as dropstone in varve deposits (unit J1). According to its geometry, this block is of supraglacial origin. e: Striated metavolcanic dropstone clast deposited in a silty matrix (diamictite, unit J1). According to its geometry, this rock is of subglacial origin. - 68 -

Figure 32: a: Diamictite with silty laminated beds and impacted by dropstones in unit J1 of Juwayl Formation. b: Tabular, cross-bedded siltstone overlain by a gravel carpet. Weak erosional base points to ice scratching, probably by an oscillating ice margin. Unit J1 of Juwayl Formation. c: Local thrust fold within diamictite most probably caused by scratching of an iceberg keel. Unit J1 of Juwayl Formation. d: Local thrust fold within diamictite most probably caused by scratching of an iceberg keel. Unit J1 of Juwayl Formation. - 69 -

Figure 33: a: Liquefaction of cross-bedded, channelized sandstones forms viscous grain flows resulting in lobe-like structures (“Sorbet” facies). Unit J2 of Juwayl Formation. - 70 -

Figure 34: Schematic depositional models for all six facies associations inspired by LeHeron et al. (2010). - 71 -

Figure 35: a: Iron-cemented multi-directional striations at the erosional unconformity between units 2 and 3 within the Sanamah Formation. b: Fluted surface slightly above the erosional unconformity between units 2 and 3 within the Sanamah Formation. c: Unidirectional striations at the top of unit J3 of the Juwayl formation. d: Flutes with oblique overprint of striations at the erosional unconformity between units S2 and S3 within the Sanamah Formation. e: Iron-cemented unidirectional striations at the erosional unconformity between units S2 and S3 within the Sanamah Formation. - 73 -

Figure 36: Well log response characters after Emery et al (1996). - 78 -

Figure 37: Combined lithological and (spectral) gamma-ray log of the Dibsiyah Formation at Jabal Nafla. - 79 -

Figure 38: Combined lithological and (spectral) gamma-ray log of the Sanamah Formation at Jabal Atheer. - 80 -

Figure 39: Combined lithological and (spectral) gamma-ray log of the Khusayyayn Formation at Jabal Khusayyayn.	- 81 -
Figure 40: Combined lithological and (spectral) gamma-ray log of the Juwayl Formation at Jabal Blehan.	- 82 -
Figure 41: Combined log of (spectral) gamma-ray logs from Schönrok (2011) and the standard Wajid lithology (Chapter 5.5).	- 83 -
Figure 42: Flow chart of reservoir characterization of sedimentary rocks (after Hornung, 1999).	- 84 -
Figure 43: Box plots of porosities and permeabilities grouped by formations.	- 85 -
Figure 44: Box plots of porosities and permeabilities grouped by facies types (see chapter 5.2).	- 86 -
Figure 45: Triangular plot of oriented measurement of permeabilities with the mini permeameter.	- 87 -
Figure 46: Correlation log total Permeability vs log intrinsic permeability.	- 88 -
Figure 47: Cross plots of porosity versus total permeability from mini permeameter measurements.	- 89 -
Figure 48: Box plot of gas and water permeability in mD of selected Wajid Sandstone Samples (data from Ngole, 2012).	- 90 -
Figure 49: Cross plot of gas versus water permeability in mD.	- 91 -
Figure 50: Principal component analysis of microfacies parameters relevant for reservoir properties.	95
Figure 51: a. Thin section photograph (crossed Nichols) of iron-rich sandstone in the Dibsiyah Formation (WDh1-51). b. Thin section photograph (crossed Nichols) of iron-rich sandstone in the Sanamah Formation (WDSK-17a). c. Thin section photograph (crossed Nichols) of sandstone rich in pseudomatrix in the Juwayl Formation (Wuh-4-9-12). d. Thin section photograph (crossed Nichols) of sandstone with high secondary porosity and little carbonate cement in the Juwayl Formation (Wuh 1-4). All photographs from Heberer (2012).	96
Figure 52: Principal component analysis of microfacies parameters relevant for reservoir properties.	97

Tables:

Table 1: Outcrops logged by Schönrok (2011).	- 18 -
Table 2: Average K ₂ O and Feldspar content of Wajid Formations (Heberer 2012).	- 81 -
Table 3: Gas and water permeabilities of selected Wajid Sandstone Samples (data from Ngole, 2012).	- 90 -
Table 4: Porosities, permeabilites and potential controlling factors from thin section analysis.	- 93 -
Table 5: Comparison of hydraulic conductivities at different scales for the Wajid Sandstone Group.	- 102 -
Table 6: Detailed lithological logs of Wajid outcrops.	- 113 -
Table 7: Samples taken for palynological analysis.	- 113 -
Table 8: Sample list with Poroperm data used in this study.	- 114 -

Abstract:

This PhD thesis was embedded in a regional groundwater study in the Paleozoic Wajid Sandstone of southwest Saudi Arabia. The Wajid Sandstone holds important fossil groundwater resources in southwest Saudi Arabia which became increasingly overused due to extensive irrigation for agricultural purpose. This thesis contributed to this groundwater project by evaluating the hydraulic properties of aquifer rocks. This involved also fundamental questions about the sedimentary facies, depositional environments, stratigraphy, architecture, age, and petrology of the Wajid Sandstone Group. The fundamental concept of this PhD thesis is based on the principle of out-crop-analogue studies, i.e. properties of reservoir rocks in the subsurface are investigated in outcrops at the surface. This concept is applicable for the Wajid Sandstone because of a well exposed outcrop belt and extractions wells whose aquifer rocks are exposed only few kilometres from the well location. The outcrop-analogue studies included all basic parameters of reservoir characterization. The major focus was on 1D standard sections where samples were preferentially taken for further analysis. In particular for heterogenous glacial deposits also 2D wall panels were composed and analysed. Field surveys lasted altogether around 4 months. The extensive sample collection was sent to Germany and all laboratory and microscopic work was done at the Institut für Angewandte Geowissenschaften of TU Darmstadt. This included measurements and analysis of gamma-ray, porosity, permeability, and thin sections as well as stratigraphic work applying palynology. The multiple data were merged into one data base and analysed by multivariate statistics and principal component analysis.

The study area is located in the south-western part of the Kingdom of Saudi Arabia and comprises the entire outcrop belt of the Wajid Group (ca. 44,000 km²). Correlation of sections is mainly based on unconformities that subdivide the succession into distinct stratigraphic packages. In its outcrop belt, the Wajid Group can be subdivided into 5 formations: the Dibsiyah Formation, Sanamah Formation, Qalibah Formation, Khusayyayn Formation, and Juwayl Formation. Thirteen lithofacies have been distinguished (LF1 through LF 13), which cover the entire spectrum of siliciclastic grain size classifications. Shales and siltstones are relatively rare in the succession, whereas sandstones, especially medium-grained to coarse-grained sandstones are abundant. Conglomerates are locally abundant in the Sanamah Formation and in the Juwayl Formation. A second order descriptor is bioturbation, which is very common in the Dibsiyah Formation, but rare to absent in the other units. The 13 lithofacies have been combined in 9 lithofacies associations (LF-A1 through LF-A9). By stacking the different sections a new standard lithostratigraphic log is presented in this thesis. Sediments of the Wajid Group were deposited during approximately 200 Ma to 260 Ma, depending on the definite depositional age of the Dibsiyah Formation. Extrapolations of sedimentation rates to depositional time show that within the Wajid Group and under the assumption of very conservative sedimentation rates, 62 Ma years are represented in the sediments: 20 Ma in the Dibsiyah Formation, 2 Ma (the length of the Hirnantian) in the Sanamah Formation, 15 Ma in the Khusayyayn Formation, and 25 Ma in the Juwayl Formation. Most likely, the time represented is much less. This means that the sediments preserved do not even cover ¼ of the Palaeozoic era. This is compatible with field observations of abundant unconformities and sedimentary breaks in the starved successions. This indicates that throughout the Palaeozoic, southern Saudi Arabia was located in an epicratonal setting, in which tectonic subsidence and relative sea level changes exerted only minor control.

A specific aim of this study was to systematically explore the heterogeneous glacial and proglacial deposits, develop a genetic depositional model and compare the findings with other regions at the northern rim of Gondwana. Saudi Arabia is one of the few places where both glaciations can be studied in well-preserved sedimentary succession, which formed under similar boundary conditions. Among these are (a) incision of subglacial tunnel valleys according to the ice-loading model, (b) subsequent valley-fill by subaqueous to subaerial proglacial deposits in front of an oscillating, polythermal ice-shield, (c) intra-formational erosional events through repeated ice advance, (d) widespread and large-scale soft sediment deformation due to glacial surge during deglaciation, (e) marine transgression as a consequence of eustatic sea-level rise following deglaciation. The general pattern fits well with observations from northern Africa, pointing to closely coupled glaciological processes along the northern margin of the Gondwana ice-shield during Upper Ordovician glaciation. Although the same general patterns apply for the Permo-Carboniferous glaciation, styles and petrographical properties differ most probably due to a

more complex ice-flow pattern with a rougher topography after the Hercynian event and contrasting weathering.

This thesis presents the first statistical analysis of porosities and permeabilities over the entire Wajid Sandstone Group in the outcrop belt and links these values with lithofacies and microfacies studies in order to identify controlling factors. Furthermore, for the first time a combined approach of standard mini permeameter and sophisticated column permeameter measurements were carried out, the latter enables to convert gas in water permeabilities. Although the data of this thesis confirms the overall good reservoir quality, also wide scatter is obvious. This is particularly the case for permeabilities. High porosities do not guarantee high permeabilities and correlation of both is weak, although a positive trend exists. This means that porosities cannot be used to predict permeabilities accurately. Medians of porosities range from 23 to 27% and 15 to 28% for formations and lithofacies types respectively. Different permeability measurements all show highest medians of 1500 to 2000 mD for the Khusayyayn Formation and lowest medians of 300 to 1400 mD for the Dibsiyah Formation. The variability is highest for the Sanamah Formation and the Juwayl Formation. To analyse these heterogeneities and identifying controlling factors, two approaches were applied: (i) lithofacies types, which represent grain texture and sedimentological structures at the mesoscopic scale in the field, and (ii) microfacies analysis using thin sections and raster electron microscopy of selected samples. Referring to lithofacies, the following trends have been identified. Siltstone and fine sandstones exhibit the highest porosities, but permeability is low for silt-dominated samples. Pebbly sandstones show reduced porosities and permeabilities, most probably because of general poorer mixing. Highest porosities and permeabilities were found for cross-bedded sandstones. Thick massive sandstones in the Juwayl Formation, which are expected to have very good reservoir properties show surprisingly high variability. Anisotropy is generally low except for siltstones, and bioturbated sandstones. Porosities and permeabilities are most closely related to each other for sandy to pebbly, cross bedded lithofacies types. Bioturbated samples and massive sandstones show a relatively high permeability compared to their porosity, which may be interpreted as homogenization of the grain fabric and/or secondary porosity by leaching. Finer grained samples show the expected opposite trend, but some exceptions exist.

Referring to microfacies, the following trends have been identified. High permeabilities can be linked with open pore space, pore connectivity, and rounding, but less with sorting. Low permeabilities are linked with increased proportions of pseudo matrix and cementation by iron oxides, calcite, and/or quartz. The Khusayyayn Formation has higher feldspar content. This leads to higher secondary porosity, proportions of pseudo matrix, and some calcite cement. As destruction and formation of secondary porosity prevails the highest average permeability in the entire Wajid Sandstone Group is observed. Biomodal grain distribution in the Juwayl Formation leads to strongly reduced permeability despite the favourable main grain texture. Secondary leaching in the Juwayl Formation is more heterogeneous and cemented or matrix rich patches are common. Furthermore, the Juwayl Formation exhibits lower porosities at the same permeabilities, which is interpreted as a more efficient connectivity due to secondary leaching. Iron cementation is strongest in the lower Wajid Sandstone Group, in particular in the Dibsiyah Formation. This seems to be the major reason for reduced permeabilities there. Likely, the iron originates from continental weathering of shield areas during the warm Cambro-Ordovician period and was remobilized during burial. The Qusaiba Shale presumably hindered the circulating pore waters to penetrate the upper Wajid Sandstone equally.

When comparing water permeabilities of matrix samples with pumping tests, both are surprisingly close and point out the high relevance of matrix permeabilities for groundwater storage and groundwater flow in the Wajid Sandstone. Pumping tests yield a slightly higher hydraulic conductivity for the Lower Wajid Aquifer. Matrix permeabilities for water show the same trend but differences are even lower. Whereas hydraulic permeabilities for matrix and pumping tests are very close in the Lower Wajid Aquifer, matrix permeabilities are almost one magnitude lower in the Upper Wajid Aquifer. In conclusion, this makes matrix permeabilities of prime importance in the Wajid Aquifers. Hence, the investigation of sedimentary heterogeneities at the outcrop and microscopic scale is of specific relevance for the prediction of reservoir quality in the Wajid Sandstone Group.

Zusammenfassung:

Diese Dissertation ist Teil einer regionalen Grundwasserstudie im paläozoischen Wajid-Sandstein von Saudi-Arabien. Der Wajid-Sandstein enthält wichtige, fossile Grundwasserressourcen im Südwesten Saudi-Arabiens, die durch umfangreiche landwirtschaftliche Bewässerung zunehmend ausgebeutet wurden. Diese Studie trägt zu diesem Grundwasserprojekt durch Evaluierung der hydraulischen Eigenschaften der Aquifergesteine bei. Dieses beinhaltet auch fundamentale Fragestellungen über die sedimentären Fazies, Ablagerungsbedingungen, Stratigraphie, Architektur, Alter und Petrologie der Wajid-Sandsteingruppe. Das zugrundeliegende Konzept dieser Dissertation basiert auf dem Prinzip von Aufschluss-Analog-Studien; z.B. wurden Eigenschaften von Reservoirgesteinen im Untergrund anhand von Oberflächenaufschlüssen untersucht. Dieses Konzept ist deshalb für den Wajid-Sandstein gut geeignet, da es sowohl einen Gürtel mit guten Aufschlüssen sowie Produktionsbrunnen, deren Aquifergesteine nur wenige Kilometer vom Brunnen entfernt aufgeschlossen sind, gibt. Die Aufschluss-Analog-Studien umfassten alle grundlegenden Parameter der Reservoir-Charakterisierung. Hauptaugenmerk lag hierbei beim Erstellen von 1-D Standardprofilen, aus denen Proben für weitere Analysen genommen wurden. Für besonders heterogene, glazigene Ablagerungen wurden 2-D Wandpaneele erstellt und analysiert. Die Geländearbeiten dauerten insgesamt ungefähr 4 Monate. Die umfangreiche Probensammlung wurde nach Deutschland geschickt, wo alle Labor- und Mikroskopierarbeiten am Institut für Angewandte Geowissenschaften der TU Darmstadt ausgeführt wurden. Diese beinhalten Messungen und Analyse von Gamma-Ray-Daten, Porosität, Permabilität und Dünnschliffen sowie stratigraphische Arbeiten mittels angewandter Palynologie. Die verschiedenen Daten wurden in eine einzelne Datenbank zusammengeführt und durch multivariante Statistik und Hauptkomponentenanalysen ausgewertet.

Das Untersuchungsgebiet liegt im südwestlichen Teil des Königreichs von Saudi-Arabien und umfasst den gesamten Aufschlussgürtel der Wajid Gruppe (ca. 44.000 km²). Die Korrelation der einzelnen Profile basiert hauptsächlich auf Diskordanzen, die jede Abfolge in distinkte stratigraphische Pakete unterteilt. Im Aufschlussgürtel kann die Wajid Gruppe in 5 Formationen unterteilt werden: die Dibsiyah Formation, Sanamah Formation, Qalibah Formation, Khusayyayn Formation und Juwayl Formation. Dreizehn Lithofaziestypen konnten unterschieden werden (LF1 bis LF13), welche das gesamte Spektrum der siliziklastischen Korngrößenklassifikation umfassen. Shales und Siltsteine sind in der Abfolge relativ selten, während Sandsteine, besonders mittelkörnige bis grobkörnige Sandsteine, sehr häufig vorkommen. Konglomerate kommen lokal häufig in der Sanamah Formation und Juwayl Formation vor. Ein Unterscheidungsmerkmal zweiter Ordnung ist Bioturbation, welche häufig in der Dibsiyah Formation auftritt, jedoch selten bis nicht in den anderen Einheiten vorkommt. Die 13 Lithofaziestypen wurden in 9 Lithofaziesassoziationen (LF-A1 bis LF-A9) zusammengefasst. Durch Stapeln der verschiedenen Profile wird in dieser Arbeit ein neues lithostratigraphisches Standardlog vorgestellt. Die Sedimente der Wajid Gruppe wurden, abhängig vom Ablagerungsalter der Dibsiyah Formation, vor ungefähr 200 Ma bis 260 Ma abgelagert. Extrapolationen von Sedimentationsraten zur Ablagerungszeit zeigen, dass unter Annahme sehr konservativer Sedimentationsgeschwindigkeiten, innerhalb der Wajid Gruppe 62 Ma im Sediment repräsentiert sind: 20 Ma in der Dibsiyah Formation, 2 Ma (die Dauer des Hirnatiums) in der Sanamah Formation, 15 Ma in der Khusayyayn Formation und 25 Ma in der Juwayl Formation. Es ist jedoch sehr wahrscheinlich, dass die repräsentierte Zeitdauer deutlich geringer ist. Das bedeutet, dass erhaltenen Sedimente nicht einmal ein Viertel des Phanerozoikums repräsentieren. Dies ist mit Geländebeobachtungen häufig vorkommender Diskordanzen und Sedimentationsschnitten in kondensierten Abfolgen vereinbar. Das weist darauf hin, dass sich durch das gesamte Paläozoikum hindurch das südliche Saudi-Arabien in einem epikontinentalen Umfeld befand, in welchem tektonische Subsidenz und Änderungen des relativen Meeresspiegels nur untergeordneten Einfluss hatten.

Ein besonderes Ziel dieser Studie war es, die heterogenen glazialen und proglazialen Ablagerungen systematisch zu erforschen, ein genetisches Ablagerungsmodell zu entwickeln und mit Funden in anderen Regionen am Nordrand Gondwanas zu vergleichen. Saudi-Arabien ist einer der wenigen Plätze, an dem beide Vereisungen in gut erhaltenen Sedimentabfolgen, welche unter ähnlichen Rahmenbedingungen gebildet wurden, beobachtet werden können. Unter diesen finden sich (a) einschneidende Tunneltäler nach dem ice-loading Modell, (b) darauffolgende Talfüllung durch subaquatische bis subäolische, proglaziale Ablagerungen vor einem oszillierenden, polythermalen Eisschild, (c) intraformationelle

Erosionsereignisse durch wiederholte Eisvorstöße, (d) weitläufige und großräumige Deformation von weichem Sediment durch glaziale Fluten während des Eisrückzuges, (e) marine Transgression als Folge von eustatischem Meeresspiegelanstieg in Folge des Eisrückzuges. Das generelle Muster passt gut zu den Beobachtungen aus Nordafrika, was auf eng verbundene Vereisungsprozesse entlang des Nordrands des Eisschildes von Gondwana während der oberordovizischen Vereisung hindeutet. Obwohl die gleichen generellen Muster auch für die permokarbonische Vereisung zutreffen, unterscheiden sich Stil und petrographische Eigenschaften höchstwahrscheinlich durch ein komplexeres Eisflussmuster mit einer rauheren Topographie nach dem herzynischen Event und unterschiedliche Verwitterung.

Diese Studie präsentiert die erste statistische Analyse von Porositäts- und Permeabilitätswerten über die gesamte Wajid Sandsteingruppe im Aufschlussgürtel und verbindet diese mit Lithofazies- und Mikrofaziesstudien um die verantwortlichen Faktoren zu identifizieren. Des Weiteren wurde zum ersten Mal ein kombinierter Ansatz von standard Minipermeameter- und fortschrittlichen Säulenpermeametermessungen verfolgt, wobei letztere erlauben, Gas- in Wasserpermeabilitäten umzurechnen. Obwohl die Daten dieser Studie die grundlegend gute Reservoirqualität bestätigt ist eine weite Streuung der Daten offensichtlich. Dies trifft besonders auf Permeabilitätswerte zu. Hohe Porositätswerte garantieren nicht auch hohe Werte für die Permeabilität und die Korrelation zwischen beiden Faktoren ist schwach, obwohl ein positiver Trend existiert. Das bedeutet, dass Porositätswerte nicht benutzt werden können, um die Permeabilität akkurat zu berechnen. Mediane der Porosität reichen von 23 bis 27% und 15 bis 28% für Formationen und Lithofaziestypen, respektive. Verschiedene Permeabilitätsmessungen zeigen alle maximale Mediane von 1500 bis 2000 mD für die Khusayyayn Formation und minimale Mediane von 300 bis 1400 mD für die Dibsiyah Formation. Die Variabilität ist am größten für die Sanamah Formation und die Juwayl Formation. Um diese Heterogenitäten zu analysieren und die bestimmenden Faktoren zu identifizieren, kamen zwei Ansätze zur Anwendung: (i) Lithofaziestypen, welche Kornstrukturen und sedimentologische Strukturen im mesoskopischen Maßstab im Gelände repräsentieren sowie (ii) Mikrofaziesanalysen mittels Dunnschliffen und Rasterelektronenmikroskopie anhand ausgewählter Proben. In Bezug auf Lithofazies wurden folgende Trends identifiziert. Siltsteine und Feinsandsteine zeigen die höchsten Porositäten, aber mit geringen Permeabilitäten für siltdominierte Proben. Kiesige Sandsteine zeigen verringerte Porositäten und Permeabilitäten, höchstwahrscheinlich durch generell schlechtere Durchmischung. Höchste Porositäten und Permeabilitäten wurden in kreuzgeschichteten Sandsteinen gefunden. Mächtige, massive Sandsteine der Juwayl Formation, von denen gute Reservoireigenschaften erwartet werden, zeigen eine überraschend hohe Variabilität. Die Anisotropie ist generell gering, außer für Siltsteine und bioturbirte Sandsteine. Porositäten und Permeabilitäten hängen am meisten zusammen für sandige bis kiesig, kreuzgeschichtete Lithofaziestypen. Proben mit Bioturbation und massive Sandsteine zeigen eine relativ hohe Permeabilität verglichen mit ihren Porositätswerten, was interpretiert werden kann als Homogenisierung des Korngefüges und/oder Bildung von Sekundärporosität durch Auswaschung. Feinkörnigere Proben zeigen den erwarteten gegenläufigen Trend, jedoch gibt es auch einige Ausnahmen.

Die folgenden Trends wurden in Bezug auf Mikrofazies beobachtet. Hohe Permeabilitäten können mit offenem Porenraum, Porenverbindungen und Rundung verbunden werden, weniger jedoch mit Sortierung. Geringe Permeabilitäten sind verbunden mit erhöhten Anteilen von Pseudomatrix und Zementation durch Eisenoxide, Kalzit und/oder Quarz. Die Khusayyayn Formation zeigt einen hohen Feldspatgehalt. Dies führt zu hoher sekundärer Porosität, hohen Anteilen an Pseudomatrix und einigem Kalzitement. Die höchste mittlere Permeabilität in der gesamten Wajid Sandsteingruppe wird beobachtet, wo Zerstörung und Bildung von sekundärer Porosität vorherrschen. Die biomodale Kornverteilung in der Juwayl Formation führt zu einer stark reduzierten Permeabilität, entgegen der günstigen Textur der Hauptkornfraktion. Sekundäre Auswaschung in der Juwayl Formation ist heterogener und zementierte oder matrixreiche Stellen sind häufig. Des Weiteren zeigt die Juwayl Formation geringere Porositäten bei gleichen Permeabilitäten, was als effizientere Konnektivität durch sekundäre Auswaschung interpretiert wird. Eisenzementation tritt in der unteren Wajid Sandsteingruppe häufig auf, besonders in der Dibsiyah Formation. Dies erscheint als der Hauptgrund für die dortige reduzierte Permeabilität. Wahrscheinlich stammt das Eisen von der kontinentalen Verwitterung von Schildgebieten während der warmen kambroordovizischen Periode und wurde während der Versenkung remobilisiert. Vermutlich hinderte der Qusaiba Shale das zirkulierende Porenwasser daran, den oberen Wajid Sandstein gleichmäßig zu durchdringen.

Wenn man Wasserpermeabilitäten von Matrixproben mit Pumpversuchen vergleicht, sind beide überraschend ähnlich und weisen somit auf die hohe Relevanz von Matrixpermeabilitäten für die Grundwasserspeicherung und den Grundwasserfluss im Wajid Sandstein hin. Pumpversuche ergaben eine leicht erhöhte hydraulische Konduktivität für den unteren Wajid Aquifer. Matrixpermeabilitäten für Wasser zeigen den gleichen Trend, die Unterschiede sind jedoch noch geringer. Wohingegen hydraulische Matrixpermeabilitäten und Pumpversuche im unteren Wajid Aquifer eng beieinander liegen sind Matrixpermeabilitäten nahezu um eine Größenordnung geringer im oberen Wajid Aquifer. Daraus folgt die allerhöchste Bedeutung der Matrixpermeabilität in den Wajid Aquiferen. Dies verleiht der Untersuchung von sedimentären Heterogenitäten im Aufschluss und im mikroskopischen Maßstab besondere Relevanz für die Vorhersage der Reservoirqualität in der Wajid Sandsteingruppe.

1. Introduction

1.1. Context

This PhD thesis was embedded in a regional groundwater study in the Paleozoic Wajid Sandstone of southwest Saudi Arabia carried out by Gesellschaft für Internationale Zusammenarbeit (GIZ, Eschborn, Germany) and Dornier Consult (DCo, Immenstaad, Germany) in cooperation with the Ministry of Water and Electricity (MoWE, Riyadh, Kingdom of Saudi Arabia). These organisations strongly supported this PhD financially and logistically. The Wajid Sandstone holds important fossil groundwater resources in southwest Saudi Arabia which became increasingly overused due to extensive irrigation for agricultural purpose. The groundwater study of Wajid included a careful assessment of the different components of the water budget and hydraulic parameters in order to set up a regional model for groundwater flow. In addition to a compilation of existing data, own surveys of the Wajid aquifer were performed including e.g. new wells, pumping tests, and evaluation of hydraulic properties of aquifer rocks. The latter was highly a contribution of this PhD complemented by fundamental scientific questions about the sedimentology, stratigraphy, and genesis of the Wajid Sandstone.

1.2. Aims

The aims of this PhD thesis are

- A modern and systematic description of the sedimentology of the Wajid Sandstone by applying the lithofacies concept
- Set-up and revise standard sections of the specific formations by logging and re-logging
- A new interpretation of depositional environments
- A better understanding of the genesis of widespread glacial deposits and comparison with similar locations in North Africa
- An evaluation of the architecture and sequence stratigraphy of the Wajid Sandstone in the outcrop belt
- Achieving a better time control by performing palynological studies on fine-grained intercalations within the sandstones
- Correlating outcrops with wells by carrying out spectral gamma-ray measurements
- A new description of sedimentary petrology and diagenesis at thin sections and linking them with lithofacies
- A quantification of porosities and permeabilities at rock samples to assess reservoir qualities
- Assessing the relationships between lithofacies and petrology to reservoir qualities in order to improve predictions of reservoir properties
- Performing water permeability tests at rock samples
- Evaluating the relevance of the sandstone matrix for water storage and water flow by comparing matrix permeability with regional hydraulic permeability

1.3. Concept

The fundamental concept of this PhD thesis is based on the principle of out-crop-analogue studies, i.e. properties of reservoir rocks in the subsurface are investigated in outcrops at the surface. This concept is well applicable for the Wajid Sandstone because of a well exposed outcrop belt and extraction wells whose aquifer rocks are exposed only few kilometres from the well location. The outcrop-analogue studies included all basic parameters of reservoir characterization (see chapter 8). The major focus was on 1D standard sections where samples were preferentially taken for further analysis. In particular for heterogeneous glacial deposits also 2D wall panels were composed and analysed. Field surveys lasted altogether around 4 months. The extensive sample collection was sent to Germany and all laboratory and microscopic work was done at the Institut für Angewandte Geowissenschaften of TU Darmstadt. The multiple data were merged into one data base and analysed by multivariate statistics and principal component analysis. Several student's reports, diploma and master theses contributed to specific aspects of this PhD thesis, e.g. measurements and analysis of gamma-ray, porosity, permeability, and thin

sections. Without this contribution the time-consuming work on the large amount of samples would have been not possible. Several parts of this thesis are published and/or submitted to international journals or conference proceedings.

1.4. Study area

The study area is located in the south-western part of the Kingdom of Saudi Arabia and comprises the entire outcrop belt of the Wajid Group (Figure 1). To the east, the almost horizontal strata are covered by the sands of the Rub' Al Khali, earth's largest sand desert; to the north and northeast, the strata are overlain by younger Mesozoic deposits. To the west and south, the Wajid Group disappears as a consequence of uplift and erosion following the opening of the Red Sea and the uplift of the corresponding rift shoulders since the Miocene. Outliers on the basement near Abha and west of Najran (Dahran al Janub; Figure 1) testify to a much larger areal distribution of the Wajid sediments. The present outcrop area comprises approximately 44,000 km², in which not a single complete stratigraphic section is present. Correlation of sections is mainly based on unconformities that subdivide the succession into distinct stratigraphic packages.

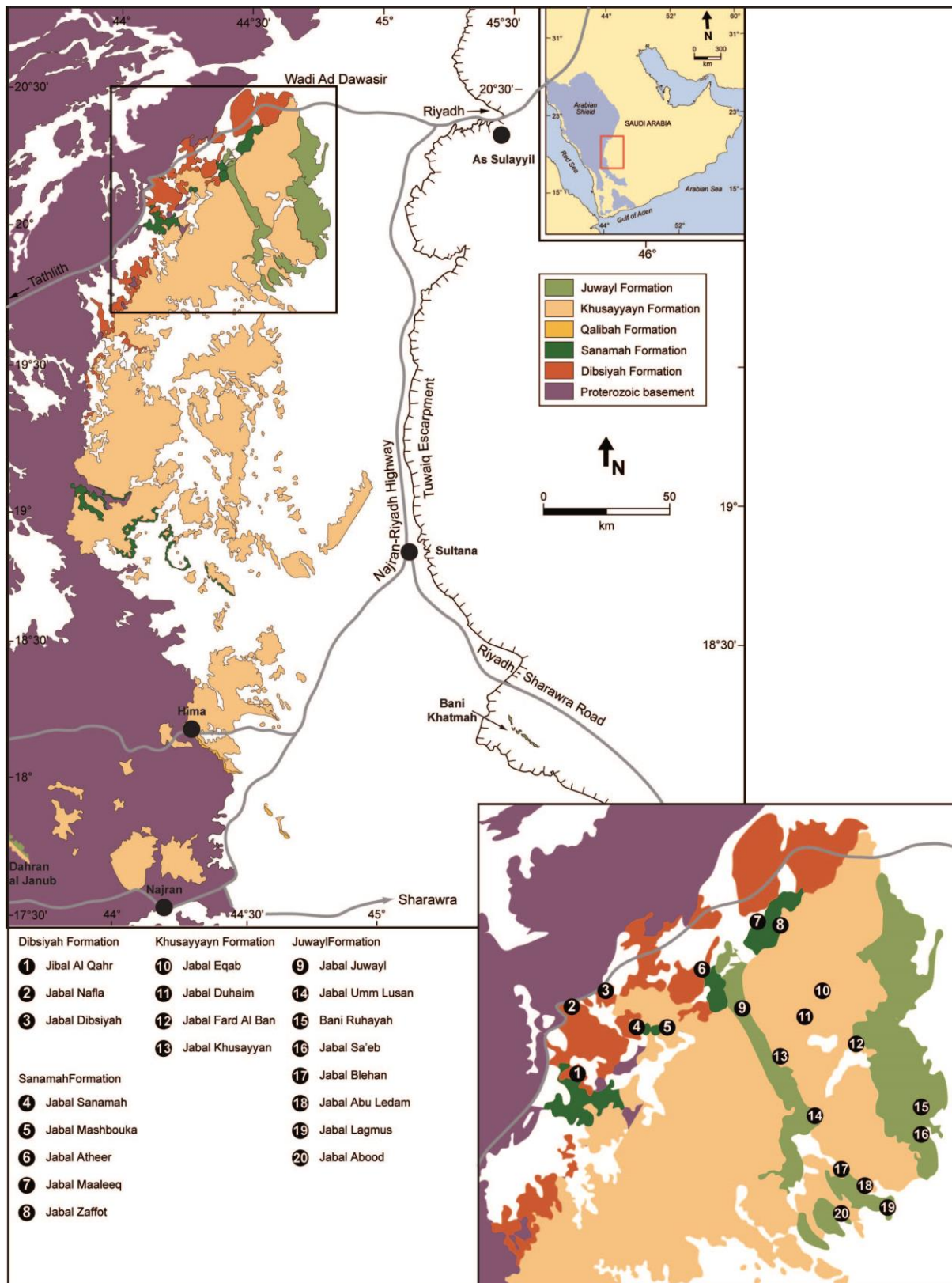


Figure 1: Geologic map of the main outcrop area of the Wajid Sandstone in southwestern Saudi Arabia. Outliers on the Arabian Shield are not shown. Insert map shows localities mentioned in text. Modified from Al Hussein (2004) and Keller et al. (2011).

2. Geological background

2.1. Evolution of the Arabian Plate

With the demise of the Pan-African orogeny and the final assembly of Gondwana, an extensive passive margin connected the Arabian-Nubian Shield with the Palaeo-Tethys (Figure 2). The passive margin sediments are found in northern Africa, Turkey, and the Iranian terranes. The Palaeozoic sediments of Arabia, in contrast, were deposited on continental crust of the shield, and hence in an intracratonic setting, today called the “Arabian Platform”. The hinge zone between the sedimentary basins on the continental crust and on the passive margin, and hence between slow and high subsidence, has yet to be documented. The Arabian Platform in its present configuration shows a shelf-margin prism extending from the basement of the Arabian Shield in the west to the frontal thrust of the Zagros Mountains in the east (Figure 1). During Cambrian time, this segment of the Gondwana margin was in a south-north position, approximately between 40°S and 20°S (Sharland et al. 2001). At that time, a vast siliciclastic epicontinental platform bordered the exposed basement of the Gondwana interior, a configuration that probably extended into the Ordovician. In southern Saudi Arabia, this constellation is reflected in the sediments of the Dibsiyah Formation.

By the Late Ordovician (Hirnantian), Gondwana had moved into a polar position and Arabia occupied latitudes between approximately 60°S and 40°S (Sharland et al. 2001), well within the reach of the Gondwana ice cap (Vaslet 1990; Le Heron & Dowdeswell 2009; Le Heron et al. 2010; Keller et al. 2011). Vestiges of this glaciation and the subsequent Early Silurian deglacial transgression are visible in the Sanamah Formation and the Qalibah Formation. Tectonically quiet conditions continued during the remainder of the Silurian and most of the Devonian until the Frasnian (Sharland et al. 2001). Sedimentation on the Arabian Platform, which was in a moderate latitudinal position, continued under epicontinental conditions, which in the study area resulted in the deposition of the Khusayyayn Formation.

During the Late Devonian and the Mississippian, the onset of subduction outboard of the Iranian terranes started to affect sedimentation on the former passive margin. Compression and extension through back-arc rifting induced a tensional regime that led to localized uplift and erosion.

Concomitantly, Gondwana again moved into a high latitudinal position and during the Pennsylvanian and Permian and the major Permo-Carboniferous glaciation spread out over much of the continent. The sedimentary products of this glaciation are well known from Arabia and adjacent areas (Helal 1964, 1966; Al Sharhan et al. 1991; Al Sharhan et al. 1993; McClure 1984; McClure et al. 1988; Melvin & Sprague 2006; Melvin et al. 2010; Kumpulainen 2009). The co-occurrence of tectonically induced erosion and of glacially induced erosion hampers the interpretation of the causes of depositional processes. This is especially true for the Wajid Sandstone, where pre-tectonic sediments (Khusayyayn Formation) are unconformably overlain by late glacial deposits (Juwayl Formation).

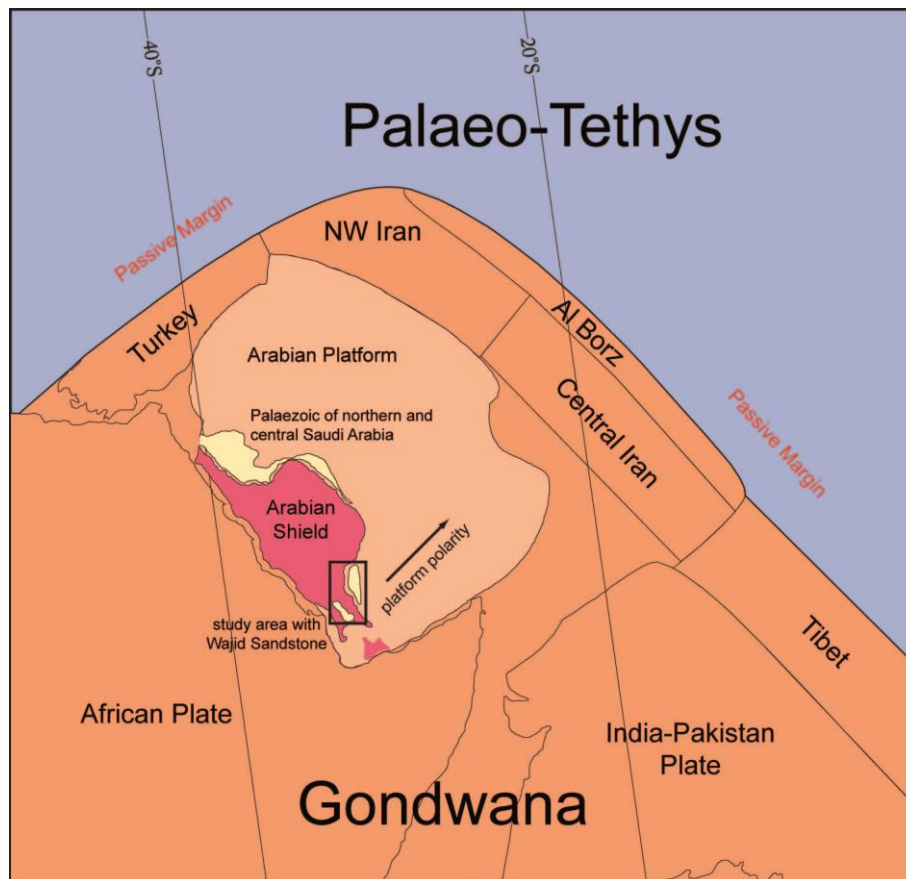


Figure 2: Palaeogeographic configuration and terranes of northwestern Gondwana during the Cambrian centered on Arabia. Arabia basically consists of the basement of the Arabian Shield and the sedimentary basin of the Arabian Platform, which during the Cambrian had the shown polarity. Also shown is the distribution of Palaeozoic sediments in Saudi Arabia and the study area with the Wajid Sandstone. Modified from Sharland et al. (2001).

2.2. Tectonic framework

The Arabian Shield (Figure 1) is represented by crystalline basement composed of Precambrian continental crust (about 870 Ma-550 Ma). The basement consists of accreted island-arc and micro-continental terranes (Stoeser & Camp 1985; Brown et al. 1989), overlain by post-cratonic sediments and volcanic rocks. The final Precambrian Amar collision (about 640-620 Ma; Brown et al. 1989) welded together the Arabian Plate along the north-trending Amar suture. North-south directed structures are a common phenomenon in the basement rocks of the Arabian Shield (Stoeser & Camp 1985). In the latest stages of the formation of the Arabian Plate basement, a major left-lateral wrench-fault system developed, the Najd Rift System (Al-Husseini 2000). Its present-day orientation is north-west - south-east as indicated by major faults and elongation of several accompanying sedimentary basins. Among these basins are the Najd Rift Basin and the Rub' Al Khali half-graben. These grabens were filled with Neoproterozoic siliciclastic rocks, carbonates, and evaporites (Johnson et al. 1994; Sharland et al. 2001; Pollastro 2003; Figure 1, Figure 3).

Today, the main structural elements in the sedimentary succession of the Arabian Platform are north-south trending structural highs such as the Ghawar Anticline and the Qatar Arch; north-west - south-east trending grabens such as the Azraq and Ma'rib grabens; and north-east - south-west trending structures such as the Syrian Platform and the Mosul and Ha'il-Kleissa trends. These structures are considered as representing the stress field of post-collisional extension with the main system being the Najd Fault System, and a perpendicular suite with the Wadi Al Batin fault and similar structures (Al-Husseini 2000). These were superimposed onto the earlier north-south trending suture zones and together provide the framework for the formation of the uplift structures. It is commonly assumed (Konert et al. 2001; Pollastro 2003; Sharland et al. 2001) that these structures and trends are inherited from the basement

through reactivation of older features during Phanerozoic tectonism. An additional effect of the late orogenic extension was the formation of major salt basins in Iran and Oman that additionally may have triggered tectonic deformation on the Arabian Platform during the Phanerozoic.

Positive features on the Arabian Platform include the Ghawar Anticline or Uplift, the Qatar Arch, the Khurais-Burgan Uplift, and the Maqalah Anticline. Almost all of these structures combine the effects of folding and reverse faulting. All of them are interpreted to have originated during the extensional collapse following Precambrian terrane accretion in the Arabian Shield (Al-Husseini 2000). Their activation, however, occurred during different episodes of the Phanerozoic.

The basement-related trends and arches subdivide the Arabian Platform in several sedimentary sub-basins, among which are the Azraq-Sirhan Basin, the Tabuk Basin, the Widyan Basin, and the Rub' Al Khali Basin. During the Jurassic and Cretaceous, the Qatar Arch and the Rimtham Arch subdivided the eastern Arabian Platform into the South Arabian sub-basin, the North Arabian sub-basin and the Gotnia Basin. The South Arabian sub-basin is essentially a prolongation of the larger Rub' Al Khali Basin.

3. Former research and state of the art

3.1. Sedimentology and stratigraphy

The entire Wajid succession was studied in detail by Powers et al. (1966). The basal strata of the Wajid Sandstone rest nonconformably on the Precambrian basement rocks of the Arabian Shield. The Wajid Sandstone is exposed from Wadi Ad Dawasir to Najran over a distance of 300 km and more. The maximum outcrop width of Wajid Sandstone is approximately 100 km (Powers et al. 1966). It is exposed in a vast area that covers almost 22000 km². To the east of the outcrop area, the strata disappear beneath the basal layers of the late-upper Permian and the Jurassic formations. The western margin of the Wajid outcrop has a convex shape against the Precambrian basement rocks. The nonconformity is exposed along the southwestern margin and can be traced into Yemen in a series of small isolated hills composed of basement rocks. The upper part of the Wajid Sandstone crops out at the foot of Bani Khatmah Escarpment beneath Jurassic strata.

The Wajid Sandstone was subdivided into four members according to their facies by Kellogg et al. 1986. These members are, in ascending order, the Dibsiyah Member, Sanamah Member, Khusayyayn Member, and the Juwayl Member. The age of these deposits was interpreted to be Cambrian and Ordovician. These members were upgraded to Formations by Stump & Van der Eem (1995), and the Wajid Formation was given Group rank. In addition, Evans et al. (1991) identified the Qusaiba Shale Member of the subsurface Qalibah Formation in the southern part of the outcrop belt, thus completing the correlation of the outcrop belt to the subsurface. Recent investigations have shown that the Wajid Group spans the entire framework of the Paleozoic, from the Cambrian to the Middle (?) Permian (Evans et al., 1991; Stump & Van Deer Eem 1996; Al-Laboun 2000, Keller et al. 2011).

In the following, a short summary of some of the most important papers and theses about previous research in the Wajid Sandstone is given. Figure 4 summarizes the different subdivisions of former authors.

ITALCONSULT (1969)

In this study, the consultant gave a detailed description of the so-called “Areas II and III” in southern Saudi Arabia. A new definition of the strata in the studied area was presented. ITALCONSULT subdivided the sequence between the Khuff Formation above and the basement below into two units. The lower part of Late Cambrian to Middle or Late Ordovician age was attributed to the Wajid Formation. A basal conglomerate generally less than one meter thick is frequently observed in outcrop at the contact between the Basement Complex and the Wajid Formation. In Wadi Ad Dawasir, the thickness of the Wajid Formation is 400 - 430 meter. But it is only 159 m thick between the Basement Complex and the black Silurian Shales in the subsurface near Sulayyil. ITALCONSULT correlated the Wajid Formation to the Saq Formation and to the lowermost Tabuk Formation in the northern part of the Kingdom. The upper part with a range from the Late Ordovician to the Early Permian was attributed to the Faw Formation. The Faw Formation was defined by ITALCONSULT (1969) based on the results of well DA-T11, located in Wadi Faw. There, the Wajid Formation is conformably overlain by the Faw Formation, which consists of three members. According to their subdivision, these members are the lower, the middle, and the upper Member. The lower member of this formation consists mainly of shale; the middle member is sandstone, whereas the upper part is shale. The Faw Formation crops out in a very limited part in the ITALCONSULT study area, but extends widely in the subsurface, especially in the southern part of the area. The maximum thickness of this formation is given with 340 m.

Dabbagh & Rogers (1983)

These authors studied the Wajid Sandstones mainly in its southern outcrop area around Najran - Bani Khatmah - outliers on the Arabian Shield. They did not give a new definition or subdivision to the Wajid Formation but discussed sedimentologic aspects of the unit. The main result of their study is a southern provenance of the sediments and the recognition that strata in the south (Khusayyayn Formation) are more strongly fluviually influenced than farther north.

Kellogg et al. (1986)

In 1986, Kellogg et al. studied the Wajid Formation during mapping of the Wadi Tathlith Quadrangle. One third of Wadi Tathlith Quadrangle is covered by the Phanerozoic sedimentary rocks, and a big deal is part of the Wajid succession, which was attributed to the Cambrian and Ordovician. They laid the actual base for the subsequent studies with their definite attribution of the Wajid Sandstone to the Cambrian and Ordovician and its internal stratigraphic subdivision. The time gap from the Silurian to the Middle or Late Permian between the Wajid Sandstone and the overlying Khuff Formation was considered as a time of erosion.

Kellogg et al subdivided the Wajid into four members:

- 1- Dibsiyah Formation
- 2- Sanamah Member
- 3- Khusayyayn Member
- 4- Juwayl Member.

Each member is separated by distinct discontinuities and a basal thin conglomeratic layer from the underlying and overlying rocks. All sediments were attributed to shallow marine to fluvial depositional environments. This study did not describe any glacial deposits in this formation. The thickness of the Wajid Sandstone was given with 550 m.

Mc Clure et al. (1988)

The authors studied the uppermost part of the Wajid Formation at three locations, Bani Khatmah, Al Arid, and a drill hole site about 200 km to the southeast of Khashm Khatmah on the southern edge of the Rub' al Khali. These locations are at the foot of the Tuwayq Mountain Escarpment. The study concentrated on the glacial deposits at the top of the formation. They determined a Carboniferous-Early Permian (Late Westphalian-Sakmarian) age for the deposits. They did not name the sediments; however, they were able to correlate them to the stratigraphic column of a drill hole in the third location mentioned above. They did not measure the thickness of the studied parts or compare it to other sections which have the same age.

Evans et al. (1991)

This study described the Wajid Formation and subdivided it according to the seismic character of the strata. The researchers gave four objectives for their work to study the Wajid Sandstone, which are:

- To differentiate the Wajid Sandstone in outcrop and determine stratigraphic equivalent rocks in other parts of the Arabian Peninsula.
- To interpret depositional environments of these Paleozoic rocks.
- To sample surface exposures of fine-grained sediments for source rock analysis.
- To sample the outcrop for petrographic analysis to characterize the reservoir potential of the mapped units.

They assigned an age of Cambrian for the base to the Middle Permian for the top of Wajid Formation.

The study considers the Wajid Sandstone to be equivalent to the Saq and Qasim, Zarqa and Sarah Formations, the Qalibah Formation, and the Unayzah Formation. They recommended eliminating the term "Wajid Sandstone" in favor of the Saq and Qasim Formations, Zarga and Sarah Formations, Qalibah Formation and Unayzah Formation to the outcrop in the studied area. This concept has heavily been criticized by Keller et al. (2011) and Al Ajmi et al. (in revision). Evans et al. (1991) gave a total thickness for the Wajid Sandstone at the surface of 480 m in comparison with a thickness of 140 m of the Saq – Qasim formations in the northern outcrop area and an additional similar value for the Zarqa-Sarah interval.

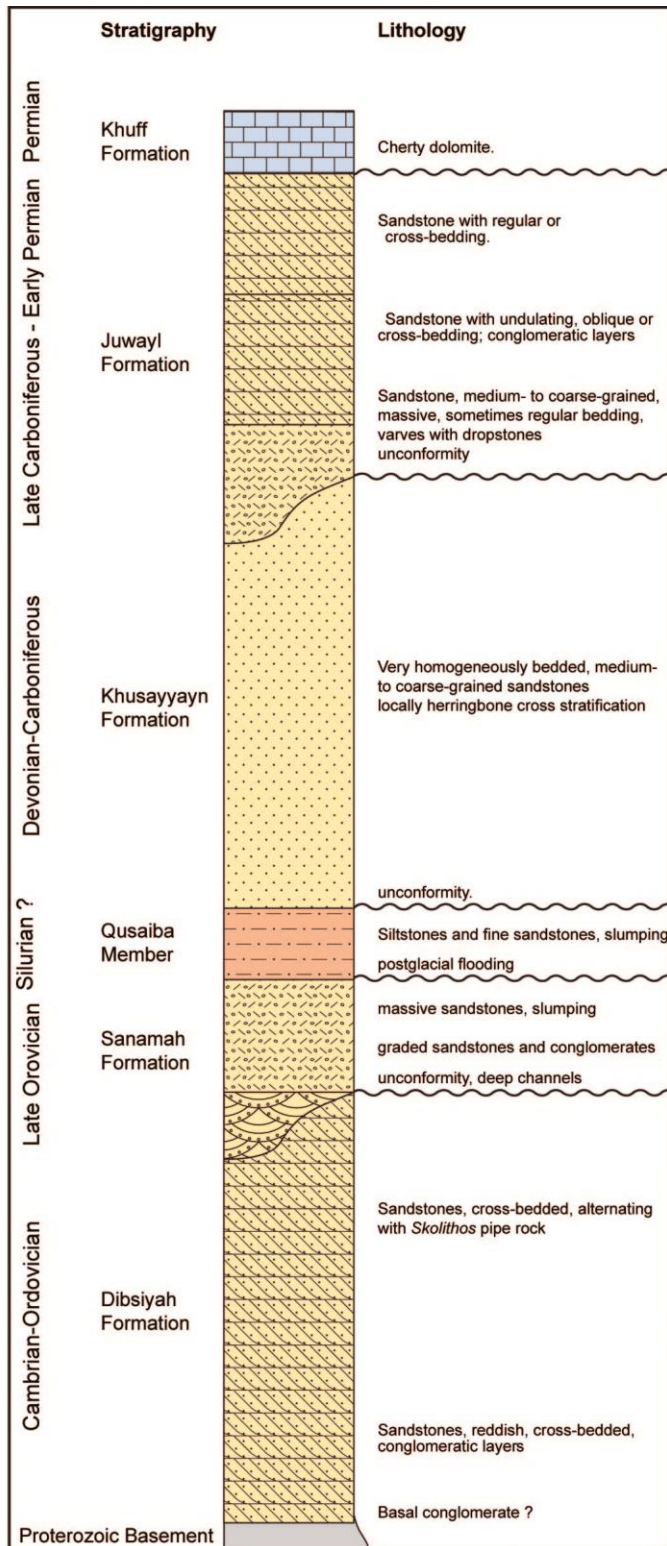


Figure 3: Lithostratigraphic subdivision of the Wajid Group (“Wajid Sandstone”) in SW Saudi Arabia, revised after Evans et al. (1991).

Halawani (1994)

In 1994, Halawani published a short study discussing the glacial sediments in the Late Ordovician. The study concentrated on a part of the Wajid outcrop area and the Ordovician glacial deposits preserved in this area. The Late Ordovician glacials in the Wajid area are represented within the Sarah Formation, considering the Sarah Formation as part of the Wajid Group. Lithologically, he divided the Sarah Formation into five members: From bottom to top, these members or units are:

- E) Silt, clay and, sandstone unit
- D) Upper boulder clay – claystone unit
- C) Sandstone unit
- B) Lower boulder clay – claystone unit
- A) Tillite unit.

The author did not include the other parts of the Wajid in his study and he did not give a total thickness of the studied part.

Stump & Van Der Eem (1995a, 1995b)

In a series of related publications, these authors studied an area of 22000 square kilometers which is the area of the outcrop of the Wajid Formation. They elevated the Wajid to a group and attributed its subunits to formations. They used the names of the Wajid suggested by Kellogg et al. (1986) previously, and added a new formation to the group, which is the Qalibah Formation. They correlate the Middle Cambrian through Early Ordovician Dibsiyah Formation with the Saq Sandstone, and the other units of the Wajid Sandstone to the units of Central Saudi Arabia following Evans et al. (1991). They describe the contacts between these formations as unconformable.

The authors elevate the Wajid sandstone to a group and the members to formations for three reasons:

- 1- Each of the former members is separated from another by hiatuses of varying magnitude.
- 2- Each former member is separated from the other by a period of regional structural deformation and erosion.
- 3- The depositional history of each former member reflects a unique series of events.

The most important features of these publications are the inference of a basic tectonic origin of these sedimentary sequences and the attribution of the units to shallow marine and fluvial environments.

Al-Laboun (2000)

This study is an unpublished report for the studied area. In this study, Al Laboun (2000) kept the former grade of a formation and subdivided the Wajid Formation into six members, according to the lithology and facies changes along the outcrop area. From bottom to top, these members are as follows:

- 1- Lower Dibsiyah; the age of this member ranges from the Middle Cambrian to the Early Ordovician. He considers this member as an equivalent to the Saq Formation in northern area of the Kingdom.
- 2- The Upper Dibsiyah Member. This member ranges from the Late Early Ordovician to Early Late Ordovician.
- 3- The Sanamah Member starts in the early Late Ordovician and reaches to the Late Ordovician. This member is equivalent to the Sarah Formation in the north.
- 4- The Madarah Member ranges from the Early Silurian to the Early Late Silurian, and it is equivalent to the Huban, Qusaibah and Sharawra.
- 5- The Khusayyayn Member is the fifth member of the Laboun study and he considers it to be Late Silurian to Early Carboniferous in age, and equivalent to Jauf, Jubah, and Unayzah Formations.
- 6- This is the uppermost member in the Al Laboun's subdivision of the Wajid Formation and it is unnamed. The age of this member is Pennsylvanian to the Late Early Permian. He considers this member to be equivalent to the Ash Sheqah Formation in his geological table of the Kingdom.

Al Laboun (2000) did not give any thicknesses for the Wajid Sandstone.

Al-Husseini (2004)

This author followed Kellogg et al. (1986) by grading the Wajid Sandstone as Formation subdivided into four members: The Dibsiyah, Sanamah, Khusayyayn and Juwayl Member. According to Al Hussaini (2004), the Dibsiyah ranges from the Late Cambrian to the Late Ordovician and it is equivalent to the Saq/Qasim Formations in the north. The Sanamah ranges from the Late Ordovician to the Late Silurian. This member is equivalent to Qalibah/Sarah/Zarqa Formations in the north. The Khusayyayn begins during the Early Devonian and extends into the Mississippian. This member is equivalent to Tawil/Jawf/Jubah/Berwath Formations in the north. The last member is the Juwayl Member, and this member comprises the Middle-Late Carboniferous to the Middle Permian. It is equivalent to the Unayzah Formation in Central Saudi Arabia. This member is separated from Khusayyayn with an unconformity surface created by the mid-Carboniferous tectonic event.

Wanas & Abdel-Maguid (2006)

This is one of the latest studies on Wajid Sandstone. This study concentrated on the petrography and geochemistry of the Wajid Sandstone. They described two sections of the Wajid Sandstone in their study area also from a sedimentary point of view. In particular, they described the orientation of cross bedding and composition of cycles and assume a north to northeast trending river system. In this study they consider the Wajid to be Cambrian – Ordovician age. The absence of recognizable fossils means that it is not possible to determine the age of the Wajid Sandstone. The study did not give a total thickness of the studied sections or place it in the stratigraphical position of the area. They discuss the environment of deposition and the source rock, and suggest correlating the Wajid Sandstone with similar deposits elsewhere in Arabia and North Africa.

Hussain et al. (2000), Hussain et al. (2004), Hussain (2007)

These researchers mainly studied the provenance of the Wajid Sandstone and tried to correlate the results to the outcrops of the Saq Formation and related strata in the northern outcrop belt of the Kingdom. As they write "...The study is a geochemical approach involving elemental chemistry of selected trace and rare earth elements (REE) to determine the exact relationships between the Saq and Wajid Formation. The study also includes investigation of a third unit, the Kahfah member of the Ordovician Qasim Formation, to provide more validity to the geochemical database of these two lower Paleozoic formations and better understanding of their stratigraphic relationships, provenance and tectonic settings. Although the original proposal included heavy minerals as a possible tool for correlation, because of the limitations of the heavy mineral data, the interpretations and conclusions of this report are largely based on the elemental chemistry data of a total of 100 sandstone samples (40 from the Wajid, 35 from the Saq, and 25 from the Kahfah, respectively) collected from the outcrop sections of these rock-stratigraphic units."

This study was done in the Abha, Khamis Mushayt, and Wadi Ad Dawasir areas with outcrops in Al Suda, Al Habalah, Ahd Rufaidah, and Wadi Ad Dawaser. In the north, the vicinity of Tabuk was studied. On the outliers on the basement, they subdivided the Wajid Sandstone into two main parts according to iron-rich horizons (ironstone) in different parts of the formation:

- 1- Red Unit; this unit is the lower part of the formation in this area.
- 2- Grey unit; the upper part of the formation in the study area.

This study did not give any age to the formation or a detailed description to the sediments of each unit and the environments of the basin in each area. In the other hand he described the basement rocks and their groups as potential source rocks for the sediments. The researcher measured the thickness of the formation in three locations of the study area:

- 1- 55 meters at Al Suda.
- 2- 110 meters at Ahad Rufaidah
- 3- 300 meters in the Al Habalah National Park.

Knox et al. (2007)

Knox et al. (2007) studied the entire succession of the Wajid Sandstone with respect to its provenance. The study shows that "...two distinct mineral compositions occur within the Dibsiyah sandstones, indicating that a major change in provenance took place during deposition of the Upper Dibsiyah sands. The boundary between the Dibsiyah and Sanamah formations is sharply defined, although the overall composition of the Sanamah sandstones is in many respects similar to that of the Dibsiyah sandstones. There is a relatively small difference in composition between the Sanamah sandstones and the associated diamictites. A major change in provenance is indicated at the base of the Khusayyayn Formation, with an increase in the proportion of monazite and staurolite. This change in composition persists into the Juwayl Formation although the greater variability displayed by the Juwayl heavy-mineral assemblages indicates contribution from several sources. Heavy-mineral assemblages in the Juwayl sandstones are comparable to those of the Unayzah C and B sandstones of central Saudi Arabia, but differences suggest mixing between a southern (Juwayl) and western (Shield) source for the Unayzah sandstones."

Diploma theses, University of Tübingen

Filomena (2007) and Dirner (2007) studied the Wajid Sandstone for the first time by applying Miall's concept of lithofacies and architectural elements and analysed cycle hierarchies. Filomena (2007) studied the Lower Wajid Succession. He described braided-fluvial to braided delta deposits for the lower Dibsiyah succession and shallow-marine environments for the upper Dibsiyah succession (both interpreted as Cambrian and Ordovician). He documented in detail the facies inventory of the glaciation-related deposits of the Upper Ordovician Sanamah Formation. Dirner (2007) studied the Upper Wajid Succession sedimentologically. He described alluvial-fan, braided-fluvial, and shallow-marine deposits for the Khusayyayn succession and glacio-fluvial to glacio-marine sediments with some aeolian intercalations for the Juwayl Formation. He documented in detail the facies inventory of the Late Paleozoic Gondwana, glaciation-related deposits of the Juwayl Formation. These theses were part of the mentioned hydrogeological of GIZ/DCo and data were available for this PhD thesis.



Figure 4: Evolution of the stratigraphic framework of the Wajid Group through time and proposed in this thesis. Note the definitive assignment of the Sanamah Formation to the Hirnantian and the short depositional ages assigned to the formations. For explanation see chapter 5.

3.2. Reservoir quality

The Wajid Sandstone Group acts as important hydrocarbon and water reservoir in the Kingdom of Saudi Arabia but also in adjacent countries. The lower part contains important structural gas traps, whereas the upper part also bears some productive stratigraphic oil traps (Evans et al. 1997; Konert et al. 2001). Hydrocarbons are mainly sourced from the Qalibah Formation, which subdivides the Wajid Sandstone group into two reservoirs and shows increasing thickness and carbon content towards the east in the subsurface (Konert et al. 2001).

Little research has been done so far concerning petrophysical properties of the Wajid Sandstone Group. Evans et al. (1991) investigated outcrops and wells and report average porosities of 20% for the Dibsiyah, 21-25% for the Sanamah, 23% for the Khusayyayn, and locally 30% for the Juwayl Formations. They also measured some permeabilities and found values up to 4217 mD (Dibsiyah Formation). They classified the Wajid Sandstone Group as an excellent to good reservoir rock. In the subsurface of the United Arab Emirates up to 6 km deep, Alsharhan (1994) found somewhat lower mean porosities and permeabilities and intense overprint by diagenesis for the Unayzah Formation and qualified the rocks as moderate to good reservoirs.

These classifications are based on few petrophysical data. So far, a systematic survey only exists for the lowermost unit of the succession, i.e. the Dibsiyah Formation (Abdulkadir et al. 2010), which only covers a small portion of lithofacies types and sedimentary facies associations present in the entire succession (see chapter 5). These authors analysed a total of 153 samples with regard to porosity and permeability, using a mini permeameter. They found a limited range of porosity, but a wide range of permeability. Based on some thin sections, they interpreted the high variability of permeability by sedimentary structures, dissolution of unstable minerals together with inhomogeneous grain packing and poor connectivity.

Zeeb et al. (2010) studied the discrete fracture network of the Upper Wajid Sandstone Group to analyse the hydraulic relevance of fracture versus matrix permeabilities for groundwater flow. They used remote sensing data and outcrop studies at a scale of 100 x 100 m. Combining with actual pumping tests and matrix hydraulic conductivity data, they estimated in-situ hydraulic fracture apertures for the upper Wajid Sandstone aquifer to be about ~1,500 μm , which is in concordance with field observations. From fracture flow modelling of the discrete fracture networks they found a conductivity ratio $k(\text{fracture})/k(\text{matrix})$ of 10.4. Although fractures dominate in hydraulic behaviour, stored water volumes must be higher in the matrix, thus making porosity and permeability data important in estimating groundwater quantities.

3.3. Hydrogeology

As mentioned in the introductory part, this PhD thesis was embedded in a hydrogeological study of GIZ/DCo. Therefore, the following background information on the hydrogeology of the Arabian Platform and the Wajid Group is directly taken from a GIZ/DCo report for the MoWE (GIZ/DCo 2009).

The aquifers on the Arabian Platform can be divided into two mega-aquifer systems. The Lower Mega-Aquifer System comprises of a sedimentary succession of mainly sandstones with interbedded shales and siltstones, spanning from the Cambrian to the Early Jurassic and includes the Wajid Group. Other important aquifers in the system are the Khuff-Kumdah and Dhurma-Minjur aquifers. Separating them are predominantly shaley aquitards like the Lower Khuff and Jilh-Sudair aquitards. The Upper Mega-Aquifer System, stretching from the Cretaceous to the Tertiary, comprises of the Wasia-Biyadh, Umm Er Radhuma, Dammam and Neogene aquifers. It is made up of mainly sandstones in the lower part and carbonates and evaporates in the upper part. The aquifers are separated by the lower Aruma shale and the Rus aquitards. Since the hydraulic separation is imperfect, cross-formation flow between the different aquifers occurs. Hydraulically separating the Lower and Upper Mega-Aquifer Systems is a succession of Lower to Middle Jurassic aquitards and aquicludes, consisting of carbonates, shales and anhydrite. Groundwater from both aquifer systems is considered fossil, since the main recharge happened mostly during the last pluvial period, with more humid climate conditions. This period ended about 5,000 years ago.

The Wajid aquifer itself is again subdivided into a lower and upper aquifer, being hydraulically separated by the shaley Qusaiba Member of the Qalibah Formation. The Lower Wajid can be defined as a confined, fractured bedrock aquifer, with its primary porosity and permeability reduced by cementation. Outcrops are exposed in a 90 km wide strip for ~300 km south of Wadi Ad Dawasir to Najran. The bottom of the succession is formed by the crystalline basement, the top by the basal shales of the Qusaiba Member of the Qalibah Formation; its thickness increases from <200 m in the western part of the Wadi Ad Dawasir to >2,000 m in the central Rub' Al Khali basin. The groundwater salinity ranges between 338 mg/l and 5,470 mg/l, with an average of 1,010 mg/l, thus being classified as fresh to moderately saline. The Upper Wajid aquifer has similar properties like the Lower Wajid, also being a confined, fractured bedrock aquifer, and the same outcrop area. Its thickness ranges from <100 m west of Wadi Ad Dawasir to >1,500 m in the central Rub' Al Khali basin. The bottom and top boundaries are the Qusaiba Member of the Qalibah Formation and the basal shales of the Khuff Formation, respectively. The groundwater is fresh to moderately saline with values between 83 mg/l and 7,490 mg/l, with an average of 1,200 mg/l.

4. Methods and material

4.1. Field work

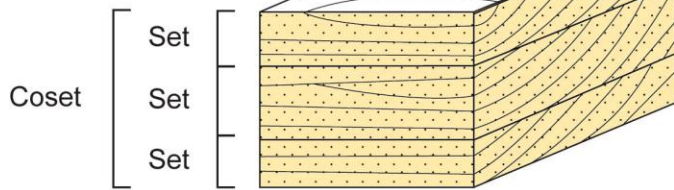
4.1.1. Sedimentological logging

This study is based on several field surveys in the outcrop belt of the Wajid Sandstone. The focus was on the type localities used to define the lithostratigraphy of the Wajid Group (Kellogg et al., 1986). The observations there were complemented with field investigations across the entire outcrop belt between Wadi Ad Dawasir in the north and Najran in the south (Figure 1). In addition, a short survey was carried out in the outcrops west of Najran and the outliers on the Arabian Shield. Sedimentary facies were analysed at various hierarchies, including cm-to dm-scale logging of sections, 2D and 3D analysis of architectural elements, and facies associations, as well as large-scale photo panels. Along several sections, spectral gamma-ray spectra have been measured in order to compare the outcrops with their subsurface counterparts (Schönrok, 2011).

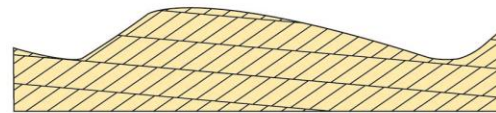
The significance of the Wajid Group for water resources management and hydrocarbon exploration results from the dominance of sandstones and conglomeratic sandstones, mostly only moderately cemented and hence rather porous and with good permeability. Correspondingly, only a minor amount of fine-grained siliciclastic sediments is present in the sedimentary succession. Within this succession, thirteen lithofacies have been identified. The lithofacies description used in this study (LF types) follows the concept of Miall (1978) using grain size, textural maturity, sedimentary structures, bedform dimensions, and bioturbation. However, this thesis does not follow his nomenclature as this was developed and is used dominantly in fluvial systems. In the classification of the subaqueous bedforms, especially the large-scale bedforms of the Dibsiyah Formation and the Khusayyayn Formation, this thesis follows the proposals of Ashley (1990). In the description of bedform dimensions, a subdivision into micro-scale (5 cm – 40 cm), meso-scale (40 cm – 75 cm), macro-scale (75 cm – 200 cm), and giant (> 200 cm) was applied in the field. Within individual beds, the shape and thickness of the foresets varies considerably as a function of grain size modality and current velocity (Reineck & Singh 1970). The geometries are shown in Figure 5 and are used in the description of the internal structure of the bedforms.

A characterization of lithofacies based on sediment petrography alone seems to be too perfunctory. Thus, petrography plus bedforms and their dimensions as first order descriptors were used. In the Dibsiyah Formation, and to a much lesser extent in the other units, textural changes of the primary sedimentary fabrics through bioturbation are of prime importance. Hence, all lithofacies which have been affected by bioturbation, have been designated a separate lithofacies sub-unit with the bioturbation index (Taylor & Goldring 1993) as a second order descriptor. The interpretation of sedimentary successions (“cycles”) is based on trends of these parameters (e.g., fining vs. coarsening upward), and interpreted in terms of base level change (accommodation vs. sediment supply). Small-scale sedimentary successions are a synthesis of grain size development (fining or coarsening upward), set height (accommodation, sediment supply), and the ichnofabrics. Small-scale successions are stacked to form large-scale succession, which in turn reflect long term changes in environmental conditions, and which are used to subdivide the sedimentary succession of the Wajid Sandstone into genetic units (lithofacies associations, LF-A). From all lithofacies, samples for thin sections, geochemistry, porosity, and permeability have been taken. For a better biostratigraphic control on the sediments, 20 samples for palynological investigations.

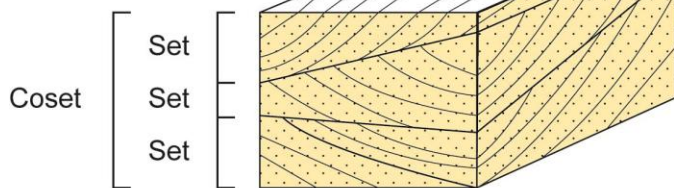
Planar tabular cross beds



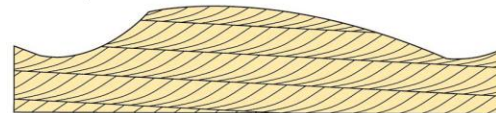
Angular foresets, partial preservation of lee slopes



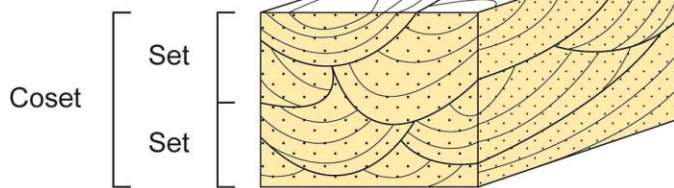
Planar wedge-shaped cross beds



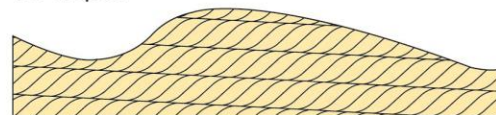
Concave foresets, partial preservation of lee slopes



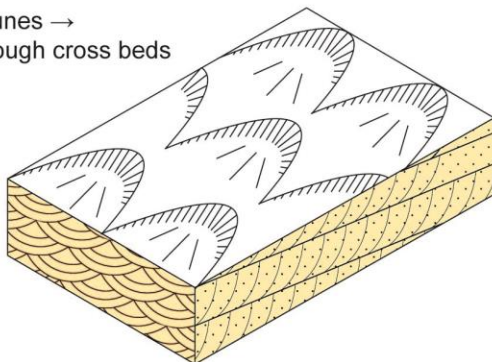
3D trough cross stratification



Sigmoidal foresets, complete preservation of lee slopes



3D dunes →
2D trough cross beds



2D dunes → tabular
cross beds, planar
or wedge-
shaped

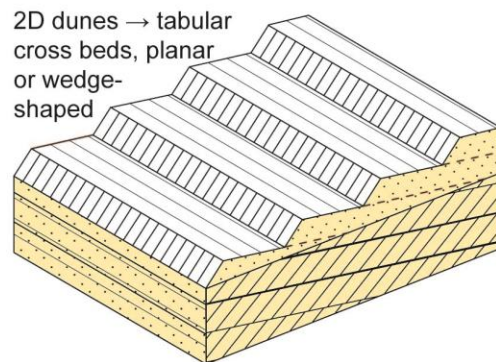


Figure 5: Descriptive nomenclature of bedforms (ripples and subaqueous dunes) and their internal structures as applied in this study.

4.1.2. Gamma-ray logging

Schönrok (2011) logged a total of seven outcrops with a handheld gamma-ray detector (see Table 1). The outcrops have previously been described for this thesis and cover the Lower and Upper Wajid. The RS-230 BGO Super-Spec Portable Radiation Detector by Radiation Solutions Inc. was used to obtain spectral gamma-ray data. Measuring specifications were:

-0.3 m measuring point interval

-30 sec measuring time per point

-measured radionuclides:

K in [%]

U in [ppm]

Th in [ppm]

Table 1: Outcrops logged by Schönrok (2011). Section numbers refer to Figure 1.

Section number	Coordinates	Designation	Elevation [m a.s.l.]	Measured profile [m]	Stratigraphic position
2	N 20°09'17.8" E 44°09'33.7"	Jabal Nafla	915	141.6	Dibsiyah Fm.
5	N 20°10'53.7" E 44°14'21.6"	Jabal Mashbouka	938	104.7	Sanamah Fm.
6	N 20°14'50.3" E 44°17'04.4"	Jabal Atheer	883	152.65	Sanamah Fm.
13	N 20°04'56.1" E 44°39'46.8"	Jabal Khusayyayn	797	53.4	Khussayyan Fm.
12	N 20°07'09.8" E 4°30'54.4"	Jabal Fard Al-Ban	844	30.6	Khussayyan Fm.
17	N 19°55'01.9" E 44°38'57.1"	Jabal Blehan	855	35.1	Juwayl Fm.
9	N 20°08'46.9" E 44°28'40.4"	Jabal Juwayl	847	36.9	Juwayl Fm.

4.2. Laboratory work

4.2.1. Thin sections

A total of 43 samples from the logged sections of Dibsiyah, Sanamah, Khusayyayn and Juwayl Formations have been studied by Heberer (2012) with a petrographic microscope to identify the mineral composition. For the preparation of thin sections only pieces without weathering alterations have been isolated from each sample. Because of their crumbly consistence, some samples had to be stabilized with resin. Assessment of the mineral suite was done by estimation. Grain size, roundness and sorting have also been determined. Grain contact types comprise punctual, concave-convex and structured contacts. The sandstones have been classified using a QFL ternary plot after McBride (1963), which can also be adapted for provenance analysis. Other than thin section microscopy, Heberer (2012) also used REM analysis on a total of 9 samples in order to investigate transport mechanisms as well as geochemical analysis (17 samples total) to gain more information about the provenance. The results of this diploma thesis are incorporated in the overall data base and used for statistical analysis of reservoir properties (see Chapter 8).

4.2.1. Palynology

For palynological studies and dating a total of 20 outcrop samples (see Annex) have been selected, mainly from the Juwayl, but also from the Khusayyayn, Sanamah and Dibsiyah Formations. All samples, each with 150 g, have been prepared using standard palynological techniques. For dissolution of carbonates and silicates, HCl (33%) and HF (43%) have been used, respectively (see Figure 6). Density separation has been done with $ZnCl_2$ solution ($D \approx 2.2 \text{ g/ml}$) and the residue has been sieved at $15 \mu\text{m}$ mesh size. For analysis with a transmitted-light microscope (magnification 40x – 100x), slides have been mounted in glycerol gelatin.



Figure 6: Sample preparation for palynological studies at TU Darmstadt: soaking of samples in HF (43%) for 24 hours.

4.2.2. Porosity and permeability

The porosity measurement was carried out using the AccuPyc II 1330 gas and GeoPyc 1360 powder pycnometers which are used in conjunction (Figure 7). They combine pure and envelope volume measurements to determine porosity. They both work based on the Archimedes principle. The Accupyc II 1330 Pycnometer determines pure density and volume by measuring the pressure changes of helium in a calibrated volume.

The principle is based on the general gas law:

Equation 1

$$P_1 (V_1 - V_p) = P_2 (V_2 - V_p)$$

The device operates with two chambers of known volume V_1 and measured pressure P_1 . In the sample chamber with helium gas pressure, the volume of the sample V_p is unknown. The sample relaxing in an expansion chamber provides a new pressure P_2 in the two chambers, one associated with volume V_2 . The equation can now be solved to get the unknown value which is the true volume of a sample (the volume in g/cm^3). In addition, the GeoPyc 1360 Pycnometer was used to measure the envelope volume and to calculate the envelope density of samples. Envelope density is the mass of an object divided by its volume. When the sample density obtained from Accupyc 1330 is inputted, then the instrument can report percentage porosity.

The final porosity results obtained for each of the samples was manually cross-checked using the formula:

Equation 2

$$(V_E - V_P) / V_E * 100\%$$

Where: V_E is the envelope or total volume and V_P is the pore volume



Figure 7: AccupycII 1330 (left) and 1360 (right) Pycnometer at the Institute for Applied Geosciences, Darmstadt.

The permeability of the samples was measured using two different methods: the minipermeameter and the column permeameter. These gave values of the apparent and intrinsic permeability respectively in Darcie's. Permeability measurements were conducted on either cube-shaped samples or core plugs. In the case of the minipermeameter, nitrogen gas was injected into the rock samples via a probe which was pressed against the sample rock face (Figure 8a, b). The software makes use of gas permeability measurements at different pressures, which are plotted against the inverse of pressure difference. The intercept of the resulting straight line with the gas permeability axis is equal to the liquid permeability. In order to receive accurate mean horizontal and mean vertical permeability, in each direction 6 measurements in x and y direction were carried out.

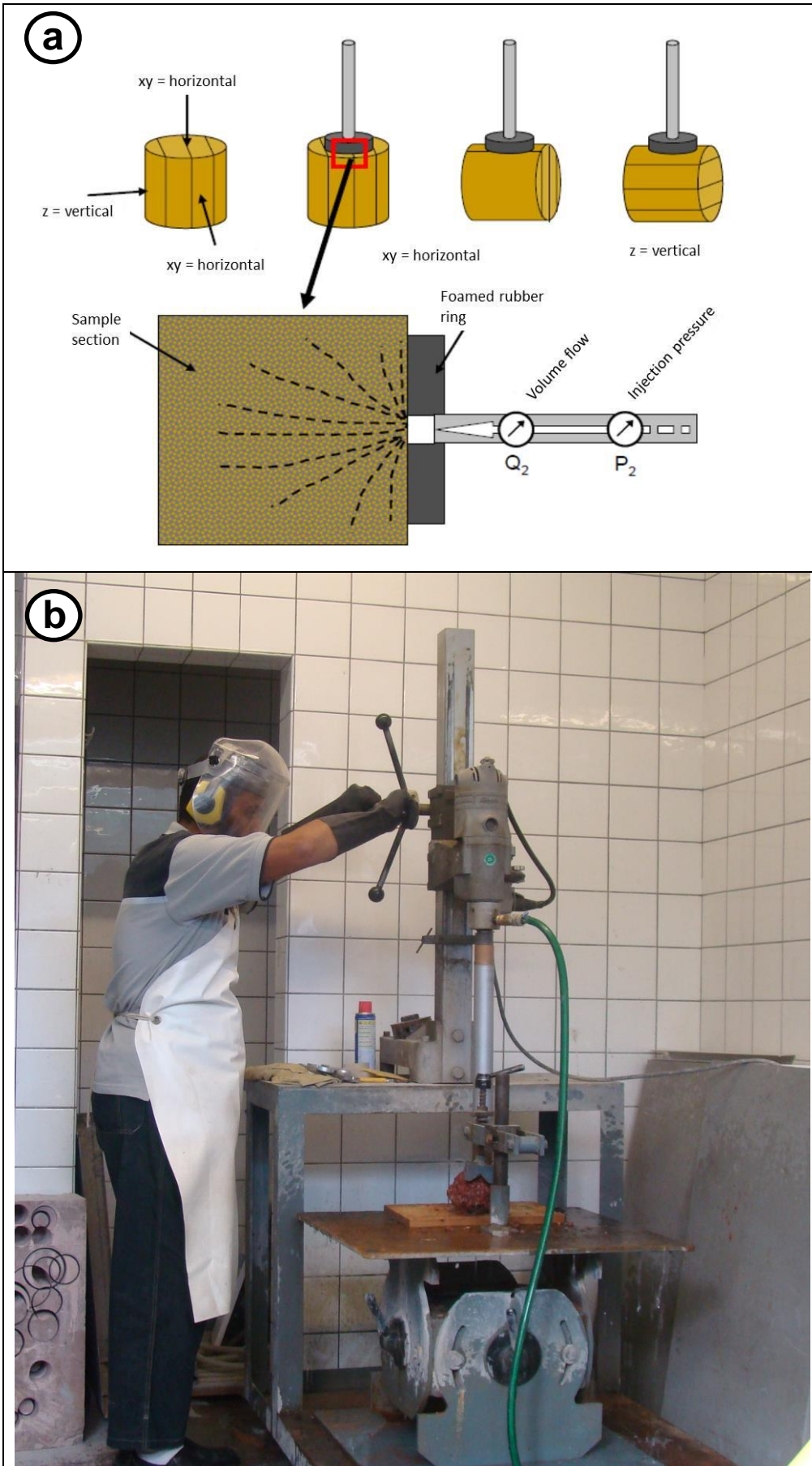


Figure 8: a Principle of mini permeameter measurements of cube-shaped or cylindrical samples (after Greb, 2006). b Drilling core plugs for Poroperm measurements.

The column permeameter measures the value of intrinsic permeability of the cylindrical sample only in one direction. Because the plugs were drilled vertical to the dip of the sedimentary beds, this permeability value is comparable and should correlate with that of the vertical z-direction, obtained from the minipermeameter. The sample is placed in an air tight cell membrane and pressured air is forced to flow through the sample from the cell inlet with pressure p_1 , then going out through the cell outlet with pressure p_2 (Figure 9). The pressure difference between the cell inlet and the outlet gives the intrinsic permeability value, which is independent of fluid property. The intrinsic permeability of a medium is largely a function of the size of pores and the degree of interconnectivity.

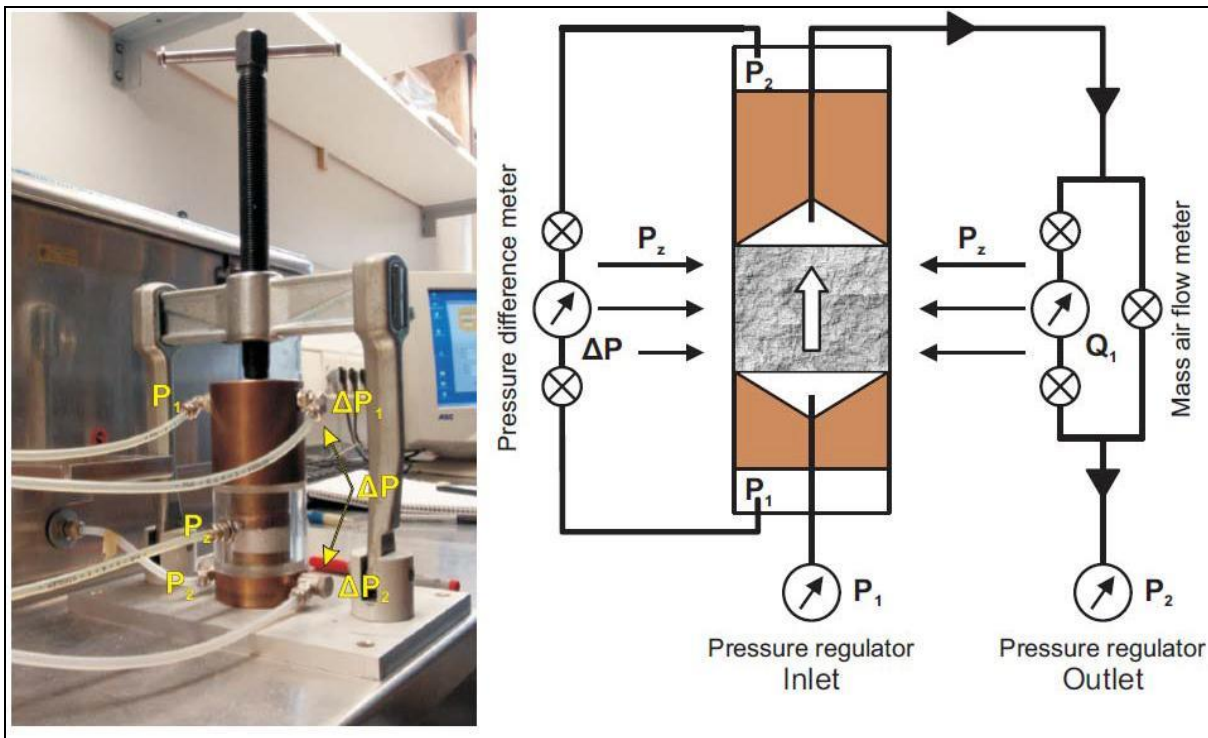


Figure 9: Gas permeameter at the Institute of Applied Geosciences, Darmstadt and principle of measurement after Bär (2008).

In order to translate gas permeabilities into water permeabilities, a specific system set-up was developed in the frame of a student's project. The following description closely refers to the report of Ngole (2012). The water permeameter system consists of four water cylinders which are interconnected by valves and tubes (Figure 10 and Figure 11). These include water inflow cylinder (P_1), outflow cylinder (P_2), high differential pressure (P_{diff} –high) and low differential pressure cylinder (P_{diff} – low). P_1 (inflow) is connected to the top of sample chamber through valve D, while on the other side on top of the sample chamber there is a tube going to P_{diff} –high through valve B. P_2 (outflow) is connected in the base of the sample chamber by a tube which is controlled by valve C. P_{diff} – low is also connected at the base of sample chamber with the tube that crosses valve A. Furthermore, P_{diff} (high) and P_{diff} (low) are linked by valve E, P_{diff} (high) and P_2 by valve F and valve G connects P_1 and P_2 in order to create short cuts between all cylinders. A vacuum pump is connected by a tube on top of P_1 cylinder through valve Y. Moreover there is a tube taking water to the P_1 or emptying the cylinders via valve Z.

An experiment starts by filling water in all four cylinders, whereby P_1 and P_2 were filled to their maximum level mark, while pressure difference cylinders were filled to their initial water level marks. In addition, the samples were evacuated from air by a suction pump and saturated with water before any measurement was done. This was done by opening valve D and Y and therefore having full access to the sample from the pump, which produces a vacuum of 30 mbar. During this stage all other valves were closed including valve 7 in the software. After sucking of the air, the samples were then saturated with water from P_2 by simply opening valve C while pump is still on. After this, the system was pressurized by assigning 6000 mbar output pressure and 3000 mbar input pressure. This minimizes possible relicts of air.

The inflation of sealing was done by allowing air from pressure chamber to fill the sample chamber. This step prevents water to bypass the sample. Like in air permeability, before starting any measurement all sensors were zeroed and then a reasonable pressure gradient was applied to enable water to flow from P_1 to P_2 . This was done by opening valves A, B, C, and D while closing all other valves to avoid shortcuts. The input pressure, output pressure, differential pressure and discharge were recorded and finally used in calculating the intrinsic permeability.

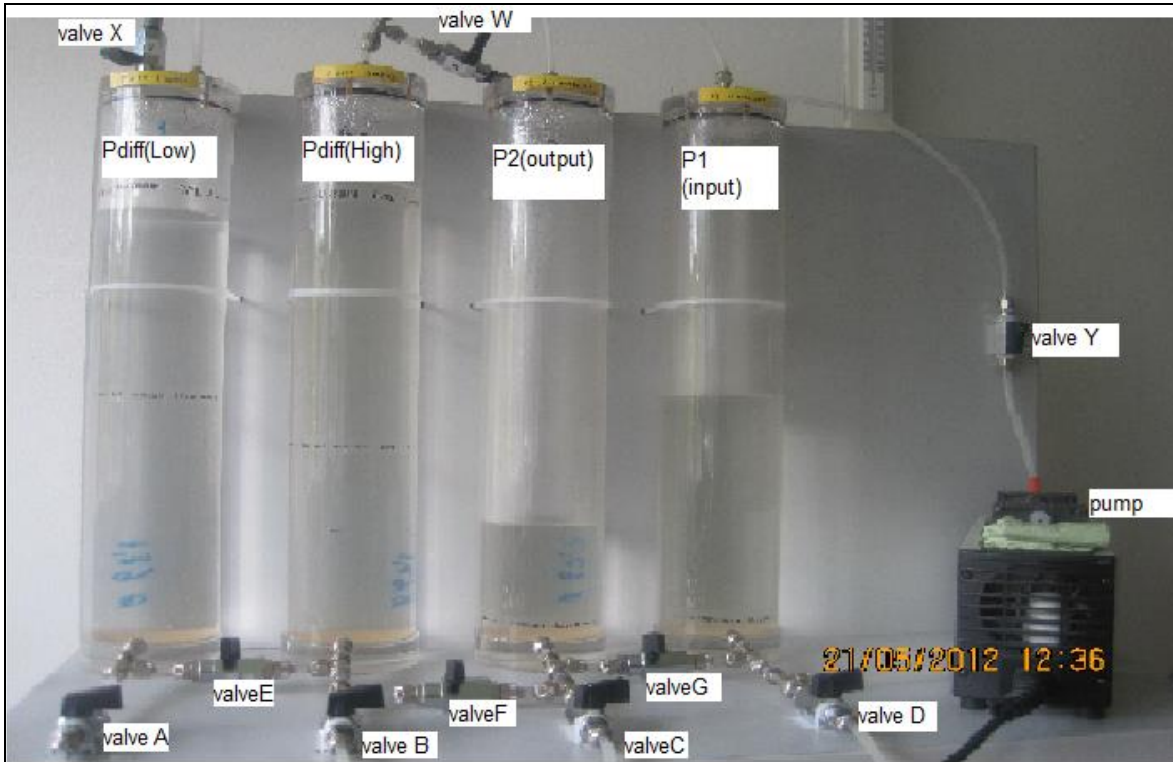


Figure 10: Set-up of water permeability equipment as developed for this project (from Ngole, 2012).

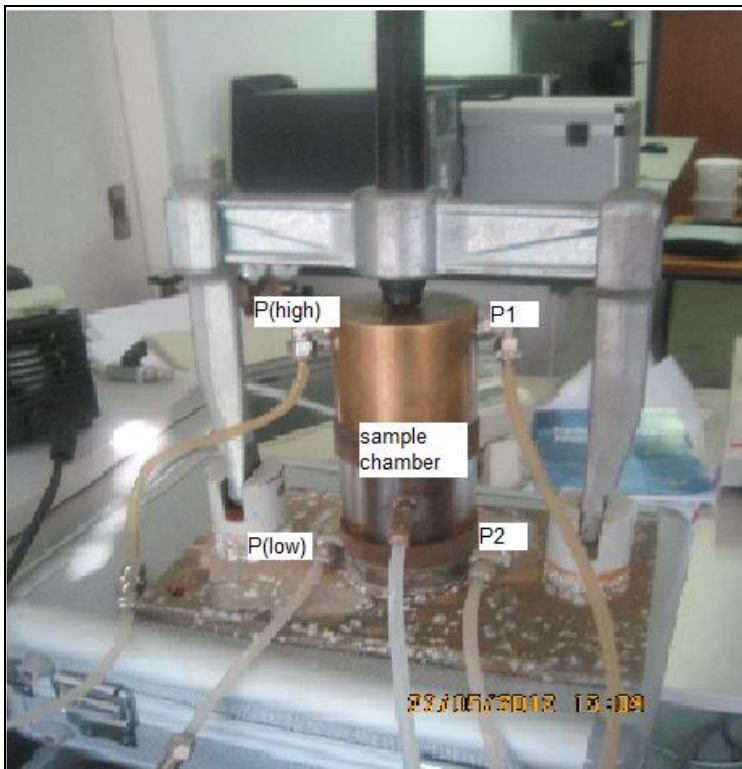


Figure 11: Sample chamber with connecting pipes to the hydraulic cylinders (from Ngole, 2012).

5. Sedimentology and stratigraphy

5.1. Lithostratigraphy

As pointed out in chapter 3.1 the concepts of the internal lithostratigraphic subdivision of the units within the Wajid Sandstone are still a matter of debate and exemplified by the papers of Kellogg et al. (1986), Al Sharhan et al. (1991), Evans et al. (1991), Stump and Van der Eem (1995, 1996), Al Laboun (2000) and Al Husseini (2004). Basically, this study follows Stump and Van der Eem (1995) in subdividing the Wajid Group into five formations: The Dibsiyah, Sanamah, Qalibah, Khusayyayn, and Juwayl formations (Figure 4). The results of this thesis, however, lead to a modification of correlations and time intervals (see discussion in chapter 5.6).

5.1.1. Dibsiyah Formation

The Dibsiyah Formation is a succession of medium-grained to conglomeratic sandstones with few intercalations of finer siliciclastic horizons. Its characteristic feature is the presence of the *Skolithos* and *Cruziana* ichnofacies. Some of the major aspects and components of these ichnofacies are shown in Figure 12.

Stratigraphic relationships

The base of the Dibsiyah Formation is always covered by debris from the buttes and mesas in which the formation is exposed. At Jabal Maqarib, a few meters of coarse-grained, only slightly lithified sandstones and conglomerates are exposed immediately above the Precambrian basement; the contact, however, is nowhere clearly exposed. The sediments consist of quartz pebble conglomerates much coarser than those of the Dibsiyah sediments proper. In addition, data from several wells, drilled into the basement during the investigations of the Wajid aquifer (GTZ/DCo 2009), have nowhere encountered a good basal coarse conglomerate. Instead, the basal layers are represented by a thin weathering horizon with angular to rounded quartz pebbles and feldspar fragments similar to those encountered in the overlying lithofacies associations of the Dibsiyah Formation. Although the sediments at Jabal Maqarib seem to onlap the Precambrian basement, they might well be derived from the outcrops of the Dibsiyah Formation. The upper boundary of the Dibsiyah Formation in the study area is an erosional unconformity at the base of the overlying Sanamah Formation. As sediments of the latter were deposited in subglacial valleys (Keller et al. 2011), the depth of erosion varies strongly in dependence from the position within the valley. Locally, erosion cuts into the lower part of the Dibsiyah Formation.

Thickness

The preserved thickness of the Dibsiyah Formation is 160 m to 190 m.



Figure 12: Meter-scale facies changes between piperock and tabular sandstones without *Skolithos*, outer part of sand sheet complex b *Monocraterion* city in medium-grained sandstone. Note concentric layers on wall, what might indicate that these tubes are actually *Rosselia* c Strongly segmented tubes of unknown origin d *Skolithos* piperock. In the lower part, individual beds are preserved and individual *Skolithos* pipes do not cross bedding surfaces. In the upper part, *Skolithos* burrowing has obliterated bedding and burrows cross bedding surfaces e *Cruziana* sp f Various types of *Skolithoturbation*: basal layers show individual *Skolithos* burrows, cross bedding is still visible. Above is a succession, in which *Skolithoturbation* has obliterated most of the primary structures. Reactivation within this package is recognized through burrows that stop at former bedding planes and others that cross them. Upper part is separated by a bedding plane indicating a major break in sedimentation.

5.1.2. Qalibah Formation

In the subsurface, known from wells (GTZ/Dco 2009) and seismic lines (Evans et al. 1991), the Qalibah Formation consists of two members: the lower Qusaiba Member and the upper Sharawra Member. The Qusaiba Member is a succession of dominantly shale with minor siltstones and sandstones; the upper unit of dominantly siltstones and sandstones is called Sharawra Member. In the absence of biostratigraphic control and based on seismic investigations, the Qusaiba Member is interpreted to be equivalent to the Lower Silurian “hot shales” of northern Arabia and northern Africa (Lüning et al. 2000).

Stratigraphic relationships

The Qalibah Formation is only exposed in a narrow strip in the south-central part of the study area (Figure 1). There, several meters of calcareous fine-grained siliciclastic sediments unconformably rest on Precambrian basement. These sediments are attributed to the Qusaiba Member. The upper contact to the Khusayyayn Formation is very sharp and unconformable.

Thickness

A maximum of 6 to 10 m is preserved in the outcrops of the Qusaiba Member.

5.1.3. Khusayyayn Formation

Sediments of the Khusayyayn Formation really dominate the outcrops of the Wajid Group (**Figure 1**). The Khusayyayn Formation is a rather uniform succession of dominantly coarse sandstones deposited in medium to giant tabular foreset sets.

Stratigraphic relationships

The base of the Khusayyayn Formation is a regionally developed unconformity. Near Najran, the Khusayyayn Formation directly rests on Precambrian Basement. Near Hima (Figure 1), the basal unconformity can be traced from outcrops, in which the Khusayyayn sandstones successively cut out the Qusaiba Member, directly to outcrops where it rests on the basement. South of Wadi Ad Dawasir, the Khusayyayn rests on different horizons of the Sanamah Formation. Evans et al. (1991) report on an undetermined fish fragment apparently indicating a Devonian age. However, details on this finding have never been published and cannot be verified.

Thickness

The most continuous succession is that at the type locality Jabal Khusayyayn, where 55 m are exposed; however, neither the lower nor the upper boundary is exposed there. The combination and correlation of sections in the northern study area indicate thicknesses of around 150 m. Values of 200 m as reported by Kellogg et al. (1986) and Stump and Van der Eem (1995, 1996) could not be verified.

5.1.4. Juwayl Formation

Outcrops of the Juwayl Formation are known from three different, not interconnected areas: In the northern part of the study area, two NW – SE trending channels are present (Figure 1; Kellogg et al. 1986; Keller et al. 2011), in which Juwayl sediments are found. In addition, in the interchannel area, there are some outcrops of the Juwayl Formation. To the east, the Juwayl sediments disappear beneath the unconformity with Late Permian Khuff Formation, which trends approximately north-south (Kellogg et al. 1986). In the southeast, Juwayl sediments are exposed along the Tuwaiq Mountain escarpment (Figure 1) at Bani Khatmah and Khashm Khatmah. The underlying sediments are not known. The succession is capped by the Jurassic unconformity, which brings the Tuwaiq Mountain Limestone on top of the Juwayl sediments. The outcrops west of Najran (Dahran Al Janub; Figure 1) show a succession of fluvial sediments on top of undoubted Khusayyayn strata. These fluvial deposits with their sharp basal surface have been described by Dabbagh & Rogers (1983); however they refused to give a stratigraphic assignment to these rocks. Al Sharhan et al. (1991) compared these rocks with those of Bani Khatmah and concluded that they might represent the same stratigraphic interval. It is assumed, that the presence of siliciclastic sediment distinctly finer than that of the Khusayyayn Formation together with the overall fining-upward also observed in other Juwayl outcrop areas are indicators that these sediments have to be attributed to the Juwayl Formation.

Stratigraphic relationships

The Juwayl Formation rests unconformably on the Khusayyayn Formation. The unconformity has different expressions in the Wajid outcrop belt: In the north, the unconformity is the result of subglacial erosion (tunnel valleys), in the other areas, it seems to be a paraconformity. The only age constraint on the Juwayl deposits was given by McClure (1980) and Besems and Schuurmann (1987) through palynomorphs from Bani Khatmah, which indicate a Sakmarian (Early Permian) age of these deposits. Above a major unconformity, the overlying carbonates of the Khuff Formation mark the onset of a completely different tectono-sedimentary regime that lasted from the latest Permian well into the Mesozoic.

Thickness

The composite section for the northern area including the channel fills is approximately 125 m thick. A similar thickness was determined for the Bani Khatmah area with its lake facies was reported by McClure (1980), whereas Hadley & Schmidt (1975) report thicknesses between 50 m and 135 m from that area.

5.2. Lithofacies types

LF 1: Shale

Shales (LF 1) are very rare in the sedimentary succession of the Wajid Group. Individual packages of more than 20 cm thickness have only been found in the Qalibah Formation, where they are grey to beige, and in the Juwayl Formation (Figure 13a), where they are often entirely silicified.

Shales are a typical product of stagnant water bodies (e.g., lakes) or slack water in the nearshore marine environment, where settling out of suspension is the dominant depositional process.

LF 2: Shale and siltstone

Intimate alternations of shale and siltstone represent LF 2. The sediments are variegated and locally form successions of several meters thickness. In the Juwayl Formation, shale and siltstones laminae form characteristic dark-light couplets with a thickness of a few mm (Figure 13b). Packages of these couplets locally accumulated to packages of several meters (Figure 13c). In several sections, these sediments are strongly silicified. The shales and siltstones were deposited in stagnant waters as evidenced by the absence of any kind of current induced structures. The rhythmic alternation of light silty and dark shaly laminae together with associated glacial deposits is characteristic of varve sediments, typical of glacial lake environments (Keller et al. 2011). Some of the individual layers may have originated from distal turbidity currents, which are not uncommon in lakes (Einsele 2000).



Figure 13: Fine-grained lithofacies of the Wajid Group. a Massive green shale (LF 1), Juwayl Formation, Section. b Shale-siltstone alternation (LF-2) strongly silicified, Juwayl Formation, Section. The rhythmic alternation of light and dark layers is typical of varve sediments. c Shale-siltstone alternations with conglomerate layers represent lake sediments with ice-rafted debris. d Siltstones with ripples (LF-3.2), Juwayl Formation Section e Variegated siltstones in the upper part of the Juwayl Formation f Wave ripples in fine sandstone (LF-5) g Thin-bedded sandstone with flaser bedding (LF-6), Juwayl Formation h White sandstone with horizontal bedding (LF-7.1), Juwayl Formation.

LF 3: Siltstone

Massive siltstones (LF 3.1) have only been observed in the Sanamah Formation and the Juwayl Formation, where these brown and beige sediments attain several 10s of centimetre thickness. Siltstones of LF 3.2 and LF 3.3 are usually thin bedded, show horizontal lamination, and are of reddish to brown and beige colour (Figure 13d). In LF 3.3 of the Dibsiyah Formation most of the primary sedimentary structures have been obliterated by burrowing; the corresponding bioturbation index (Taylor & Goldring 1993) is 4 to 5. The massive siltstones of LF 3.1 represent some kind of mass flow deposit as shown by the absence of current induced structures. The siltstones likely were deposited through distal turbidity currents that originated close to the mouth of a glacially-fed river.

Sedimentary structures indicate that the siltstones of LF 3.2 and LF 3.3 were formed from bed load transport under lower flow regime conditions. Where these deposits are associated with 2D or 3D dunes, they likely are the product of the vast interdune areas where current velocities are distinctly lower than in the dune fields themselves (Ashley 1990).

LF 4: Siltstone to fine sandstone

Siltstones and sandstones form thin- to medium bedded horizons of intensively red or locally yellow colours. Internal stratification is almost absent; locally, low-angle cross bedding and ripple-drift cross bedding have been observed. The sediments were deposited in micro-scale or meso-scale bedforms. They show strong and large-scale soft-sediment deformation, including truncated folds, dome-like, and large-scale ball-and-pillow structures (Figure 14). The sediments record low energy conditions with an alternation or a combination of bedload transport and fall out of suspension. Nevertheless, a large amount of sediment was provided, which was rapidly deposited and subsequently subject to dewatering. As these deposits are found in the Sanamah Formation and the Juwayl Formation, and as these deposits are part of a glacial succession, they are interpreted as ice distal products. Decreasing energy of the rivers draining the glaciers led to the deposition of coarse sediment close to the glacial front, but further downstream only silts and sands were delivered. Locally, these sediments may even represent deposits of a delta in a glacial lake. Deformation of the sediment, especially when associated with shearing and thrusting, is interpreted to result from subsequent glacier advance (Keller et al. 2011).

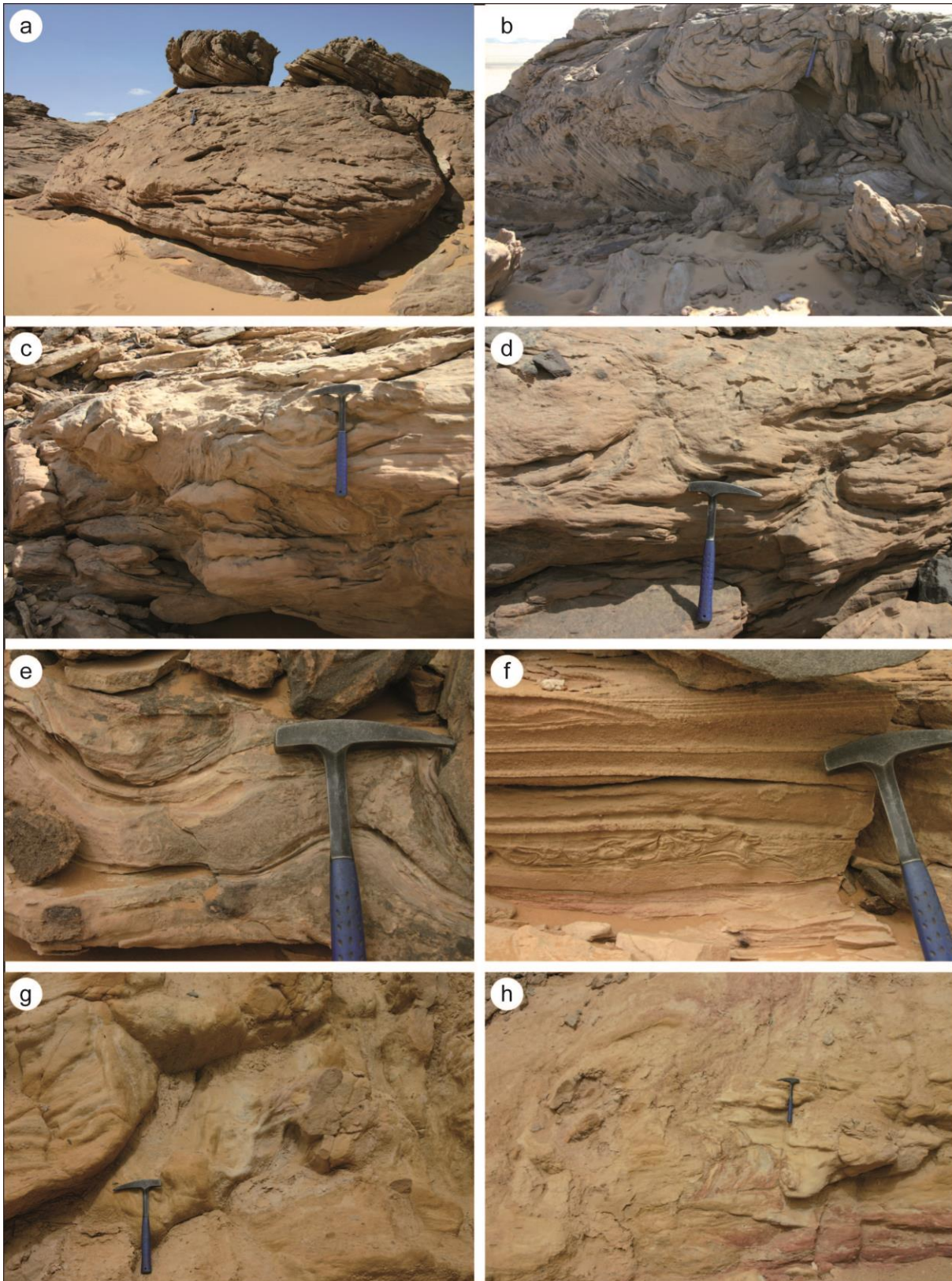


Figure 14: Soft- sediment deformation in the Wajid Group a Large, almost recumbent folds in coarse sandstones (LF-8.2) of the Khusayyayn Formation, Section , b Slumping in sandstones of the Khusayyayn Formation, Section , c Slumping in the sandstones of the Dibsiyah Formation, Jibal Al Qahr d Dewatering (flame) structures in sandstones of the Dibsiyah Formation, Jibal Al Qahr e Sliding and bed-internal folding in rapidly deposited sandstones, Juwayl Formatio, Jabal Blehan f Sliding with bed-internal folding in a single sandstone layer of the Juwayl Formation, Jabal Blehan g Massive siltstones strongly deformed by grounding icebergs, Juwayl Formation, Bani Khatmah h Total destruction of primary sedimentary structures in lake sediments of Bani Khatmah, Juwayl Formation.

LF 5: Sandstone, ripple-drift cross bedding

Fine to medium grained sandstones in dominantly micro-scale beds with cross bedding of different origin represent LF 5. The sediment is moderately sorted to sorted. Whereas in many horizons, the cross bedding originated from unidirectional flow, in others bidirectional cross bedding, often symmetrical, was observed. From 3D outcrops it becomes apparent that the latter are wave ripples (Figure 13f). The sediment is the product of a moderate to low energy environment, in which bedload transport was the main agent. Bedforms indicate unidirectional and bidirectional transport. Although well-developed mud flasers or mud drapes are absent, the bidirectional bedforms are likely to represent tidal influence.

LF 6: Sandstone, flaser bedding

LF 6 is composed of fine to medium grained sandstones, moderately to well sorted, with well-developed flaser bedding (Figure 13g). The sediments are generally present in micro-scale beds and may be stacked to bedsets of more than one meter thickness. The sandstones were deposited in moderate to low energy environments with dominantly bedload transport. Slack-water periods are documented through the fall-out of mud, which gave rise to the flaser texture of the sediment.

LF 7: Sandstone, horizontal to low-angle cross bedding

LF 7 is made up of fine to coarse grained sandstones in meso-scale to macro-scale beds. All of these deposits are horizontally bedded or show low-angle cross bedding. As there are distinct differences in the grain size, LF 7.1 represents fine to medium grained sandstones (Fig 7h), whereas LF 7.2 is composed of almost unimodal white coarse sand (Fig 8a). LF 7.3 is medium to coarse sand, which served as a substrate for burrowers, who effectively destroyed many but not all of the primary sedimentary structures. The corresponding Bioturbation Index is 4 to 5. All these sediments show beige to intensively red colours. The individual laminae locally are graded. Sometimes, the lamination is accentuated by heavy mineral stringers. From the studies of Paola et al. (1989) and Cheel (1984), it seems that horizontal lamination is mainly produced under high-energy, upper flow regime conditions. High frequency scouring and subsequent filling and low frequency migration of bedforms with a height of several grain and amplitudes of up to 100 cm are superimposed to form the laminae. In flume studies, these processes were able to produce graded laminae and to produce heavy mineral segregations.

LF 8: Sandstone, fine to medium, tabular cross bedding

LF 8 is composed of fine, medium, and coarse sandstones deposited in beds a few tens of centimetres (micro-scale) to almost two meters (macro-scale) thick. The bounding surfaces of the foreset sets are planar and commonly almost horizontal. All geometries from purely angular (Figure 12c) to increasingly curved with a tangential basal contact of the foresets (Figure 12d) to sigmoidal geometries (Figure 12e) have been observed and partly used to distinguish between the subfacies.

- LF 8.1.1 (Figure 12d) is distinctly white fine to medium sandstone in meso-scale beds. The foresets are mm-thick and of the angular type or slightly curved.
- LF 8.1.2 is fine- to medium-grained sandstone, yellowish to red, deposited in micro- to meso-scale beds. The foresets are mm-thick and moderately to strongly curved.
- LF 8.2 consists of locally pebbly, medium- and coarse-grained sandstones in meso-scale to macro-scale beds (Figure 12f). LF 8.2.1 with micro-scale to meso-scale foreset and cosets locally contains abundant feldspar fragments, and, in the Dibsiyah Formation, is frequently burrowed. Individual foresets are mm-thick to several mm thick and dominantly moderately curved. LF 8.2.2 shows medium to thick foresets that locally are close to 150 cm thick (Figure 12e). The foresets are of the angular type. Where these sediments of LF 8.2.2 are frequently slumped (Khusayyayn Formation), they have been designated LF 8.2.3.
- LF 8.3 (LF 8.3.1) is represented by medium and coarse sandstones, also with medium to thick foreset sets (Figure 12g). In contrast to LF 8.2, however, the individual foresets are thick and often graded from basal pebble laminae into sand of coarse or medium grain size (Figure 13a). Here too, feldspar clasts are abundant in some horizons. LF 8.3.2 is distinguished on the presence of abundant burrows of *Skolithos sp.* and related species and of *Cruziana sp.* and only observed in the Dibsiyah Formation.

- LF 8.4 is petrographically similar to LF 8.3. However, the individual bed shows a fining-upward succession of graded beds, that is, individual foresets are graded and the foresets at the base of the bed are coarser grained than those towards the top.
- LF 8.5 again is medium to coarse sandstone; however, here the entire bed is graded.

Throughout the Wajid Group, sets and cosets of micro-scale, meso-scale, and macro-scale LF 8 sediments have been observed. In addition, giant sets with a height > 200 cm are present in the Khusayyayn Formation. The tabular sandstone beds originated in moderate to high energy environments. Tabular sandstones are the typical product of migrating large 2D dunes (Ashley 1990) under unidirectional flow conditions with bedload transport.

LF 9: Sandstone, macro-scale 2D-trough cross bedding

Although in general rather similar, LF 9 and LF 10 are distinguished because of the distinct grain size association of coarse sand and abundant quartz pebbles in LF 10. Quartz pebbles are absent in LF 9 and the sorting in general is better. The typical feature of these deposits is their depositional geometry in trough cross beds, usually several times wider than deep. In many cases, the 3D outcrops permit the recognition of the third bounding surface as a planar surface. In general, sediments have been deposited in meso-scale and macro-scale bedforms. Micro-scale units are present only to a minor extent.

- LF 9.1 is moderately sorted and of medium to coarse composition.
- LF 9.2 is sandstone deposited in 2D trough cross beds (Figure 14c), which is relatively well sorted, either within the medium sand fraction or in the coarse sand fraction. Quartz grains are moderately rounded to rounded.
- LF 9.3 is similar to LF 9.1; however, bioturbation is prominent, the corresponding Bioturbation Index (*Skolithos* ichnofacies) varies between 2 and 5.

In all subfacies, siltstone intraclasts have been frequently observed at the base of the scour fills (Figure 14d). Similar to LF 8, sandstones of LF 9 were deposited under medium to high energy conditions. As pointed out by Ashley (1990), 2D through cross bedded sandstones result from the migration of 3D dunes. In comparison with their 2D counterparts, transport energy must be at least slightly higher to produce 3D geometries. Mudstone intraclasts suggest the presence of low energy environments in the vicinity (inter-dune environments).

LF 10: Sandstone to pebbly sandstone, macro-scale 2D-trough cross bedding

LF 10 is mainly present in macro-scale bedforms and to a lesser extent in meso-scale forms. The following subfacies have been identified:

- LF 10.1 is conglomeratic sandstone, deposited in 2D trough cross beds. Rounding of the quartz grains varies between subangular to rounded, sorting is moderate to poor.
- LF 10.2 is represented by medium and coarse sandstones in which grading is preserved. In LF 10.2.1, the entire bed of coarse to medium or fine sand is graded. LF 10.2.2 shows medium to thick foresets, in which the individual foresets are graded from basal pebble laminae into coarse and rarely medium sand (Figure 14d).
- LF 10.3 is a rare type of sediment in the Wajid Group and only present close to the contact between the Sanamah Formation and the underlying Dibsiyah Formation. It consists of inversely graded conglomeratic sandstones with large tabular clasts of grey siltstone.
- LF 10.4 and LF 10.5 both preserve the record of moderate to intensive bioturbation. Whereas the pebbly or conglomeratic sandstones of LF 10.4 were the home of trilobites that left a variety of *Cruziana* tracks (BI 2-4), sands of LF 10.5 were haunted by vertical burrowers whose activities are recorded as *Skolithos* sp. and related forms (Figure 15; BI 2-5).

The hydrodynamic interpretation for LF 10 is the same as for LF 9. However, the absence of quartz pebbles in LF 9 indicates an important shift in environmental conditions in the depositional system. The reasons for this shift will be discussed later.

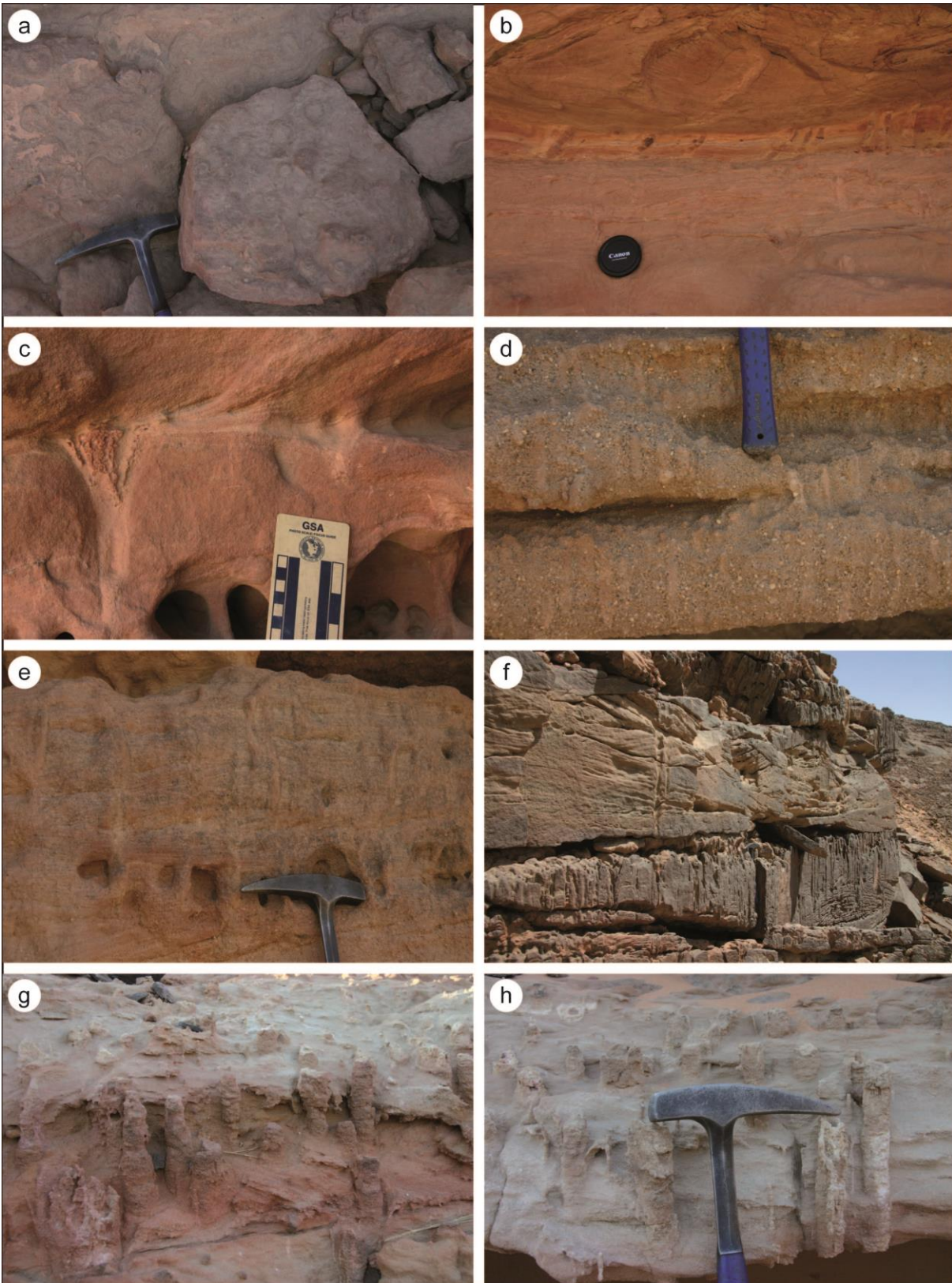


Figure 15: Aspects of bioturbation in the Dibsiyah Formation at Jabal Nafla a Bedding plane surface with *Monocraterion* b Sandstones and siltstones, lower bed is strongly bioturbated, no bioturbation in overlying siltstones c Well-developed longitudinal cross section of *Monocraterion* sp. d Conglomeratic piperock, Bioturbation Index 4 to 5 e *Skolithos* tubes in micro-scale cross bedded tabular sandstones f Piperock with various generations and penetration depths of *Skolithos* eroded and overlain by 2D dune sandstone g *Monocraterion*? tubes and small interspersed *Skolithos* tubes. *Monocraterion* tubes are up to 5 cm in diameter h similar to g but with longitudinal sections through *Monocraterion*. Some of them might actually represent *Rosselia* sp.

LF 11: Sandstone to pebbly sandstone, 3D trough cross beds

The following subfacies have been identified:

- LF 11.1.: medium, but dominantly coarse sandstones with varying amounts of pebbles with 3D trough cross bedding (Figure 14g). Locally in the Sanamah Formation, individual foresets are up to 25 cm thick and graded.
- LF 11.2 is distinguished on the presence of graded foresets, often several mm to rarely 15 mm thick, in which a basal pebble layer successively grades into fine to medium sand (Figure 14h). The 3D troughs represent channels, a few tens of meters wide at most and up to a few meters swarms of channels. Vertically, stacks of no more than 3 or 4 channel sets were found.

These sandstones represent high energy deposits of a (glacio-) fluvial environment, in which channels were frequently fluctuating and transported large amounts of sediment. LF 11.2 was deposited more episodically, probably as a response to thawing-freezing (seasonal) events. The channel systems with their grain size distribution are typical of braided rivers, which originate beneath the glacier and which transport the subglacially eroded material to the plains in front of the glacier or ice shield.

LF 12: Sandstone, massive

The following subfacies have been identified:

- LF 12.1 is massive sandstone with pebbles, cobbles or boulders. Floating blocks with sizes up to several meters have been observed, which consist of the same material as the matrix they are associated with. The sandstones were deposited in irregular channel-like features with an erosional base. Some of the erosive bases form vertical walls pointing to unusual environmental conditions. Locally, faint slab-like, strongly concave internal cross bedding is visible. Individual packages of these yellowish to brownish unstructured sediments are up to 30 m thick (Figure 16b).
- LF 12.2 is yellow to beige and grey medium to coarse massive sandstone with a varying amount of pebbles or cobbles. These sandstones and conglomeratic sandstones were deposited in medium to thick horizons without apparent bedding (Figure 16d). Only locally, a weak large-scale cross-stratification can be observed. In general, the clasts are mainly randomly distributed but locally they are concentrated in patches. Some of the sandstones have an erosional base, other were deposited in channels some 10 m wide. Locally, slumping disrupted the beds and generated floating intraclasts.
- LF 12.3 is structureless fine to medium sandstone only observed in the Sanamah Formation. It is mainly red but also yellow to beige, and in contrast to the other sandstones of LF 12, at least moderately sorted.
- LF 12.4 is a rather frequent deposit in the upper part of the Dibsiyah Formation. It consists of coarse, locally pebbly sandstones, in which any original depositional feature has been entirely obliterated by the burrowing activity of *Skolithos sp.* and related animals (Figure 16a).

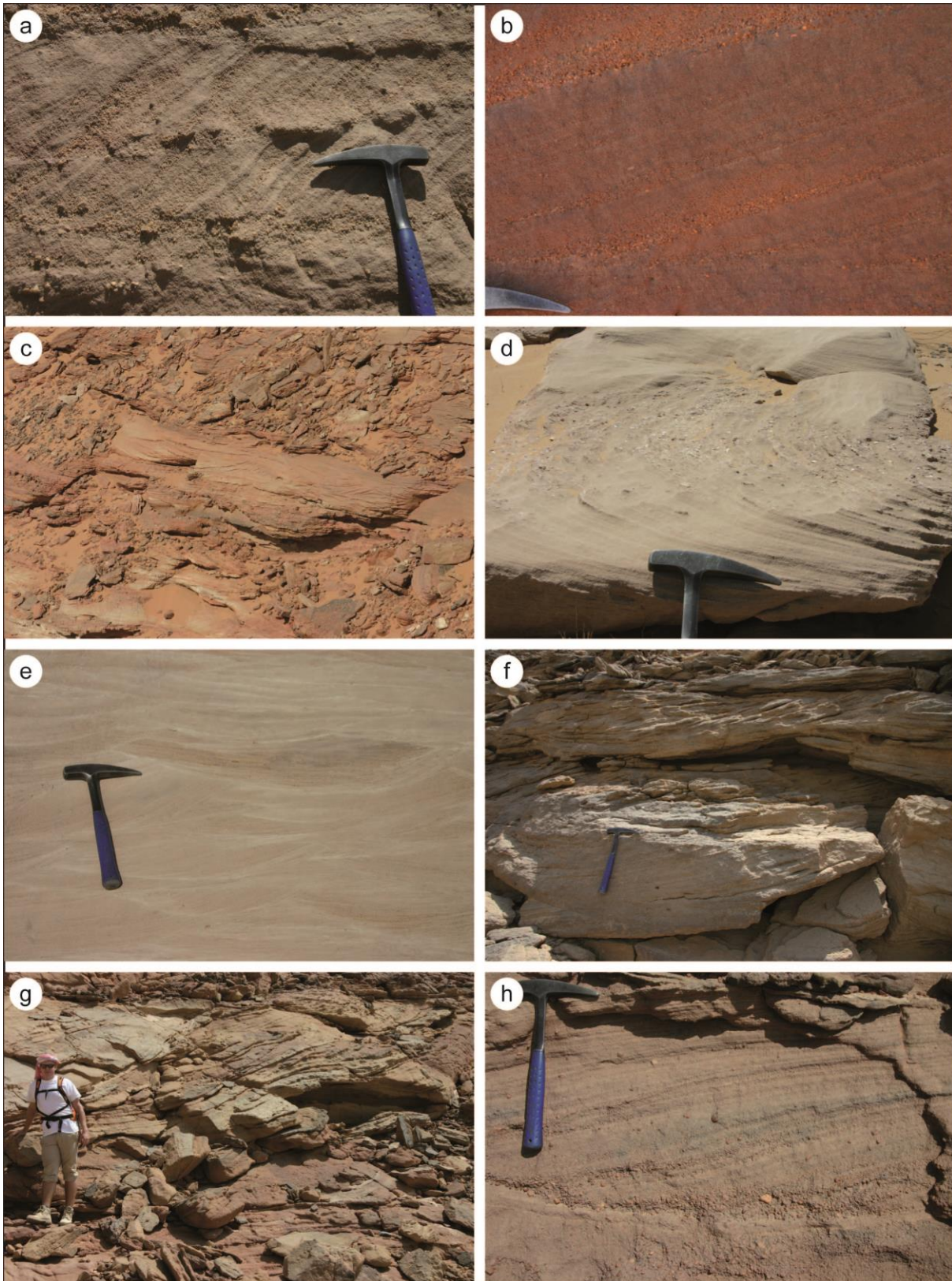


Figure 16: Steeply dipping, slightly curved, graded foresets of a package of micro-scale bedforms of 2D dunes (LF-8.1.2), Dibsiyah Formation, Jabal Dibsiyah b meso-scale angular cross beds. Each of the cross beds is graded from fine pebble to coarse sand (LF-8.3.1), Dibsiyah Formation, Jabal Nafla c 2D cross bed is a cross section through 3D dune (LF-9.2), Dibsiyah Formation, Jabal Nafla d Set of 2D cross beds in white sandstones. Each of the individual sets has a basal layer of slitstone intraclasts, Section , Juwayl Formation e Micro-scale stack of 2D cross beds in the core of the sand sheet complex of the Dibsiyah Formation, Jabal Nafla f Meso-scale to macro-scale 2D trough cross beds in the Khusayyayn Formation (LF-10.1) g 3D through cross bedded conglomeratic sandstones (LF-11.1) of glacio-fluvial origin, Sanamah Formation, Jabal Sanamah g Channel fill sandstone, in which almost all foresets are graded from fine pebbles to coarse or medium sand (LF-11.2).

The massive rocks of LF 12.1 interfinger with the 3D trough cross-bedded sandstones of LF 11. Apparently, they developed from large-scale synsedimentary liquefaction of LF 11. Hyperconcentrated flows transported large blocks of coarse sandstone and caused oversteepened and vertical channel walls, and diffuse lobe structures. The massive facies results from temporal liquefaction during short pulses of deglaciation (thawing) or even temperature rise in summer. As the transport processes were highly viscous and honey-like and as it results from temporary thawing, this unique facies association has been termed “Sorbet” facies by Keller et al. (2011). LF 12.2 and LF 12.3 are present in both glacially influenced units of the Wajid Group, the Sanamah Formation and the Juwayl Formation. Sediment was provided in large quantities and transported under high energy conditions. The absence of internal textures points to deposition from hyperconcentrated flows. In modern glacial environments, these facies are typical of sandur flats in front of ice sheets or glaciers (Maizels 1997, Russell et al. 2006).

The better sorting and rounding in LF 12.3, which is present in the Sanamah Formation only, may indicate greater distances to the (subglacial) source area or, more likely, recycling of older sediments.

LF 12.4 is actually an end member of the weakly to strongly bioturbated coarse sandstones of LF 9 and LF 10 in the Dibsiyah Formation and has a Bioturbation Index of 6 (Taylor & Goldring 1993); hence, the original bedforms most probably were 2D and 3D dunes.

LF 13: Conglomerate

The following subfacies have been identified:

- LF 13.1 contains abundant pebbles and cobbles; sorting is poor. The mainly reddish “matrix” is composed of medium to coarse sand (Figure 16c). The conglomerate is mainly monomictic to oligomictic with rounded to well-rounded clasts of vein-quartz origin.
 - In LF 13.1.1, the pebbles are of low sphericity and have a rather long a-axis. In the Sanamah Formation, big slabs of grey silty sandstones were apparently eroded from the underlying Dibsiyah Formation. The thickness of the individual conglomerate horizons varies between 20 cm and 3 m (Figure 16e).
 - LF 13.1.2 is fine to medium quartz pebble conglomerate with subordinate coarse sand. The grains are rounded to well-rounded clasts of high sphericity. In addition, siltstone clasts and shale intraclasts have been observed. Individual layers are up to 20 cm thick but stacks of these sediments may accumulate to 200 cm thickness. Sedimentary structures include angular foresets in planar cross beds and rare sigmoidal foresets.
- LF 13.2 is matrix-supported conglomerates. Many of the clasts of LF 13.2 show glacial striations, the distinct shape of glacially transported clasts, and shatter marks.
 - LF 13.2.1: Monomictic matrix-supported conglomerates are dominant in the Sanamah Formation. They are poorly sorted and have a sandy to silty matrix, in which subangular to rounded clasts of vein-quartz origin are found. Some of these clasts show shatter marks and striations. In addition, slabs of the clast-supported conglomerates (LF 13.1) are present in some horizons.
 - LF 13.2.2 is represented by polymictic matrix-supported conglomerates with a sandy to silty matrix (Figure 16h); they are found both in the Sanamah Formation and the Juwayl Formation. These sediments form mostly poorly sorted structureless horizons with beds up to 6 m thick, in which pebbles and boulders are irregularly distributed within the matrix. Sometimes however, they are concentrated in nests and pavements. In the Sanamah Formation, the clast spectrum of LF 13.2.2 is relatively restricted with vein quartz, feldspar clasts, pebbles and boulders from the underlying strata including the Dibsiyah Formation, and very few basement clasts. In the Juwayl Formation, magmatic, metamorphic and sedimentary rocks are represented in the clast spectrum.
 - LF 13.2.3 is only observed in the Juwayl Formation consisting of polymictic conglomerates with a shaly matrix. They are in general present as well bedded horizons, in which the clasts are irregularly distributed and often show impact structures (Figure 16g).

5.3. Facies associations and depositional environments

Standing alone, several of the lithofacies described above are non-diagnostic for a specific depositional environment. However, when grouped into lithofacies associations, these associations characterize well-defined depositional environments. Nine lithofacies associations have been recognized in the sediments of the Wajid Group (LF-A1 through LF-A9). Figure 17 shows the new lithostratigraphic master log for the Wajid Group with these facies associations and their presence within the different formations. Some of the associations (LF-A4 through LF-A6 and LF-A9) have recently been documented by Keller et al. (2011). Table 1 lists the lithofacies associations and the constituting lithofacies (LF) in addition to the attribution to the formations of the Wajid Group.

LF-A1: Conglomeratic 3D dunes association (Dibsiyah Formation)

This lithofacies association is composed of quartz pebble conglomerates (LF 13.1.2) and a variety of (pebbly) sandstones deposited with 2D trough cross beds of LF 10.1, 10.2, and 10.3 (Figure 18a). In addition, siltstone layers (LF 3.2., 3.3) are present in often laterally discontinuous beds (Figure 18c), because they have been eroded by the currents responsible for the formation of the 2D trough cross beds. Consequently, the former presence of fine-grained material locally is not documented in the sedimentary succession itself, but by their fragments in coarser sediments, into which they were incorporated through erosion and redeposition. The contacts between the beds are often sharp and show reactivation surfaces. Bed amalgamation is common. Beds and bedsets are of macro and meso scale, only locally micro-scale beds have been observed. Bioturbation is present throughout this association (Figure 15), mainly represented by *Skolithos sp.* and *Monocraterion sp.*; other unidentified tubes are common (Figure 12). *Cruziana* and other trilobite tracks have also been found.

Interpretation

LF-A1 records high energy, marine conditions dominated by the presence of 3D dunes. 3D dunes with their relatively simple internal structure as described above are the result of strong unidirectional flows (Ashley 1990). On shelves or epicontinental platforms, storms, geostrophic currents, or strong tidal currents are the main transport agents. No evidence of storm deposition has been encountered in the Dibsiyah Formation, so that either geostrophic or strong asymmetrical tidal currents were responsible for sediment transport. Strong uni-directional flow is corroborated by steeply inclined foresets with angles > 25° (Harms et al. 1982; Fleming 1982). Bidirectional currents regularly produce slipfaces smaller than 20°. 2D dunes and 3D dunes are relatively stable phenomena when compared to small-scale bedforms (ripples). They may be quasi-stationary for months or years (Allen 1980; Allen and Collinson 1979; Bokuniewicz et al. 1977); hence in the interdune areas, which are protected from the currents, low-energy depositional pools are present, in which fine-grained material (mud or silt) can be deposited. Scouring in front of the large-scale bedforms during lateral migration then leads to erosion of the interdune sediment and its incorporation into the dunes as intraclasts.

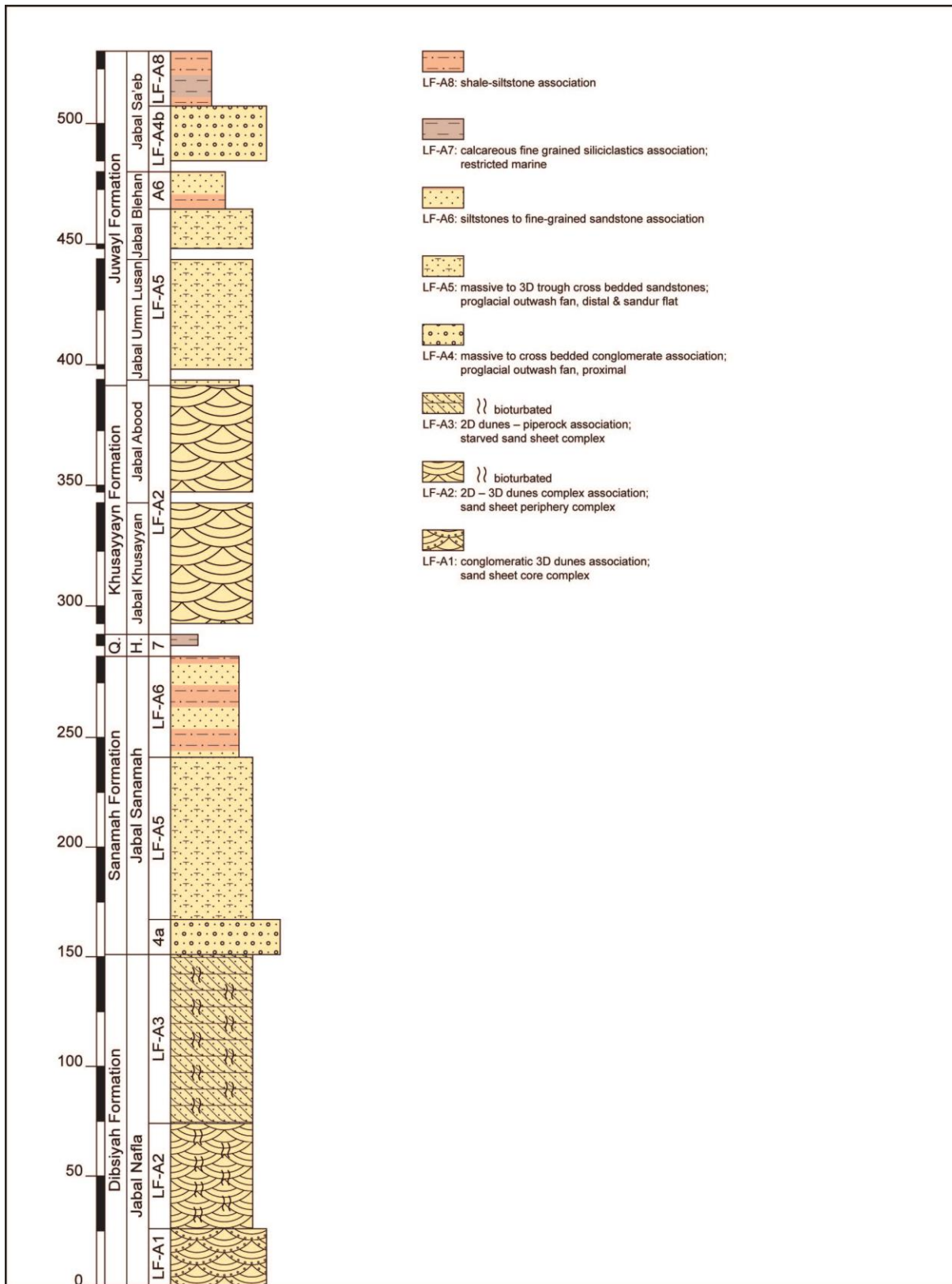


Figure 17: Composite lithostratigraphic masterlog and succession of lithofacies associations for the Wajid Group, mainly based on outcrops in the northern study area. Break in the column marks shift to another section (section name in second column) or interval not observed in the outcrops. The approximate paleogeographic position of each section is given in Figure 22. Section localities are those of Figure 1. H = Hima; Q = Qalibah Formation

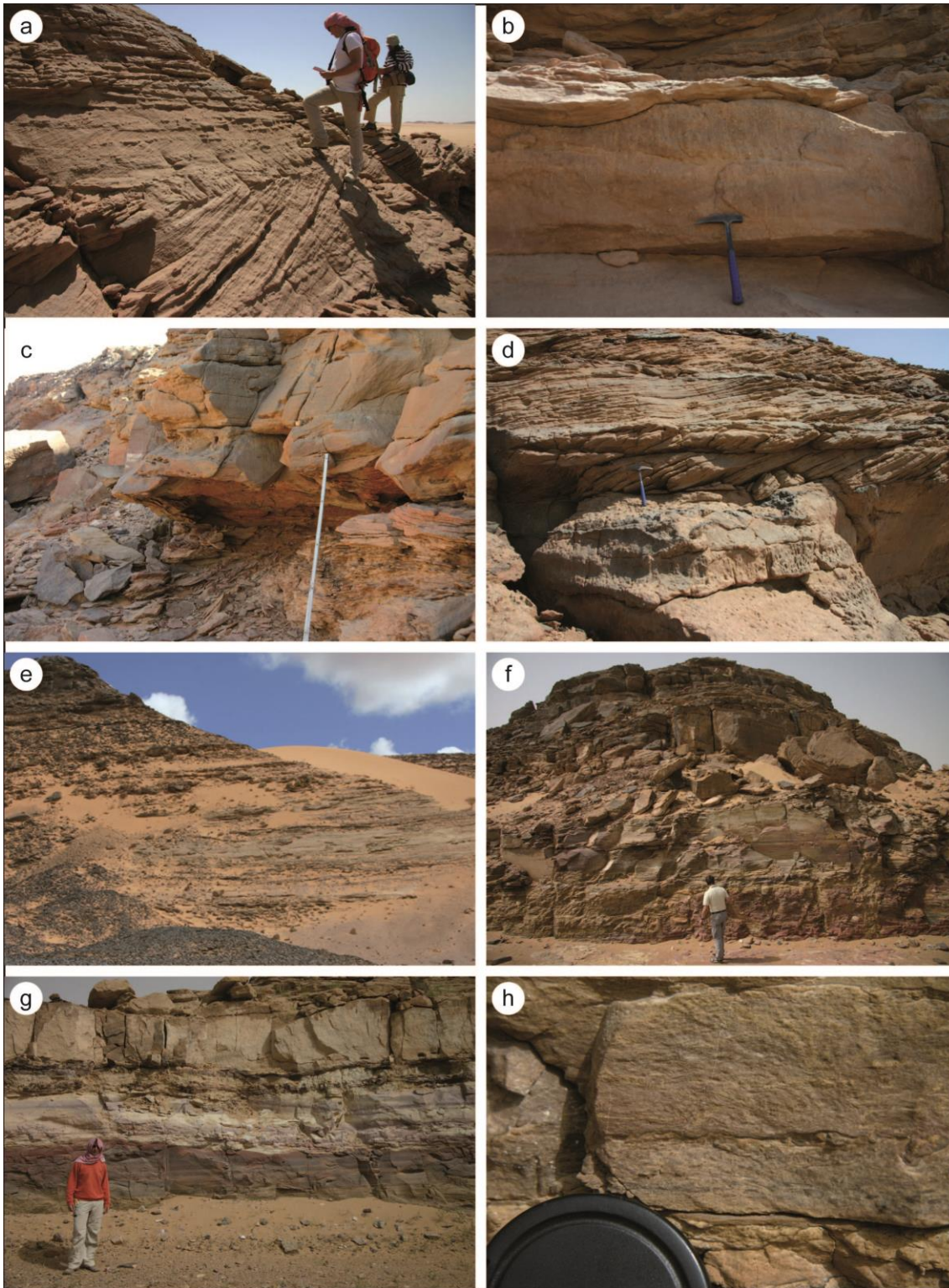


Figure 18: Sedimentary successions of the Wajid Group a Alternation (LF-A2) of sandstones with tangential basal contact (LF-8.1.2) and purely tabular sandstones (LF-8.2), Dibsiyah Formation, Jabal Nafla b Piperock, Bioturbation Index 4 to 5, sharply overlain by 2D trough cross-bedded sandstones, Dibsiyah Formation, Jabal Nafla c Remnant of red siltstones (LF-3.2) within tabular sandstones of LF-8.1.2. Migration of 2D dunes over interdune areas led to erosion of the siltstones d Set of tabular sandstones (LF-8) erosionally cover piperock with a Bioturbation Index of 5 to 6. e Sedimentary succession of the upper Sanamah Formation (LF-A6) with micro-scale to medium-scale sandstones and siltstones. Massive beds on top of outcrop are unconformable Khusayyayn Formation, Jibal Al Qahr f Outcrop of Qalibah Formation (LF-A7) with alternation of fine-grained siliciclastic rocks, roadcut south of Hima g Qalibah Formation with variegated fine-grained siliciclastics overlain by white calcareous sandstone. Massive tabular cross beds are base of unconformable Khusayyayn Formation. Roadcut south of Hima. h Detail of g, calcareous sandstone with a few undetermined shells.

LF-A2: 2D – 3D dunes complex association (Dibsiyah Formation, Khusayyayn Formation)

Although a rather monotonous succession, it is the most spectacular and most easily recognized association in the outcrop belt of the Wajid Group because of the giant and thick foresets of the tabular cross beds so typical of the Khusayyayn Formation (Figure 19b, c). Individual foresets of several centimetre thickness and 200 cm height have been observed. The association comprises basically sediments that are arranged in tabular cross beds (LF 8). In addition, sediments with 2D trough cross bedding (LF 9, LF 10) are present and a few horizons with parallel bedding (LF 7) have been observed. The bounding surfaces are always sharp and in many cases show signs of erosion and reactivation. Locally, beds are arranged to show typical patterns of herringbone cross stratification. Sedimentary structures (Figure 14b, c) include slumping, ball-and-pillow structures, and large scale overturned folds (Figure 14a). The presence of ball-and-pillow structures is remarkable, given the coarse sandy nature of the sediment. Apparently, subtle changes in the texture between underlying and overlying bed were sufficient to permit these processes to take place. In the Dibsiyah Formation, the amount of vertical burrows in the beds varies considerably; in the Khusayyayn Formation only a few *Skolithos* burrows have been observed.

Interpretation

Similar to LF-A1, this association records deposition under high-energy, marine conditions. The sediments are the product of strong uni-directional currents responsible for the formation of 2D dunes and 3D dunes. However, the co-occurrence of 2D dunes (tabular sandstone bodies) and 3D dunes (trough cross bedded sandstones) indicates fluctuations in the transport energy in the environment (Ashley 1990) and an overall decrease when compared to LF-A1. This is corroborated by the drastic decrease in conglomeratic layers and pebbles in the sediment. Previous authors (Dabbagh & Rogers 1983; Stump & Van der Eem 1995) attributed the Khusayyayn Formation to a fluvial environment. Although except for the few *Skolithos* burrows no unequivocal marine indicators are present, it is likely that all the bedforms of the Khusayyayn Formation are of marine origin. Individual beds are traceable over hundred meters in the outcrop and so are bedsets. Giant dunes near Hima are traceable over several hundreds of meters, and the few lithofacies types described from the formation are observed in all outcrops from Najran to the north of the study area. No 3D through cross bedded sandstones or conglomerates are present that would indicate stacking of braided river channels. In addition, no other lithology or architectural element of a braided river (or a meandering river) system has been identified. Hence, a high-energy, shallow-marine depositional environment similar to that of the Dibsiyah Formation is most likely for the Khusayyayn Formation.

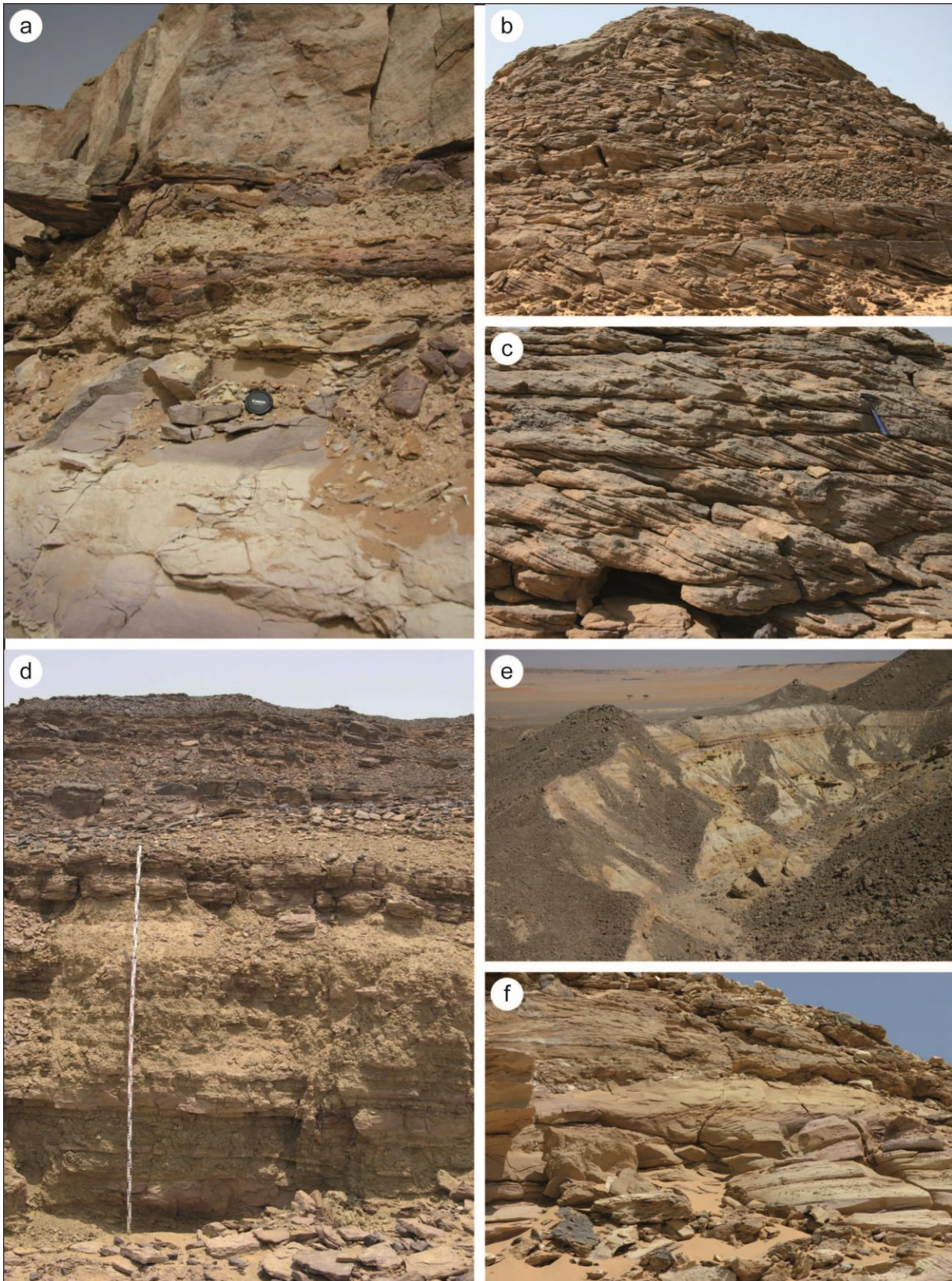


Figure 19: Sedimentary successions of the Wajid Group a Qalibah Formation with thick-bedded sandstones and unconformable Khusayyayn Formation, Hima b Typical outcrop of Khusayyayn Formation with macro-scale to giant bedforms and rocks of LF-A2. Section approximately 15 m high, Jabal Khusayyayn c Very uniformly dipping meso-scale tabular cross beds of the Dibsiyah Formation (LF-A2). Beds are part of outer sand sheet complex, Jabal Dibsiyah d Light-coloured sandstones and siltstones with conglomerate layer (LF-A6) in the Juwayl Formation, Bani Ruhayyah e The glacial lake succession at Bani Khatmah. Section is approximately 40 m thick and consists of fine-grained siliciclastics and matrix-supported conglomerates (LF-A9).

LF-A3: 2D dunes – piperock association (Dibsiyah Formation)

The most characteristic feature of this association are horizons, locally 7 m thick, that are entirely burrowed by *Skolithos* sp. and related organisms (Figure 20a). No primary structure is found in these massive rocks. Some of these very thick horizons show undulating surfaces and given the fact that these horizons weather out as positive forms, some of them appear as “reef-like” mound structures. Internally, tubes of up to 100 cm length (!) have been observed. These totally burrowed horizons are known as “Tigillites”. They alternate regularly with thick beds of tabular cross bedded sandstones (Figure 15f, Figure 12a). The lower and upper contacts of the horizons are always sharp.

Interpretation

In general, the physical conditions of sediment transport and the depositional environment are similar to LF-A2. In contrast to LF-A2, however, there is no more quartz-pebble conglomerate in the succession and pebbles are almost absent from the sediment. In comparison to LF-A2, this association is the product of a more episodic sediment accumulation. Almost all dunes show reactivation or erosional surfaces. Whereas in many of the well preserved layers, the Bioturbation Index is 0 or locally 1 to 2, the massive piperock has an index of 7. Together with the length of the tubes (100 cm), this indicates that the *Skolithos* animals had sufficient time for colonization and that they were able to retreat to their homes during accommodation events (Desjardins et al. 2010). This probably also indicates that the individual burrows are not one-time burrowing structures but a succession of superimposed burrows.

LF-A4: Glacio-fluvial conglomerate association (Sanamah Formation, Juwayl Formation)

In both formations, conglomeratic associations are present, which originated from glacio-fluvial processes. The association in the Sanamah Formation is dominated by conglomerates and coarse sandstones. No silt or clay is present at all. In contrast, in the Juwayl Formation fine and medium sandstones and locally some siltstones are present. Hence this association is subdivided into LF-A4a: Massive to coarse glacio-fluvial conglomerate association (Sanamah Formation) and LF-A4b: diverse glacio-fluvial conglomerate association (Juwayl Formation). LF-A4a is dominated by conglomerates deposited in bedded or massive units. The association is composed of LF 11.1, LF 12.2, LF 13.1, and LF 13.2.1. Sediments of LF 13.2.2 (polymictic matrix-supported conglomerate) are present but rare. Within this facies association, almost all contacts between beds are erosional (Figure 16g). The depth of the scours and channels varies from centimetres to several tens of meters. The largest erosional phenomena are the basal depositional surfaces across which this facies association was distributed. They are palaeovalleys several hundred meters wide and several tens of meters deep. In LF-A4b, massive and conglomeratic rocks of LF 10, LF 11.1, LF 12.4, and LF 13.2.2 alternate with finer grained siliciclastic deposits of LF 7.1 and LF 8.2. In addition, massive siltstones (LF 3.1) are locally present. Massive sandstone laterally passes into 3D through cross bedded sandstones and the base of the coarse units is mostly erosional. Channels are several meters wide and a rarely more than one meter deep.

Interpretation

In the Sanamah Formation, based on the presence of clasts of undoubted glacial origin and the succession of facies this association was interpreted to be a proglacial outwash fan in front of the glacier with its sediment provided by strong subglacial melt water streams (Keller et al. 2011; facies S1). These streams deposited their load within the channels that had previously been carved.

A similar scenario can be developed for the Juwayl Formation. There, however, the presence of finer grained sandstones and some siltstones indicate that the melt water streams were not as strongly laterally confined as in the Sanamah Formation. Instead, between individual glacier outlets, sandur flats, braided river remnants, and probably small lakes were present that added to the more diverse lithologies preserved. These differences between Ordovician and Permian deposits may simply be due to different ice dynamics and the distance to the glacier front with the Permian deposits recording a more ice distal setting.

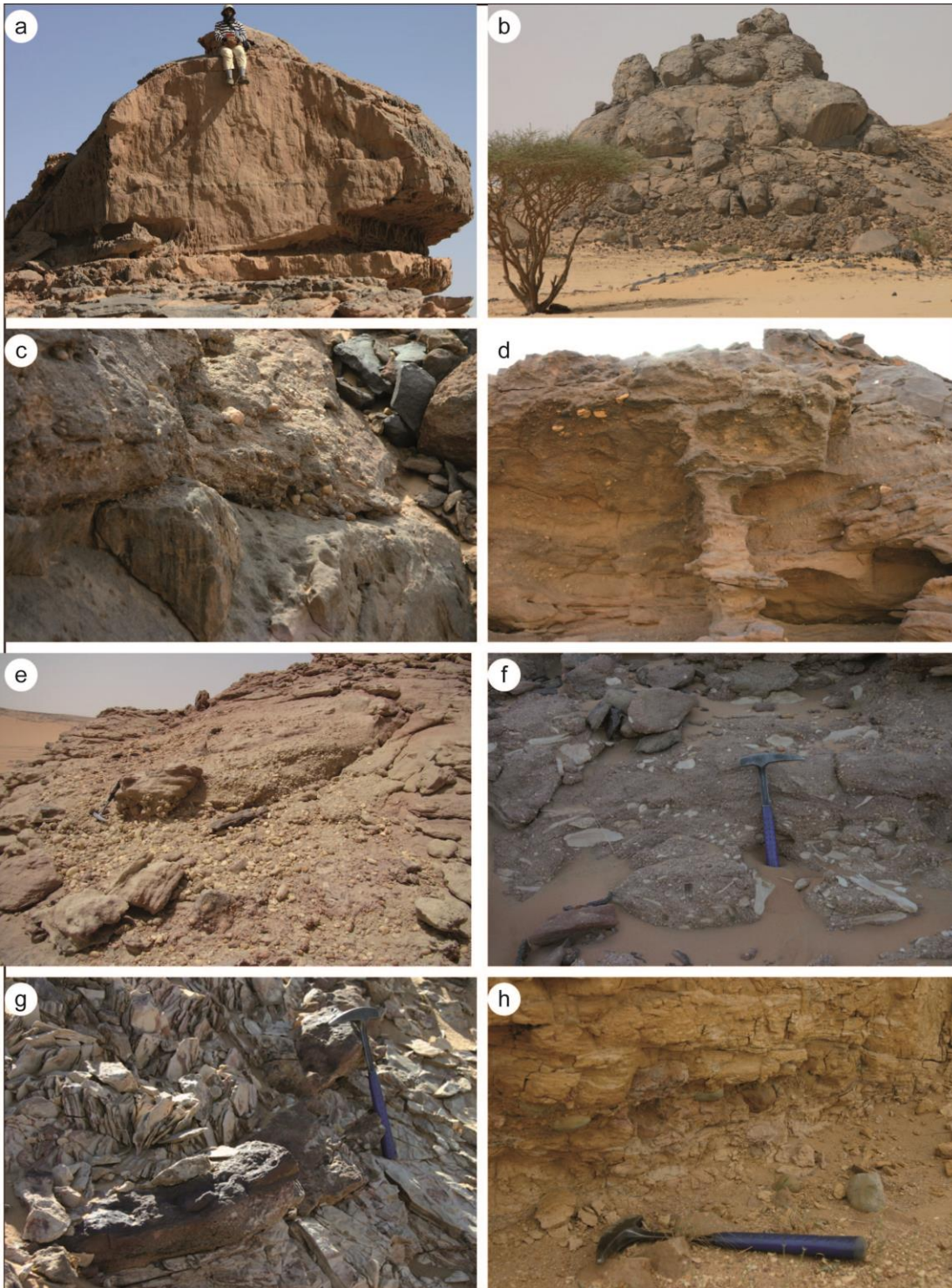


Figure 20: Massive sandstones and conglomerates of the Wajid Group a Massive “Tigillites” or piperock of the Dibsiyah Formation (LF-12.4). The entire primary structure is destroyed by bioturbation, individual pipes are more than one meter long, Jabal Nafla b Massive sandstone of the Juwayl Formation (“Sorbet Facies”, LF-12.1). The outcrop is approximately 25 m high, Jabal Overheat c Basal conglomerate of the Sanamah Formation overlying Dibsiyah piperock. The conglomerate (LF-13.1) is poorly sorted and mainly consists of quartz pebbles d Massive to 3D cross bedded conglomerates, poorly sorted (LF-12.1 to LF-11). The quartz pebbles show glacial striations and shatter marks, Sanamah Formation, Jabal Dibsiyah e Almost pure quartz pebble conglomerate with clasts of low sphericity and long a-axis (LF-13.1.1), Sanamah Formation, Jabal Sanamah f Sanamah conglomerate (LF-13-1) with large siltstone slabs eroded from the underlying Dibsiyah Formation, Section g Matrix-supported conglomerate with large basement boulder (LF-13.2.2) interpreted as dropstone. The varves and the dropstone have been deformed by a later glacier advance, Jabal , Juwayl Formation h Matrix-supported conglomerate of siltstone and shale with abundant pebbles of basement origin (LF-13.2.3). The pebbles are interpreted as rainout from icebergs, the fine-grained sediments are glacial-lake sediments, Juwayl Formation, Bani Khatmah.

LF-A5: Massive to 3D cross-bedded sandstone association (Sanamah Formation, Juwayl Formation)

This facies association is composed of massive sandstones of LF 12 together with pebbly, 3D trough cross bedded sandstones of LF 11.1. In the Juwayl Formation, these facies interfinger with well bedded sandstones and siltstones (LF 4). These sediment packages are organized in irregular channel-like features cutting deeply into the underlying rocks. Locally, faint slab-like, strongly concave internal cross bedding is visible. The most prominent feature of this association is its arrangement in large clinofolds up to 50 m high, which can be traced over several hundreds of meters (see Keller et al. 2011).

Interpretation

Sediment was provided in large quantities and transported by high-energy subglacial melt waters (Keller et al. 2011, facies S2). The absence in many beds of internal bedding features points to hyperconcentrated mass-flow deposition. These facies are typical of sandur flats in proglacial settings downstream of proximal fluvial conglomerates of LF-A5 (Maizels 1997; Russell et al. 2006). As the sediments in the Juwayl Formation are in general slightly finer, they represent a more distal glacio-fluvial setting than those of the Sanamah Formation. Large-scale deformation structures observed in these sediments are typical of glacial shearing of not yet fully lithified sediment (Figure 14g, h; Figure 20g). Locally in the Sanamah Formation, this facies association is organized in large scale clinofolds, several meters thick and hundreds of meters wide. They are typical of Gilbert-type deltas that may have developed within the water-filled channels or in ice-dammed lakes in front of the glaciers.

LF-A6: Siltstones to fine-grained sandstone association (Sanamah Formation, Juwayl Formation)

This association is rapidly alternating succession of shales (LF 1), shale-siltstone alternations, (LF 2) siltstones (LF 3.1, LF 3.2), siltstones to fine sandstones (LF 4) and occasionally some sandstones of LF 5 (Figure 18e). The rocks are arranged in centimetre to a few decimetre thick depositional units. Characteristically, many of the siltstones and sandstones show truncated folds, dome-like and large-scale ball-and-pillow structures. The successions are brown to grey and individual stacks may be several meters to few tens of meters thick.

Interpretation

Deposition occurred partly from falling out of suspension but dominantly through bedload transport. Some massive siltstones and sandstones were deposited from mass flows. In this facies association, the entire suite of lithologies originated in an ice distal setting (Keller et al. 2011). The increase in fine-grained material towards the top of the succession indicates increasing distance to the retreating glaciers. Sediments of this facies association record rapid sediment accumulation with dewatering giving rise to slumping, ball-and-pillow structures and associated phenomena.

LF-A7: Calcareous fine-grained siliciclastics association (Qalibah Formation)

In the southern outcrop area, several outcrops have been visited, in which a thin succession of fine-grained calcareous siliciclastic sediments is present (Figure 18g, h). As this succession is rarely more than 6 m thick and as the individual beds are rarely present in beds more than a few centimetres thick, the sediments themselves have not been described as separate lithofacies units. The succession consists of reddish calcareous siltstones with shell fragments (braquiopods?) and locally intensive bioturbation (Figure 18h), of green shales, and calcareous white sandstones. Intercalated are white crinkly calcareous layers which resemble microbial mats.

Interpretation

The facies association records a restricted marine environment, probably slightly hypersaline, as indicated by a monospecific fauna, microbial mats, and some structures that can be attributed to haloturbation, e.g. the disturbance of sediment by the growth of salt crystals. As the Qusaiba Member is stratigraphically related to the Lower Silurian post-glacial flooding successions of northern Arabia and northern Africa, these sediments described here most probably reflect the early marine onlap of fine-grained sediment onto the exposed glacial topography of southern Arabia. Basinward, these restricted marine sediments grade into still finer grained and organic-rich deposits as known from the subsurface.

LF-A8: Shale-siltstone association (Juwayl Formation)

This association is composed of thick packages of relatively pure clay shales in alternation with massive (LF 3.1) and laminated (LF 3.2) siltstones. Micro-scale bedforms dominate (Figure 19e, f). Locally, white fine-grained sandstones with low-angle tabular cross beds are present (LF 8.1.1) in micro-scale to meso-scale units.

Interpretation

The sediments record basically low-energy conditions. Whereas the shales were deposited in stagnant water, the siltstones record both mass flow deposition (LF 3.1) and current activity in the lower flow regime. The massive siltstones likely are distal turbidites. The white sandstones are difficult to interpret. Evans et al. (1991) and Melvin & Sprague (2006) interpreted similar deposits in central Saudi Arabia as aeolian deposits; they may similarly reflect shallow-marine deposits, in which tidal activity accounts for the sorting and rounding of the sediment. This facies association represents a succession deposited during a relative rise in water level. This could have been a rise in the level of the glacial lake that existed in much of southern Arabia, or it was sea-level rise during advanced deglaciation. No unequivocal evidence is present to support either possibility. Vestiges of glacial processes are no longer visible in this succession, which terminates the Wajid Sandstone Group in the Bani Ruhayyah section, and which is erosionally overlain by the Khuff carbonate rocks.

LF-A9: Diamictic siltstone and shale association (Juwayl Formation)

Fine-grained sediments (LF 1, LF 2, and LF 3.1) are the fundamental building block of this association. In addition, and most important for the environmental interpretation, is the presence of LF 13.2.3 (polymictic conglomerates in a clay or silt matrix). This succession is tens of meters thick and characterized by beige and yellow, partly reddish colours (Figure 19d, e). The entire succession shows large-scale soft-sediment deformation structures (folding, thrusting, dragging, water escape; Figure 14g, h).

Interpretation

The presence of LF 2, representing varve deposits, together with the polymictic conglomerates of LF 13.2.3, indicate that this facies association was deposited in a vast glacial lake, existing during the Late Palaeozoic Gondwana glaciation. This conclusion was drawn by Pollastro (2003), Osterloff et al. (2004) and Bussert & Schrank (2007) for adjacent areas of southern Saudi Arabia and Oman into Ethiopia and recently also confirmed for the Wajid Group by Keller et al. (2011). In this context, the fine grained material was provided by subglacial melt waters draining into the lake, where fractionation created buoyant plumes of suspended sediment. Settling out of suspension is then reflected in the mm thick laminae of light and dark particles usually attributed to seasonal variations of supply in sediment and organic matter. Boulder pavements or pebble carpets and outsized boulders record the presence of icebergs. Drift of icebergs across the lake is reflected in deformation structures caused by impact of the keels onto the lake bottom.

5.4. Sediment logs and depositional models

Figures 6 to 16 show logged sections, outcrop photographs and 2D architectural models from the field work of this thesis. In the following, these results are presented and interpreted in the frame of depositional models, geodynamic evolution of the Arabian Plate, and sea-level fluctuation.

5.4.1. Dibsiyah Formation

The depositional model for the Dibsiyah Formation is based on the assumption that during the Cambrian, an epicontinental sea bordered the Arabian Shield (Figure 2). In many places of northern Arabia and adjacent Africa, the Precambrian – Cambrian unconformity is marked by deeply weathered crystalline rocks with a prominent palaeosoil on top of it (Avigad et al. 2005). This soil marks the top of a vast peneplain developed immediately after the fading away of the Pan-African orogeny. Above this soil, arkosic sandstones of fluvial origin are rapidly transgressed by shallow marine sands (Avigad et al. 2005; Kolodner et al. 2006). These sands were delivered by a braided river system draining the Arabian-Nubian

Shield consistently in a northward direction. In southern Saudi Arabia, fully marine strata of the lower Dibsiyah Formation are separated from the basement by a thin zone of weathering and arkosic conglomeratic sandstones. No fluvial deposits have been encountered (GTZ/DCo 2009). This zone is here regarded as a transgressive lag deposits at the base of the Cambrian-Ordovician marine succession. Hence, nearshore deposits and their transition into hypothetical braid planes at the lower end of the braided river system should have been located farther south and west.

The coarse material delivered through the braided river – braid plane system makes up much of the lowermost part of the Dibsiyah succession (LF-A1; Figure 21). The sedimentary structures with 3D dunes and abundant conglomeratic layers testify to very high energy conditions. The Cambrian and Early Ordovician are a time of overall sea-level rise (Ross & Ross 1988, 1995; Miller et al. 2005). With the gradual sea-level rise and the concomitant migration of the shoreline, the sediments were deposited in slightly deeper and less energetic environments as manifested in the transition to increasing 2D dune structures and the reduction in conglomeratic layers and pebbles (LF-A2). This overall trend continues into LF-A3, the upper part of the Dibsiyah Formation. This unit is regarded as an almost starved succession with episodic sediment accumulation and redistribution and a prospering fauna that took advantage of these conditions.

The three lithofacies associations of the Dibsiyah Formation together (Figure 17, Figure 21) represent parts a vast sand sheet complex (Stride et al 1982). Nearest to the shore, large compound dunes form the core of the complex; in the Dibsiyah Formation this core is represented by LF-A1 and LF-A2. Farther offshore, smaller dunes follow, in the Dibsiyah Formation LF-A2 and LF A3. The zone of small ripples with increasing fine-grained material still farther offshore is not preserved in the Wajid Group. The evolution from a supply-dominated regime in the lower Dibsiyah Formation towards an accommodation-dominated regime in its upper part is roughly reflected in the ichnofabrics. Many of the overall observations in the Dibsiyah Formation have been recently described in detail from the Lower Cambrian Gog Group in the southern Rocky Mountains by Desjardins et al. (2010). Their model and interpretations will be followed here.

In the lower part of the Dibsiyah Formation, relatively short and narrow burrows (< 10 mm and 5 mm, respectively), widely spaced are present in the foresets and the upper surfaces of 2D and 3D dunes. The Bioturbation Index varies between 1 and 2. Desjardins et al. (2010) interpreted this *Ichnofabrics 1* to represent short-lived colonization events between sedimentation events. *Ichnofabrics 2* is characterized by the co-occurrence of abundant *Skolithos* and *Diplocraterion* in beds with a Bioturbation Index of 3 to 4. *Diplocraterion* is very scarce in the Dibsiyah Formation; however, the overall characteristics of this ichnofacies are observed. It occurs in micro- to meso-scale bedforms in different lithofacies. Successions of colonization, erosion, and re-colonization are evident in the sediments and probably indicate a decrease in sediment supply and concomitantly an augmentation of the colonization windows.

Ichnofabrics 3 is characterized by the co-occurrence of *Skolithos* and *Planolites*, a frequent association in the Dibsiyah sandstones in micro- and meso-scale deposits. The burrows of *Skolithos* are more robust than in the other ichnofacies (200 mm long and 20 mm wide) and have similar dimensions as *Planolites*. The burrowers are present in moderately to intensively bioturbated horizons (index 3 to 5). The coexistence of deep-tier suspension feeders (*Skolithos*) and shallow-tier sediment feeders (*Planolites*) indicates alternating episodes of current dominated times and slack-water times. The latter were used by *Planolites* to spread across the sands without being immediately buried beneath an overriding dune. In the Dibsiyah Formation, several points have been observed, where well-preserved *Planolites* inhabit the upper part of a sandstone bed, which in turn is overlain by siltstone (Figure 15b, c). *Ichnofabrics 4* is a monospecific occurrence of *Skolithos* in beds with a Bioturbation Index of 6 and 7. These horizons, often structureless through homogenization by the burrowing activities, are up to 7 m thick and laterally continuous for more than 1 km. The burrows are rarely wider than 20 mm, but their length may exceed 100 cm (!). They cross cut internal surfaces. As described above, the mound-like surface of some of these horizons corresponds to surfaces of macro-scale dunes. Desjardins et al. (2010) concluded that such deposits with their ichnofabrics indicate inactive sediment surfaces during colonization and the capability of the organisms to retreat deep into the sediment in times of strong currents.

The evolution and succession of ichnofabrics in the Dibsiyah Formation is yet another indicator of a marine environment that developed from nearshore supply dominated to a farther offshore, accommodation dominated setting. Hence, the ichnofabrics evolution closely follows the sedimentary evolution.

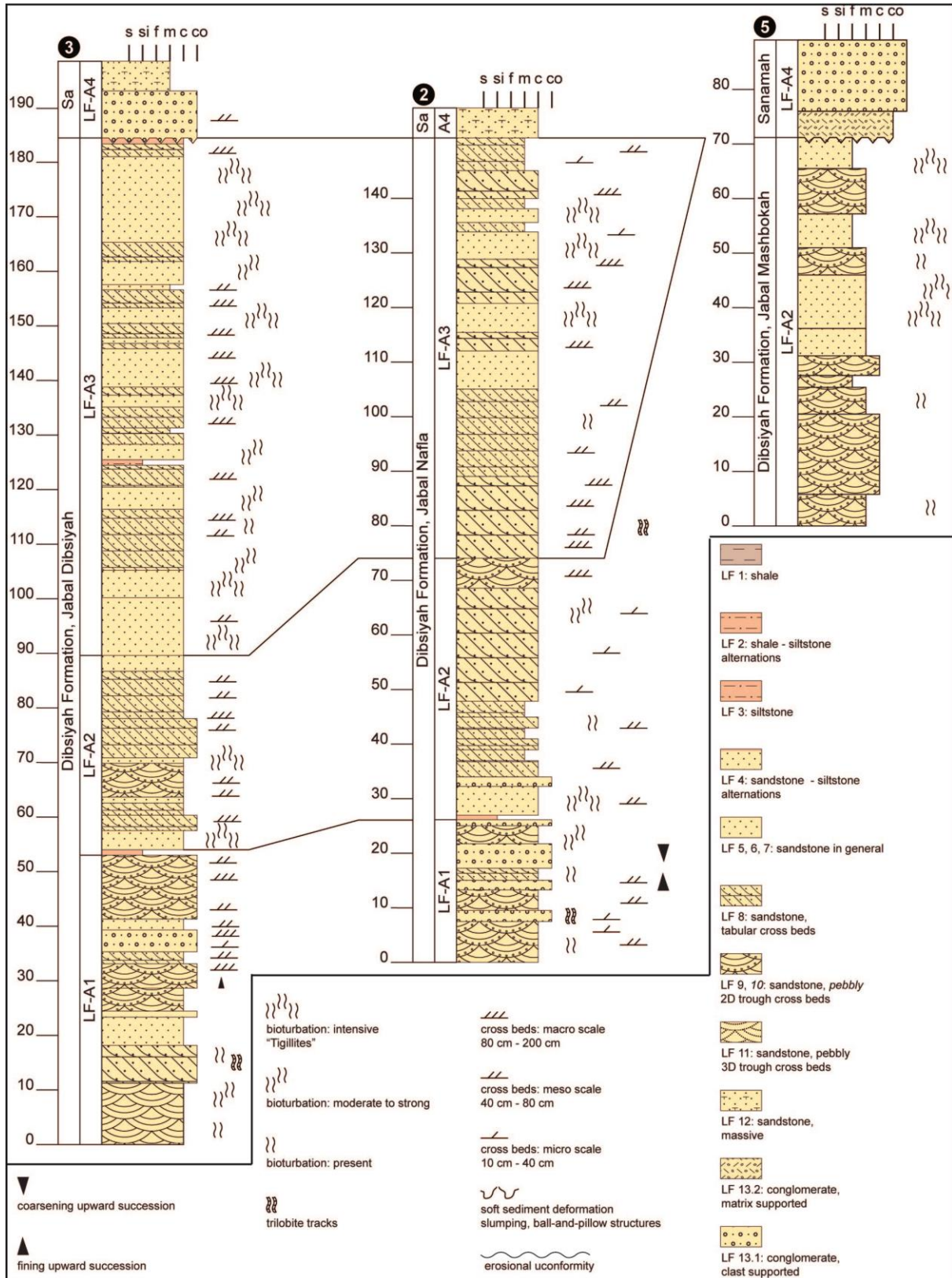


Figure 21: Lithostratigraphic logs of the Dibsiyah Formation and the basal overlying strata of the Sanamah Formation. Scale in meters. Section localities are those of Figure 1. Note the overall fining-upward from LF-A1 to LF-A3 and the concomitant increase in bioturbation and piperock.

5.4.2. Sanamah Formation

The Sanamah Formation unconformably rests on the Dibsiyah Formation. In the Wajid outcrop area, the basal unconformity was carved during initial glacier advance during the Hirnantian glaciation. Consequently, the thickest packages are preserved in sub-glacial tunnel valleys (Figure 22a), whereas from the intervening areas there is little information on the time-equivalent sediments (Keller et al. 2011). The basal unit (LF-A4a; Figure 23) represents the proximal proglacial conglomeratic channel fill of the initial glacier advance. The entire succession of LF-A4a with its numerous erosional surfaces testifies to small-scale, probably seasonal changes of sediment supply, deposition and erosion. This is characteristic of a polythermal regime (Keller et al 2011; Chapter 6). Two subsequent glacier advances are recorded in the sediments (Keller et al 2011, Chapter 6). Above the basal package is a succession of massive sandstones (LF-A5; Figure 23), which were deposited across an erosional surface with abundant striations. The overlying sediment is typical of sandur flats in front of glaciers or ice sheets. The 3rd glacial advance was only short-lived and failed to carve a major surface. Instead, following the basal coarser grained sediments, the remainder of the succession (LF-A6; Figure 23) is characteristic of large sediment supply and accommodation big enough to accommodate the sediment. The fining up of the sediments and the increasing distance of the environment to the sediment source probably reflects the last pulses of the waning ice sheet.

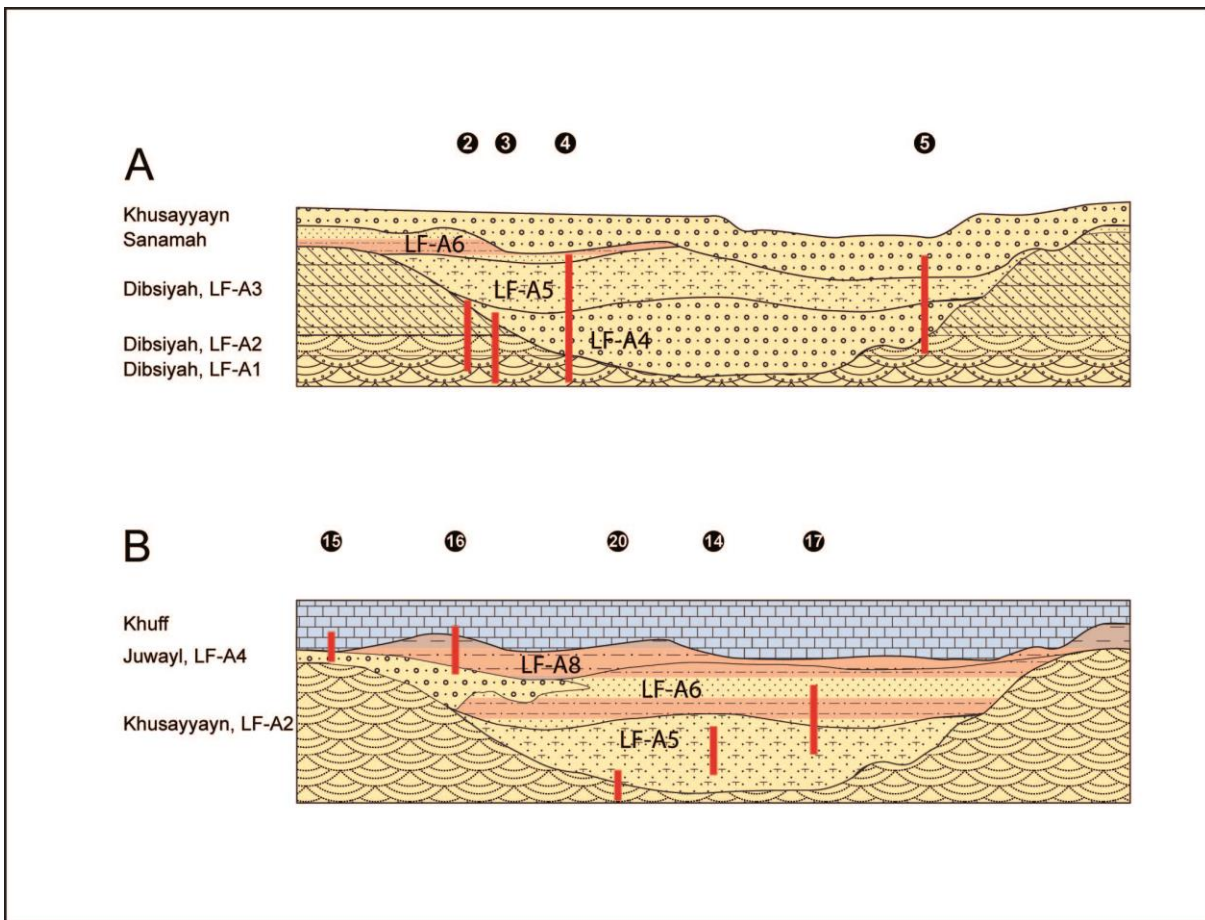


Figure 22: Spatial architecture of the Wajid Group and approximate paleogeographic position of the lithologs used for the construction of the masterlog of Figure 19. a = Dibsiyah through Khusayyayn Formations b = Khusayyayn through Khuff Formations. Legend as in Figure 21. Section localities are those of Figure 1.

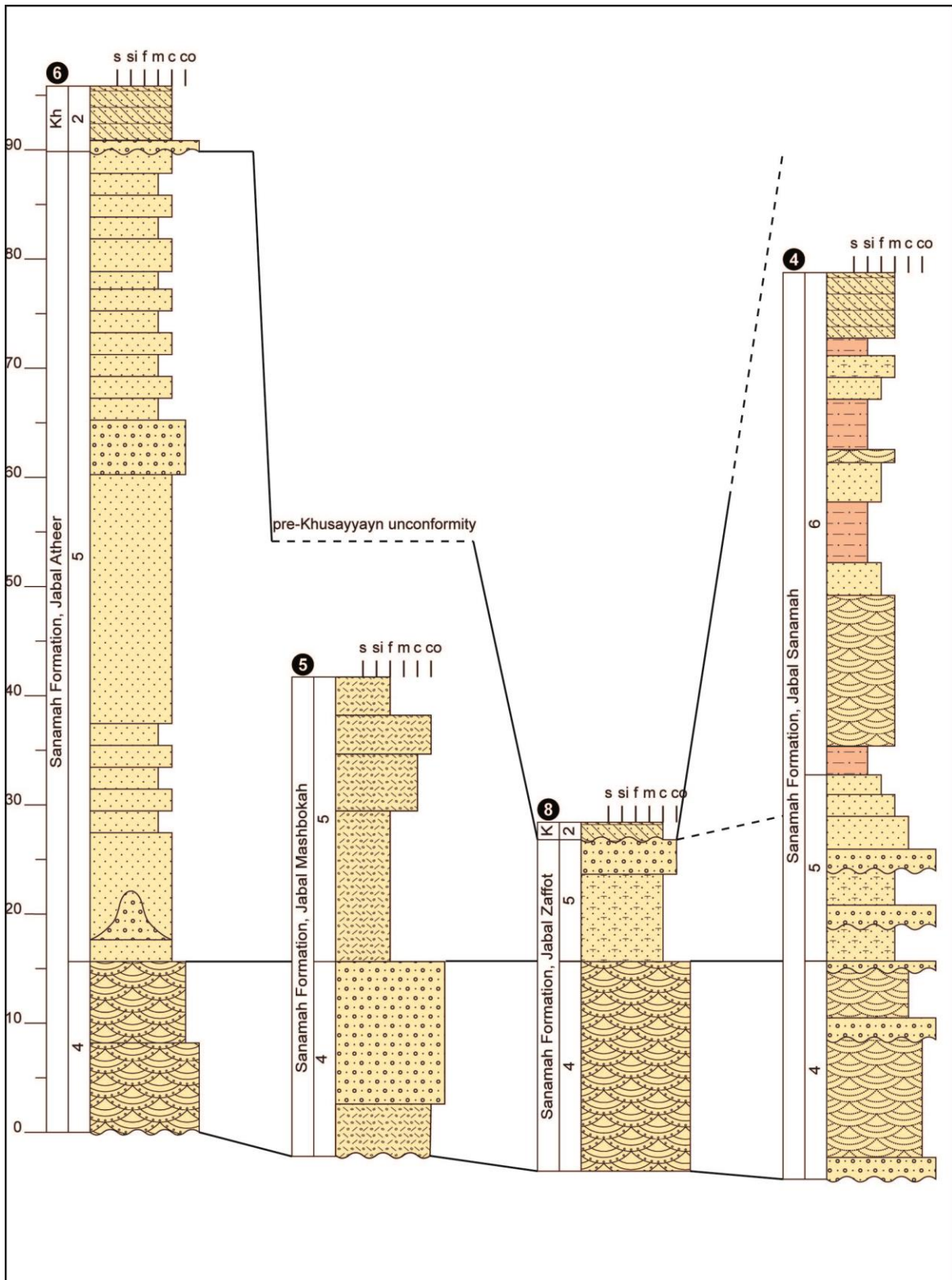


Figure 23: Lithostratigraphic logs of the Sanamah Formation. The basal correlation surface is the Dibsiyah – Sanamah unconformity, the upper correlation is hung on the pre-Khusayyayn unconformity. Section modified from Filomena (2007). Scale in meters. Legend as in Figure 21. Section localities are those of Figure 1.

5.4.3. Qalibah Formation

The outcrops present of the Qalibah Formation (Figure 18f-h) do not permit a detailed discussion of the facies architecture or palaeogeographic relationships. In general, however, if the sediments attributed to the Qusaiba Member indeed represent this unit, they should be part of the widespread transgressive deposits traceable over much of Arabia and North Africa (Lüning et al. 2000, 2005), where they are a primary source rock for hydrocarbon accumulations.

5.4.4. Khusayyayn Formation

The Khusayyayn Formation is bounded below by a major unconformity. In the northern study area, this unconformity is cut into the Sanamah Formation (Figure 22a, b). In the Jibal Al Qahr, Khusayyayn strata rest on rocks of LF-A6 of the upper Sanamah Formation; at Jabal Zaffot (Figure 22a, b), the unconformity cuts down into rocks of LF-A5. Near Hima, a thin package of the Qalibah Formation is preserved beneath the Khusayyayn (Figure 18g), but in the vicinity, the onlap of the Khusayyayn Formation onto crystalline basement can be observed. Everywhere, meso-scale or macro-scale bedforms of 2D dunes are found near the base (LF-A2). The succession above the unconformity is characterized by large-scale to giant beds and bedsets (Figure 19a). Although no continuous succession is present, the reconstruction of the approximate palaeogeographic positions of the sections measured permit a vertical reconstruction of facies shifts. At Jabal Khusayyayn (Figure 24), a package of macro-scale and giant bedforms successively passes into meso-scale and a few micro-scale bedforms. Overlying is a succession with well-developed herringbone cross stratification in meso-scale beds. This succession within LF-A2 records a relative fall of sea-level from subtidal into intertidal environments, where the loss of accommodation leads to thinner beds and bedforms and where opposing tidal currents of similar intensity produce the well-known herringbone structures. Sections representing a stratigraphic higher interval with the contact to the Juwayl Formation (Jabal Abood; Figure 24) record the return to deeper conditions and the development of meso-scale and macro-scale bedforms.

The Khusayyayn Formation is interpreted to have originated on an epicontinental platform under supply-dominated conditions. The tremendous amount of medium and coarse sand distributed over much of the outcrop belt, but also recorded from the subsurface (GTZ/DCo 2009), formed a vast sand sheet complex. This complex required a well-developed distribution system, probably in the form of braided rivers – braid plane systems. No traces of this system are preserved in the Khusayyayn Formation, but it must have been active to the west and south of the Wajid outcrop belt. The outcrops near Abha and Khamis Mushayit have been partly attributed to the Khusayyayn Formation by Babalola (1999) and Hussain et al. (2004), which from their lithology and sedimentology seems very reasonable. Farther east towards Najran, Dabbagh & Rogers (1983) describe similar deposits without giving them a stratigraphic assignment. These deposits of the “southern part of the Wajid Sandstone” clearly belong to the Khusayyayn Formation. All authors presented detailed cross bed measurements which uniformly indicate an overall southern provenance of the deposits. Although this cannot conclusively be proved here, there seem to be more vestiges of 3D dunes in the south than farther north supporting the model of a southern provenance of the sediments. This observation was also made by Dabbagh & Rogers (1983), although their stratigraphic assignments are not conclusive. The core of the sand sheet, dominated by 3D structures, was in the south, and the outer parts with dominance of 2D structures are present farther north.

Evans et al. (1991) proposed a fluvial to aeolian depositional environment for the Khusayyayn Formation. This is most unlikely given the very uniform distribution of mega-scale and giant cross beds, the grain size and sorting, which would be very atypical for an aeolian system, and the absence of any other kind of structure characteristic of a (braided) river system. Especially the absence of 3D trough cross beds and fluvial channel stacks is hardly compatible with a fluvial interpretation.

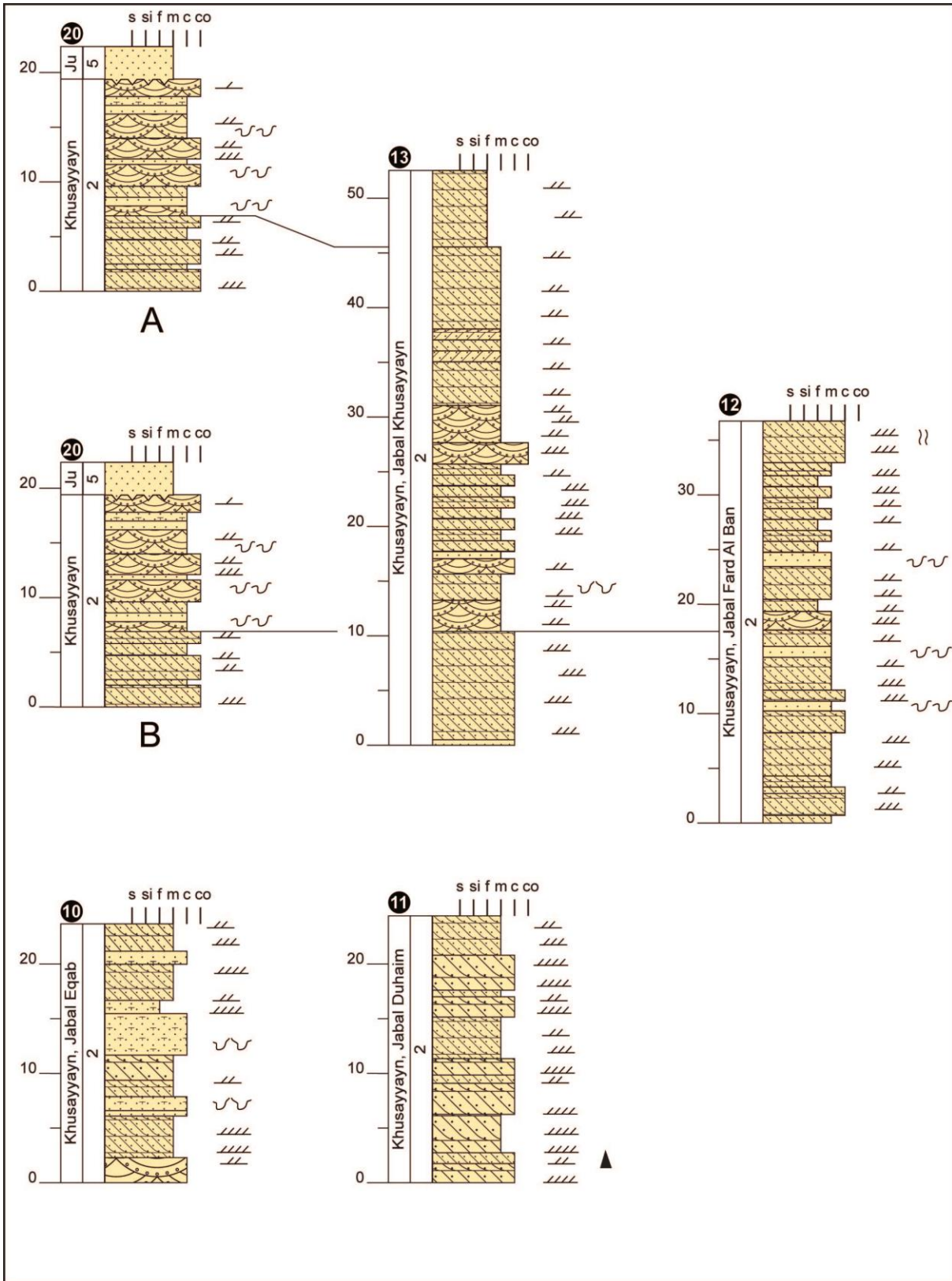


Figure 24: Lithostratigraphic correlation of the Khusayyayn Formation. "A" and "B" mark two possible correlations of the Jabal Abood section to the type sections (see discussion the text). Sections Jabal Eqab and Jabal Duham have been added to show the problems of correlations in the very uniform succession without marker beds. Scale in meters. Legend as in Figure 21. Section localities are those of Figure 1.

5.4.5. Juwayl Formation

The Juwayl Formation unconformably rests on the Khusayyayn Formation (Figure 22b). In the northern study area, the corresponding relief is that of two major glacially cut channels, whereas in the south, the geometry is not well defined due to the lack of appropriate outcrops (Figure 1).

In the northern area, the basal deposits within the channels belong to LF-A5 (massive to 3D cross bedded sandstones; Figure 22b) and mostly represent the “Sorbet” facies (Figure 20b). Locally, they form packages of more than 30 m thickness. Near the base of this unit and locally covering the flanks of the valleys, are varve deposits (LF-2) either as huge blocks in the Sorbet facies or as strongly deformed relictic beds above undeformed Khusayyayn strata. Apparently, a glacial lake was present in this area that either covered the post-Khusayyayn erosional surface or that existed in the channels. In this case, the channels must be older than the initial (varve) sediments which were later reworked by newly advancing glaciers and which dragged the varve deposits into the channels.

The sedimentary succession at Jabal Blehan (Figure 25) shows that sediments of the channel fill succession (LF-A5) up section grade into LF-A6 with siltstones and fine-grained sandstones (unit J3 of Keller et al 2011). The sedimentary evolution in this overall periglacial setting starts with deposits of a glacial lake that was driven back during glacier advance and that evolved into a vast fluvio-glacial plain on which sandstones were deposited. Maximum glacial advance probably coincides with the transition from LF-A5 to LF-A6 (Figure 22b, Figure 25). The latter represents a more ice-distal succession as a consequence of the retreat of the glacier or the ice sheet. A somewhat different succession is present at Jabal Sa'eb (Figure 25), where glacio-fluvial conglomerates are present (LF-A4b), which are overlain by shales and siltstones (LF-A8; Figure 22b). Similar to Jabal Blehan, the lower unit represents deposits of a glacier advance, whereas the overlying fine-grained siliciclastic rocks mirror a glacial retreat.

Mainly fine-grained siliciclastic sediments have been preserved in the Bani Khatmah area (Figure 13e, Figure 19c) in the vicinity of Najran. From these deposits, a glacial lake can be reconstructed and together with the observations by Pollastro (2003) and Kruck & Thiele (1983) permit the reconstruction of a vast glacial lake over much of southern Arabia. Similar deposits are known from Ethiopia (Bussert and Schrank 2007) and from other areas of adjacent Gondwana fragments (Torsvik and Cocks 2011). Whether these individual lake deposits each represent an independent depositional basin (Torsvik & Cocks 2011) or whether they were interconnected to form a single giant glacial lake (Pollastro 2003; Keller et al 2011) remains open for discussion.

If the individual outcrop areas of the Wajid Sandstone are considered, it seems that in the north depositional environments are preserved that were closer to the ice or glacier margin of the Gondwana glaciation. Sediments of LF-A4b or LF-A5 are absent in the south, where mainly distal glacio-fluvial and lake sediments are preserved. A lithologic correlation between the areas has not yet succeeded. However, the transition from glacier advance (cold phase) to glacier retreat (warm phase) postulated in the northern sections might be reflected in the southern sections near Bani Khatmah: There, the lower part of the succession shows dominantly bedded sandstones and siltstones with few dropstones and little or absent deformation. Above a marked surface with a well-developed boulder pavement, dropstones increase suddenly and this part of the succession was affected by grounding icebergs (Keller et al. 2011).

If this interpretation is correct, then the upper part of the northern sections and their southern correlatives together reflect one retreat of the Gondwana ice shield and the expansion of the glacial lake at the expense of more ice-proximal environments. Whether this episode documents the final demise of the ice shield during the Permian or not remains speculation because of the pre-Khuff unconformity, which ultimately terminates with the Wajid Sandstone sedimentation (Figure 4, Figure 25).

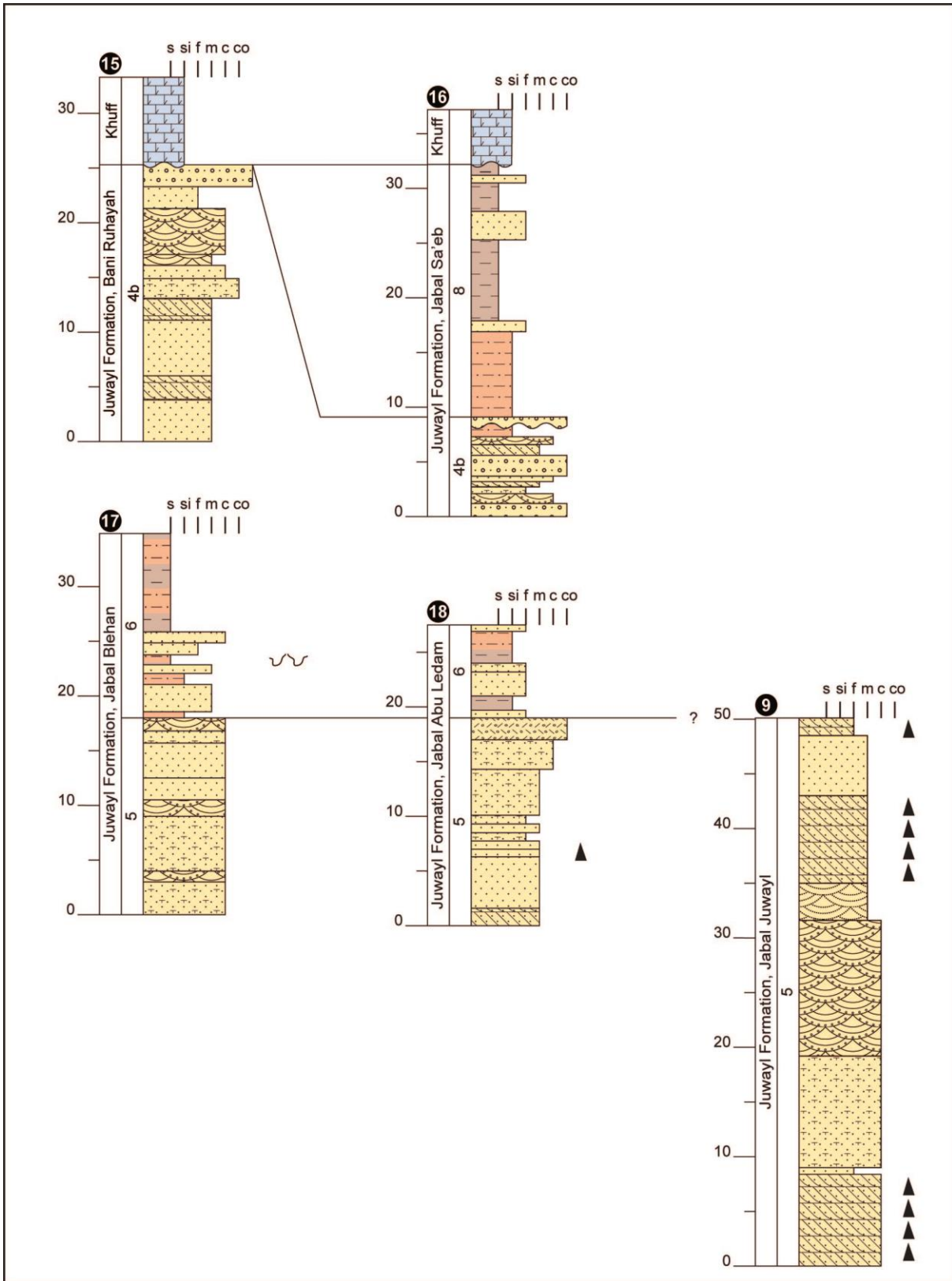


Figure 25: Lithostratigraphic logs of the Juwayl Formation. Scale in meters. Legend as in Figure 21. Section localities are those of Figure 1.

5.5. A new standard log for the Wajid Sandstone Group

As one of the outcomes of this thesis, a refined stratigraphic log (Figure 17) for the Wajid Group is presented. This log is composed of individual sections that all are described in this thesis and that are combined into one major log. As the lithostratigraphy of the Wajid Group does not follow the classical layer cake stratigraphic models (tunnel valleys in the glacial deposits, “Hercynian” tectonism), the method of combining sections from known palaeogeographic positions (Figure 22) leads to a more realistic approach to distribution and thicknesses of the individual formations and of the entire Wajid Group and to its stratigraphic architecture.

The new master log (Figure 17) starts with the sediments of the Dibsiyah Formation (Figure 21), in which 3 lithofacies associations have been recognized (LFA1 – LF-A3). The standard section for this part of the Wajid Group at Jabal Nafla (Figure 21) is approximately 150 m. The basal succession is characterized by 2D trough cross-bedded conglomeratic sandstones and sandstones (LF-A1). The presence of *Skolithos sp.* and *Cruziana* in several localities indicates that all these sediments were deposited under marine conditions. Hence, this succession has been interpreted as a high-energy, near shore marine environment with tidal channels. This part of the section varies between 25 m and 50 m thickness in the different outcrops (Figure 21). Up section (Figure 17), LF-A2 with its increasing amount of bioturbation of the *Skolithos* type indicates that the environment became even more favourable for early marine life. The decrease of conglomerates and pebbles in the succession testifies to a relative sea-level rise and increasing distances to the braided river – braid plane supply system. Thicknesses between 40 m and 50 m have been measured for this part of the succession. The third unit is an alternation of tabular cross-bedded sandstones and massive “Tigillites”. It was deposited under starved conditions in accommodation controlled regime. The overall trend to more starved conditions in an environment still farther offshore continues. This unit has a minimum thickness of 90 m as measured at Jabal Dibsiyah, but it might have been considerably more.

Above the glacially induced unconformity at the base of the Sanamah Formation, LF-A4 represents the basal sediments of the valley fills (Figure 22a, b). The reference section was chosen at Jabal Sanamah, where the most complete succession of Sanamah sediments is preserved. Massive to cross-bedded conglomerates represent outwash plain sediments deposited in front of the glaciers. Individual pulses of melt water flow are recorded as thick graded layers as observed in the Jabal Atheer section (Figure 23). This part of the section, where observed, is approximately 25 m thick (Figure 23). It is erosionally overlain by massive to cross bedded sandstones of LF-A5. Erosional features are common within this package, in which the massive units are the product of hyperconcentrated flows and the sandstones that of high-energy subglacial melt waters that transported enormous amounts of sediment. The arrangement in large-scale clinofolds points to the existence of standing water bodies, either as sediment-locked lakes in the valleys or larger scale lakes in front of the ice shield. At Jabal Atheer, 70 m of this facies association are preserved beneath the Khusayyayn unconformity (Figure 23). Yet another unconformity separates this succession from the overlying rocks of LF-A6. The siltstones and sandstones represent ice-distal environments with still high sediment input. The overall succession has a transgressive pattern to it, interpreted to reflect the waning and retreat of the Ordovician ice shield in northern Gondwana. From Jabal Sanamah, a minimum thickness of approximately 130 m has been taken for the master log (Figure 17).

The contact to the overlying Qalibah Formation is not exposed in the outcrop belt. From the subsurface (GTZ/DCo 2009; Schönrok 2011), it is known that the contact is a major transgressive surface that is represented in northern Saudi Arabia and northern Africa (Lüning et al. 2000) and that documents the post-glacial sea-level rise in this part of northern Gondwana. In the outcrop belt, only some 6 m to 10 m are preserved and shown in the master log (Figure 17). No section has been measured here, but the outcrops at Hima are chosen for the Wajid master log (LF-A7). There, the Qalibah Formation onlaps the basement and in turn is overlain unconformably by the Khusayyayn Formation with mega-scale to giant bedforms.

In the master log, most of the Khusayyayn Formation is represented by the type section, where some 55 m of a sand sheet periphery complex crop out (LF-A2; Figure 24), which is attributed to the lower part of the succession. This section is composed of dominantly macro-scale bedforms in the lower part that are overlain by meso-scale forms. In the middle of the section, tidal structures are evident in the succession. The higher part of the succession shows the return to subtidal conditions with dominantly meso-scale bedforms and an overall decrease in grain size to medium and fine sands. The transition into the Juwayl Formation is exposed at Jabal Abood (Figure 24). There, meso-scale and macro-scale bedforms with abundant slumping are exposed. In one horizon, dewatering and concomitant deformation led to overturned folds several meters “thick”. This succession is unconformably overlain by massive sandstones (“Sorbet facies”, LF 12; LF-A5) of the Juwayl Formation. In Figure 24, two possible correlations of this section to the type section at Jabal Khusayyayn are shown. If alternative “A” is correct then the entire thickness of the Wajid Group is some 20 m less than given in the master log.

At Jabal Umm Lsan (Figure 25), the type section of the “Sorbet facies”, approximately 50 m of these facies are exposed and show all details described above. Unfortunately, neither the lower nor the upper contact is exposed. A minimum thickness of 50 m has been incorporated into the master log, which continues with the strata exposed at Jabal Blehan (Figure 25), where Sorbet facies (LF-A5) pass into LF-A6 with siltstones and fine sandstones. Internal soft sediment deformation is frequently observed in this succession. According to Keller et al. (2011), this succession mirrors the first recognizable glacier advance – glacier retreat episode in the Juwayl Formation. A similar succession, although represented through LF-A4b and LF-A8 (Figure 22b), is present at Jabal Sa’eb (Figure 25) and there unconformably overlain by the carbonates of the Khuff Formation. Within the conglomerates of LF-A4b, granitic boulders and other basement components are present indicating a source area on the Arabian Shield to the west. The overlying fine-grained siliciclastic deposits (unit J3 of Keller et al. 2011) reflect the rise of the lake level and its expansion towards the north. The succession of events between the deposition of these beds and the overlying Khuff Formation remains speculative.

5.6. Palynology

The predominant number of the 20 collected samples of clayey to silty sediments contains degraded organic material that is usually poorly preserved. It can only be distinguished between opaque and translucent plant debris. Complete and well preserved palynomorphs are absent in all 20 samples. Only in five samples (Wuh-1 9, Wuh-5 varves, WKh-T 5, Ma’aleq, Fard C) fragments and bodies are preserved, which can be assigned to palynomorphs. They are possibly acritarchs, prasinophytes, spores and especially bisaccate pollen of gymnosperms (Figure 26). The latter have been found in samples, which originate from the Juwayl-Formation. Bisaccate pollen occur from the Upper Carboniferous and are later in the Mesozoic the dominant pollen in continental sediments. A more detailed and reliable stratigraphic determination is due to the lack of well-preserved palynomorphs currently not possible. Also the prasinophyte, a green alga, in sample WKh-T 5 is poorly preserved, so that no exact species can be attributed to this taxon. Prasinophytes occur throughout the entire Phanerozoic in marine sediments. The samples show at least that palynomorphs were primary preserved in the sediments. Therefore, the poor quality of palynomorphs can be explained by the fact that all samples were collected in outcrops. Consequently, these rocks were exposed to the extreme climatic conditions in Saudi Arabia. This leads to an extensive weathering and oxidation of palynomorphs, so that only plant debris like opaque and translucent phytoclasts, which have the highest preservation potential, are detectable in these outcrop samples. However, it is auspicious to carry out palynological investigations of fresh rocks from boreholes that contain material of the same age. These could provide useful stratigraphically relevant palynomorphs, because well-preserved palynomorphs of the Palaeozoic are well known for this geographical area.

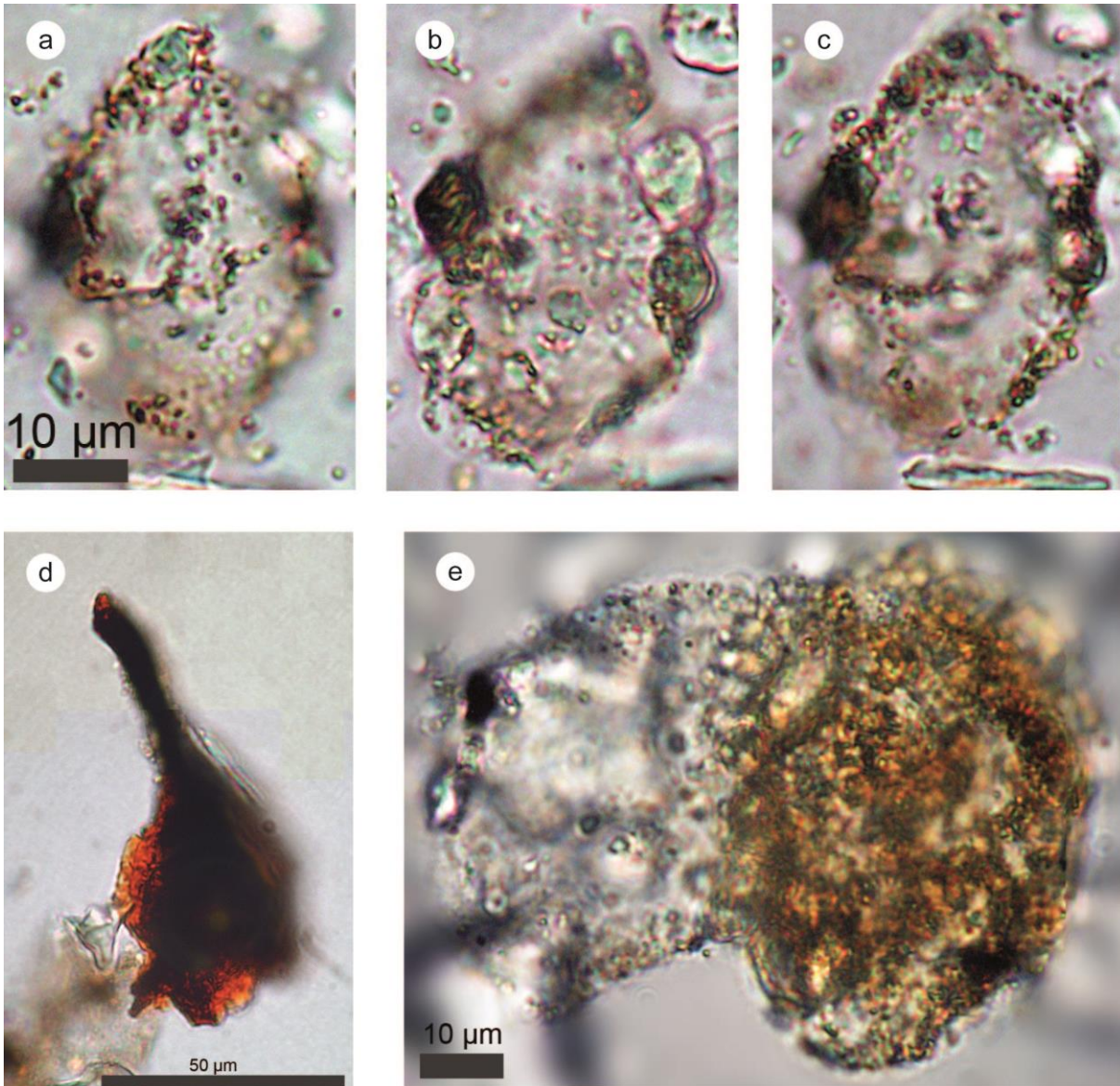


Figure 26: a, b, c: Flimsy and decomposed organic bodies, possible acritarch (sample Wuh-1 9, Juwayl Formation). d: Needle-shaped translucent phytoclast (plant debris, sample WKh-T 5, Khusayyayn Formation). e: Decomposed fragment of a bissacate gymnosperm pollen (sample Fard C, Juwayl Formation).

5.7. Discussion

5.7.1. Biostratigraphical evidences for the age of the Wajid formations

The age of the Wajid Group and its constituents are still only loosely confined and the effort of this study on palynological analysis of 20 samples from various outcrops could not improve the situation because no indicative biostratigraphic information could be derived. Hardly any biostratigraphically indicative fossil has been found also by other authors, except for some trilobite tracks, a few fish remains, and a few palynomorphs (Evans et al., 1991; McClure 1980; Besems and Schuurmann 1987). Hence, the overall stratigraphic framework is based on the lithologic comparisons with better dated successions in the northern Kingdom and the tracking of subsurface seismic surfaces into the outcrops (Evans et al., 1991).

No biostratigraphic data are available from the *Dibsiyah Formation* despite its diverse ichnofauna. On a global scale, mass occurrences of *Skolithos* piperock or “*Tigillites*” as they are known in northern Africa and Arabia (Crimes 1981) are a Cambrian and Ordovician phenomenon (Droser 1991). They are especially important around Laurentia in Cambrian strata preceding the birth of the Great American Carbonate Bank (Dejardins et al. 2011; Fedo & Cooper 2001; Droser 1991; see also Table 1 in Dejardins

et al. 2011). Tigillites are known from Cambrian and Ordovician siliciclastic shelves around Gondwana (Mángano & Buatois 2004; Mángano et al. 1996; Seilacher et al. 2002; Klitzsch 1981; Destombes et al. 1985; Gibert et al. 2011). However, nowhere they are characteristic of a certain stratigraphic interval but of environmental conditions indicating shallow-marine, nearshore siliciclastic seas with high energy conditions and hence the absence of silt and mud (Seilacher 1967; Droser & Bottjer 1989; Droser 1991). Hence, as the Dibsiyah Formation underlies sediments that are confidently correlated to the Hirnantian glaciation and as it contains *Cruziana* and other trace fossils it must be of late Early Cambrian or Ordovician, pre-Hirnantian age. At present, no more precise age attribution is possible.

The *Sanamah Formation* did not yield biostratigraphically indicative fossils. However, its lithology and sedimentology together with its inventory of glacially induced features (see Keller et al. 2011) leave little doubt that these deposits are equivalents of the Hirnantian glacial sediments of North Africa (Ghienne 2003; Ghienne & Deynoux 1998; Ghienne et al. 2003 ; Le Heron et al. 2004, 2005, 2009, 2010) and Eritrea and Ethiopia (Bussert & Schrank 2007; Kumpulainen 2009). The overlying *Khusayyayn Formation* yielded some fish remains (Evans et al. 1991), which tentatively have been assigned a lower Middle Devonian age. Evans et al. (1991) also cite Middle Devonian microfloras from a well east of Hima. In general, they assigned an Early Devonian through Mississippian age to the *Khusayyayn Formation*. The only biostratigraphically rather well dated unit is the *Juwayl Formation*, from which microflora data are available (McClure 1980; Besems and Schuurmann 1987). They constrain the depositional age of the *Juwayl Formation* to the Early Permian (Sakmarian; see also Stephenson & Filatoff 2000a, b). According to these authors, the stratigraphic gap between the *Juwayl Formation* beneath and the *Khuff Formation* above may comprise as much as the interval from the Artinskian/early Kazanian through much of the Tatarian (Figure 4).

5.7.2. Estimation of the time involved in deposition of the Wajid Group

In Figure 4, the assignments of the Wajid Sandstone to the standard international stratigraphic subdivision are shown. From the discussion above, it is evident that most of the assignments must be incorrect or need major refinements. Just two examples: How likely is it that the Dibsiyah Formation with its 180 m represents most of the Cambrian and Ordovician? How likely is it that the *Khusayyayn Formation* with its 150 m represents most of the Devonian and the Mississippian? In basin analysis, sedimentation rates provide a valuable tool for the estimation of time included in a specific succession (Ager 1973; Sadler 1981; Dott 1983; Miall 1997, 2010, in press; Einsele 2000). Sadler (1981) and Miall (in press) documented that calculated sedimentation rates are inversely correlated to the time frame for which the rate was calculated. Although the local instantaneous sedimentation rate may be extraordinarily high, with increasing time the chance increases that this package is affected by compaction, erosion, reworking etc. and that eventually the entire package is removed from the stratigraphic record. This also means that Ager's observation that "the stratigraphic record is more gap than record" becomes increasingly important if sedimentary successions of basin scale are considered.

Sedimentation rates vary over 11 orders of magnitude, from the deposition of a single lamina of quartz grains to entire packages of sedimentary basin fills (Miall 1997). If calculated at the appropriate scale, sedimentation rates indeed reflect sedimentary processes acting over the corresponding time scale. From these sedimentation-rates – time-frame relationships, Miall (in press) developed a hierarchical scheme called "Sedimentation Rate Scale (SRS)" with 11 SRS units. These units show the relations between time scale, instantaneous sedimentation rates, sedimentary processes, preservational boundary conditions, and cyclicity. The SRS are based on measured sections whose depositional time frame is well known. A shelf margin succession for example, of 25 m to 160 m thickness deposited over 25.000 years, gives sedimentation rates of 1 m/ka to 6,4 m/ka (Suter et al. 1987). By implication, if a sedimentary succession is present with a well-defined depositional framework, a plausible recurrence interval, and a known thickness, it should be legitimate to calculate the time involved in deposition of this specific succession.

The Dibsiyah Formation is a sand sheet complex much like the present day North Sea (Stride et al. 1982) or other shelf areas bordering North America (Suter et al. 1987; Suter 2006). This depositional system with its variety of submarine dunes corresponds to SRS 8 and SRS 9 of Miall (in press). Recurrence times vary between 10^4 and 10^6 years and sedimentation rates between 10^0 and 10^{-2} m/ka. If for the sake of

simplification a thickness of 200 m is assumed for the Dibsiyah Formation, the depositional time frame for the Dibsiyah Formation would be:

Sedimentation rate 10^0 m/ka \rightarrow depositional time 0.2 Ma

Sedimentation rate 10^{-1} m/ka \rightarrow depositional time 2 Ma

Sedimentation rate 10^{-2} m/ka \rightarrow depositional time 20 Ma

Examples from recent sediments have shown (Suter et al. 1987; Suter 2006) that values between 10^0 m/ka and 10^{-1} m/ka are widespread in modern environments. Hence, a depositional time between 0.2 Ma and 2 Ma for the Dibsiyah Formation is a reasonable assumption. Even if one considers that there might be an order of magnitude difference due to differences in the subsidence rates of modern shelves and the ancient epicontinental platform rooted on the Arabian-Nubian Shield, the time span during which the Dibsiyah Formation was certainly not greater than 20 Ma. Given that the occurrence of trilobites occurred some 20 Ma after the onset of the Early Cambrian, the Dibsiyah Formation could occupy any 20 Ma (or less) interval between the uppermost Early Cambrian and the Katian. It could for example represent the Cambrian Series 2 and 3 interval or similarly the late Darriwilian through Katian interval. However, as the Dibsiyah Formation is a siliciclastic deepening-upward succession of an epicontinental basin, the deepening upward and the concomitant increase in accommodation must be directly related to coastal onlap. Coastal onlap curves for the Cambrian and Ordovician (Vail et al. 1977; Ross and Ross, 1988; Miller et al. 2005, Haq & Schutter 2008) consistently show an increase of coastal onlap from the base of the Cambrian into the Early Ordovician, then a sharp decrease (regression) and a renewed increase in onlap into the Caradocian/Katian. It is speculated here that the Dibsiyah Formation might correspond to the most important onlap event around the Furongian – Tremadocian (Late Cambrian – earliest Ordovician). Hence, the Dibsiyah Formation would represent a highstand system above maximum flooding surface O10 or O20 of Sharland et al. (2001).

Similarly, the Khusayyayn Formation, which reflects a similar depositional environment as the Dibsiyah Formation, must have been deposited between 1.5 Ma and 15 Ma if the measured thickness of 150 m is taken as a basis and sedimentation rates are on the order of 10^{-1} m/ka to 10^{-2} m/ka. If the biostratigraphic data given by Evans et al. (1991) are correct and the (base of the) Khusayyayn Formation belongs to the basal Middle Devonian, the Khusayyayn Formation should comprise the Eifelian, Givetian, and parts of the Frasnian, if sedimentation rates are assumed at 10^{-2} m/ka. Hence, the Khusayyayn Formation and the Juwayl Formation should be separated by a major stratigraphic break of 50 Ma to 60 Ma. If these calculations come only near to the truth, the existing stratigraphic distribution charts for the Wajid Group have to be modified considerably. The proposal is shown in the right column of Figure 4.

5.7.3. Geotectonic setting of the Wajid Basin

Sharland et al. (2001) subdivided the Phanerozoic geotectonic history of the Arabian Plate (AP) into 11 tectono-stratigraphic megasequences (AP 1 to 11). The stratigraphic sequences are “genetic stratigraphic sequences” in the sense of Galloway (1989), in which maximum flooding surfaces or maximum coastal onlap define the upper limits of genetic stratigraphic sequences. During the Cambrian, south-western Saudi Arabia occupied a position well within the cratonic interior of Gondwana (Figure 2). Although one cannot attribute the Dibsiyah Formation definitely to a certain time interval of the Cambrian or Ordovician, one can attribute it to AP 2 of the Sharland et al. (2001) scheme. Whereas AP 1 still comprises Neoproterozoic sediments, which are genetically related to the latest stages of the Pan-African orogeny and the assembly of Gondwana, AP 2 is the first post-tectonic sequence and is of Cambrian and Ordovician age. The upper bounding surface is the glacially induced erosional unconformity at the base of the Hirnantian deposits. Hence the Dibsiyah Formation constitutes part of AP 2 of Sharland et al. (2001), whereas the glacial deposits of the Sanamah Formation form the base of AP 3 in south-western Arabia.

As the top of AP 3 is located close to the base of the Famennian, the Khusayyayn Formation also belongs to this AP 3. According to Sharland et al. (2001), AP 3 still reflects intracratonic conditions, which is also clearly shown in the Wajid Sandstone. The Sanamah Formation is a terrestrial succession, in which sediment accumulation was dominantly controlled by the depth of erosion at the base of the glaciers. As the Upper Ordovician ice shield covered much of northern Africa and Arabia and probably extended into Turkey (Monod et al. 2003), the ultimate control of accommodation lay with a base level under regional,

intracratonic control, probably a lake level, yet another indicator of an epicontinental depositional environment. As the Khusayyayn Formation is very similar in depositional environment to the Dibsiyah Formation, and as sedimentation rates are similar, and as the onlap of the Khusayyayn Formation onto the basement is observed in the study area, the epicratonic system must have persisted into the Middle Devonian. Similar to the Dibsiyah Formation, the Khusayyayn Formation must have been deposited during a time of major coastal onlap but a plate-wide correlative maximum flooding interval has not yet been identified (Sharland et al. 2001).

AP 4 (Famennian through mid-“Stephanian”), is characterized by changes in the tectonic regime along the margins of Gondwana and its rotation. This AP is attributed to the Hercynian tectonic cycle (Sharland et al. 2001). Although uplift and tectonic inversion have been interpreted to be responsible for erosion and non-deposition of Devonian and Carboniferous sediments and for the formation of some anticlinal structures, nothing of these processes is seen in southern Saudi Arabia. Although apparently no sediment of this AP is preserved in the Wajid Group, it can be concluded that the area remained in a tectonically quiet state, because there is no folding or faulting documented in the older strata; there is nowhere sediment preserved that would testify to increased or abnormal sedimentation rates; and there is no angular unconformity between the sediments of AP 3 (Khusayyayn Formation) and AP 5 (Juwayl Formation). The latter belongs to the basal part of AP 5, which comprises the deposits of the Late Palaeozoic Gondwana glaciation. Similar to the Sanamah Formation, the ultimate control on erosional depth of the glaciers and preserved sediment thickness was the regional base level of the glacial lake that covered southern Arabia at that time. Abundant basement clasts in the Juwayl sediments (Keller et al. 2011) testify to the proximity of an area, in which the glacier or the ice sheet directly eroded the Precambrian basement through stripping off the thin remaining sedimentary cover of Cambrian, Hirnantian, and Devonian sediments of the Wajid Group.

The entire scenario of marine sediment packages with abundant indications of short-term sedimentary breaks due to sediment starvation, terrestrial glacial deposits whose thickness was controlled by glacial lake base level and major stratigraphic gaps between the units of several 10s of millions of years, indicates that the Wajid Sandstone was deposited in an epicratonic setting not affected by the tectonic processes at the distant margins of Gondwana.

5.7.4. Provenance of the Wajid Sandstone Group

The source area and lithology of the Wajid Sandstone is still under debate, although recently the opinion seemed to settle for a major source area somewhere in present-day Yemen. Plots of normalized Al_2O_3 , Fe_2O_3 and $Al_2O_3/(Al_2O_3+Fe_2O_3)$ vs. Fe_2O_3/TiO_2 imply Yemen highlands as a likely source for the Lower Wajid units. They were derived from a tectonically stable, passive margin setting, as bivariate plots of K_2O/Na_2O and SiO_2 show, and deposited in a braided river system (Babalola, 1999). This is supported not only by geochemical analysis, but also by paleocurrent observations and heavy mineral assemblages. A stable cratonic setting is supported by the maturity of the sediments (> 90% quartz). A secondary, minor source area may lie somewhere on the Arabian Shield, as indicated by variations in the paleocurrent data (Babalola, 1999). This is in contrast to the younger clastic sequences in the area, which mainly originate from a western source area on the Shield.

Hussain et al. (2004) further supported this hypothesis by identifying the Neoproterozoic Afif, Abas, Al-Bayda, Al-Mahfid and Al-Mukalla terranes as well as older, recycled sediments from the infra-Cambrian as sources for the Dibsiyah and Khusayyayn Formations. The high ZTR (zircon, tourmaline, rutile) index of heavy minerals from the Wajid Sandstone and its maturity indicate intermediate/acidic igneous rocks and/or recycled sediments as source(s). A source further south than Yemen is unlikely due to the lack of Neoproterozoic rocks in Somalia, Eritrea and Ethiopia (Hussain et al., 2004). Similar conclusions are drawn by Wanas & Abdel-Maguid (2006) in their study, utilizing petrographic as well as major and trace mineral analysis. They identify metamorphic and plutonic rocks from a cratonic interior, passive margin setting as a source for the Wajid sediments. The southeastern margin of the Arabian Shield is suggested as a probable source area. Wanas & Abdel-Maguid (2006) further correlate the Wajid Sandstone with equivalents in North Africa and other parts of Arabia, indicating their deposition on a stable continental shelf formed by a low-lying landmass on the margin of the Arabian-Nubian shield.

Several shifts in heavy mineral-derived provenance signals occur within the Wajid succession, namely within the Upper Dibsiyah Formation, between the Upper Dibsiyah and Sanamah Formations and at the base of the Khusayyayn Formation. The heavy mineral assemblage from the Khusayyayn Formation mainly persists in the Juwayl Formation, although a greater variability points towards a contribution from several sources. Changes in the stratigraphic provenance signals mainly correlate with Formation boundaries, with the exception of the Dibsiyah Formation. The change in the heavy mineral suite within the Upper Dibsiyah Formation could not be linked to a discontinuity. All these shifts in provenance signals are not attributed to shifts of the source region(s), but rather to shifts in exposed source rocks in the same area(s), possibly caused by progressive denudation, changes in uplift patterns and/or drainage systems (Knox et al., 2007).

Petrography and geochemistry of samples from the sections in this thesis analysed by Heberer (2012) confirmed former results on sand provenance of the Wajid Group. According to the QFL discrimination diagram of sandstone provenance according to Dickinson et al. (1984), the sandstone samples plot in the field of cratonic interior. Generally, the Khussayyayn Formation has a higher feldspar content compared to the other formations and tends to the field of basement uplift. Major chemical components vary little among the formations. The Khusayyayn formation shows a higher K_2O content consistent with the higher proportion of feldspars. Other deviations can be assigned to diagenetic control, i.e. CaO and Fe_2O_3 . The latter is enriched in the Sanamah Formation which reflects more widespread iron cementation in this formation. Compared to the average composition of the upper Crust, SiO_2 is enriched and other components are mostly depleted. Depletion is weaker for the Dibsiyah and Sanamah Formations and higher for the Khussayyayn and Juwayl Formations which may be interpreted as increased weathering in the source regions and/or increased diagenetic overprint. Applications of various discrimination diagrams, in particular those of Roser & Korsch (1985) and Bhatia (1983), yield a passive margin setting for most samples. Some samples of the Dibsiyah Formation also plot in the field of active continental margin which may be interpreted as a result of erosion of pan-Africanic orogenic basement rocks. A passive margin setting is also confirmed by trace elements, e.g. the discrimination diagram $La-Th-Sc$ and $Th-Sc-Zr/10$ after Bhatia & Crook (1986).

6. Glacial depositional environments

6.1. Glacial deposits in the Wajid Group

The Wajid Sandstone Group bears an exceptional good record of both Paleozoic glacial episodes affecting Gondwana. Recently, the sedimentary environments of the Hirnantian glaciation have been studied in detail in northern Africa e.g. by Ghienne & Deynoux (1998), Ghienne et al. (2003), Le Heron et al. (2004, 2005). A similar modern sedimentological study of Paleozoic glacial and proglacial environments was missing for Saudi Arabia and reports on glaciogenic deposits in the Wajid Group are scarce and not well constrained so far (see chapter 3.1). The Hirnantian glaciation is represented by the Sanamah Formation and the Permocarboiferous glaciation by the Lower Juwayl Formation. Therefore, a specific aim of this study was to systematically explore the heterogeneous glacial and proglacial deposits, develop a genetic depositional model and compare the findings with other regions at the northern rim of Gondwana. Most parts of this chapter have been published in Keller et al. (2011), however, the classification of lithofacies types and facies associations in this paper refers to the Sanamah and Juwayl Formations only. In the following the lithofacies classification has been modified and adopted to the overall classification of the Wajid Sandstone Group as presented in chapter 5.2. Keller et al. (2011) subdivided both formations in three units and described them as facies associations. This subdivision is kept in the following and the corresponding facies associations according to chapter 5.3 are mentioned in addition.

6.2. Facies associations, glaciogenic processes and depositional model

Several of the lithofacies described above *per se* are non-diagnostic for a certain environment. However, when grouped into lithofacies associations, these associations characterize well-defined depositional environments. In the Sanamah Formation, three units (S1 - S3; Figure 27a, b) have been identified, and three also in the Juwayl Formation (J1 - J3; Figure 27c, d). Concomitantly, in the Sanamah Formation, these units also represent facies associations and depositional sequences, separated by major surfaces. Figure 27 shows cross sections and longitudinal sections through the channels in SW Saudi Arabia for both glacial episodes. Figure 30 shows glaciological scenarios to explain the observed sedimentary facies, depositional architecture, and glacial phenomena for both the Sanamah and Juwayl Formations. Figure 34 shows schematic depositional models for all six facies associations inspired by LeHeron et al. (2010).

Massive to cross-bedded conglomerate facies association (Unit S1)

This unit corresponds to facies association LF-A4 and consists of clast-supported conglomerates (LF 13.1), matrix-supported conglomerates (LF 13.2), and coarse, conglomeratic sandstones (LF 10). It is interpreted as a subaqueous outwash fan, its sediments deposited by sediment-laden, high-energy subglacial meltwater jets. Strong turbulence in the flowing water together with discontinuous sediment supply is responsible for repeated erosional events and the frequent changes between water-lain sediments and gravitationally-induced mass transport by hyperconcentrated flows. No silt or clay is present in the sediments, pointing to a complete fractionation of the sediment load into underflow and overflow in the water column, where fine particles become buoyant and are transported further down current (Le Heron *et al.* 2004). High-pressure meltwater flow also prevented any deposition of pure till deposits. Only few pockets of weakly-sorted, clast-supported conglomerates are preserved locally on the channel floor.

This facies association is typical of outburst floods or jökulhlaups and has been described from modern environments in detail by Maizels (1991, 1993, 1997). Deposition from hyperpycnical flows is responsible for the generation of lobes composed of graded beds such as observed at Jabel Atheer as the basal channel fill. This unit characterizes the lower part of the channel fill (Figure 28). Meltwater flows and hyperconcentrated flows modified the original glacial topography and created an erosional topography superimposed onto the pre-existing morphology. The lobes gently dip down valley towards the southeast. Geometries and thicknesses of the ice-proximal outwash fans indicate ample accommodation of several 10s of metres and probably up to 80 m must be assumed.

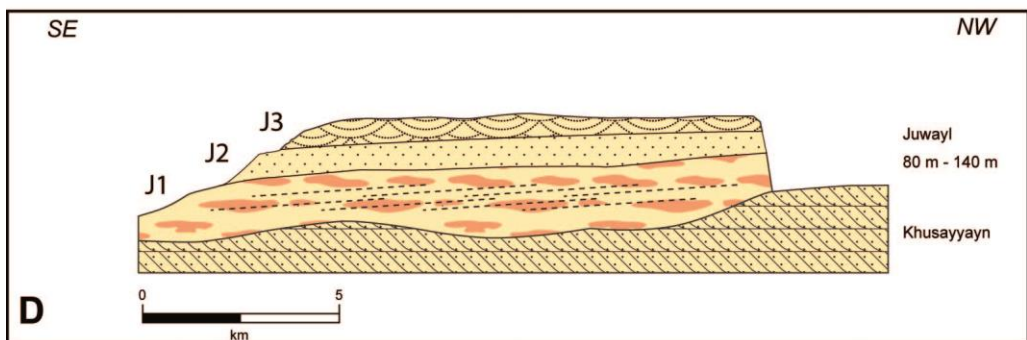
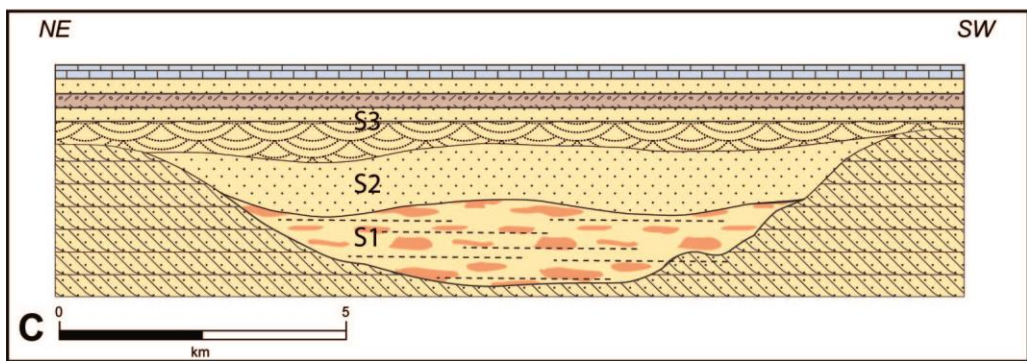
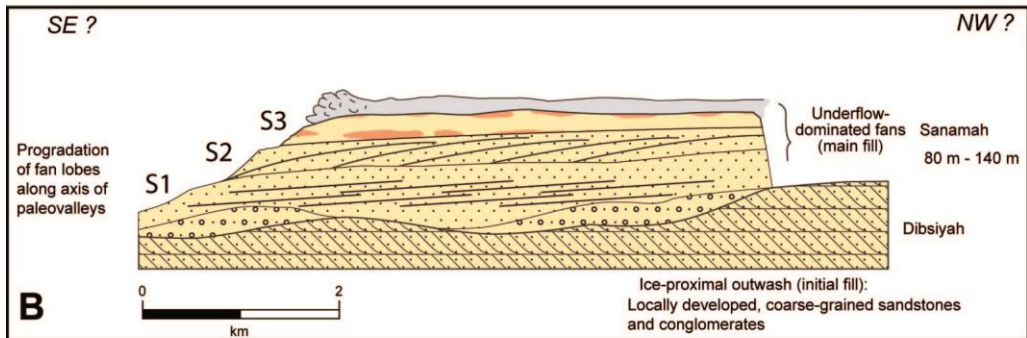
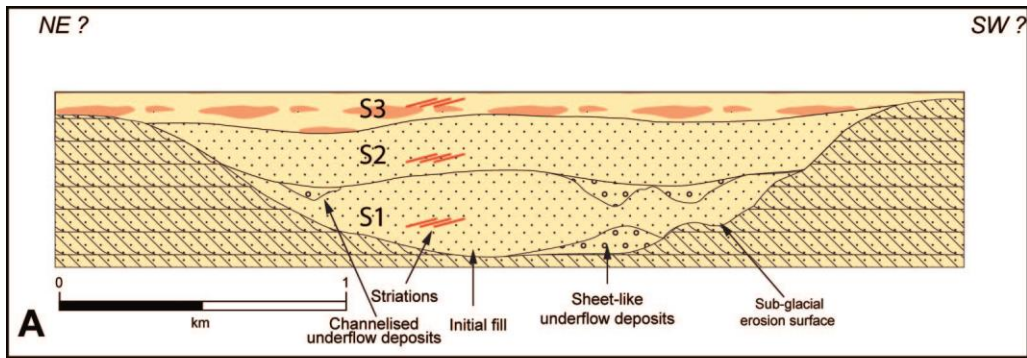


Figure 27: Schematic model of the sedimentary architecture of the fill of tunnel valleys and onlapping glacial to postglacial successions for the Late Ordovician (a, b) and the Permo-Carboniferous (c, d) glaciations in SW Saudi Arabia (Wajid Sandstone). S1-S3 and J1-J3 correspond to the units described in the text. a and c are cross sections through the valleys, b and d are sections parallel to the axis of the valleys (modified from Le Heron *et al.* 2004).

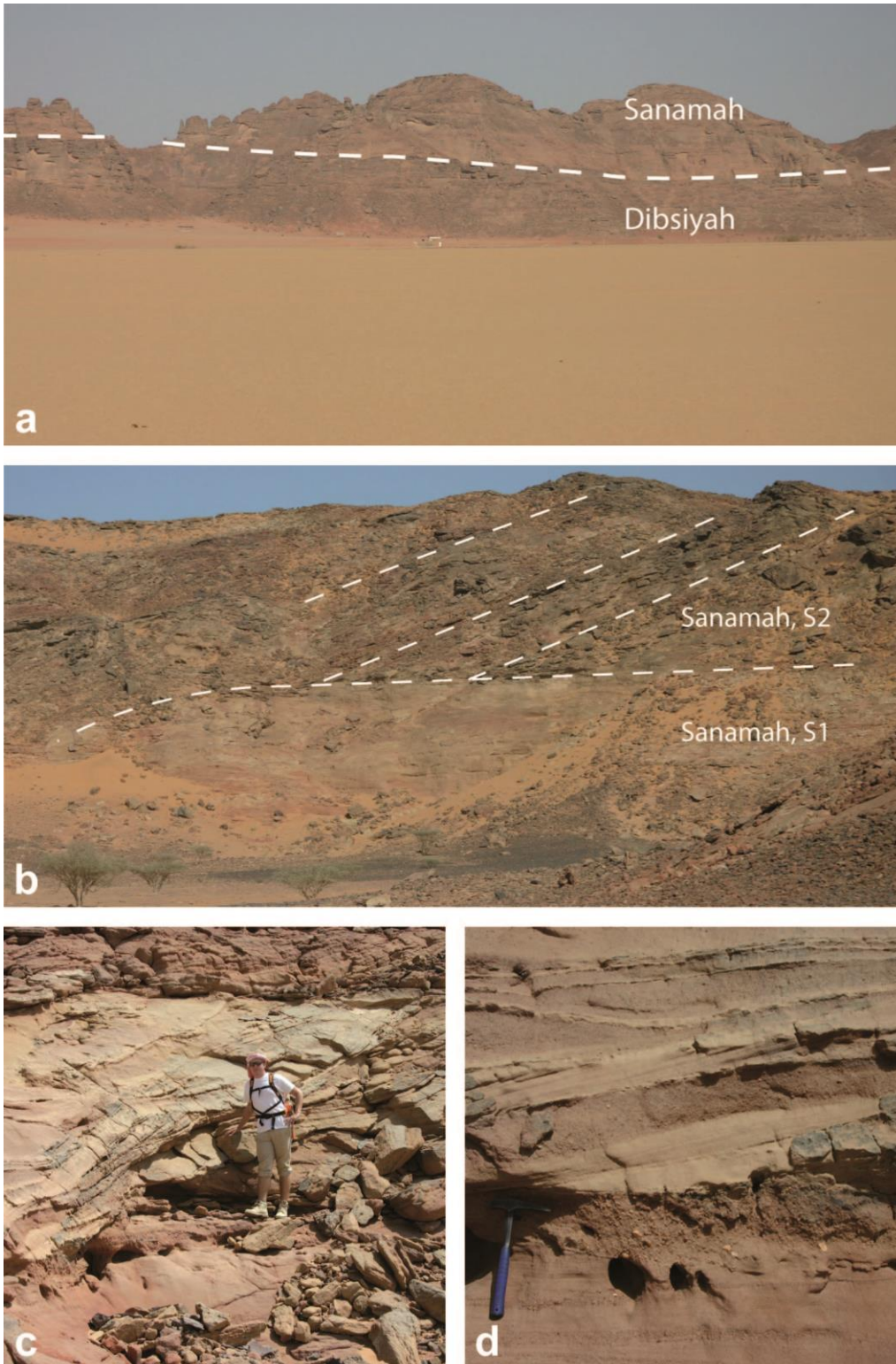


Figure 28: a: Erosional unconformity of a palaeovalley incised into the shallow-marine Dibsiyah Formation and filled with glacial to proglacial deposits of the Sanamah Formation. b: Sedimentary architecture of an Upper Ordovician palaeovalley fill showing low-angle prograding sediments of the basal conglomeratic unit S1. They are overlain by steeply downlapping clinofolds of the sandy unit S2. Clinofolds dip towards the south. c: Low-angle cross-bedded lobes of conglomeratic unit S1 with erosional base (Sanamah Formation). d: Low-angle cross-bedded medium- to coarse-grained sandstones with nests of pebbles in unit S2 (Sanamah Formation).

Massive to cross-bedded sandstone facies association (Unit S2)

This unit corresponds to facies association LF-A5 and is dominated by medium to coarse sand, often pebbly. The facies association is composed of massive, medium- to coarse -grained lithofacies (LF 11), of cross-bedded medium- to coarse-grained facies (LF 9), and of massive coarse sandstones (LF 12). Sediment was provided in large quantities and transported by high-energy subglacial melt waters. The absence in many beds of internal bedding features points to hyperconcentrated mass-flow deposition. These facies are typical of sandur flats in proglacial settings in front of glaciers or ice sheets (Maizels 1997; Russell *et al.* 2006). Locally, this facies association is organized in large clinofolds up to 50 m high (Figure 28). They are typical of Gilbert-type deltas that may have developed within the water-filled channels or in ice-dammed lakes in front of the glaciers.

Units S1 and S2 are separated by a surface marked by striations and a kettle hole shown in Figure 29. Although still present, the content of granules and gravels diminishes considerably across this boundary. Apparently, this surface marks the transition from aggradation towards retrogradation and consequently from a stationary or advancing glacier system to retreat. At the base of unit S3, a prominent, irregular erosional discontinuity is developed, which cuts down approximately 20 m into unit S2 (Figure 27a). Fluted surfaces and striations constrain a second glacier advance which conserved most of the valleys fill and spread out over the glaciofluvial plain, whose sediments were deposited during the former glacier retreat. Flutes and striations point to a polythermal regime; that is, parts of the sediments must have been frozen.

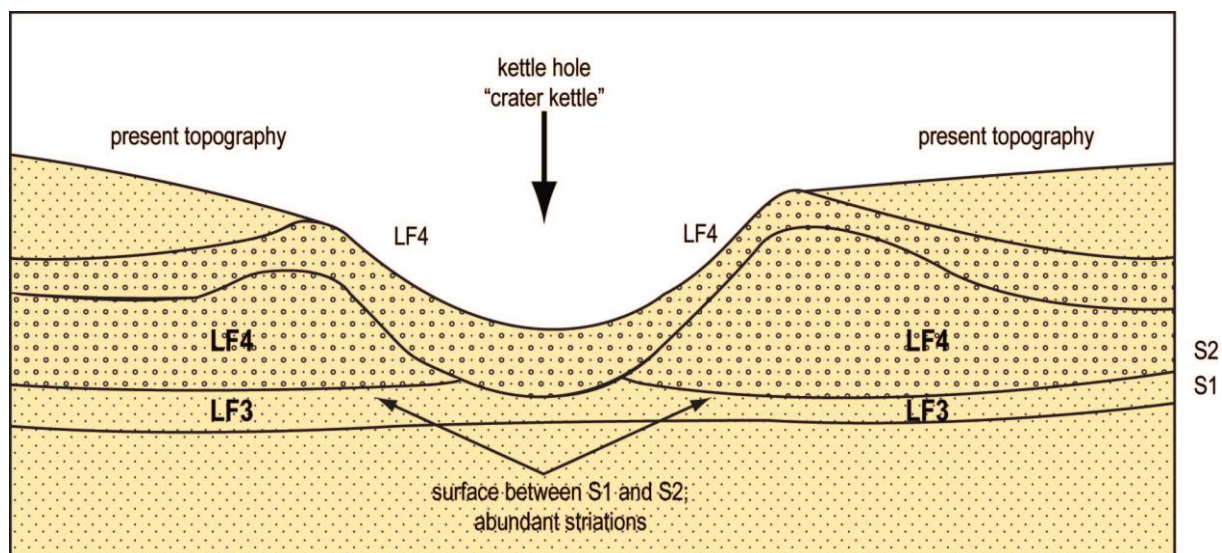


Figure 29: Sketch of a kettle hole in S2 at Jabal Maaleeq. According to its geometry, it corresponds to a “crater” or “rimmed” kettle hole in the sense of Maizels (1997).

Siltstones to fine-grained sandstone facies association (Unit S3)

This unit corresponds to facies association LF-A6. The general decrease of grain size, the preservation of silt, absence of mass-flow deposits despite some local slumps, and few and less pronounced internal erosional surfaces indicate less turbulent flow conditions and a decrease of transport energy when compared to unit S2. This succession is interpreted as a proglacial product of a subaerial, ice-distal, glacio-fluvial plain. Following Le Heron *et al.* (2005), who found similar features in the Murzuq Basin in SW Libya, the soft-sediment deformation features are interpreted as the result of glacial soft-sediment deformation of unfrozen, waterlogged sediments, most presumably by a glacial surge over the glacio-fluvial plain during a late stage of deglaciation. This soft-sediment deformation indicates yet another glacier advance over unfrozen sediments after deposition of unit S3. The corresponding disconformity is non-erosive and flat. Therefore it is concluded that this glacial advance represents a short-term glacial surge during deglaciation (Figure 30a). This might have been caused by rising temperatures establishing warm-based conditions and reducing ice viscosity, as well as by postglacial sea-level rise and buoyant uplift of the ice shield. The Qusaibah Shale overlying the unconformity is interpreted to represent the major marine transgression following the Ordovician glaciation (Sharland *et al.*, 2004).

Diamictic siltstone and shale facies association (Unit J1)

This unit corresponds to facies association LF-A9 and shows matrix-supported conglomerates (LF 13.2) alternating rapidly with siltstones and shales (LF 2, LF3). The shales are interpreted as subaqueous varve deposits in an ice-distal lake setting (Figure 31b). Most probably, they are the product of buoyant plumes of suspended matter fractionated from subglacial, high-pressure meltwaters draining into the lakes. Some icebergs reached these lakes and delivered dropstones. The diamictites, best exposed at Bani Khatmah (Figure 1) far from the other outcrops, are interpreted as ice-proximal equivalents to the varve facies. Outsized conglomeratic clasts and their arrangement as pebble carpets and nests can be only explained by debris rafting through icebergs (Figure 32c, d). This interpretation is supported by localized soft-sediment deformation structures, which are most probably formed by scratching of iceberg keels over soft sediment. Extensive pebble carpets and associated erosional surfaces (Figure 32b) might be also produced by short-term advances of an oscillating ice margin. Altogether a glacio-lacustrine environment is assigned to this facies association. This interpretation is corroborated by observations by Pollastro (2003) and Osterloff *et al.* (2004). Apparently, a vast glacial lake covered much of south-eastern Saudi Arabia and adjacent Oman. As lake sediments are also found in Ethiopia (Bussert & Schrank 2007) this lake probably extended across much vaster areas.

Coarse-grained sandstone facies association (Unit J2)

This unit corresponds to facies association LF-A5 with few intercalations of LF-A4. It is composed of coarse-grained lithofacies (LF 11 and LF 12) in combination with finer-grained sediments (LF 9 and LF 4). The massive to slab-like, weakly cross-bedded sandstones show identical grain-size spectra to the cross-bedded sandstone facies, and together with intraclasts and close interfingering there is no doubt that this facies is produced by localized, synsedimentary liquefaction of the surrounding cross-bedded sandstones. The facies represents the product of repeated hyperconcentrated flows (Figure 33a, c). Preservation of floating blocks of coarse sandstones, oversteepened to vertical channel walls, and weak internal lobe structures point to smooth, highly viscous, honey-like (“Sorbet!”) mass flow within the sedimentary succession. Consequently, it is called “Sorbet” facies in this thesis. Similar facies associations have been reported from modern proglacial settings in Iceland (Maizels 1993, 1997), where massive sandstones with only faint internal structures are typical of outburst floods on sandur planes. The difference to modern environments, however, is the dimension of the features observed in the Juwayl Formation. This may have to do with ice-shield dynamics vs. local glacier dynamics on Iceland.

The channelized, cross-bedded sandstones are interpreted as having been deposited in a large glacio-fluvial plain in front of the ice margin. The meltwater streams were directed towards the pre-existing large-scale channels with their high accommodation and rapid sediment accumulation. Features like vertical channel walls, floating blocks of unlithified coarse sand, undisturbed overlying sediments, and the lens-shape geometry of the massive sand bodies can be only explained by a polythermal regime in this glacio-fluvial plain. It is argued here, that these bodies originate from temporal liquefaction of frozen glacio-fluvial deposits during short pulses of deglaciation or seasonal temperature rises during summer. The highly viscous sands behaved like sorbet, hence the name “Sorbet” facies. LF 9 and LF 4 represent a more ice-distal glacio-fluvial setting. The large-scale deformation structures are interpreted as having been caused by glacial shearing of soft sediments, most presumably during a glacial surge in the late stage of deglaciation. The intimate association of LF 11 and LF 12 with LF 9 and LF 4 indicates oscillation of the ice margin and consequently the migration of depositional environments.

Unit J2 is interpreted to represent a rapid progradation of glacio-fluvial to deltaic sediments. This was presumably caused by increased sediment supply as seen in modern environments (Maizels 1993, 1997) and/or base level fall due to water-level drop of the pre-existing glacial lake, which is assumed to have covered large areas of the southwestern Arabian Platform during this time (Kruck & Thiele 1983; Pollastro 2003; Bussert & Schrank 2007). A forced lake-level fall during peak glacial conditions implies reduced meltwater discharge and subaerial exposure of former subaqueous delta and lake deposits.

Well-bedded shale to sandstone facies association (Unit J3)

This unit corresponds to facies association LF-A6 and LF-A8. This unit represents a transgressive succession, most probably due to sea-level rise during advanced deglaciation. In northern Saudi Arabia, similar coarse-grained, large-scale cross-bedded sandstones have been interpreted as eolian (Unayzah A, Evans et al. 1997; Melvin & Sprague 2006); however, based on the relative poor sorting and the coarse sand, and taking into account their stratigraphic position in a transgressive sequence, an interpretation of tidally influenced channels in a shallow-marine setting is preferred. Such channels are repeatedly observed towards the top of the succession; however, they become increasingly smaller and less frequent. Evidence for glacial processes is no longer visible in this succession, which terminates the Wajid Sandstone Group, and which is erosionally overlain by the Khuff carbonate rocks. During deposition of unit J3, the glacio-fluvial plain became more distal to the ice front. This finer-grained unit shows intense soft-sediment deformation similar to that observed in the Sanamah Formation but less thick. Therefore, a similar scenario of a short-term glacier surge running over the glacio-fluvial plain during deglaciation is suggested (Figure 30b). Above the basal, almost planar disconformity, the deposition of transgressive marine beds started under tidal control and much reduced sediment supply. Similar to the Qusaibah Shale above the Ordovician sediments, this can be related to a eustatic, postglacial sea-level rise. Later on, in late Permian time, the first platform-wide marine transgression took place depositing the Khuff carbonates. This fundamental change of depositional style on the Arabian Platform was controlled by tectonic subsidence (Sharland et al. 2001).

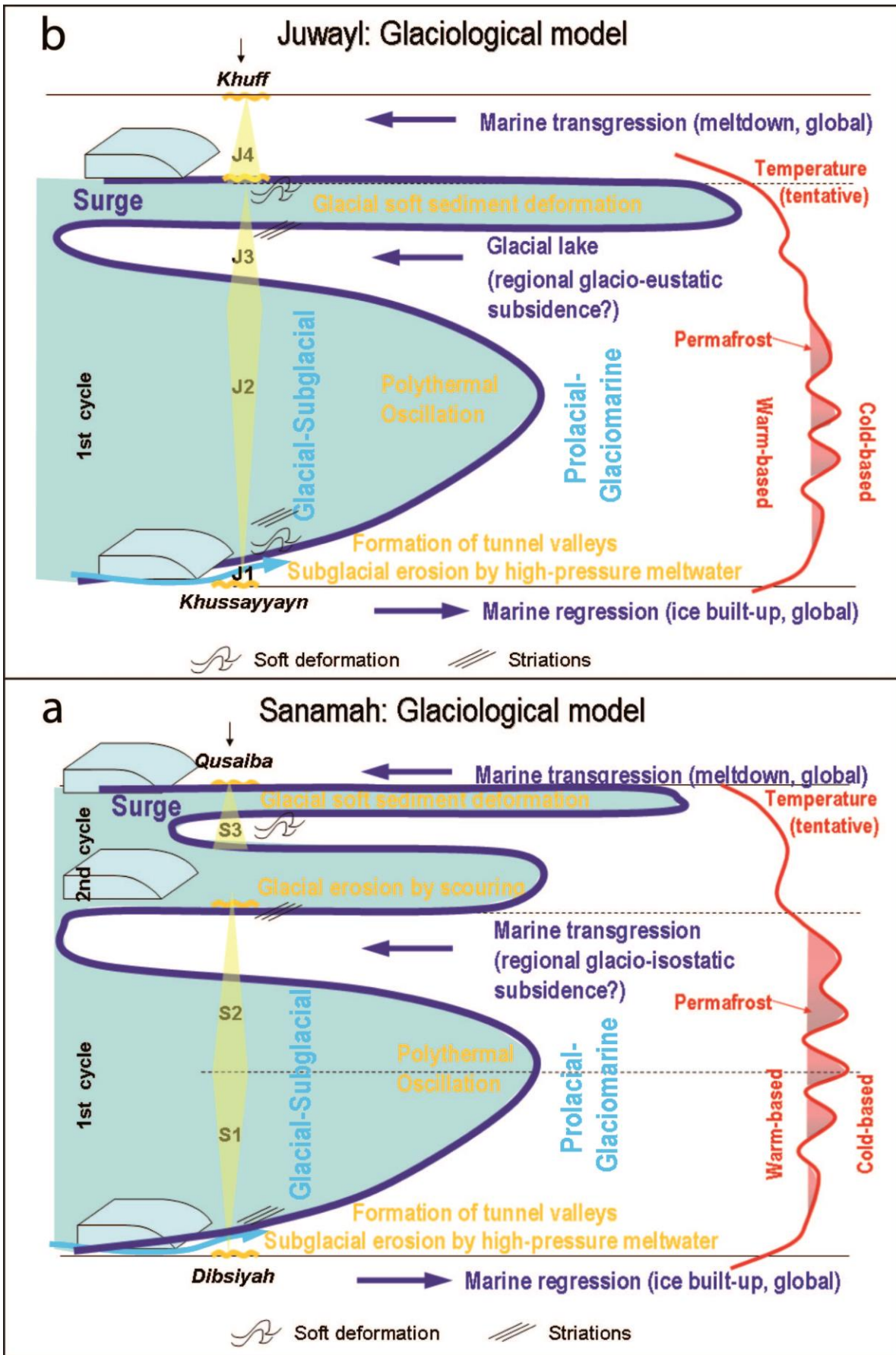


Figure 30: Glaciological model for the Late Ordovician (A) and Permo-Carboniferous (B) glaciation based on sedimentary facies and glaciogenic signatures in the outcrop area of the Wajid sandstone in SW Saudi Arabia. The black arrow indicates the position of the studied outcrops. Note that more glacial cycles may have been active, which are not preserved in the sedimentary record. See text for further explanation.

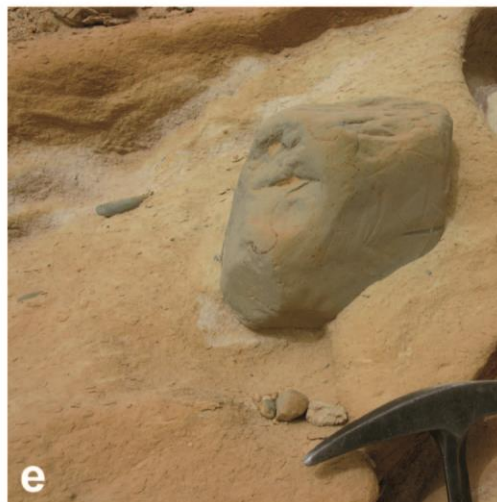
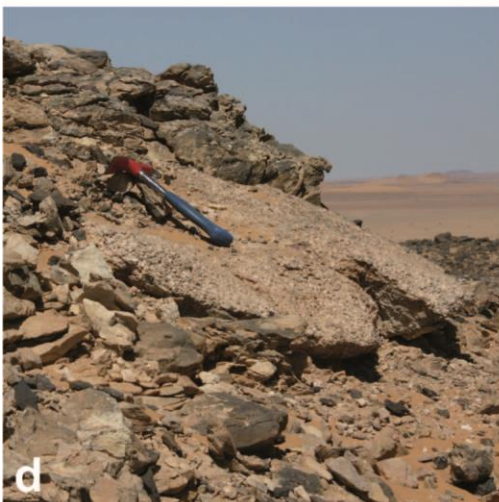
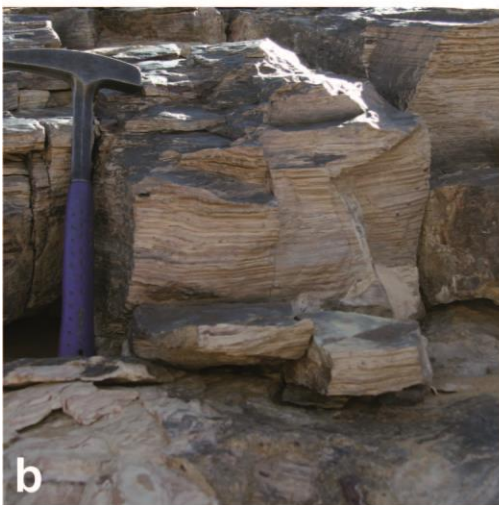


Figure 31: a: Downbending of clayey varve beds of unit J1 at the rim of a Permo-Carboniferous tunnel valley. b: Silicified shales interpreted as varves (unit J1). c: Slumped varve deposits with intercalated sandstone bed (unit J1). d: Angular granitic block deposited as dropstone in varve deposits (unit J1). According to its geometry, this block is of supraglacial origin. e: Striated metavolcanic dropstone clast deposited in a silty matrix (diamictite, unit J1). According to its geometry, this rock is of subglacial origin.

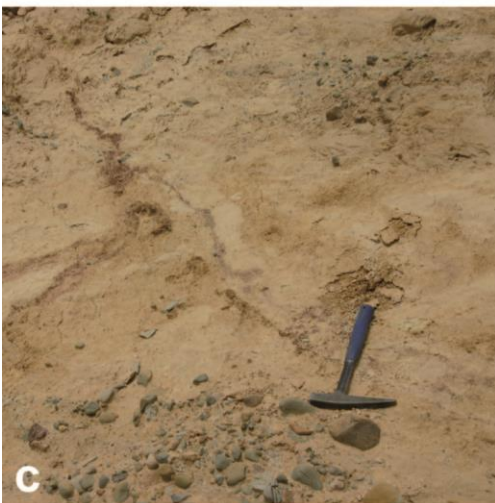


Figure 32: a: Diamictite with silty laminated beds and impacted by dropstones in unit J1 of Juwayl Formation. b: Tabular, cross-bedded siltstone overlain by a gravel carpet. Weak erosional base points to ice scratching, probably by an oscillating ice margin. Unit J1 of Juwayl Formation. c: Local thrust fold within diamictite most probably caused by scratching of an iceberg keel. Unit J1 of Juwayl Formation. d: Local thrust fold within diamictite most probably caused by scratching of an iceberg keel. Unit J1 of Juwayl Formation.

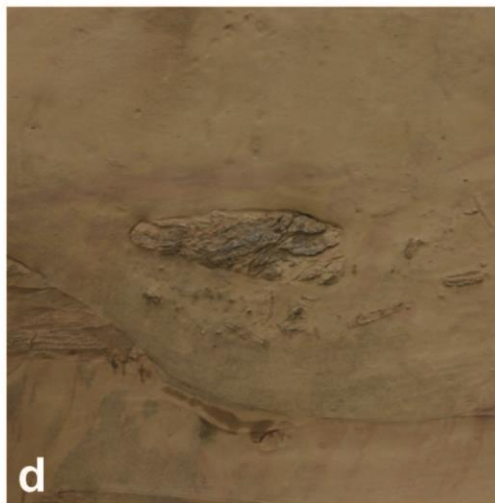
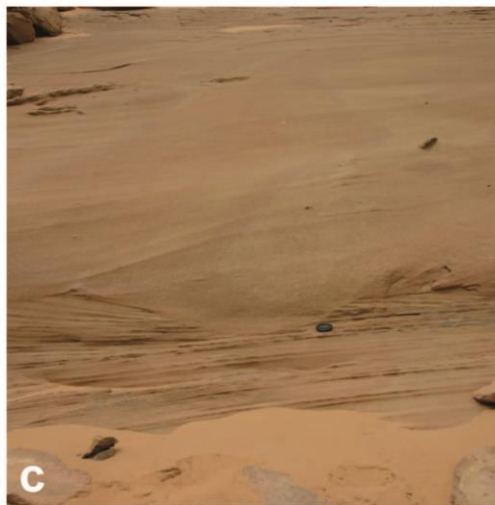
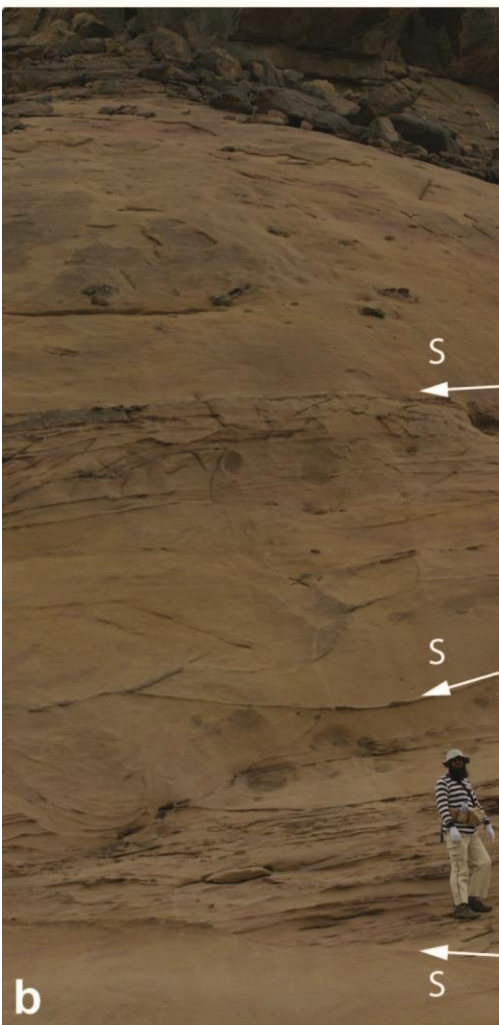


Figure 33: a: Liquefaction of cross-bedded, channelized sandstones forms viscous grain flows resulting in lobe-like structures (“Sorbet” facies). Unit J2 of Juwayl Formation.
 b: Large scale, multistory “Sorbet” facies (arrows with “S” show base of successive levels of “Sorbet” facies at Jabal Um Lsan). c: Erosional base of “Sorbet” facies. d: Floating intraformational block of cross-bedded sandstones.

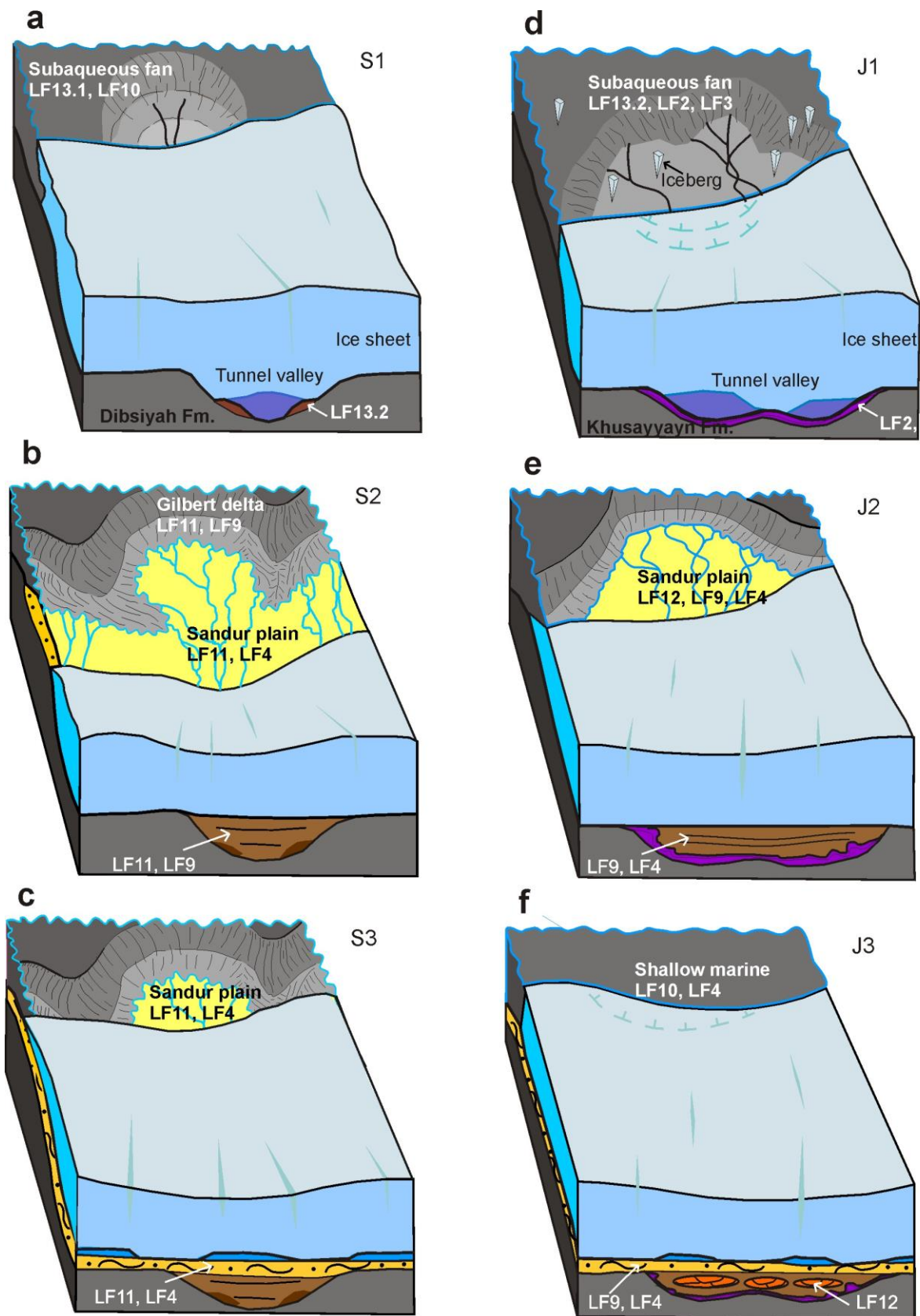


Figure 34: Schematic depositional models for all six facies associations inspired by LeHeron et al. (2010). Sanamah Formation (Upper Ordovician) (a) Massive to cross-bedded conglomerate facies association (Unit S1). (b) Massive to cross-bedded sandstone facies association (Unit S2). (c) Siltstone to medium-grained sandstone facies association (Unit S3). Juwayl Formation (Permo-Carboniferous). (d) Diamictic siltstone and shale facies association (Unit J1). (e) Coarse-grained sandstone facies association (Unit J2). (f) Well-bedded shale to sandstone facies association (Unit J3).

6.3. Analysis and evaluation of selected structures as evidence of ancient glaciations

Although typical till deposits are missing in southwest Saudi Arabia, much evidence of a glacial to proglacial setting of the deposits can be found. This includes specific lithofacies types described above, which can only be explained if sediments had been temporarily frozen (such as LF11, LF12). In addition, sand-gravel mixtures and massive to weakly cross-bedded sands without clay and silt could be explained by unsteady, strongly sediment-laden currents since they typically occur by meltwater outbursts in proglacial settings (LF13.1, LF13.2, LF10). Here some specific glaciogenic features in the Wajid Group of southwest Saudi Arabia are described in the following sections.

6.3.1. Striations

In both the Sanamah and Juwayl formations, striations have been observed on disconformable surfaces and bedding planes. In a single section (Jabal Maaleeq, Sanamah Formation), five horizons have been observed in which the striae run parallel to those on the underlying and overlying horizons (Figure 35e). In the vicinity of Jabal Atheer, such a horizon was also observed in the uppermost part of the non-glacial Dibsiyah Formation just beneath the unconformity with the Sanamah Formation. Other striations were observed near Bani Ruhayah in the upper part of the Juwayl Formation (Figure 35c). Most of the striae are well preserved because they are diagenetically cemented by iron oxides.

Striations in the Sanamah Formation show a very consistent direction between 110° and 130°; in the Juwayl Formation, directions between 130° and 150° have been measured. In both formations, striations are more or less parallel to the axis of the channels in which the sediments were deposited. Locally in the Sanamah Formation, two sets of highly divergent striations have been observed (Figure 35a).

Striations are characteristic of a glacial environment; some facts, however, indicate that these striations cannot have been created through direct glacier contact. In most known examples of true glacial striations, these striations are preserved in hard rocks at the base of the glacial succession. Magmatic and metamorphic rocks are suitable for the preservation of striae, but also quartz arenites and occasionally carbonate rocks. Secondly, in some horizons cross-cutting relationships have been observed between two generations of striations. This may be due to deviation of the ice movement by local obstructions, by changing movement direction of a single glaciers during its thinning and retreat or, if found extensively, formed by two glaciers advancing from different directions (Flint 1957; Benn & Evans 1998). There is no sufficient information on the distribution of divergent striations in the Sanamah Formation to confidently establish a specific cause except perhaps some local obstruction associated with the development of adjacent soft-sediment deformation. All striations observed in the Sanamah and Juwayl formations were most likely formed on unconsolidated sediments. Soft-sediment striated surfaces have been observed in other African Palaeozoic units where they have been also interpreted as glacially induced (Deynoux & Ghienne 2004; Le Heron et al. 2005). Le Heron et al. (2005) interpret these features as formed by shearing along bedding planes of over-pressured sand packages, most probably by ice load.

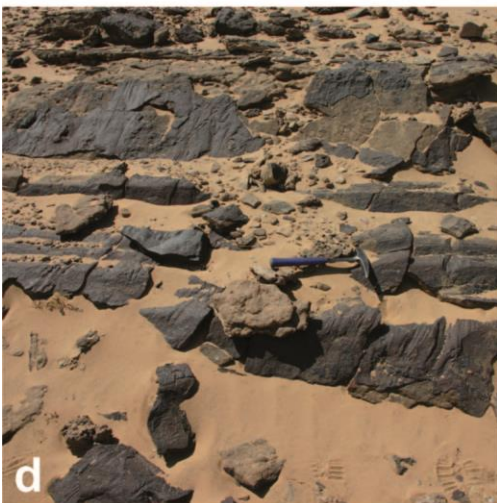
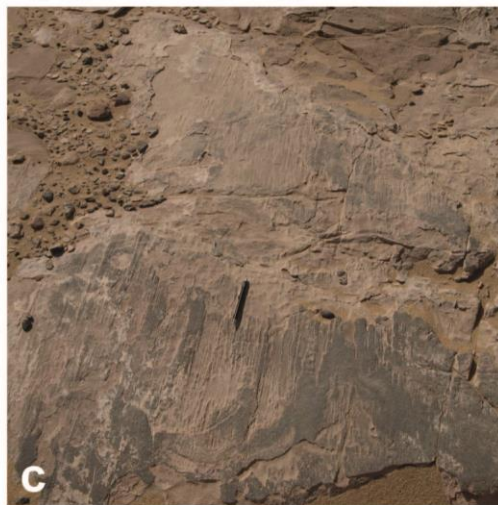
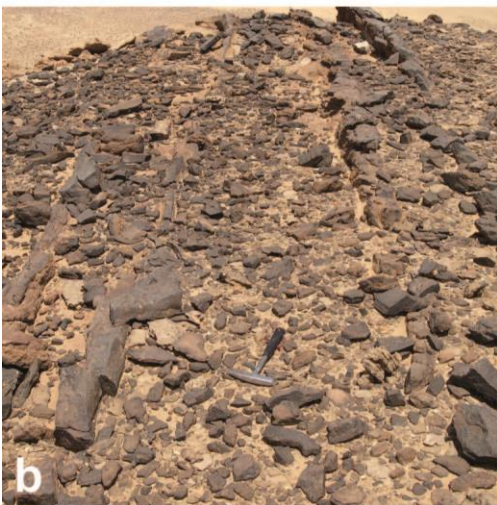


Figure 35: a: Iron-cemented multi-directional striations at the erosional unconformity between units 2 and 3 within the Sanamah Formation. b: Fluted surface slightly above the erosional unconformity between units 2 and 3 within the Sanamah Formation. c: Unidirectional striations at the top of unit J3 of the Juwayl formation. d: Flutes with oblique overprint of striations at the erosional unconformity between units S2 and S3 within the Sanamah Formation. e: Iron-cemented unidirectional striations at the erosional unconformity between units S2 and S3 within the Sanamah Formation.

6.3.2. Fluted surfaces

Within the Sanamah Formation there is an unconformity (S2/S3) along which well-developed iron crusts are preserved. This iron-cemented unconformity can be taken as a marker horizon and can be traced over large areas. On this surface, flute structures similar to those described by Le Heron et al. (2005) have locally been observed (Figure 35b). Direction of the flutes coincides with those of the striations and show directions between 110° and 130°.

6.3.3. Dropstones and boulder pavements

Many sediments of the Juwayl Formation were deposited in a vast lake (Pollastro 2003). Within these fine-grained sediments, exotic clasts of pebble to boulder size are present. Magmatic rocks (granite), metamorphic rocks (especially metagreywackes) and sedimentary rocks of older Wajid Group units have been identified (McClure et al. 1988). Frequently, the clasts show faceting and striations, in particular the fine-grained pebbles of metagreywacke (Figure 31e). They also deform the laminae of sediments they rest on (Figure 32a). These clasts can be reasonably interpreted as ice-rafted dropstones. At Bani Khatmah, a succession of fine siltstones to sandstones containing dropstones is abruptly overlain by a clast-supported conglomerate whose clasts show striations (Figure 32b). The accumulation of these boulders most likely represents remnants of a conglomeratic pavement associated with the oscillation of an ice front.

6.3.4. Local post-depositional sedimentary deformation

At Bani Khatmah and at Jabal Overheat, the lacustrine sedimentary succession of the Juwayl Formation show large-scale, post-depositional deformation structures consisting of folds and thrust faults (Figure 32c, d). Some of the horizons are almost entirely deformed. These structures may be partly associated with pressure exerted by icebergs drifting across stagnant water and occasionally touching down on the sediment surface.

6.3.5. Origin and possible significance of the large valleys

Both the Sanamah Formation and the Juwayl Formation were partly deposited in broad valleys up to several kilometres wide and more than 100 m deep. In northern Saudi Arabia, similar Ordovician structures on seismic lines are up to 600 m deep (McGillivray & Hussein 1992). Seismic mapping of these valleys in northern Saudi Arabia show a radial orientation and longitudinal shape with low sinuosity (Sharland et al. 2001). These features are therefore preferentially interpreted as tunnel valleys. However, other models also exist which have been reviewed by Sharland et al. (2001) for northern Saudi Arabia and Le Heron et al. (2004) for northern Africa. They consider a subglacial origin as well as pure fluvial incision and fluvial incision coupled with ice isostasy. A tectonic origin as proposed by Stump & Van der Eem (1995, 1996) is rather unlikely, given the tectonic quiescence at that time and the dimensions of uplift, erosion and subsidence required within a rather limited time interval. A radial pattern of valleys would also be unlikely.

The lithofacies associations with vestiges of repeated outburst floods indicate that these valleys might have originated as tunnel valleys (Piotrowski 1994; Ghienne & Deynoux 1998; Le Heron et al. 2009). This interpretation implies subglacial erosion by meltwater during the ice maximum and shortly thereafter, when the hydraulic transmissivity of ice sheet stratum was insufficient to drain all basal meltwater and meltwater excess was evacuated via open channels at very high discharge rates and flow velocities (Piotrowski 1997). These sudden repeated outbursts caused efficient subglacial meltwater erosion close to the margin of the ice shield and may have prevented till deposition in the valleys as has been described from Pleistocene examples. The depth of the Palaeozoic valleys in the study area of up to 100 m is surprisingly close to those reported from Pleistocene examples of northern Germany (Piotrowski 1997). One distinct property of subglacial tunnel valleys is the irregularity of their gradient. It could not be decided whether this is true for the valleys in the study area, because valley floors were not exposed along longitudinal profiles and geophysical surveys have not yet been carried out.

6.3.6. Large-scale soft-sediment deformation by glacier push

Glaciogenic large-scale soft-sediment deformation structures are well known from Quaternary ice sheets, but have rarely been recognized in Palaeozoic deposits. Le Heron et al. (2005) showed that structures

such as large thrust-and-fold systems, giant ball-and-pillow structures and dome-like structures are widespread in front of the Upper Ordovician ice sheet in Libya and that they have important glaciological and stratigraphic significance. These structures were produced by glacier push and by load-induced diapirism. Similar features are present at the top of the Sanamah Formation and within the upper part of the Juwayl Formation, where these phenomena attain dimensions of up to 30 m. They are not restricted to the presumed tunnel valleys, and thus are valuable marker beds. The deformation is most probably caused by a short-term glacial surge during deglaciation and potentially of chronostratigraphic value (Le Heron et al. 2005).

6.3.7. Palaeozoic glaciological models for SW Saudi Arabia

Based on observed facies associations, architecture and glaciogenic sedimentological features as described before, a conceptual model for the two Palaeozoic glacial episodes in SW Saudi Arabia is presented (Figure 33a, b). Three and two-glacial advances for the Ordovician and Permo-Carboniferous are proposed, respectively, which include additional high-frequency fluctuations as deduced from the sedimentary deposits. The sedimentary record starts at or shortly after the ice maximum when subglacially eroded tunnel valleys began to be filled up. Here, a polythermal regime for this time is suggested. In the Ordovician, a second advance led to erosion and created widespread striations in underlying beds (discontinuity S2/S3). In both the Ordovician and Permo-Carboniferous cases, the upper part of the glaciogenic successions show distinct horizons of widespread soft-sediment deformation followed by post-glacial flooding. The observed features of soft-sediment deformation could be explained by glacial shearing under mostly warm-based conditions. However, clear till deposits are absent. Here a short-term surge scenario for these late re-advances is proposed, probably initiated by the buoyancy of the ice sheet due to meltwater ponding in downwarped marginal areas and/or a postglacial sea-level rise. Reduced ice viscosity due to temperature rise may also have played a role. In both cases, the glaciogenic succession is covered by pronounced marine transgressive sequences which correspond to primary maximum flooding surfaces in the sequence stratigraphic framework of the Arabian Plate (S10 and P20: Sharland et al. 2001).

6.4. Palaeozoic glaciations of Gondwana

The sedimentary record of the two glacial episodes in southern Saudi Arabia shows striking similarities and indicates rather similar glaciological conditions during the Late Ordovician and during the Permo-Carboniferous. In addition, sedimentary facies and architecture of Upper Ordovician deposits of the Arabian Platform can be compared with those recently described from Mauritania (Ghienne & Deynoux 1998; Ghienne et al. 2003) and the Murzuq Basin in Libya (Le Heron et al. 2004). Le Heron et al. (2004, 2005) described many similar features and suggested a model of a polythermal regime at an oscillating ice front, followed by deglaciation and a late glacial surge. Finally, postglacial eustatic sea-level rise led to transgression and the deposition of marine beds above the glacial succession. The almost identical pattern of glaciological regimes over a distance of more than 1000 km along the northern margin of Gondwana supports the hypothesis of a large, coupled ice shield over at least North Africa and Arabia as has been suggested by Le Heron & Dowdeswell (2009), rather than an isolated ice sheet on the Arabian Shield.

Some differences remain, however, concerning the number of ice advances and ice retreats. While Le Heron et al. (2004) found incision of the tunnel valleys into glaciogenic deposits of an earlier ice advance, and Ghienne et al. (2003) as well as Le Heron et al. (2006) suggested four glacial cycles from observations in Mauritania and Libya, Ordovician glaciogenic deposits in SW Saudi Arabia are restricted to the valley fill and thin onlapping on the valley margins. Together with a first glacier advance which eroded the subglacial valleys and deposited a first glaciolacustrine to deltaic sequence (S1), two further advances are indicated by a major intra-formatonal erosional unconformity (S2/S3) and widespread soft deformation at the top (S3) (Figure 20b). Vaslet et al. (1991) concluded from observations on outcrops and seismic data from northern Saudi Arabia that two erosional episodes formed the tunnel valleys, which were subsequently filled by the Zarqa Formation and after the second erosional episode by the Sarah Formation. Both units together are the northern equivalent of the Sanamah Formation of the Wajid Group.

Repeated ice advance-retreat episodes have also been reported from the subsurface of west-central Saudi Arabia (Melvin & Miller 2002). It is suggested that these two erosional events in glaciogenic Upper Ordovician sequences of the northern and central Arabian platform can be correlated with the two unconformities observed in SW Saudi Arabia, and might be of high chronostratigraphic value. The second erosional event, however, is less pronounced in the SW and failed to cut down to the bottom of the valleys as has been reported from northern Saudi Arabia (pre-Sarah unconformity).

The lack of pre-incision glaciogenic deposits on the Arabian Platform that are present in Libya might be explained by topographic effects such as a flatter morphology and the absence of prominent intracratonic basins on the Arabian Shield. This would have resulted in low accommodation and a lower potential for preservation of the sediments. Another explanation would be that tunnel valley formation was not exclusively restricted to one distinct glacial stage along the entire margin, but that it may have occurred repeatedly at an oscillating ice margin. It will probably never be possible to resolve these events biostratigraphically because of the absence of any fauna. Hence, a correlation to the North African events must necessarily remain speculative. As recent research (Saltzman & Young 2005; Buggisch et al. 2010) has shown that the Hirnantian glaciation was only the peak event of a succession of larger-scale glacial episodes since the Katian, a correlation entirely based on sedimentological criteria would be audacious. Hence it may be that not all of the events in Saudi Arabia correspond to the Hirnantian glaciation proper.

The Permo-Carboniferous glacial episode is not well documented in northern Africa; it is, however, well constrained by biostratigraphical data from Oman (Pollastro 2003; Osterloff et al. 2004), Yemen (Kruck & Thiele 1983) and Ethiopia (Bussert & Schrank 2007). Here, glaciogenic deposits were deposited in glacial valleys cutting down to the Precambrian basement. For Ethiopia, Bussert & Schrank (2007) suggested that the sediments were deposited in a glaciolacustrine to glaciofluvial environment, similar to the model presented here. Similarly, Kruck & Thiele (1983) and Pollastro (2003) assume that large areas of the south-western Arabian Platform have been covered by a glacial lake during this time. This hypothesis could be confirmed by describing typical glaciolacustrine facies associations from the Wajid Group.

Several indications exist that the Permo-Carboniferous ice sheet was much more heterogeneous than that of the Late Ordovician. During the early Carboniferous, the Hercynian tectonic event led to a major unconformity on the Arabian Platform; up to several hundred metres of sediments were removed by erosion (Sharland et al. 2004). The presence of large angular basement blocks in the Juwayl deposits can only be explained by supraglacial transport and rock fall from a mountain range or nunataks. Such elevated areas seem to have existed not only around the Arabian Shield but also at the southern edge of the Arabian Platform in Oman, Yemen and Ethiopia (Kruck & Thiele 1983; Bussert & Schrank 2007). The glaciogenic deposits of Bani Khatma, 250 km south of the other outcrops (Figure 1), show a spectrum of dropstone petrography not known from the presently exposed rocks of the Arabian Shield (McClure et al. 1988). The clasts were presumably shed from a southern source located at the opposite margin of the glacial lake. Kruck & Thiele (1983) found a SW-directed and Bussert & Schrank (2007) a north-south directed ice flow. Both are opposite to the model of a single huge Gondwana ice shield with a unidirectional north-NW directed ice flow. Therefore, Bussert & Schrank (2007) concluded that an independent ice cap must have existed in Eritrea and/or in southern or central Saudi Arabia, which was probably restricted to the area of the Hercynian uplift in this region.

The incision of tunnel valleys, a polythermal setting in front of an oscillating ice sheet and extensive glacial surge during a late stage of glaciation reflects similar glaciological processes in the Carboniferous and in the Ordovician. This includes large ice sheets which discharge to sea- or lakelocked coastal areas. A remarkable difference is the quartzose petrography of the Ordovician conglomerates and accompanying sandstones compared to the Permo-Carboniferous deposits. Upper Ordovician glacial erosion mostly reworked mature shelf sediments poor in clay, which had been deposited across the Precambrian-Cambrian peneplain of the Arabian Shield (Avigad et al. 2005). No pebbles of basement rocks were found, which indicates that the Arabian Shield was not exposed or was poorly exposed during the Late Ordovician and that it did not act as a major sediment source. This drastically changed during the Hercynian tectonic event. In addition, less intense chemical weathering and enhanced production of clay

minerals with the advent of land plants may be responsible for a quite different composition of the Carboniferous sediments (Keller & Lehnert 2010).

7. Gamma ray logging

7.1. Theoretical background

Natural gamma radiation is caused by three main radionuclides: ^{40}K , ^{232}Th and ^{238}U . These elements occur primarily in magmatic rocks but can accumulate in sediments through erosion and redeposition. From the three main radionuclides, potassium is the most abundant, followed by Uranium. Thorium is the rarest of the main radionuclides. Potassium is mainly found in clay minerals and therefore in sedimentary rocks like claystones and shales, as well as in evaporites that contain KCl. Other rock-forming minerals that contain potassium are the feldspars orthoclase and microcline (Rider, 2002). Naturally occurring Uranium consist of mostly ^{238}U and to very small parts of ^{235}U and ^{234}U . They originate primarily from igneous rocks and pass from solution into sediments in three principal ways (Rider, 2002):

- 1) Chemical precipitation in stagnant, anoxic waters with slow sedimentation rates
- 2) Adsorption by organic matter under reducing conditions
- 3) Complexation with phosphate

Thorium also originates from igneous rocks but unlike Uranium has only poor solubility in water. Thus Thorium is mainly contained in heavy minerals whereas U may be also significantly adsorbed on clay minerals (Rider, 2002).

Natural γ -ray logging is a type of passive nuclear measurement and is applicable to both boreholes and outcrops. The method is widely used in borehole logging to identify lithologies, especially shale beds, and correlate different wells. There are two different types of γ -ray logs: total and spectral γ -ray logs. The former method is faster, cheaper and provides enough information for lithological and correlation purposes and is thus more common in borehole measurements, but does not specify the source of the γ -radiation (K, U or Th). Values are shown in a joint graph and represent the total (combined) γ -activity of K, U and Th. Common units are [cp/s] (counts per second) or [API]. The latter type provides information about the source of the radiation and is therefore a more accurate, but also more expensive and time-consuming method. The specific activities of K, U and Th are shown in separate graphs. Common units are [%] (K) and [ppm] (U, Th). Outcrop measurements are usually done as spectral γ -ray logs, utilizing handheld devices. One of the advantages of γ -ray logging is that it can be used in cased wells. Thus the method has been applied extensively in groundwater drilling projects of the GIZ/DCo in Saudi Arabia (Schönrok 2011). For correlation purposes or the identification of trends, the natural γ -ray log is usually sufficient, whereas spectral γ -ray data can be vital for the analysis of single anomalies or peaks.

In this study, γ -ray logs taken by Schönrok (2011) have been analysed and compared with lithological logs. Special attention was given to trends in the γ -ray patterns, which are referred to as “dirtying-up”, “cleaning-up” and “bow” trends after Emery et al. (1996) (Figure 36).

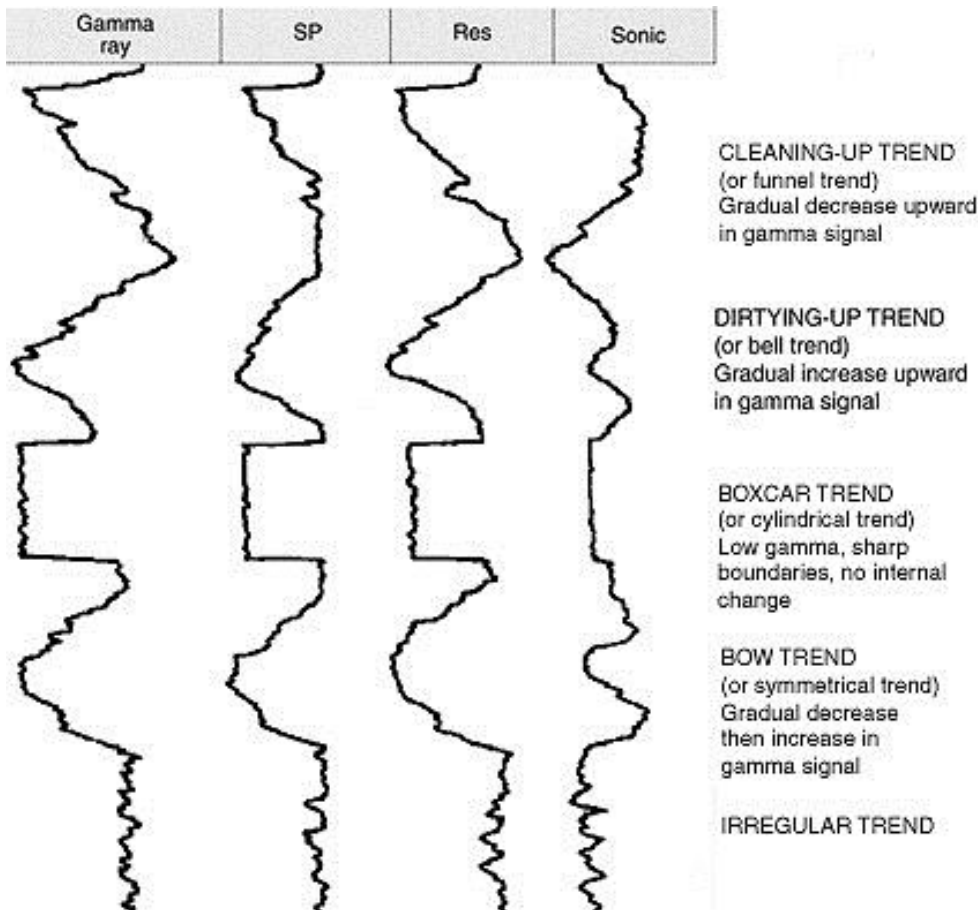


Figure 36: Well log response characters after Emery et al (1996).

7.2. Natural gamma-ray of sections

Gamma-ray logs measured by Schönrok (2011) were correlated with lithological logs of this study from the same outcrops.

The potassium concentrations are stated as “less than 1%”, which is probably due to detection limits on the handheld gamma-ray detector. Unfortunately, this is not clearly stated by Schönrok (2011).

Dibsiyah Formation (Jabal Nafla)

The gamma-ray log of the Dibsiyah Formation at Jabal Nafla (see Figure 37) has a total average API of 50. Average concentrations for the particular elements are less than 1% K, ~ 3 ppm U and ~ 8 ppm Th. The trends as well as the overall gamma-ray level are dominated by thorium. Peaks of uranium coincide with thorium peaks. While most of the log shows repeated bow trends of both thorium and uranium, at the top of the log is a prominent dirtying up trend dominated by thorium. Two major thorium peaks, with coincide with two minor uranium peaks, stand out in the log and are associated with iron-cemented sandstones in lithofacies LF 8. The trends and peaks are not related to grain size.

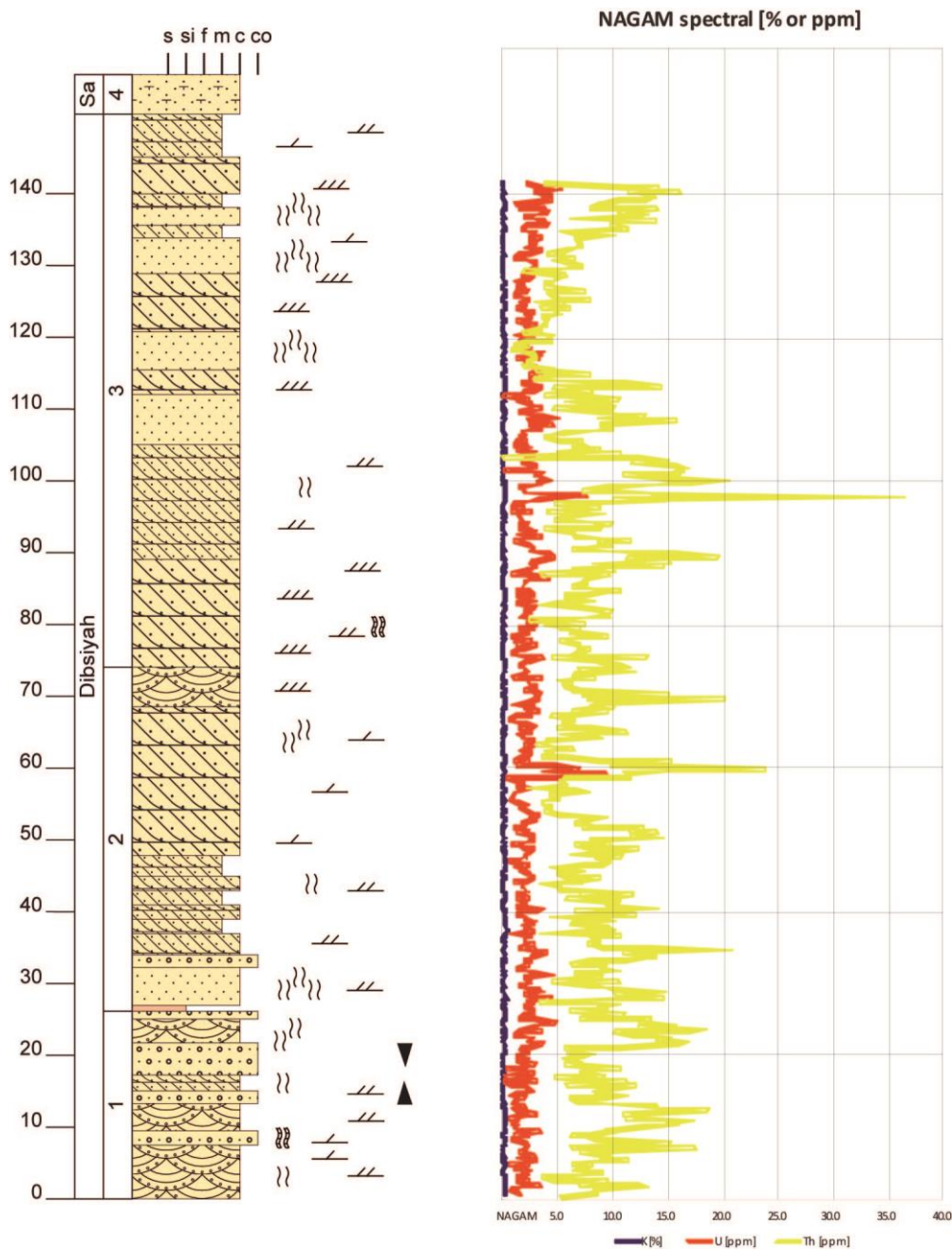


Figure 37: Combined lithological and (spectral) gamma-ray log of the Dibsiyah Formation at Jabal Nafla. Gamma-ray data taken from Schönrok (2011).

Sanamah Formation (Jabal Atheer)

The gamma-ray log of the Sanamah Formation at Jabal Atheer (Figure 38) has a total average API of 50. Average concentrations for the particular elements are less than 1% K, ~ 3 ppm U and ~ 8 ppm Th, which is the same as for the Dibsiyah formation. Trends are mostly bow trends of both thorium and uranium. One cleaning up trend of thorium has been identified in the middle of the log. The most prominent feature of the log is given by two prominent uranium peaks of up to 190 ppm, caused by iron-cemented crusts. They also seem to be associated with a change in both facies and grain size, occurring on the top and bottom of a bank of clast supported conglomerate (LF 13.1). The conglomerate layer is bordered by coarse sandstones on the bottom and medium grained sandstones at the top. The change in facies and grain size is likely cause for the genesis of iron cemented crusts enriched in uranium. Aside from the two uranium peaks, the overall level of U and Th gamma radiation increases towards the top of the log. A minor peak of both Th and U is at the top of the succession, in alternating layers of medium and coarse grained sandstone.

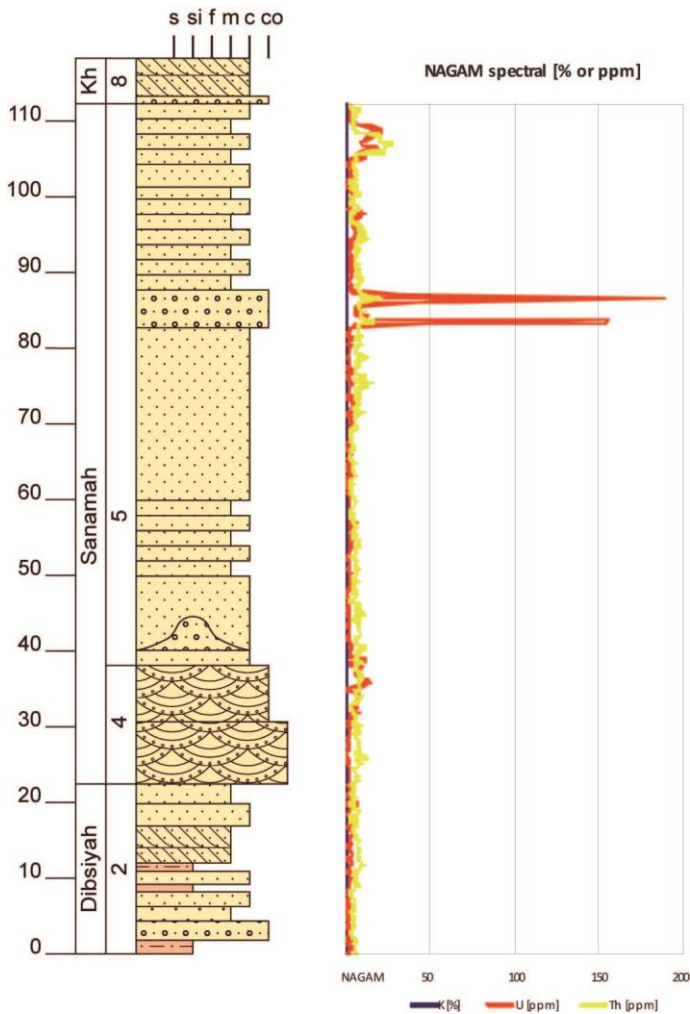


Figure 38: Combined lithological and (spectral) gamma-ray log of the Sanamah Formation at Jabal Atheer. Gamma-ray data taken from Schönrok (2011).

Khusayyayn Formation (Jabal Khusayyayn)

The gamma-ray log of the Khusayyayn Formation at Jabal Khusayyayn (Figure 39) shows an overall dirtying up trend from an average gamma-ray level of 60 API at the bottom to 160 API at the top. There is also an increase of both quantity and intensity of single peaks from bottom to top. Overall concentrations are mostly stable for U with roughly 4 ppm and K at 1%, but with a slight increase towards the top. The low amount of K is surprising given the higher content of K-feldspar reported by Heberer (2012) for samples from the Khusayyayn formation (Table 2). This may again be an issue with detection limits of the handheld gamma-ray detector. Unfortunately, the initial data measured in the outcrop by Schönrok (2011) was not accessible. Th concentration shows an increase from 5 ppm at the bottom to 25 ppm at the top, resulting in a strong Th-dominated dirtying up trend. This trend coincides with a fining-upward trend in grain size across the whole profile. A possible explanation could be the enrichment of Th in the finer grained fraction, resulting in a negative correlation between Th concentration and grain size. This does not account for single peaks in the more or less homogenous upper parts, though. A prominent feature is a negative thorium and uranium peak between 25 m and 30 m, in a layer of pebbly trough cross-bedded sandstones of lithofacies LF 9. This change in lithofacies and drop of Th concentration fits with the observed negative correlation between Th concentrations and grain size for this log.

NAGAM spectral [% or ppm]

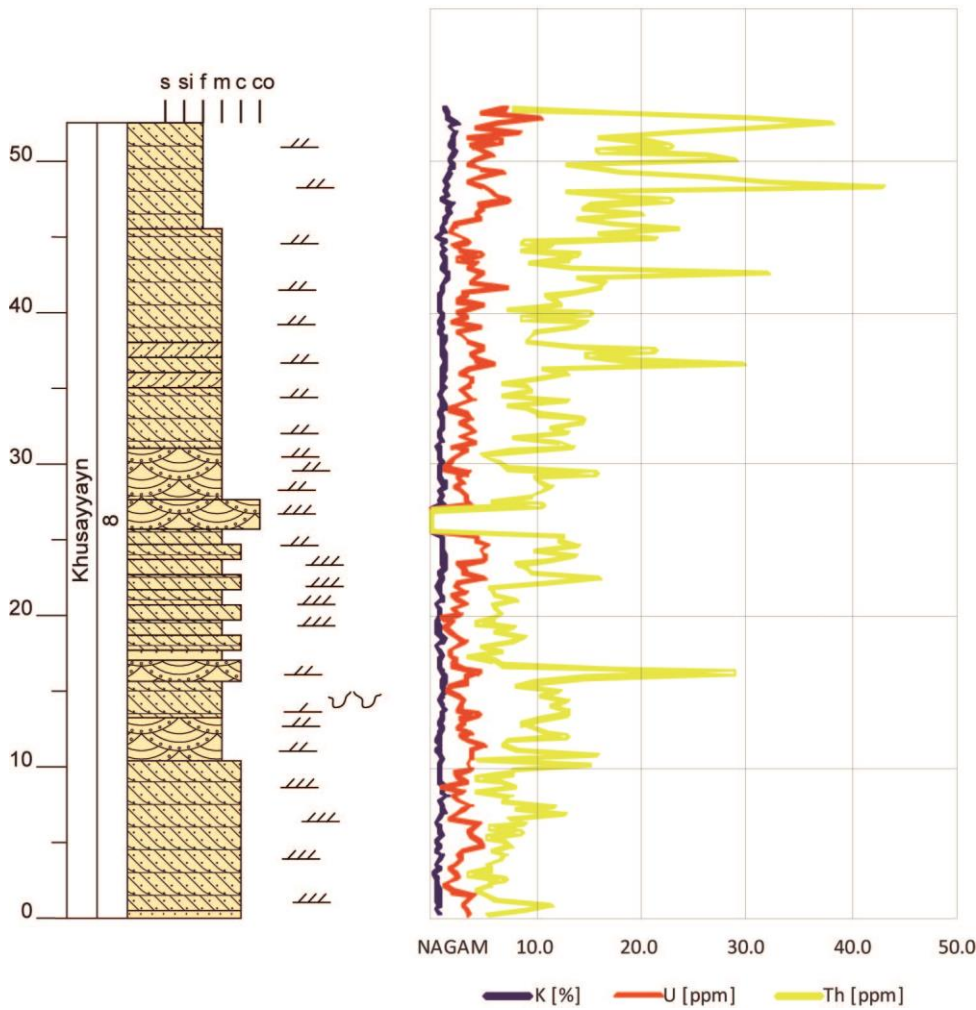


Figure 39: Combined lithological and (spectral) gamma-ray log of the Khusayyayn Formation at Jabal Khusayyayn. Gamma-ray data taken from Schönrok (2011).

Table 2: Average K_2O and Feldspar content of Wajid Formations (Heberer 2012).

Formation	Average K_2O [%]	Average estimated feldspar content [%]
Juwayl	0.036	1.9
Khusayyayn	0.54	15
Sanamah	0.04	1.7
Dibsiyah	0.02	1.4

Juwayl Formation (Jabal Blehan)

The gamma-ray log of the Juwayl Formation at Jabal Blehan (Figure 40) has a total average API of 15 at the bottom, 60 API in the middle and 30 API at the top. Average concentrations for the particular elements are less than 1% K, ~ 2 ppm U and between ~ 2 ppm and 14 ppm Th. The log is strongly dominated by Thorium, which shows a dirtying up trend comprising almost the entire section. Highest overall readings of Thorium as well as a single high spike correlate to silty lithofacies at the top. Like in the log from the Jabal Khusayyayn there is a negative correlation between grain size and Th concentration, shown by coinciding fining-up and dirtying-up trends. A minor U peak seems to fall together with a change in lithology from coarse grained, massive sandstone (LF 12) to shale-siltstone alterations (LF 2), similar to the much more prominent U-peaks in the Jabal Atheer (Figure 38). Besides that, uranium readings neither show trends nor high single peaks.

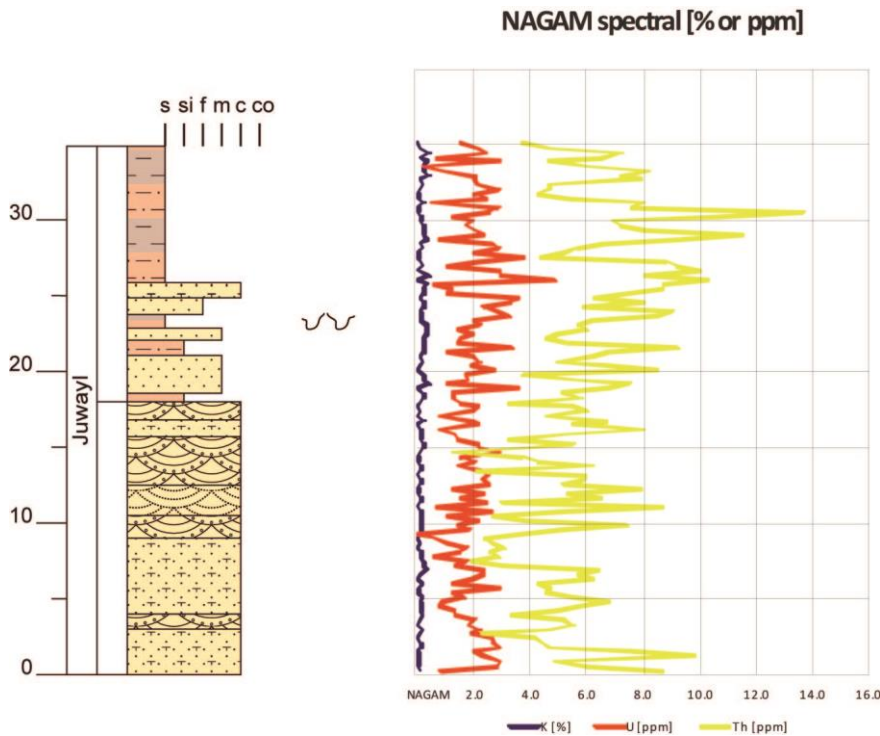


Figure 40: Combined lithological and (spectral) gamma-ray log of the Juwayl Formation at Jabal Blehan. Gamma-ray data taken from Schönrok (2011).

7.3. Natural gamma-ray and the standard Wajid log

Using the correlated gamma-ray and lithological logs from chapter 7.2 and the standard Wajid lithological log of chapter 5.5, a composite spectral gamma-ray log for most of the Wajid succession has been created (Figure 41). The overall gamma-log trends are dominated by thorium, with uranium being important only locally and often mimicking the thorium trends on a smaller scale. Potassium is in this scale irrelevant for trends throughout the logged succession; there is only one slight increase in potassium concentration visible, at the top of the lower Khusayyayn Formation, which coincides with a general increase of thorium and uranium concentrations. As increased K-feldspar contents are reported from samples from the Khusayyayn formation (Heberer 2012), it is surprising that the log does not reflect this more. This may be a matter of scale and detection limit of the handheld gamma-ray detector though. The uranium concentration shows two prominent spikes: In the middle part of the Sanamah Formation, uranium concentration eclipses thorium concentration by far. This is believed to be caused by iron crusts.

The total natural gamma radiation stays constant, except an increase at the top of the Khusayyayn Formation and a reduction in the Juwayl Formation. Within the overall constant concentration levels – especially of thorium – there are two major bow trends visible, as well as several minor ones. One prominent dirtying up trend was located in the lower Khusayyayn Formation, as well as a minor one in the Juwayl Formation. These coincide with finig-up trends, implying at least a remote connection between grain size and Th concentration. Sudden positive as well as negative changes of concentration levels (spikes) also occur. Positive spikes of the thorium concentration can be found in the lower part of the upper Dibsiyah Formation and throughout the Khusayyayn Formation. Uranium concentration spikes are not necessarily linked with increased thorium concentrations. Negative concentration spikes (sudden drops of the concentration level) occur in the upper Dibsiyah Formation. Here, thorium concentration drops independently of the uranium readings, whereas in the middle Sanamah and lower Khusayyayn Formations, drops of thorium and uranium concentrations coincide. In the available scale, potassium concentrations show neither positive nor negative spikes, with the exception of one minor increase in K-readings at the top of the lower Khusayyayn Formation (Figure 39). This fits with the increased K-feldspar content of the Khusayyayn formation reported by Heberer (2012), but nevertheless K concentrations are surprisingly low compared to the feldspar content.

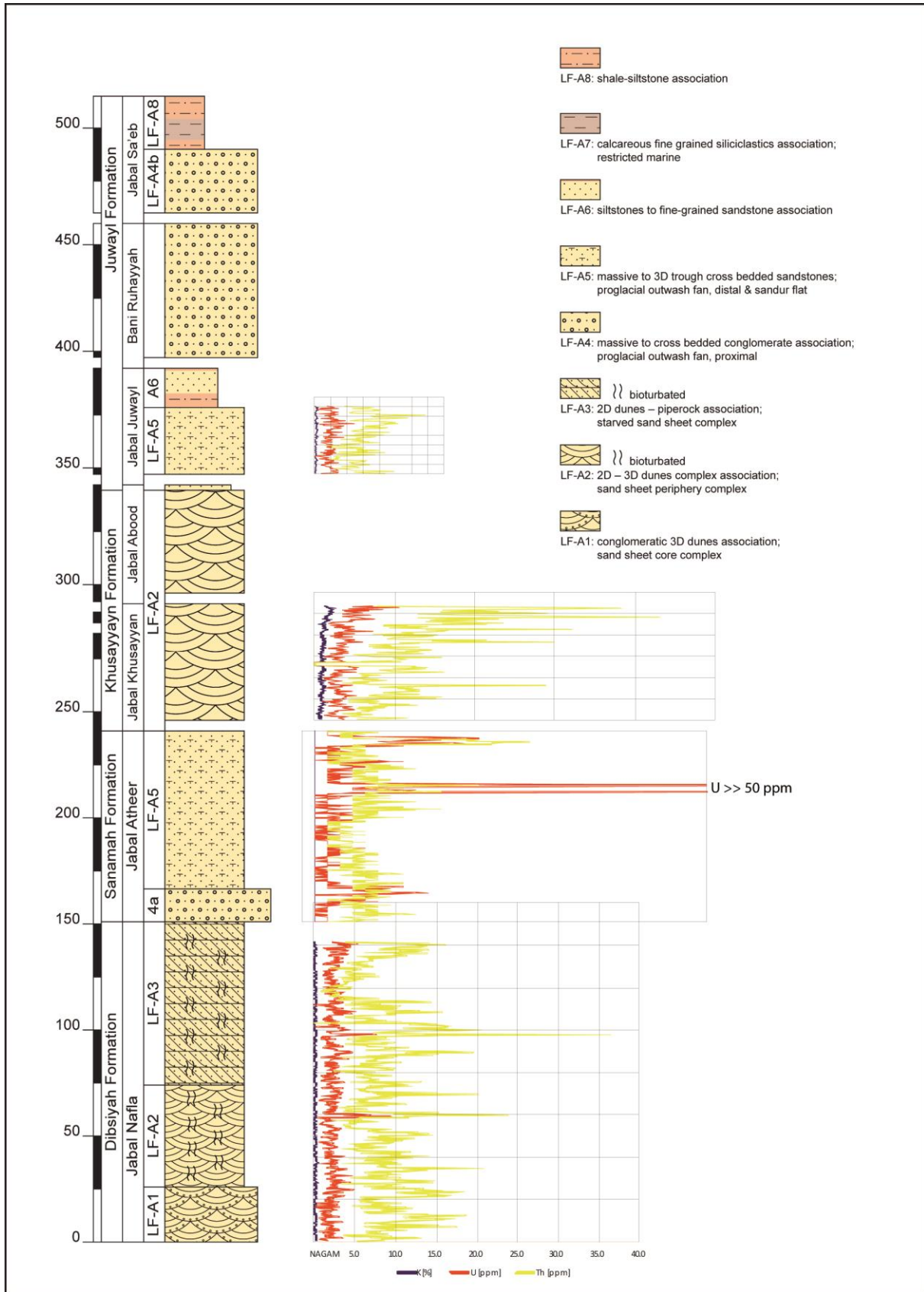


Figure 41: Combined log of (spectral) gamma-ray logs from Schönrok (2011) and the standard Wajid lithology (Chapter 5.5).

8. Reservoir characteristics

8.1. Theoretical background

Reservoir studies involve a large set of tools and scales, ranging from analysis of well cores, outcrop studies to basin analysis (Figure 42). The latter makes large-scale seismic data necessary and includes modelling. This study aims at contributing to a reservoir model of the Wajid Sandstone Group by an outcrop-analogue approach and a statistical analysis of petrophysical parameters from rock samples. Among those, porosity and permeability are the most important attributes of reservoir rock. They determine the amount of fluid a rock can contain and the rate at which that fluid can be produced (Bloch, 1994; in SEPM Short course 30). Prediction and/or interpolation of porosity and permeability are of fundamental importance to set-up mathematical reservoir models. Therefore a process-oriented understanding of both parameters is needed, because their variety is a result of complex geological processes. This includes rock texture, environment of deposition, and physical and chemical diagenesis during burial. These processes can only be resolved by studying the microfacies of rock samples, e.g. thin section analysis and raster electron microscopy (REM), sometimes complemented by mineralogical and geochemical analysis. In this study, a statistical analysis of 160 own petrophysical and hydraulic measurements within the Wajid Sandstone is carried out (chapter 8.2), which is complemented by a petrographical study of 38 samples in order to evaluate the reasons for variable porosities and permeabilities in the Wajid Sandstone Group (chapter 8.3). The reservoir characterization of the Wajid Sandstone Group in this thesis includes measurements and petrographical work of several student's projects and master theses, which are merged and analysed together here. The student's projects are Olowale (2010), Osemwegie (2011), and Ngole (2012). Diploma and master theses are: Filomena (2007), Dirner (2007), Olawale (2010), and Heberer (2012).

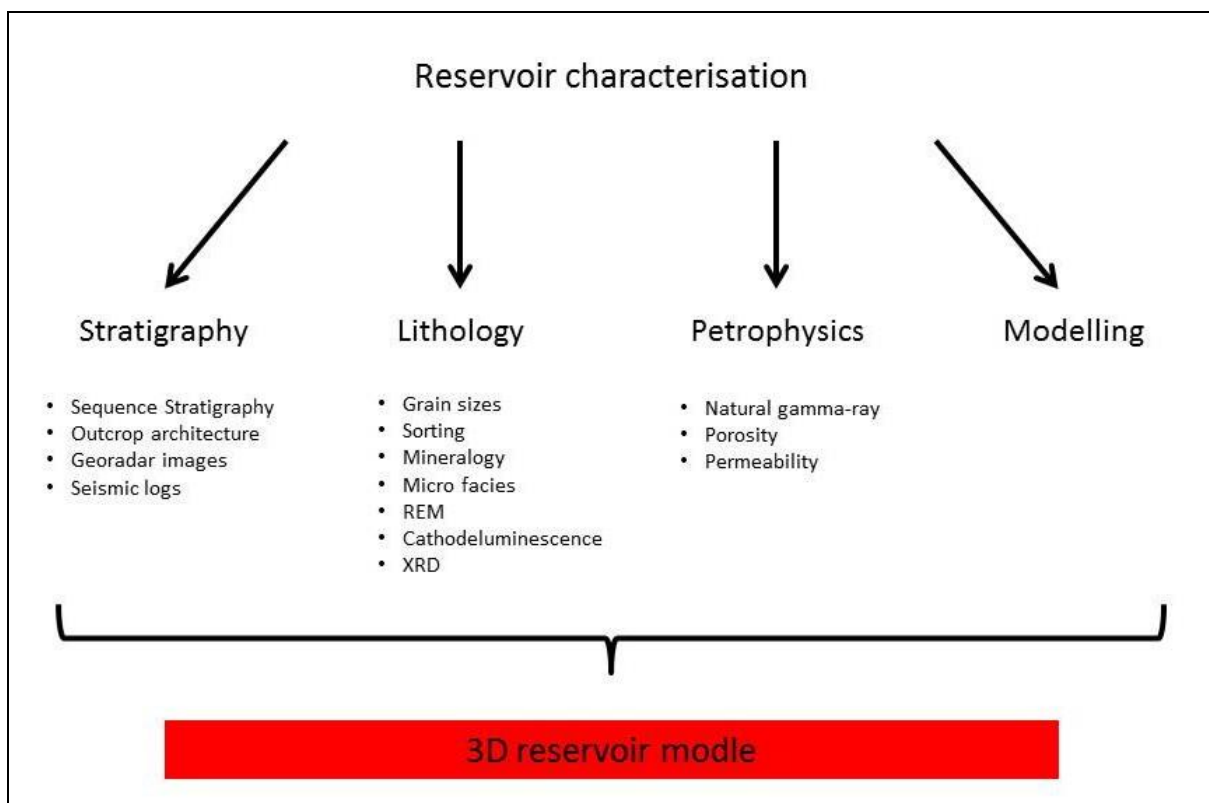


Figure 42: Flow chart of reservoir characterization of sedimentary rocks (after Hornung, 1999). This study focuses on lithology and petrophysics.

8.2. Porosity and permeability

8.2.1. Statistics

Figure 43 and Figure 44 give a visual summary of measured porosities and permeabilities grouped by formations and lithofacies. Some lithofacies types are not represented, because they are finer than siltstones or they have only little extension. The median of porosities varies little among the formations and ranges between 23 and 27%. Scatter of data is very low in the Khusayyan Formation (ca. 4% non-outlier range) and highest in the Juwayl Formation (ca. 40% non-outlier range). The Dibsiyah and Sanamah Formations show moderate scatter with ca. 10% non-outlier range. According to the median, Sanamah and Juwayl Formations show positively skewed distribution, i.e. low porosities are dying out over a larger range. Different permeability measurements all show highest medians of 1500 to 2000 mD for the Khusayyan Formation and lowest medians of 300 to 1400 mD for the Dibsiyah Formation. The variability is highest for the Sanamah Formation and the Juwayl Formation. The permeability measurements are further compared in chapter 8.2.2.

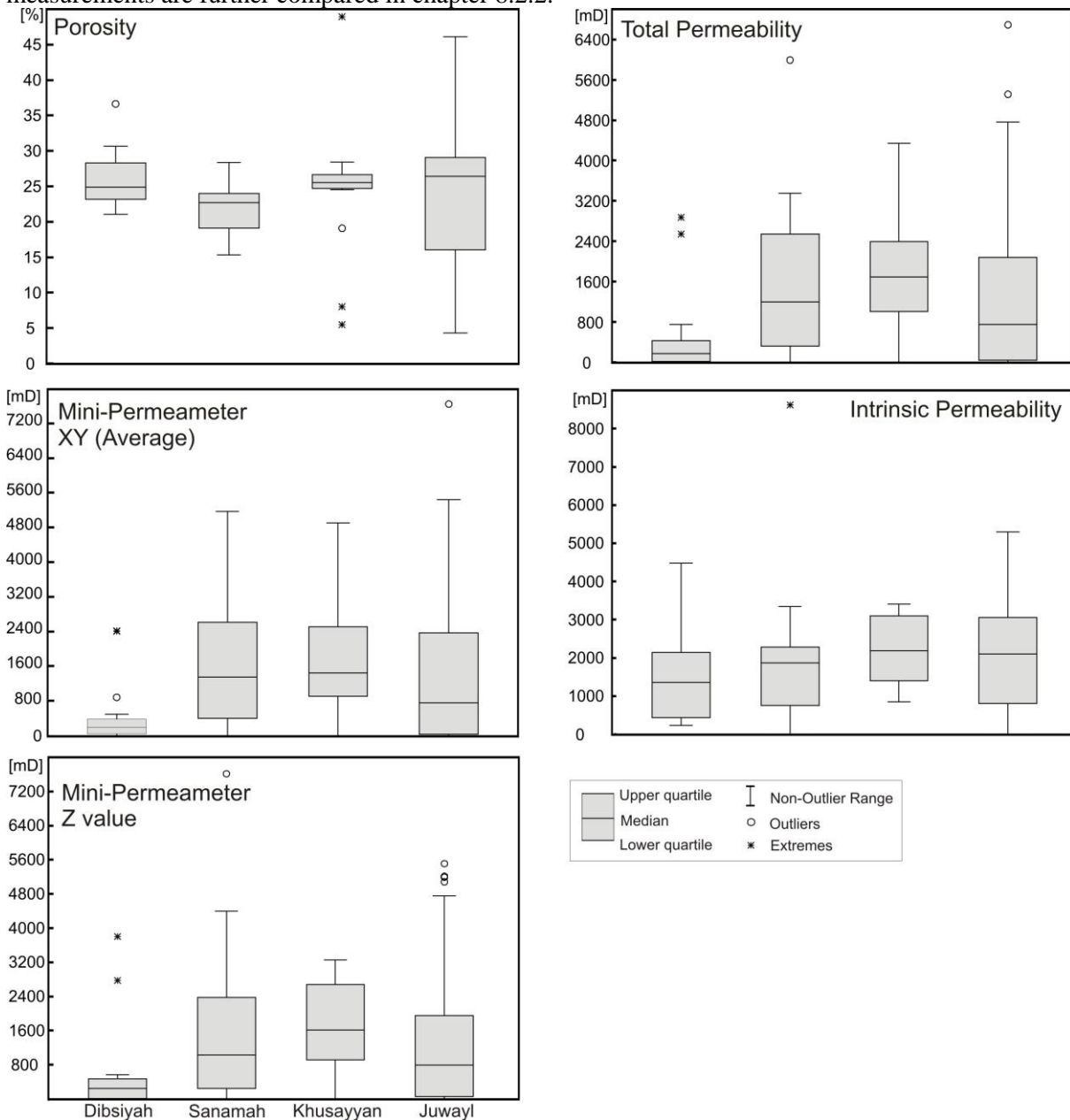


Figure 43: Box plots of porosities and permeabilities grouped by formations.

Lithofacies types are roughly arranged by increasing grain sizes and decreasing sorting. The median of porosity is highest for siltstone to fine sandstone (LF4), and lowest for siltstone (LF3). Mixing with pebbles (LF 10 and LF11) tend to reduce porosity, most probably because of poorer mixing. Surprisingly, the massive sandstone LF12, which looks very homogenous in hand specimen, has a relatively low porosity. The reasons will be investigated in chapter 8.3. by petrographical analysis. The different permeabilities roughly follow porosities, except the fine-grained LF4. This indicates that the connectivity of pores is reduced here.

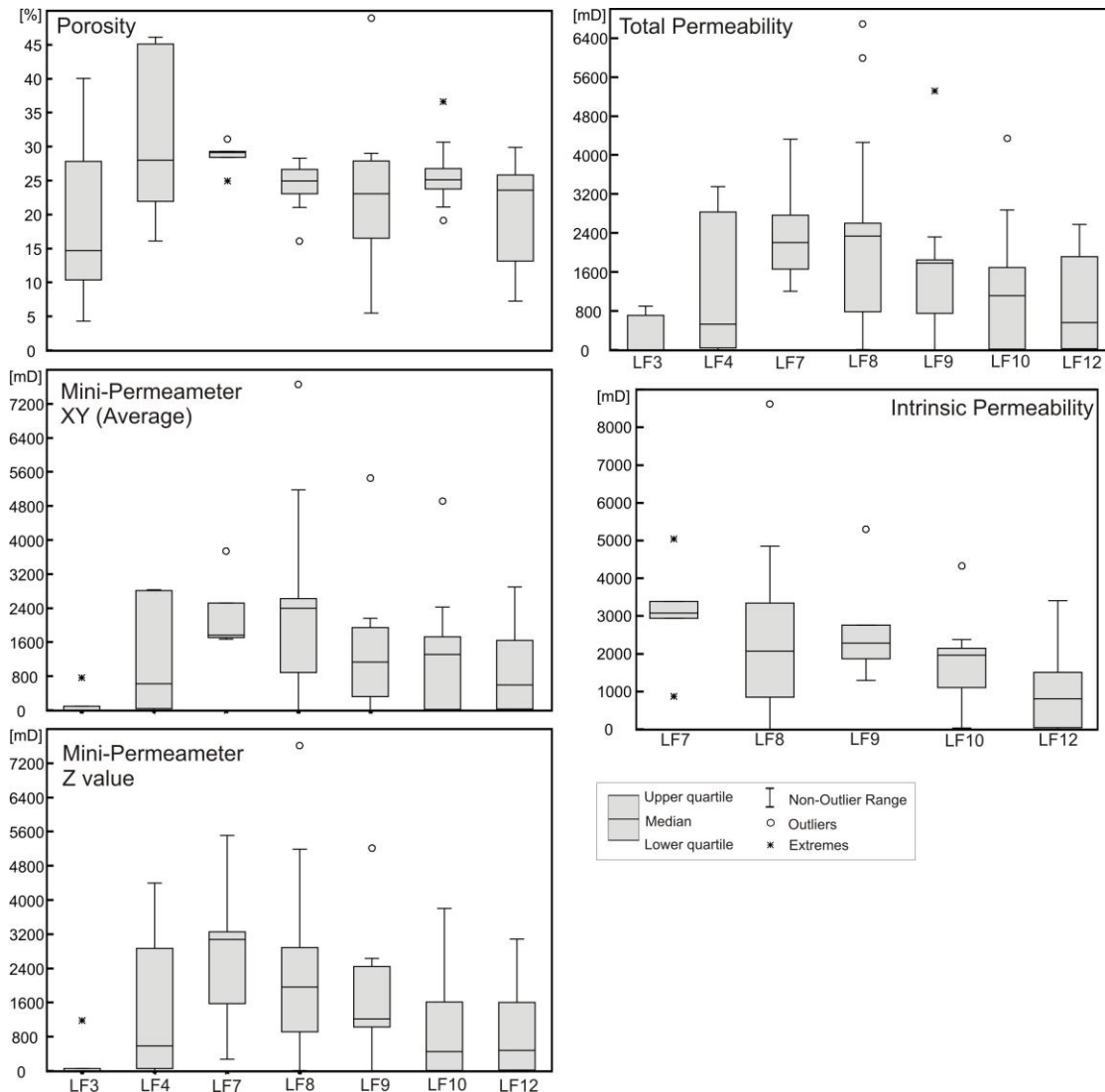


Figure 44: Box plots of porosities and permeabilities grouped by facies types (see chapter 5.2).

8.2.2. Anisotropy

Anisotropy was tested by a triangular plot of oriented measurements with the mini-permeameter, where x,y are horizontal permeabilities, and z vertical permeabilities (Figure 45). Samples outside the central triangle show anisotropy of more than 50% in one direction. The majority of samples plot inside the triangle, i.e. they are not significantly anisotropic. The Dibsiyah and Sanamah Formations show the most anisotropic samples, whereas anisotropy in the Khusayyayn and Juwayl Formations are rarer. Referring to lithofacies types, LF3, LF10 and LF12, they show strongest scatter and to be the most anisotropic samples. This can be explained by oriented texture for the fine-grained texture in LF3 and strong bioturbation in LF10. Again, LF12 shows often anisotropy, although the massive sandstone looks quite homogenous.

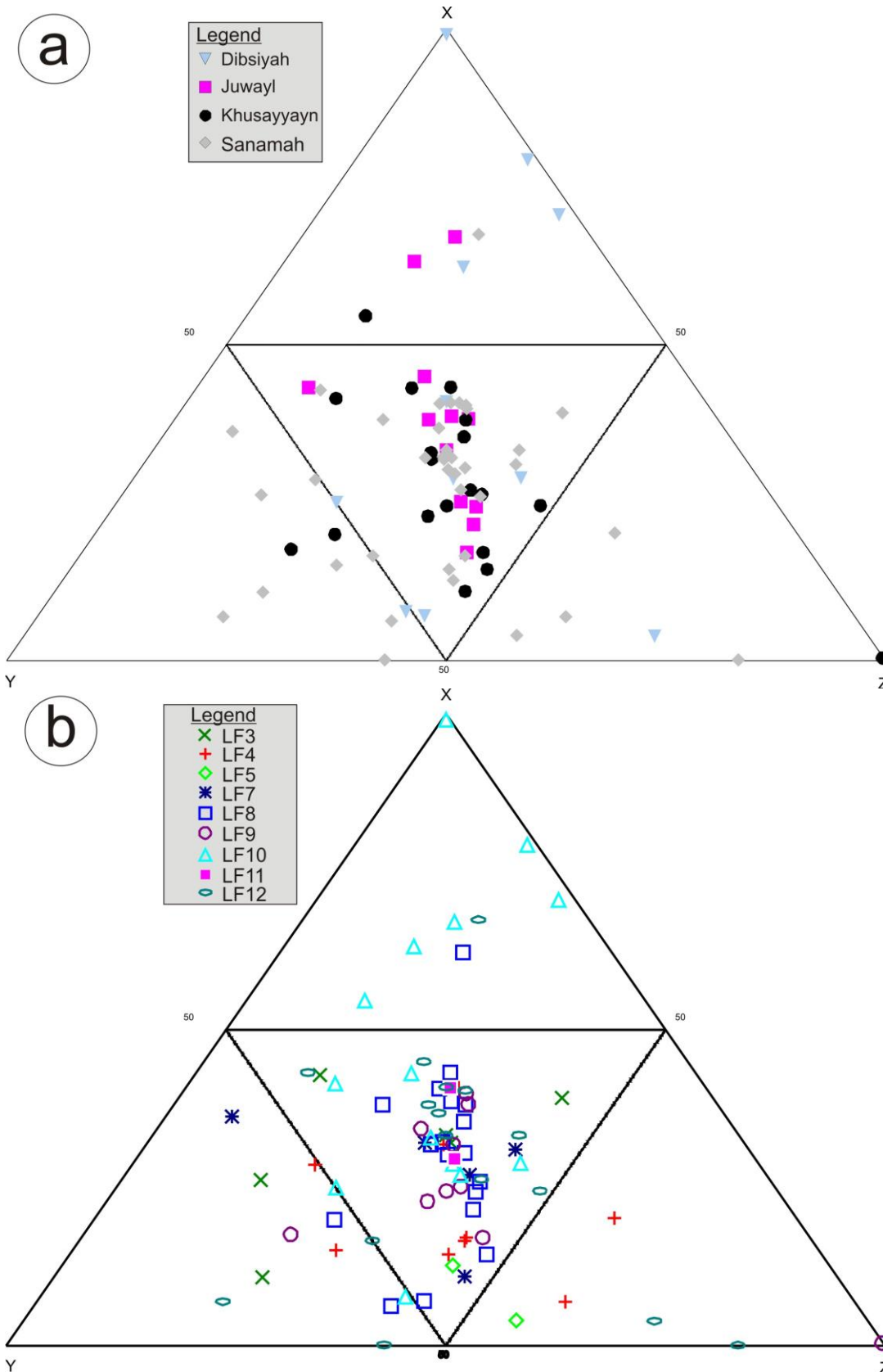


Figure 45: Triangular plot of oriented measurement of permeabilities with the mini permeameter. a. Grouped according to formations, b. grouped according to lithofacies.

8.2.3. Total and intrinsic permeability

In order to compare the two different methods of permeability measurements, the average from x,y,z orientations from the mini-permeamter and the intrinsic permeability of 70 column measurements are

plotted together (Figure 46). Both correlate very well with a correlation coefficient of $r^2 = 0.96$. This means that mini-permeameter measurements are representative also for liquid permeabilities such as water. Because of the larger data set and the information about orientations, only mini-permeameter measurements are used for further analysis.

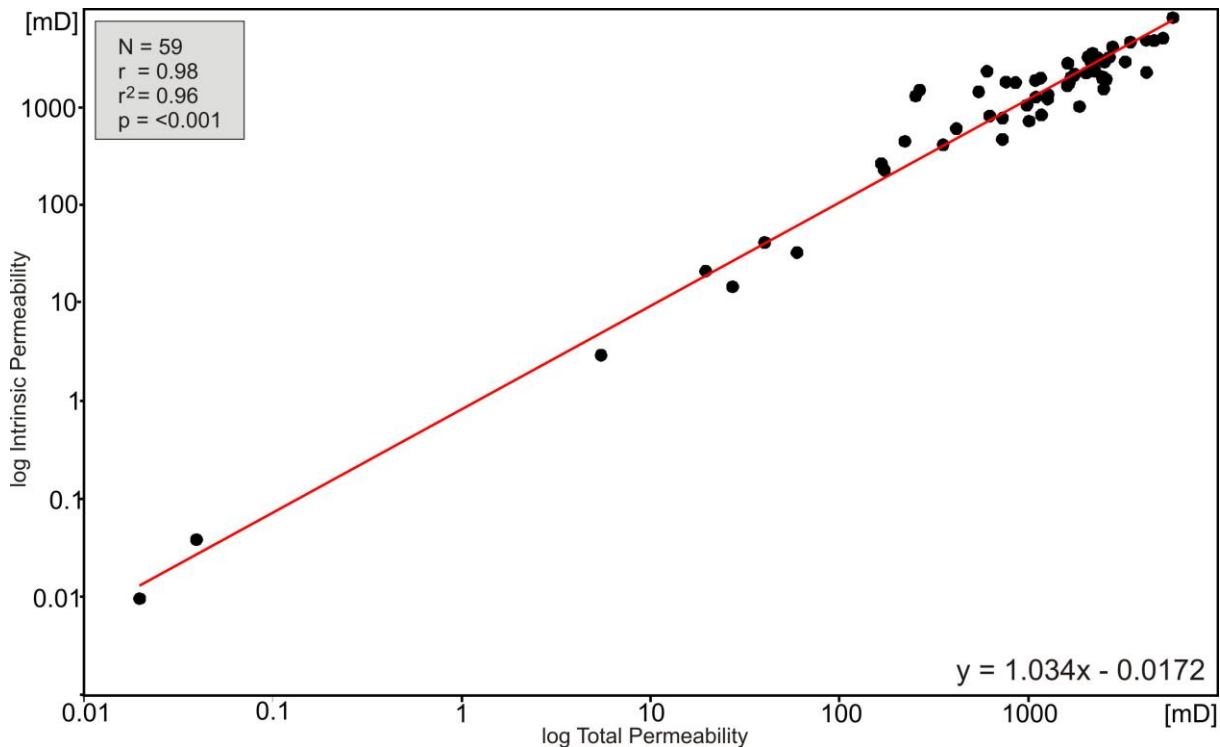


Figure 46: Correlation log total Permeability vs log intrinsic permeability.

8.2.4. Crossplots porosity and permeability

The correlation of porosity versus permeability depends on the geometry and connectivity of pores in a sample and is often relatively poor. This is also the case for the Wajid Sandstone samples. Correlation coefficients for formations and lithofacies are both weak with r^2 ca. 0.2, but both show a significant positive trend (Figure 47). Identical porosities can result in permeabilities ranging over five magnitudes. Again, specific trends can be detected. The Dibsiyah and Sanamah Formations show strongest deviation from the regression line, except two samples from the Khusayyayn Formation. Furthermore, the Juwayl Formation tends to lower porosities at the same permeabilities than the other formations, i.e. pointing to a more efficient connectivity and pore distribution compared to the others. Sandy to pebbly, cross bedded lithofacies types plot close to the regression line such as LF7 and 8, and with exceptions also LF10. Bioturbated samples and massive sandstones show a relatively high permeability compared to their porosity, which may be interpreted as homogenization of the grain fabric (LF9, LF12). Finer grained samples show the expected opposite trend, but some exceptions exist (LF3, LF4).

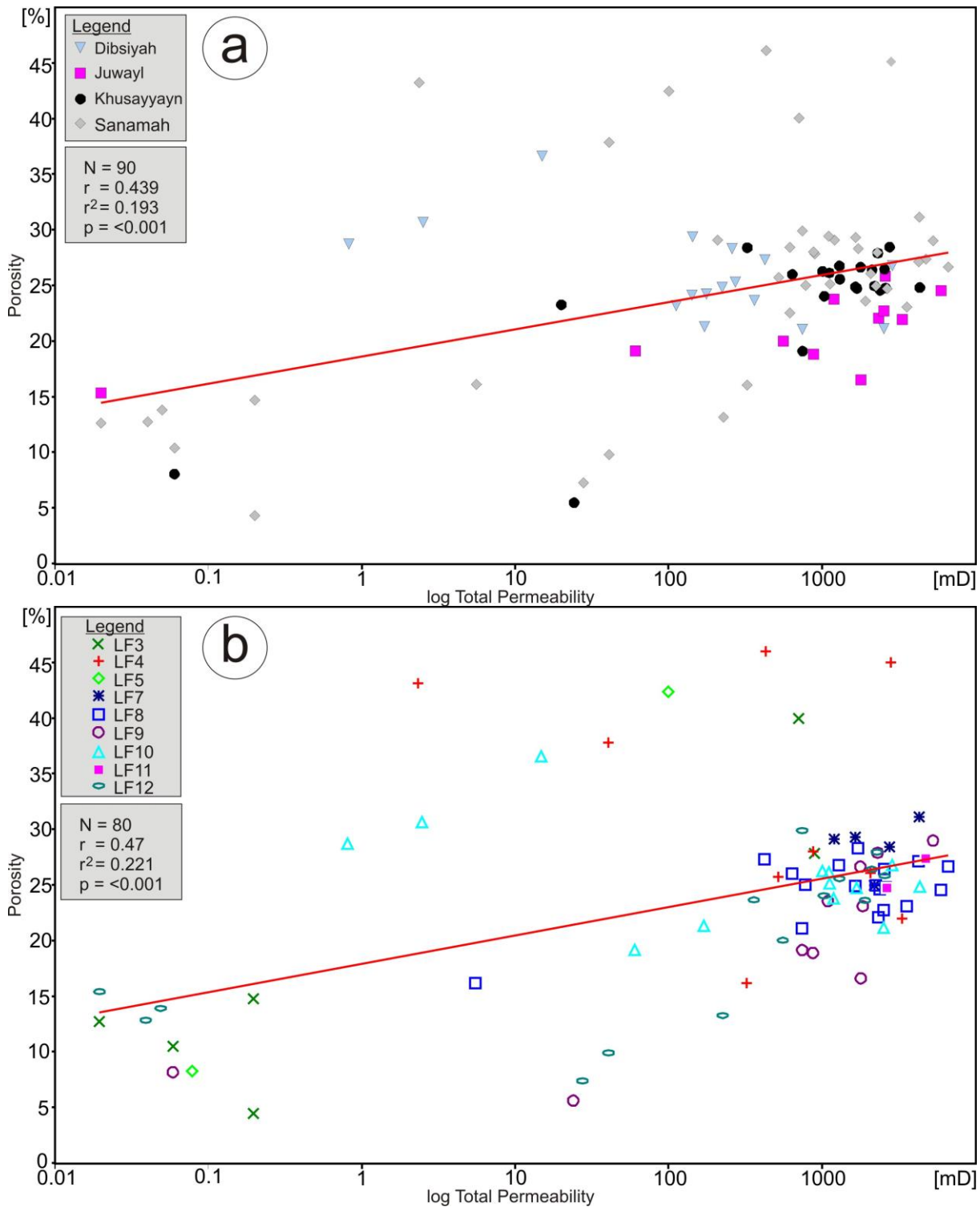


Figure 47: Cross plots of porosity versus total permeability from mini permeameter measurements. a. Grouped according to formations, b. grouped according to lithofacies.

8.2.5. Hydraulic permeability

Table 3 and Figure 48 show measured gas and water permeabilities. Gas permeability has relatively higher values than water permeability as shown by their maximum and minimum values and their means or medians. Both are often skewed to lower values. Nevertheless, there is strong scatter to which degree water are lower than gas permeabilities ranging from 4 to 95%. This underlines the individual geometrical conditions of the pore space in the samples. The differences in gas permeabilities between the formations as shown in section 8.2.1, hence, are also valid for water permeabilities. Fig x shows that gas and water permeabilities correlate well with a correlation coefficient of $r^2 = 0.86$ (Figure 49). This means that in

principle gas permeabilities can be used to predict water permeabilities. In particular, this is valid for higher permeabilities, which are of specific practical importance.

Table 3: Gas and water permeabilities of selected Wajid Sandstone Samples (data from Ngole, 2012). Conversion factor of 1D into m s⁻¹ = 9.66x10⁻⁶ (Freeze & cherry, 1979).

Sample ID	Formation	Lithofacies	Gas (intrinsic) permeability [mD]	Water permeability		Proportion of water from gas permeability
				[mD]	[ms ⁻¹]	
Wuh-1-9	Juwayl	-	4044,3	2583,81	2,5E-05	0,64
Wuh 3(4)	Juwayl	LF 8.2.1	1131,3	322	3,1E-06	0,28
Wkh-T-2	Khusayyayn	LF 10	111,3	3,68	3,6E-08	0,03
Wsh-1-18	Sanamah	LF 12.4	1042,3	306,98	3,0E-06	0,29
Wuh-4-3	Juwayl	LF 7	1671,4	1308,8	1,3E-05	0,78
Wuh-2-10	Juwayl	LF 4	3718,4	2256,56	2,2E-05	0,61
Wkh-3-13	Khusayyayn	LF 8.2	871,51	567,5	5,5E-06	0,65
WDSK 5	Sanamah	LF 8.5	3085	2339,4	2,3E-05	0,76
Wuh-3 (6a)	Juwayl	LF 8.6	1593,5	367,08	3,5E-06	0,23
WS-1-17	Sanamah	LF 12.2	2,9	2,32	2,2E-08	0,80
WDSK 17a	Sanamah	LF 9	1715,7	410,8	4,0E-06	0,24
Wuh-2-1	Juwayl	LF 11.2	2265,8	134,2	1,3E-06	0,06
S-1-1	Sanamah	LF 8.5	1734,1	1127,5	1,1E-05	0,65
Wuh-2-16	Juwayl	LF 8.1	4,8	0,2	1,9E-09	0,04
WKh-T-10	Khusayyayn	LF 8.2	1847,9	481,76	4,7E-06	0,26
WD - 1 a	Dibsiyah	-	4676,7	4551,94	4,4E-05	0,97
WD - 05	Dibsiyah	-	1330,1	221,95	2,1E-06	0,17
WD - 06 a)	Dibsiyah	-	1952,6	665,17	6,4E-06	0,34
WD - 12	Dibsiyah	-	2388,9	1646,12	1,6E-05	0,69
WS - 04	Sanamah	-	23,4	4,13	4,0E-08	0,18
SWJ 3.2	-	-	2718,3	2581,15	2,5E-05	0,95
WJ 1.2	-	-	4361,8	1075,48	1,0E-05	0,25
WJ 1.3	-	-	4467,3	1549,43	1,5E-05	0,35
WJ 5	-	-	2066,9	672,28	6,5E-06	0,33
Wuh-1-5/Fard base	Khusayyayn	-	1481	737,6	7,1E-06	0,50

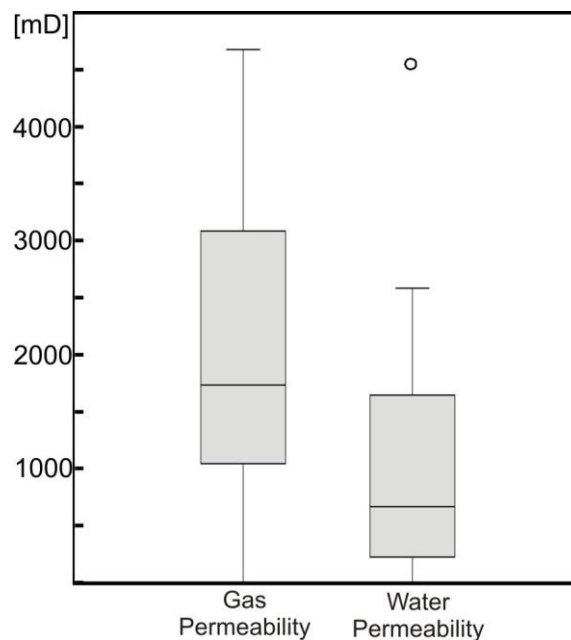


Figure 48: Box plot of gas and water permeability in mD of selected Wajid Sandstone Samples (data from Ngole, 2012).

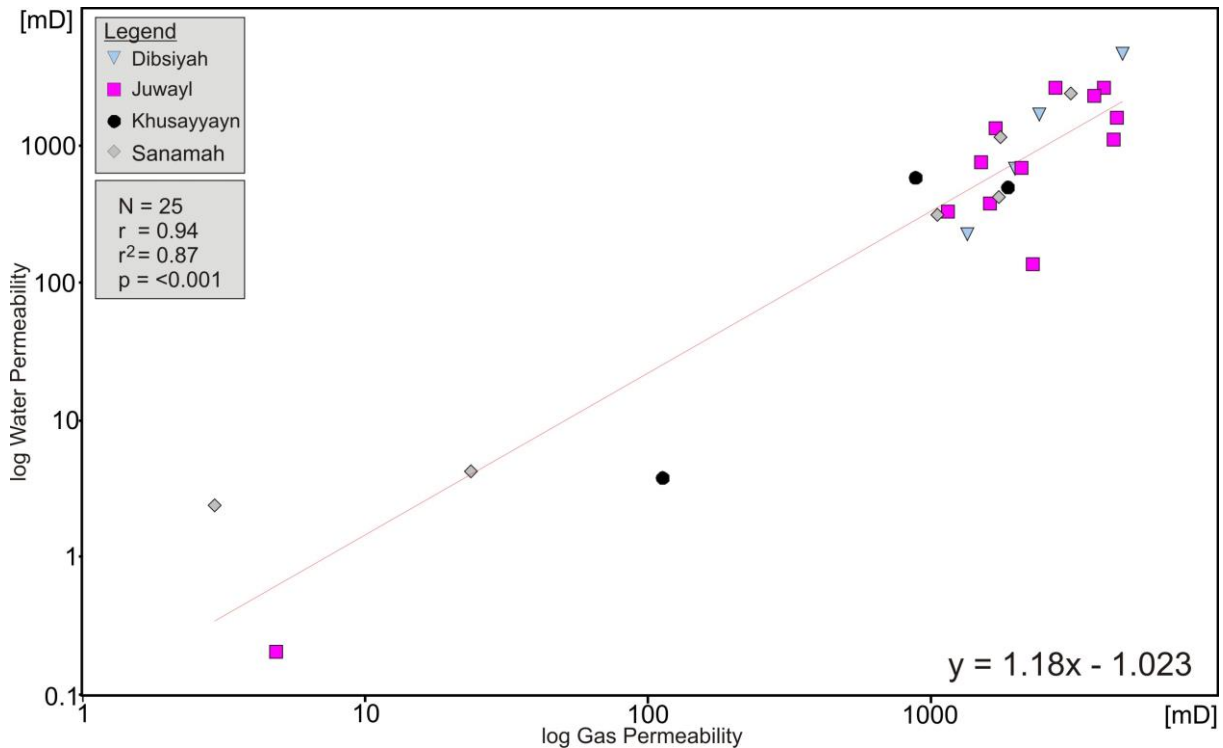


Figure 49: Cross plot of gas versus water permeability in mD.

8.3. Reservoir characterisation

8.3.1. Poroperm and sedimentary facies

Statistical analysis of porosities and permeabilities in chapter 8.2 demonstrated that grain texture (e.g. grain sizes, sorting) is obviously a controlling factor, however, it does not explain some wide scatter and significant differences between similar lithofacies types. Some additional factors could be identified by sedimentological analysis in the field, such as anisotropies and fabric rearrangements due to bioturbation. The different formations of the Wajid sandstone group comprise distinct lithofacies types and thus different depositional environments (Chapter 5). In turn, this leads to distinct pattern of porosities and permeabilities. Although porosities are not significantly different between the formations, their variability mirrors heterogeneities. They have been found being minor in the Khusayyayn Formation and pronounced in the Juwayl Formation. The Khusayyayn also show the highest permeabilities on average. Variabilities are again high in the Juwayl Formation and also in the Sanamah Formation. Both show strong variation in grain textures and lithofacies types due to their proglacial setting representing very different hydraulic conditions and including glacial impact (chapter 6). Anisotropy is highest in the Dibsiyah and Sanamah Formations which is at least partly caused by bioturbation.

Both also show strongest deviation from the regression line porosity versus permeability. The Juwayl Formation exhibits lower porosities at the same permeabilities, which was interpreted as a more efficient connectivity and pore distribution.

8.3.2. Poroperm and petrology

The question of wide scatter of porosities and permeabilities as well as weak correlation of some lithofacies types with permeability still needs to be solved, because it cannot simply be based on grain texture and sedimentary structures. Heberer (2012) carried out a detailed microfacies study using thin sections and raster electron microscopy of selected rock samples of sections in this thesis. For 38 samples, petrological results can now be compared with porosity and permeability measurements. In particular, diagenetic imprint and primary versus secondary porosities can be evaluated as additional controlling factors.

Table 4 displays permeabilities and selected petrological data from Heberer (2012) which are believed to play a role in controlling reservoir properties, matrix, cement, sorting, and rounding. Qualitative estimates were converted in numerical classes in order to perform statistical analysis. To evaluate the relative importance of factors a principal component analysis (PCA) was carried out for column and mini permeameter measurements separately.

The PCA for intrinsic permeability show similar weighting with pore space, connectivity and rounding, whereas matrix and cement show opposite trends (Figure 50a). This corresponds more or less to what is theoretically expected. The Dibsiyah and Sanamah Formations preferentially group in the lower quadrangles. The major reason is widespread iron cementation (Fig Figure 51a), which is also obvious from the intense red colours of these sandstones in the field (Chapter 5). Furthermore, rounding is usually good to very good which is a result of very mature, multi-cycled, quartz-rich sand (Wanas & Abdel-Maguid, 2006). The Khusayyayn Formation is closely grouped and again shows minor heterogeneity. Thin sections show a large amount of altered feldspar, in particular orthoclase, but also microcline is present. The Khusayyayn sandstones are exceptional in the Wajid Sandstone Group because of their arkosic composition. Conserved feldspar content reach 20%. On the one hand side, feldspar alteration leads to secondary porosity, on the other hand side the proportion of pseudo matrix increases. Feldspar alteration also produces higher amounts of calcitic cement. Both lead to the unique grouping of the Khusayyayn Formation in the PCA plot. The highest scatter is observed again for the Juwayl Formation. Thin section analysis shows samples with iron cementation (Wuh-1-2) similar to the lower Wajid formations, but also some with increased pseudo matrix (Wuh-4-9-12). Others show strong leaching and voluminous secondary porosities (e.g. Wuh1-1, Wuh-1-4, Wuh-4-2, Wuh-4-3, Figure 51). The PCA plot in Figure 50b based on mini permeameter measurements shows a similar pattern as described for intrinsic permeability. Permeability shows same tendencies such as sorting and pore space and opposite trends to cementation and rounding. The close orientation of x,y,z directions show low relevance of anisotropy at the microfacies scale, where bioturbation may only indirectly interfere textures and cementation

Table 4: Porosities, permeabilities and potential controlling factors from thin section analysis. Percentage estimates are taken directly from Heberer (2012), whereas matrix, cement, sorting, and rounding were classified from qualitative estimates in order to carry out statistical analysis.

Legend (classes): 1 = existing, 2 = present, 3 = abundant.

Sample and Facies			Permeability					Petrology								
			MINI-PERMEAMETER				COLUMN-Perm	Cement + Pseudo-Matrix %	Pores %	Cement Ca class	Cement Fe class	Cement Qz class	Pseudo-Matrix class	Connec-tivity class	Rounding class	Sorting class
Sample Name	Formation	Lithofacies units	X mD	Y mD	XY (avg.) mD	Z mD	Intrinsic mD									
Wuh-4-9-12	Juwayl	LF-12.4, LF-7.1	1008,17	687,26	847,71	798	811,05	8	5	2	2	3	2	4	2	3
WDSK-18	Sanamah	LF-4	1720,53	3932,73	2826,64	4400,04	3045,9	10	20	1	2	1	3	4	3	3
WDSK-1	Sanamah	LF-10, 10.1, 10.2, 10.21	122,81	28,23	75,52	32,01	34,20	30	2	2	2	2	3	1	3,5	2,5
WKh-T-9	Khusayyayn	LF-12.2	3840,4	713,67	2510,03	1139	1065,3	25	10	2	2	2	2	1	3	4
WDSK-5b	Sanamah	LF-8.5	3879,97	6483,34	5181,66	7613,76	8617,4	10	25	1	2	2	1	4	3	2
WKh-T-12	Khusayyayn	LF-12.1	1033,35	1284,97	1159,16	1603,86	1405,2	10	8	2	2	3	2	3	3	3
WDSK-16	Sanamah	LF-12.1	3473,1	2317,34	2895,22	1931,72	1605,3	20	20	1	3	2	3	2	2,5	3
Wuh-1-4	Juwayl	LF-7.1	4038,29	3438,44	3738,37	5510,65	5043,4	5	40	1	1	2	1	1	2	4
WDh-1-top	Dibsiyah	LF-12.5	445,74	320,41	383,07	321,82	433	10	25	1	1	1	2	2	3,5	2,5
WKh-T-2	Khusayyayn	LF-10	5621,68	4210,24	4915,96	3194,85	2374,6	15	10	2	2	2	2	1	2,5	3
WKh-T-1	Khusayyayn	-	1106,86	1154,38	1129,95	1213,34	1300,5	20	5	2	2	2	3	4	2,5	3
Wuh-4-3	Juwayl	LF-7	1308,88	2030,08	1669,48	273	872,4	3	30	1	2	3	0	4	3	3
WDSK-5	Sanamah	LF-8.5	1712,34	2408,05	2060,19	2891,39	3343,7	5	30	2	2	2	2	4	1,5	3,5
WDh-1-9	Dibsiyah	LF-10	2191,2	2653,29	2422,24	2773,95	2143,5	2	30	1	2	1	1	1	3	2
WDSK-17-a	Sanamah	LF-9	664,79	939,89	802,34	1030,8	1340,8	10	30	1	3	2	0	1	3,5	1
Wuh-4-5	Juwayl	LF-8.2.1	2691,96	2059,93	2375,94	2230,64	3079,1	3	30	1	2	1	0	2	3	1,5
Wuh-1-2	Juwayl	LF-8.1	1673,66	1768,1	1720,88	1734,33	2101,8	5	30	2	3	2	2	1	3	2,5
WKh-T-10	Khusayyayn	LF-8.2	1435,78	3782,76	2609,27	1962,82	3343,7	20	5	2	1	2	3	2	3	2,5
WKh-T-11	Khusayyayn	LF-10.4	1391,64	1399,73	1395,67	560,51	1110,7	15	10	1	2	2	2	2	2	2,5

WDh-1-52	Dibsiyah	LF-8.5	1402,37	381,4	891,89	468,92	492,1	20	1	2	2	1	2	2	3	3
WDh-1-13	Dibsiyah	LF-10	39,61	259,48	149,54	212,62	277,66	8	20	1	2	1	2	4	3,5	1
WKh-T-3	Khusayyayn	LF-8.2	1685,85	1083,83	1384,84	1124,75	1265,4	20	5	2	2	2	3	1	3	3
WKh-T-6	Khusayyayn	LF-8	1894,59	1424,89	1659,74	1647,52	1734,8	10	5	2	2	2	2	2	2,5	3
WDSK-9	Sanamah	LF-10.2, LF-12.5	1947,11	679,04	1313,08	455	1975,2	5	30	2	2	2	2	3	3	3
WKh-T-8	Khusayyayn	LF-10.1	1669,81	1787,6	1728,71	1613,04	1847,7	5	20	3	2	2	1	1	2	3
Wuh-1-1	Juwayl	LF-7.1	1602	1806,6	1704,61	1574,8	2321,5	5	25	1	1	3	1	4	3	4
WDh-1-7	Dibsiyah	LF-10.4	2490,88	2332,34	2411,61	3802,4	4325,8	3	25	1	2	1	1	1	3,5	3
Wuh-4-2	Juwayl	LF-9.1	6444,92	4464,68	5454,8	5214,05	5300,2	5	20	1	2	3	1	1	2,5	2,5
WDh-1-51	Dibsiyah	LF-8.2.2	91,1	626,2	358,65	562,73	634	25	5	2	3	2	1	1	3	2,5
Wuh-5-26-31	Juwayl	LF-8.3	2131,42	1934,49	2032,95	2032,95	2776,8	5	12	2	2	2	2	2	3	3
WDh-1	Dibsiyah	-	13,21	81,62	47,42	241,21	-	10	20	1	2	2	1	2	4	2
Wuh-5-32-33	Juwayl	LF-4	400,85	1455,64	928,25	793,4	-	5	10	2	1	1	0	7	2,5	3
Wuh-1-5	Juwayl	LF-9.2	660	1171,74	915,89	1052,41	-	2	5	1	1	2	2	1	3	4
Wuh-1-top	Juwayl	LF-4	1,44	1,47	1,45	4,21	-	5	20	1	3	2	3	1	2,5	3
Wuh-5-1	Juwayl	LF-4	2707,24	2915,06	2811,15	2866,23	-	40	1	2	1	2	1	1	3	2,5
Wuh-4-1	Juwayl	LF-4	450,41	796,98	623,7	327,61	-	2	30	1	1	3	1	1	2,5	2
Fard A	Juwayl	LF-3.1	0,28	0,29	0,29	0,3	-	5	30	2	2	2	-	6	3	3
Fard B	Juwayl	LF-3.1	25,87	155,2	90,54	56,33	-	10	2	2	2	3	-	3	2,5	3

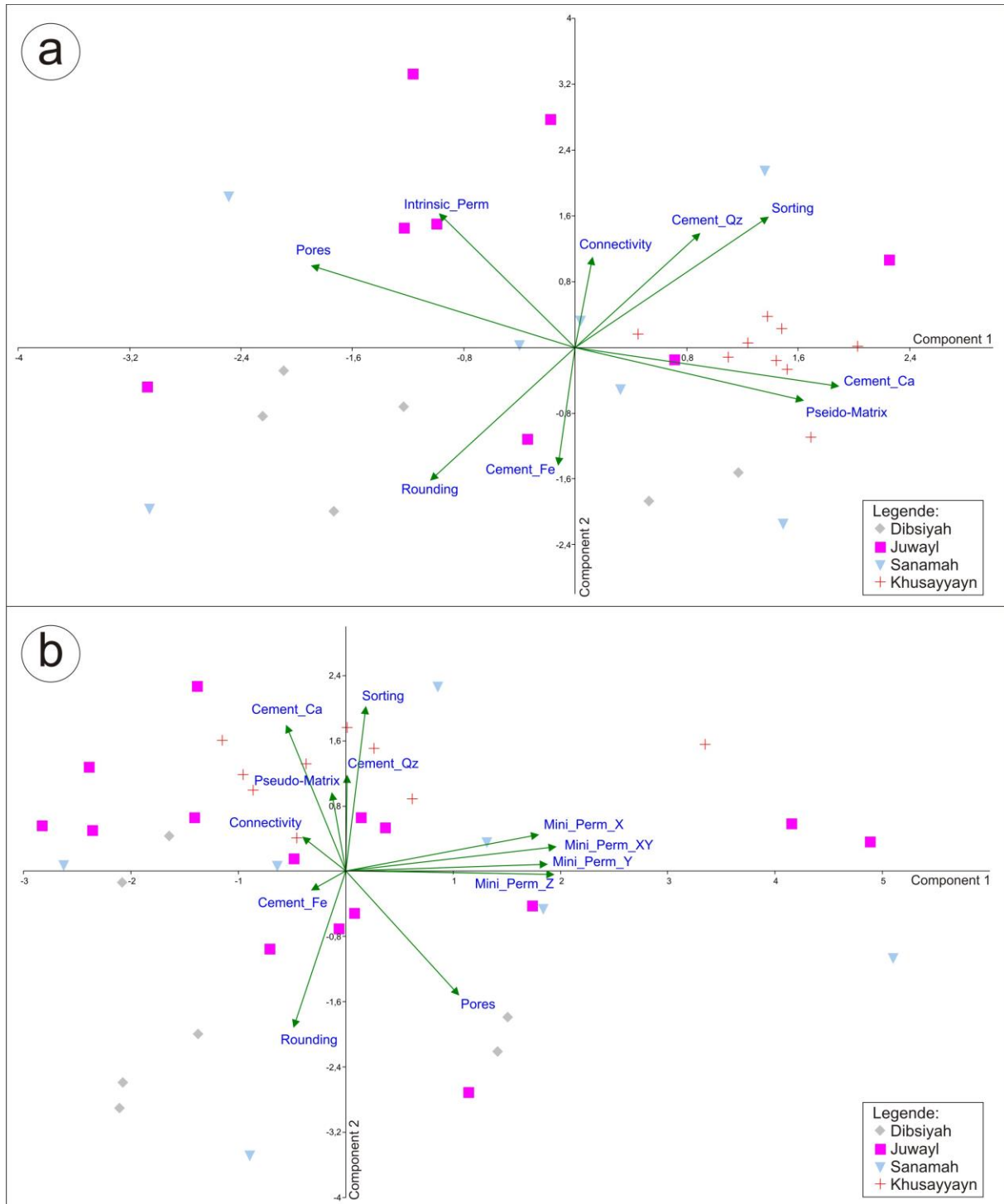


Figure 50: Principal component analysis of microfacies parameters relevant for reservoir properties. Grouped according to formations. A. Intrinsic permeability, b. x,y,z directions measured by a mini permeameter.

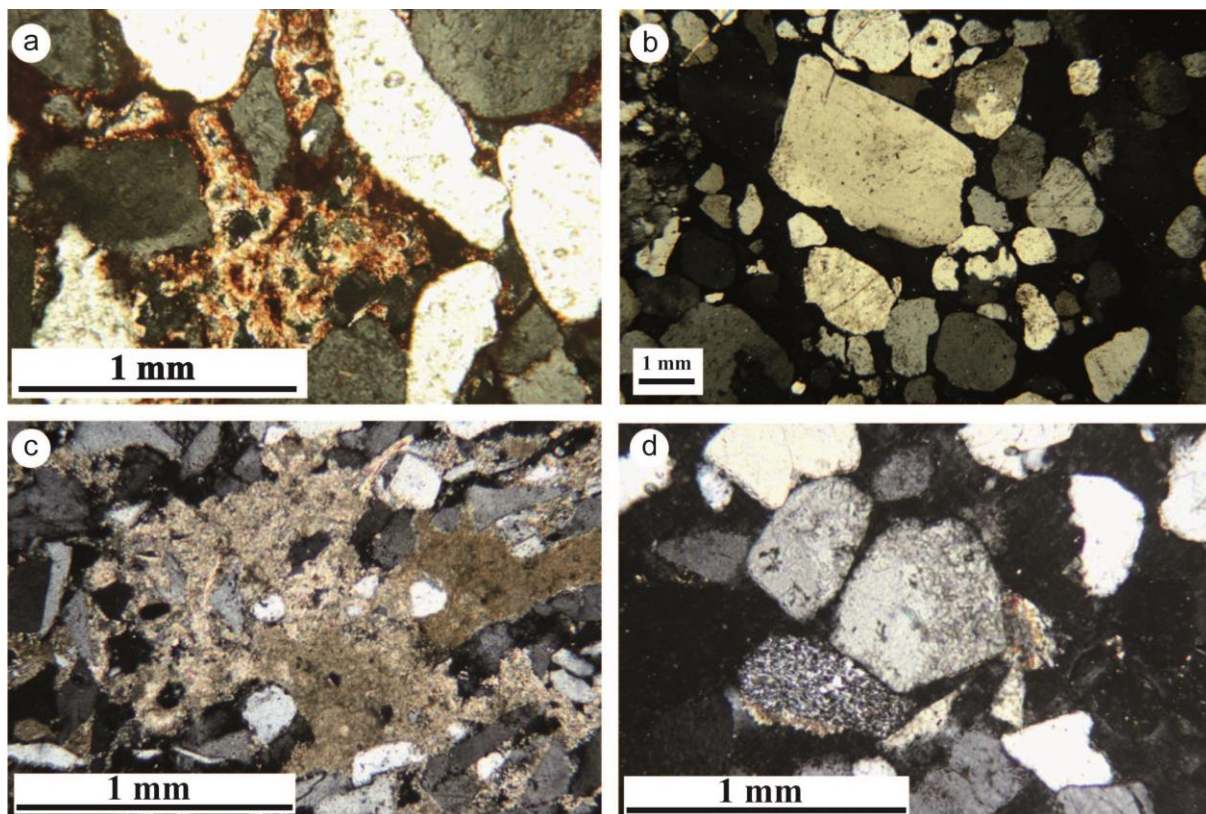


Figure 51: a. Thin section photograph (crossed Nichols) of iron-rich sandstone in the Dibsiyah Formation (WDh1-51). b. Thin section photograph (crossed Nichols) of iron-rich sandstone in the Sanamah Formation (WDSK-17a). c. Thin section photograph (crossed Nichols) of sandstone rich in pseudomatrix in the Juwayl Formation (Wuh-4-9-12). d. Thin section photograph (crossed Nichols) of sandstone with high secondary porosity and little carbonate cement in the Juwayl Formation (Wuh 1-4). All photographs from Heberer (2012).

Figure 52 a and b show the same PCA plots but visualized for different lithofacies types. Because of the lower number of samples not all lithofacies types are represented and some only by few samples. LF7 and partly LF8 cross-bedded sandstones have been shown before to be very good reservoir rocks. This is confirmed by plotting preferentially in the upper two quadrangles. The porous Juwayl samples with secondary porosities belong to these types. LF10, pebbly sandstone, is more variable. Here, the mineral composition overprints textural factors, because samples from the Khusayyayn formation from the lithofacies type are shifted to the right in the diagram due to formation of pseudo matrix from feldspar alteration. LF12 which resembles to a homogenous sandstone and good reservoir rock in the field seems to be affected by both, pseudo matrix formation and cementation and hence shows a variable reservoir quality. Heberer (2012) found a high amount of crushed quartz grains making up a large proportion of the matrix and underpinning the specific nature of these mass flow deposits in a proglacial setting (Chapter 6).

Heberer (2012) also carried out a SEM study on transport mechanisms on selected samples of the Wajid Group. The samples were selected to contain as little cement as possible. Calcite and iron cement were removed by cooking the samples with HCl. Quartz cements on the other hand could not be removed and proved to be problematic. After treatment with HCl, quartz grains have been studied under the SEM for features indicating transport mechanisms. A total of 10 samples have been analysed: 2 from the Dibsiyah, 3 from the Sanamah, 2 from the Khusayyayn and 3 from the Juwayl Formation. Although a final association of the samples to certain transport mechanisms was not possible, tendencies have been identified: The Dibsiyah Formation shows features of fluvial transport and the Sanamah Formation indicates glacial transport, while the Khusayyayn Formation is either of fluvial or marine and the Juwayl Formation of fluvial, marine or glacial origin. Samples from the Juwayl and Khusayyayn Formations show quartz grains with partially abraded, old surfaces. These indicate reworked sediments which have experienced significant weathering between first deposition and remobilisation.

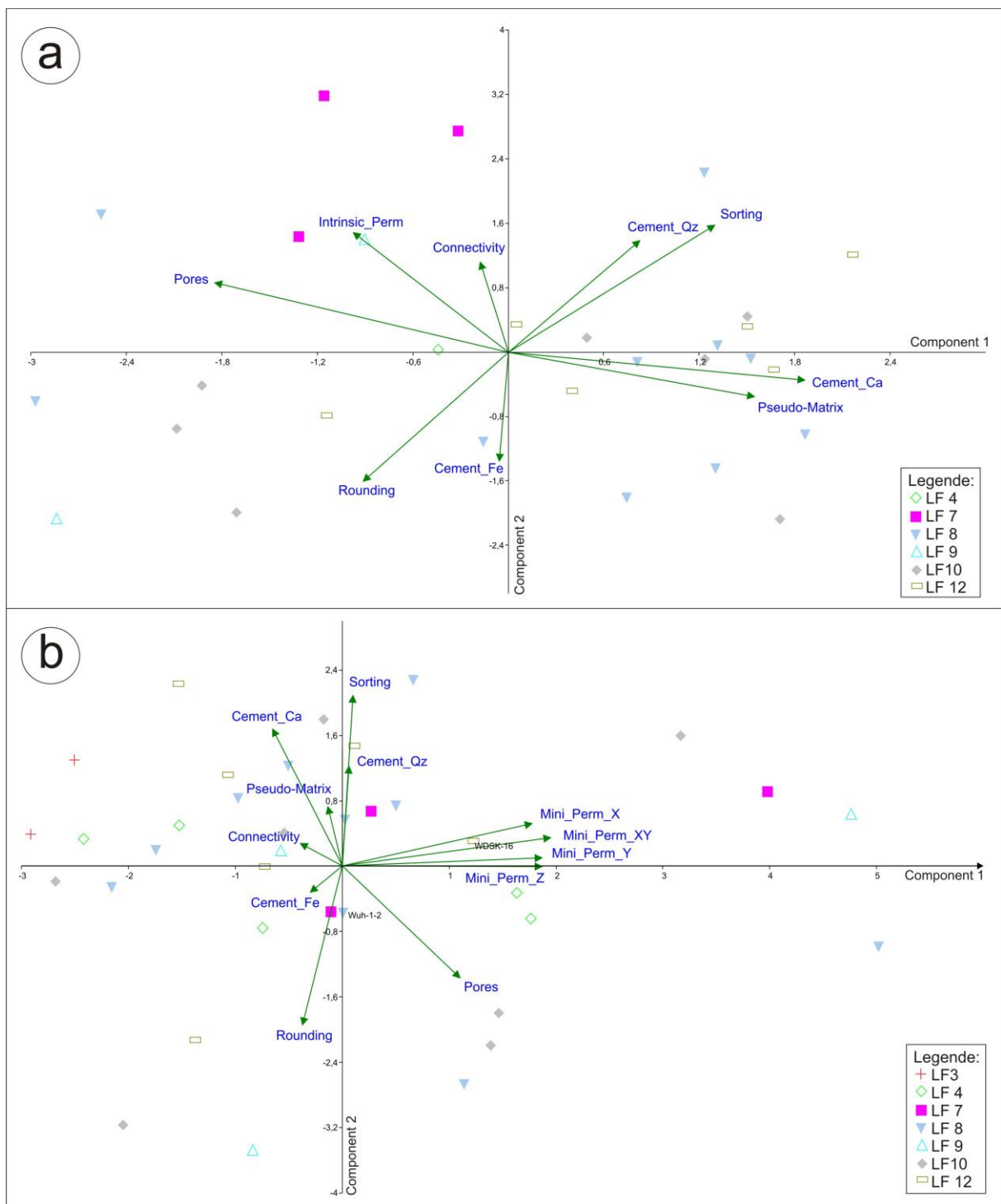


Figure 52: Principal component analysis of microfacies parameters relevant for reservoir properties. Grouped according to lithofacies types. A. Intrinsic permeability, b. x,y,z directions measured by a mini permeameter.

9. Discussion and conclusion

9.1. Sedimentary facies and stratigraphy

In its outcrop belt, the Wajid Group of southern Saudi Arabia can be subdivided into 5 formations: the Dibsiyah Formation, Sanamah Formation, Qalibah Formation, Khusayyayn Formation, and Juwayl Formation. Thirteen lithofacies have been distinguished (LF1 through LF 13), which cover the entire spectrum of siliciclastic grain size classifications. Shales and siltstones are relatively rare in the succession, whereas sandstones, especially medium-grained to coarse-grained sandstones abound. Conglomerates are locally abundant in the Sanamah Formation and in the Juwayl Formation. A second order descriptor is bioturbation, which is very common in the Dibsiyah Formation, but rare to absent in the other units. These 13 lithofacies have been combined in 9 lithofacies associations (LF-A1 through LF-A9).

LF-A1 through LF-A3 together describe large-scale submarine sand sheet complexes. These complexes are present in the Dibsiyah Formation and the Khusayyayn Formation. The sedimentologic and ichnofaunal characteristics of both units indicate marine depositional environments throughout. A fluvial environment for the basal Dibsiyah Formation as interpreted by Evans et al. (1991) and Stump and Van der Eem (1995, 1996) is most unlikely. The results of this study are more consistent with a shallow marine pro-deltaic environment. LF-A4 through LF-A6 are the product of glacial environments. In the Sanamah Formation, this was the Hirnantian glaciation, in the Juwayl Formation it was the Permian part of the Late Palaeozoic Permo-Carboniferous Gondwana glaciation. In combination, all three facies associations record proximal to distal glacial environments. The succession of lithofacies and facies associations permits the recognition of three glacier advance – retreat cycles in the Sanamah Formation and of two in the Juwayl Formation. Whereas in the Sanamah Formation only deposits of subglacial tunnel valleys and the adjacent proglacial environments are preserved, in the Juwayl Formation additionally remnants of a large glacial lake are preserved. LF-A8 and LF-A9 of the Juwayl Formation are dominantly fine-grained associations. A few conglomeratic layers testify to the proximity of glaciers or an ice sheet from where the coarse components were provided by fluvial processes or as fallout from icebergs. Together these two associations record a rise in water level, most likely of a large glacial lake. This glacial lake was present over much of the southern Arabian Peninsula and might have extended into Africa.

The few meters of sediment preserved of the Qalibah Formation do not permit a definite assignment to a facies belt. However, fine-grained calcareous sediments with stromatolitic structures point to a restricted marine environment, probably present during the early post-Hirnantian sea level rise. Sediments of the Wajid Group were deposited during approximately 200 Ma to 260 Ma, depending on the definite depositional age of the Dibsiyah Formation. Extrapolations of sedimentation rates to depositional time show that within the Wajid Group and under the assumption of very conservative sedimentation rates, 62 Ma years are represented in the sediments: 20 Ma in the Dibsiyah Formation, 2 Ma (the length of the Hirnantian) in the Sanamah Formation, 15 Ma in the Khusayyayn Formation, and 25 Ma in the Juwayl Formation. Most likely, the time represented is much less. This means that the sediments preserved do not even cover $\frac{1}{4}$ of the Palaeozoic era. This is compatible with field observations of abundant unconformities and sedimentary breaks in the starved successions. The sedimentary processes, starved shallow-marine and terrestrial-glaciogenic, and the relationship between preserved and non-preserved time in the sediments indicate that throughout the Palaeozoic, southern Saudi Arabia was located in an epicratonal setting, in which tectonic subsidence and relative sea level changes exerted only minor control.

9.2. Glacial depositional environments

Based on detailed analysis of sedimentary facies and architectural geometries of Upper Ordovician and Permo-Carboniferous glacial deposits, a genetic model for both glacial episodes is proposed and compared with other locations in northern and north-eastern Gondwana. Saudi Arabia is one of the few places where both glaciations can be studied in well-preserved sedimentary succession, which formed under similar boundary conditions. Among these are (a) incision of subglacial tunnel valleys according to the ice-loading model, (b) subsequent valley-fill by subaqueous to subaerial proglacial deposits in front of an oscillating, polythermal ice-shield, (c) intra-formational erosional events through repeated ice advance, (d) widespread and large-scale soft sediment deformation due to glacial surge during deglaciation, (e) marine transgression as a consequence of eustatic sea-level rise following deglaciation. The general pattern fits well with observations recently published by Ghiene et al. (2003) and Le Heron et al. (2004, 2005, 2009) from northern Africa, pointing to closely coupled glaciological processes along the northern margin of the Gondwana ice-shield during Upper Ordovician glaciation. Although the same general patterns apply for the Permo-Carboniferous glaciation, styles and petrographical properties differ most probably due to a more complex ice-flow pattern with a rougher topography after the Hercynian event and contrasting weathering.

9.3. Natural gamma-ray

As shown by Schönrok (2011), spectral gamma-ray measurements from outcrops correlate with spectral and natural gamma-ray logs from wells and boreholes. The gamma-ray data, together with lithologs, show evidence of the typical tripartite division of the Wajid Sandstone, with the Lower and Upper Wajid being hydraulically separated by the shaly and silty Qalibah Formation. The Qalibah Formation is also a key formation for correlating well data, as it is easily recognizable, especially features like the maximum flooding surface at the boundary between the Qusaiba and Sharawa Members and the Pre Tawil Unconformity at the boundary between the Sharawa Member and the Khusayyayn Formation. While a differentiation of the Lower Wajid and Qalibah Formation into different units is possible through log patterns, a further differentiation of the Upper Wajid was impossible, neither was delimitation to the lithological equivalent of the overlying, sandy Khuff Formation, due to similar log patterns. Gamma-ray trends throughout the log are dominated by thorium and consist of mostly bow – or barrel – trends with two singled out dirtying up trends. Where uranium trends have been identified, they are in accordance with thorium trends. Potassium exhibits no significant trends except one minor dirtying up trend at the top of the lower Khusayyayn Formation, where a general dirtying up trend is observable. The lack of visible K trends may be due to both scale of the logs and the detection limit of the handheld gamma-ray detector. Unfortunately no further data was available from Schönrok (2011). Thus, trends in gamma-readings are mainly caused by thorium and, in rare occasions, uranium.

This is quite surprising since thorium and uranium are usually associated with different enrichment processes.

Thorium is regarded as mostly immobile and its sources are detrital heavy minerals. This is reflected in the log trends for both elements, which don't show a clear connection. A connection between thorium enrichment and sedimentary facies has not been observed, though the dirtying-up trends for thorium in the logs of the Jabal Blehan (Juwayl formation) and Jabal Khusayyayn (Khusayyayn formation) seem related to fining-up trends in grain size. Uranium is commonly linked to diagenetic processes and secondary enrichment. This is most notably observable in the log from the Jabal Atheer (Sanamah formation), where 2 significant peaks in uranium concentration coincide with diagenetically precipitated iron crusts (Schönrok 2011). The controlling factors for the spectral gamma radiation are therefore spread out between different sources: Uranium occurrence is mainly influenced by diagenetic effects, thorium by provenance and transport mechanisms and potassium, since it is mainly contained in feldspar, is linked to factors controlling feldspar distribution and preservation, like weathering, provenance and transport mechanisms. In order to better understand the natural gamma-ray characteristics of the Wajid sandstone, further study is necessary.

9.4. Reservoir quality

Generally, the Wajid Sandstone Group is known as good reservoir rock and bears important gas and water resources in central and southern Saudi Arabia (Evans et al., 1997; Konert et al., 2001). This thesis presents the first statistical analysis of porosities and permeabilities over the entire Wajid Sandstone Group in the outcrop belt and links these values with lithofacies and microfacies studies in order to identify controlling factors. Furthermore, for the first time a combined approach of standard mini permeameter and sophisticated column permeameter measurements were carried out, the latter enables to convert gas in water permeabilities. Generally, both methods yield comparable results, i.e. standard mini permeameter measurements are a good approach also for liquid permeabilities, as far as they will be corrected. Here, independent hydraulic tests were performed (chapter 9.5).

Although the data of this thesis confirms the overall good reservoir quality, also wide scatter is obvious. This is particularly the case for permeabilities. High porosities do not guarantee high permeabilities and correlation of both is weak, although a positive trend exists. This means that porosities cannot be used to predict permeabilities accurately. Medians of porosities range from 23 to 27% and 15 to 28% for formations and lithofacies types respectively. Different permeability measurements all show highest medians of 1500 to 2000 mD for the Khusayyayn Formation and lowest medians of 300 to 1400 mD for the Dibsiyah Formation. The variability is highest for the Sanamah Formation and the Juwayl Formation. To analyse these heterogeneities and identifying controlling factors, two approaches were applied: (i) lithofacies types, which represent grain texture and sedimentological structures at the mesoscopic scale in the field, and (ii) microfacies analysis using thin sections and raster electron microscopy of selected samples.

Referring to lithofacies, the following trends have been identified:

- Siltstone and fine sandstones exhibit the highest porosities, but permeability is low for silt-dominated samples. Pebbly sandstones show reduced porosities and permeabilities, most probably because of general poorer mixing. Highest porosities and permeabilities were found for cross-bedded sandstones. Thick massive sandstones in the Juwayl Formation, which are expected to have very good reservoir properties show surprisingly high variability.
- Anisotropy is generally low for the Wajid Sandstone samples, except for siltstones, and bioturbated sandstones. Siltstones show oriented texture because of compaction and increased proportions of platy sheet silicates (clay minerals, micas). Again the massive sandstones in the Juwayl Formation show strong scatter with anisotropic samples.
- Porosities and permeabilities are most closely related for sandy to pebbly, cross bedded lithofacies types. Bioturbated samples and massive sandstones show a relatively high permeability compared to their porosity, which may be interpreted as homogenization of the grain fabric and/or secondary porosity by leaching. Finer grained samples show the expected opposite trend, but some exceptions exist.

Referring to microfacies, the following trends have been identified:

- High permeabilities can be linked with open pore space, pore connectivity, and rounding, but less with sorting. Low permeabilities are linked with increased proportions of pseudo matrix (mostly clay-rich impregnations from alteration of primary minerals or lithoclasts or primary matrix from depositional processes), and cementation by iron oxides, calcite, and/or quartz.
- The mineral composition of the sandstones also matter. Most sandstones of the Wajid group are quartz arenites. However, the Khusayyayn Formation is an exception and has arkosic composition. On the one hand side, feldspar alteration leads to secondary porosity, on the other hand side the proportion of pseudo matrix increases. Feldspar alteration also produces higher amounts of calcitic cement. Both lead to the unique grouping of the Khusayyayn Formation in the PCA plot. Nevertheless, destruction and formation of secondary porosity prevails and leads to the highest average permeability in the entire Wajid Sandstone Group.
- Pseudo matrix has also a competing effect in the massive sandstones of the Juwayl Formation. Heberer (2012) found a high amount of crushed quartz grains making up a large proportion of the matrix and underpinning the specific nature of these mass flow deposits in a proglacial setting. This bimodal grain distribution led to strongly reduced permeability despite the

favourable main grain texture. Secondary leaching, however, recovered good permeabilities in some cases.

- Secondary porosity is most obvious in the Upper Wajid Sandstone Group. In the case of the Khusayyayn Formation, feldspar alteration leads to a relatively uniform enhancement of permeabilities. In contrast, leaching in the Juwayl formation is more heterogeneous and cemented or matrix rich patches are common. Nevertheless, highest permeabilities in the Wajid Sandstone Group with more than 5 D are related to secondary porosity and open pore space more than 20% in thin sections. Furthermore, the Juwayl Formation exhibits lower porosities at the same permeabilities, which was interpreted as a more efficient connectivity due to secondary leaching. The spatial distribution of these leached realms must be a primary goal for further reservoir studies and ongoing exploration in the Wajid Sandstone and its equivalents.

Iron cementation is strongest in the lower Wajid Sandstone Group, in particular in the Dibsiyah Formation. This seems to be the major reason for reduced permeabilities. Likely, the iron originates from continental weathering of shield areas during the warm Cambro-Ordovician period and was remobilized during burial. The Qusaiba Shale presumably hindered the circulating pore waters to penetrate the upper Wajid Sandstone equally.

9.5. Implications for hydrogeology

The Wajid Sandstone Group hosts the most important groundwater resources in southwest Saudi Arabia and was used to develop agriculture in the Wadi Ad-Dawasir area. Intense water abstraction led to strong draw-down of groundwater levels up to more than 100 m within two decades and initiated a detailed survey of the regional groundwater system, which was carried out by GIZ/DCo (2010). This study has shown that in the subsurface, the Wajid Sandstone succession represents two aquifers: a lower aquifer, represented by the Dibsiyah and the Sanamah Formations, and an upper aquifer, represented by the Khusayyayn and the Juwayl Formations. The aquitard comprises the siltstones and shales of the Qusaiba Shale equivalent to the Qalibah Formation in the outcrop belt. Some connection also exists to local Quaternary Wadi deposits. The Upper Wajid is the only aquifer with significant exploitable groundwater resources because the Lower Wajid aquifer occurs in greater depth and its major water volume is not exploitable by recent pumping technologies. Water quality is usually good with salinities from 338 mg/l to 5,470 mg/l (average 1,010 mg/l) and from 83 to 7,490 mg/l (average 1,200 mg/l) in the lower and upper Wajid aquifer, respectively (GIZ/DCo, 2010).

Results of a total of 28 pumping tests, 21 in the upper Wajid and 7 in the lower Wajid, were available, either from reports from GTZ/DCO (2010) or Italconsult (1969). Pumping tests performed by GTZ/DCO (21 of 28) were analyzed using the Cooper and Jacob large time approximation of the Theis nonequilibrium method for nonleaky, confined aquifers (Cooper and Jacob, 1946). No clear indications for a double porosity behavior were found in the time-drawdown data and the straight line solution was applied for the determination of transmissivity and storativity. Using the drilling profiles, hydraulic conductivities were calculated based on aquifer thickness. The arithmetic mean of the hydraulic conductivities derived from the pumping tests was about 4 times higher in the upper Wajid (8.3×10^{-5} m/s) compared to the lower Wajid (2.2×10^{-5} m/s) (Tab. 1).

For comparison, measured water permeabilities (mD) for the sandstone samples obtained in the laboratory column experiments were converted into hydraulic conductivities (m/s). In the four formations, hydraulic conductivities varied by a factor of 3 only, with highest values for the Dibsiyah formation (Tab. 1). Whereas hydraulic conductivities for matrix and pumping tests are within a factor of 2 in the Lower Wajid Aquifer, matrix conductivities are more than one magnitude lower in the Upper Wajid Aquifer.

Castaing et al. (2002) showed that the ratio between fracture permeability and matrix permeability (in m^2) indicates whether fracture flow or matrix flow dominates. Castaing et al. (2002) could show, that at ratios of about 100 the influence of a fracture system on groundwater flow becomes visible and might dominate at a ratio of 10,000. In principal, also hydraulic conductivities (in m/s) can be used for comparison. Toubanc (2005) suggested, that the overall conductivity is the sum of matrix

conductivity and fracture conductivity ($K_{f\ overall} = K_{f\ matrix} + K_{f\ fracture}$) and therefore fracture conductivity for the upper and lower Wajid can be calculated by rearrangement of the equation (Tab. 1). Ratios are 14 for the upper Wajid and 0.8 for the lower Wajid, indicating the matrix flow is most likely to dominate. This was also shown by Zeeb et al. (2010) in a similar approach.

This data show surprisingly close hydraulic conductivities of matrix, fracture networks and pumping tests for the Wajid Sandstone aquifer, although these methods deal with different scales and measurement methods. Fracture conductivities are in the same order of magnitude as the matrix conductivities. This is not enough for the fracture network to become dominant in regional groundwater flow. In addition, matrix provides a much larger volume for storage of fossil groundwater than fractures. This makes matrix permeabilities of prime importance in the Wajid Aquifers for both, stored groundwater volumes and groundwater flow. The reason of this high hydrogeological importance of the sandstone matrix is given by a relatively homogenous grain size spectrum (sand to gravel) over the whole succession, a weak cementation, and the almost complete absence of fine-grained sediments except the sealing layer between the Upper and Lower Aquifer. This specific sedimentological preconditions enables overall high porosities and good pore connectivities. This case study illustrates, that a priori geological knowledge combined with sedimentological outcrop-analogue studies and petrophysical measurements of representative samples in the laboratory can be of specific relevance to derive reasonable input parameters for regional groundwater models and thus groundwater management.

Table 5: Comparison of hydraulic conductivities at different scales for the Wajid Sandstone Group. All values in $m\ s^{-1}$.

	Hydraulic conductivity overall* (ms^{-1})	Hydraulic conductivity matrix** (ms^{-1})	Hydraulic conductivity fractures*** (ms^{-1})
Upper Wajid sandstone	8.3×10^{-5} ($\pm 6.7 \times 10^{-5}$)	5.5×10^{-6}	7.7×10^{-5}
- Juwayl formation	-	1.1×10^{-5} ($\pm 8.6 \times 10^{-6}$)	-
- Khusayyayn formation	-	3.9×10^{-6} ($\pm 2.4 \times 10^{-6}$)	-
Lower Wajid sandstone	2.2×10^{-5} ($\pm 1.8 \times 10^{-5}$)	1.1×10^{-5}	1.0×10^{-5}
- Sanamah formation	-	5.9×10^{-6} ($\pm 8.0 \times 10^{-6}$)	-
- Dibsiyah formation	-	1.7×10^{-5} ($\pm 1.6 \times 10^{-5}$)	-

*pumping tests, GTZ/DCO (2010), Italconsult (1969). **Column experiments, this study. ***calculated after Castaing et al. (2002).

Acknowledgement

The completion of my dissertation and subsequent Ph.D. has been a long journey. It's true that "Life is what happens" when you are completing your dissertation. Life doesn't stand still, nor wait until you are finished and have time to manage it. Much as happened and changed in the time I've been involved with this project, or as some of my dear friends have so affectionately referred to it "The Paper." Many have questioned whether I would finish my dissertation, as have doubted my commitment to it. I, on the other hand, barring losing confidence so many times I've lost count, getting writer's block just as many times, ending one relationship, moving, beginning another relationship, computers crashing, needing to work as much as possible, and pure frustration in general, knew I'd complete my Ph.D. I just had to do it in my own time and on my own terms.

My dissertation has always been a priority, but as most know, there are several priorities in a person's life at any one time. Unfortunately due to life's challenges and the changes that followed, my dissertation could not always be the number one priority. At any rate, I have finished, but not alone, and am elated. I could not have succeeded without the help, support and reconcile of my God ALLAH ALMIGHTY (Sobhanah Wa Ta'ala) first So I've to thank my God first and say (Al Hamdolellah), Then the invaluable support of several faithful and honest persons. Without these supporters, especially the select few I'm about to mention, I may not have gotten to where I am today.

I'd like to give my special to thank the Ministry of Water and Electricity represented in His Excellency Engineer Abdullah Al-Husayen and The Deputy ministers, Dr. Ali Al-Tukhais and Dr. Mohammad Al-Saud to give me this chance to do my PhD, and for their unlimited support. His Excellency Dr. Al Saud, is keeping following my study and ask for any support from his side all the time. So thank you Dr. Al Saud.

To this selected scientific group, I'd like to give heartfelt special thanks, beginning with Prof. Dr. Matthias Hinderer. He helped and gently pushed me through the last chapter. His flexibility in scheduling, gentle encouragement and relaxed demeanour made for a good working relationship and the impetus for me to finish. He was not only my Prof. He was working and advising me as my oldest loyal and sincere brother. Thank you Prof. Matthias.

I'd also like to give special thanks to Prof. Dr. Martin Keller, who stepped in as my Chair late in the process. He was not only my co-advisor, but my mentor and friend. His patience, flexibility, genuine caring and concern, and faith in me during the dissertation process enabled me to attend to the scientific environmental life while also earning my Ph.D. He's been motivating, encouraging, and enlightening. He has never judged nor pushed when he knew I need to juggle priorities. We've laughed together, spent nights and days together in the desert during my field work. I couldn't have completed all the required paperwork and delivered it to the correct place without him.

My gratitude is also extended to Prof. Dr. Christoph Schüth (and his beautiful family) who has known the answer to every question. He was one of the first friendly faces to greet me when I began this doctoral program and has always been a tremendous help no matter the task or circumstance. Thank you Christoph, you shall always be remembered as a smiling face, a warm and friendly heart and one of the few who assisted me in completing my doctoral program.

My heartfelt special thanks should also go to my good friend Dr. Eng. Andreas Kallioras. He was the first face who greeting me when I arrived in the airport for the first time in Germany, he was close to me all the time, I felt that I know him since years. He supported and helped me morally and financially with his gentle and nice wife Maria. I cannot thank both of you enough. I am forever grateful. Thank You Andreas and Maria!

My special thanks should go to Dr. Helmut Bock, he was gentle flexible and nice during the field work. He was the first who introduced me to the study area. When others doubted, he remained a fan. When I became too serious, his humour and friendly sarcasm allowed me to laugh and lightened my perspective.

Even after his retirement, he remained a supporter and provided insight and direction-right up to the end. For this, I cannot thank him enough. I am forever grateful. Thank You Dr. Helmut!

I am very grateful to the remaining members of my dissertation committee, in The Ministry of Water and Electricity, (Sa'ed Duair, Ahmad Khalefah, and Ibraheem Shabeebi).

Second the colleagues in the GIZ company office: Prof Dr. Randolph Rausch, Johannes Doehler, Mazen El Hallaq, Heiko Dirks, Lahher, Waseem, Mosa, Abdulrazaq Maqsoud and Jack Kapreal. Another good colleague is Abdulmutaleb Al Noor, he was the first who work with me in the beginning of my study and field work for more than one month. Thank you Mr. Al noor

Thirdly the other good colleagues, teachers and technicians in TU-Darmstadt (Dr. Jens Hornung, Dr. Olaf Lenz., Kirsten Herrmann, Holger Scheibner, Alexander Bassis, Isiaka Olawale, Isimemem Osimwegie, Terence Ngole, Susanne Heberer and the special friend Nils Michelsen), in addition to Daniel Bendeas from Tübingen University, for his support in the beginning of my field work, and all other colleagues who gave help or support from other sectors. Their academic support, input and personal cheering are greatly appreciated.

Forth, my dearest , lovable and faithful friend and brother, Mohammad Al Ateeq in King Abdul Aziz City For Science And Technology (KACST), I'm very grateful to him for his support and help from the first days of my study, he was always feel happy to support me. Thank you Mohammad, and thanks to all of your colleagues, teachers, and friends.

I am very grateful to The National Agricultural Development Company NADEC, for there venerable support during my fieldwork in the study area, they gave me the chance to use their guest hose for months. I couldn't have completed the fieldwork without their help. My thanks go especially to the General Director of Nadic Abdul AZIZ Al Babtain, Eng. Salem Al Shawi, Eng. Ali Al Ghsham, Eng. Adel Al Otaibi, Faris Ad Dawsari and all other staff in the company in the main office in Riyadh, the project in Hail and in Wadi Ad Dawaser Project.

Next I'd like to thank Eng. Saud Ad Dehan and Prof. Dr. Naser Al Ajami they were always happy to help me, Eng. Saud used to push others in his company to help me in the field, in the labs of his company and in the electronic library. And he used to push me too to work hard and honest; he gave the chance to use some of his own expensive field measuring tools to use it in the field e.g. the radioactive measurement field server. So thank you Eng. Saud and all staff in Technology experts.

Dr. Naser was always interested to help me in the field, he accompanied me for two weeks during my field work, he used to give me valuable scientific advises and some lectures about my study and how to develop my new own tools in the discovery of the different sedimentological data from the field, so thank you Prof. Dr. Naser.

I cannot begin to express my gratitude and feelings for my brother Dr. Mohammad Al Ajmi. We laughed, fought, shouted and discussed, among other things. Having met in this very doctoral program, Mohammad had the first-hand knowledge of the dissertation process and what I was experiencing. This understanding was priceless. He has played the part of friend, confidant, conscience, humourist, phone comrade, etc., etc. Need I say more? He's been as tough on me as he's been supportive and caring.

For all these reasons and many, many more, I am eternally grateful. Thank you Mohammad for being persistent and encouraging, for believing in me, and for the many precious memories along the way.

Another staunch supporter and fan was my youngest brother, Abdullah. He was taking care of my family in my absence for long time when I was working in the field where there were not mobile connection, for months in the desert, and when I was in Germany for few months. He was giving much care and he spent a lot of money for my family from his own pocket. Thank you, Abdullah.

One other friend I must mention is Abdullah Al Humain. He was our previous General Director in the Ministry. He was the first who fought and worked hard to give me this chance in this project in 2008, through the Ministry and GIZ Company. He constantly asked me "are you done yet?" and

affectionately referred to me as his friend the ‘professional student’. Thank you for your encouragement, support and most of all your humour.

In addition, these acknowledgements would not be complete if I did not mention my wife, Jawhara. She went through every excruciating step and mood change with me, and all of my kids (Anfal, Abdullah, Musab, Atheer, Reema, and Haneen). They have been a twinkle in my eye. They have been central to my completion of this study as they have given me confidence and motivated me in so many ways. Throughout my doctoral program, they have been a bright light, often sending supportive e-mails and letters, and calling me to encourage me, asking about mine when I’m out in the field or in Germany, always concerned with how stressed I might be. There are no words that can express my gratitude and appreciation for all you’ve done and been for me. As I ramble, I still have not found the words that describe or express how I feel for my wife and my kids and what their presence in my life has meant. Thanks to all of you.

Of course these acknowledgments wouldn’t be complete without giving my special thanks to my mother and sister. Both have instilled many admirable qualities in me and given me a good foundation with which to meet life. They’ve taught me about hard work and self-respect, about persistence and about how to be independent. Mom, especially, was a great role model of resilience, strength and character. Both have always expressed how proud they are of me and how much they love me. I’m proud of them too and love them very much. I am grateful for them both and for the ‘smart genes’ they passed on to me.

References

- Abdulkadir IT, Sahin A, Abdullatif OM (2010) Distribution of petrophysical parameters in the Cambro-Ordovician Dibsiyah Member of the Wajid Sandstone, SW Saudi Arabia. *Journal of Petroleum Geology* 33.3: 269-280
- Ager DV (1973) *The nature of the stratigraphical record*. John Wiley, New York
- Al-Husseini MI (2004) Pre-Unayzah unconformity, Saudi Arabia. In: Al-Husseini MI (ed) *Carboniferous, Permian and Early Triassic Arabian Stratigraphy*. *GeoArabia Special Publication* 3: 15-59
- Al-Laboun (2000) *Lithostratigraphy and oil and gas fields of Saudi Arabia*. 4th edition, Saudi Society for Earth Sciences, King Saud University, Saudi Arabia
- Alsharhan AS (1994) Geology and hydrocarbon occurrences of the clastic Permo-Carboniferous in the central and eastern Arabian Basin. *Geologie en Mijnbouw* 73a: 63-78
- Alsharhan AS, Nairn AE, Mohammed AA (1993) Late Palaeozoic glacial sediments of the Southern Arabian Peninsula: their lithofacies and hydrocarbon potential. *Marine and Petroleum Geology* 10: 71-78
- Alsharhan AS, Nairn AE, Shegawi O (1991) Paleozoic Sandstones of the Rub al Khali, Arabia – A review. *Paleogeogr. Paleoclim. Paleoecol.* 85: 161-168
- Allen JRL (1980) Sand waves; a model of origin and internal structure: *Sedimentary Geology* 26: 281-328
- Allen JRL, Collinson J (1979) The superposition and classification of dunes formed by unidirectional flow. *Sedimentary Geology* 12: 169-178
- Ashley GM (1990) Classification of large-scale subaqueous bedform: a new look at an old problem. *Journal of Sedimentary Petrology* 60: 160-172
- Avigad A, Sandler A, Kolodner K, Stern RJ, McWilliams M, Miller N, Beyth M (2005) Mass-production of Cambro-Ordovician quartz-rich sandstone as a consequence of chemical weathering of Pan-terranes: Environmental implications. *Earth and Planetary Science Letters*, 240, 818-826
- Babalola LO (1999) *Depositional Environments and Provenance of the Wajid Sandstone, Abha-Khamis Mishayt Area, Southwestern Saudi Arabia*. PhD Thesis, Faculty of the College of Graduate Studies King Fahd University of Petroleum & Minerals Dahrhan, Saudi Arabia, 259 pp
- Benn ID, Evans DJA (1998) *Glaciers and Glaciation*. Arnold, London
- Besems RE, Schuurman WML (1987) Palynostratigraphy of Late Palaeozoic glacial deposits of the Arabian Peninsula with special reference to Oman Palynology 11: 37-53
- Bokuniewicz HJ, Gordon RB, Kastens KA (1977) Form and migration of sand waves in a large estuary, Long Island Sound. *Marine Geology* 24: 185-199
- Brown GF, Schmidt DL, Huffman AC (1989) *Geology of the Arabian Peninsula: shield area of western Saudi Arabia*. U.S. Geological Survey Professional Paper: 560-A
- Buggisch W, Joachimski MM, Lehnert O (2010) Late Ordovician (Turinian-Chatfieldian) climate of Laurentia. *Geology* (in press)
- Bussert R, Schrank E (2007) Palynological Evidence for a latest Carboniferous Early Permian Glaciation in Northern Ethiopia. *Journal of African Earth Sciences* 49: 201-210
- Castaing C, Genter A, Bourguine B, Chilès JP, Wendling J, Siegel P (2002) Taking into account the complexity of natural fracture systems in reservoir single-phase flow modelling. *Journal of Hydrology* 266.: 83-98.
- Cheel RJ (1984) Heavy Mineral Shadows, A New Sedimentary Structure Formed Under Upper-flow-regime Conditions: Its Directional And Hydraulic Significance. *J.Sedim. Petrol.* 54: 1175-1182

Crimes TP (1981) Lower Palaeozoic trace fossils of Africa. In: Holland CH (ed) Lower Palaeozoic of the Middle East, Eastern and Southern Africa, and Antarctica, John Wiley & Sons, New York, pp 189-198

Dabbagh ME, Rogers, JJW (1983). Depositional environments and tectonic significance of the Wajid Sandstone of Saudi Arabia. *Journal of African Earth Sciences* 1: 47-57

Desjardins PR, Mángano MG, Buatois LA, Pratt BR (2010) Skolithos pipe rock and associated ichnofabrics from the southern Rocky Mountains, Canada: colonization trends and environmental controls in an early Cambrian sand-sheet complex. *Lethaia* 43: 507–528

Destombes J, Hollard H, Willefert S (1985) Lower Palaeozoic Rocks Of Morocco, In: Holland C (ed) Lower Palaeozoic Rocks Of Northwestern And Western Africa. Wiley New York, pp 91-336

Deynoux M, Ghienne JF (2004) Late Ordovician glacial pavements revisited – a reappraisal of the origin of striated surfaces. *Terranova* 16: 95-101

Dirner S (2007) The Upper Wajid Group south of Wadi Ad Dawasir (KSA), an outcrop analogue study of a Palaeozoic aquifer. Diploma Thesis, Eberhard-Karls-Universität Tübingen

Dott RH Jr (1983) Episodic sedimentation—how normal is average? How rare is rare? Does it matter? *Journal of Sedimentary Petrology* 53: 5-23

Droser ML (1991) Ichnofabrics of the Palaeozoic Skolithos ichnofacies and the nature and distribution of the Skolithos piperock. *Palaios* 6: 316–325

Droser ML, Bottjer DJ (1989) Ichnofabrics of sandstones deposited under high-energy nearshore environments: measurement and utilization. *Palaios* 4: 598-604

Einsele G (2000) *Sedimentary Basins. Evolution, Facies, and Sediment Budget*. 2nd edn. Springer Berlin

Emery D, Myers K, Bertram GT (1996) *Sequence Stratigraphy*. Blackwell Science, Blackwell Publishing Company, Oxford, 297p

Evans DS, Bahabri BH, Al-OTAIBI AM (1997) Stratigraphie Trap in the Permian Unayzah Formation Central Saudi Arabia. *Geo Arabia* 2: 259-278

Evans DS, Lathon RB, Senalp M, Conally TC (1991) Stratigraphy of the Wajid Sandstone of South-western Saudi Arabia. Paper Society of Petroleum Engineers SPE 21449: 947-960

Fedo CM, Cooper JD (2001) Sedimentology and sequence stratigraphy of Neoproterozoic and Cambrian units across a craton-margin hinge zone, southeastern California, and implications for the early evolution of the Cordilleran margin: *Sedimentary Geology* 141-142: 501-522

Filomena, CM (2007) Sedimentary Evolution of a Palaeozoic Sandstone Aquifer: The Lower Wajid Group in Wadi Ad Dawasir, South Western Saudi Arabia. Diploma thesis, University of Tübingen

Flint RF (1957) *Glacial and Pleistocene Geology*. John Wiley & Sons, Inc., New York

Galloway WE (1989) Genetic Stratigraphic Sequences in Basin Analysis I: Architecture and Genesis of Flooding-Surface Bounded Depositional Units. *AAPG Bulletin* 73: 125-142

Ghienne JF (2003) Late Ordovician sedimentary environments, glacial cycles, and post-glacial transgression in the Taoudeni Basin, West Africa. *Palaeogeography, Palaeoclimatology, Palaeoecology* 189: 117–145

Ghienne JF, Deynoux M (1998) Large-scale channel fill structures in Late Ordovician glacial deposits in Mauritania, Western Africa. *Sedimentary Geology* 119: 141-159

Ghienne JF, Deynoux M, Manatschal G, Rubino JL (2003) Palaeovalleys and fault-controlled depocentres in the Late Ordovician glacial record of the Murzuq Basin (central Libya). *Comptes Rendus Geosciences* 335: 1091–1100

-
- Gibert JM, Ramos E, Marzo M (2011) Trace fossils and depositional environments in the Hawaz Formation, Middle Ordovician, western Libya. *Journal of African Earth Sciences*, 60: 28-37
- GIZ/DCo (2010) Detailed water resources studies of Wajid and overlying aquifers, Volume 10, Drilling Investigations. Ministry of Water and Electricity, Kingdom of Saudi Arabia
- Hadley DG, Schmidt DL (1975) Non-glacial origin for conglomerate beds in the Wajid sandstone of Saudi Arabia. In: Campbell KSW (ed) *Gondwana Geology*. Australian National University Press, Canberra, pp 357-371
- Halawani MA (1994) Late Ordovician Glacial Sediments In Northwest Saudi Arabia. Second Int. Conf. Geology of The Arab World, Cairo University
- Haq BU, Schutter SR (2008) A chronology of Paleozoic sea level changes. *Science* 322: 64-68
- Harms JC, Southard JB, Walker RG (1982) Structures and Sequences in Clastic Rocks. Soc. Econ. Petrol. Miner. Short Course 9
- Heberer S (2012) Petrografische und geochemische Untersuchungen an den Wajid-Sandsteinen, Saudi-Arabien. Diploma Thesis, TU Darmstadt
- Helal AH (1963) Jungpaläozoische Glazialspuren auf dem Arabischen Schild. *Eiszeitalter und Gegenw* 14: 121-123
- Helal AH (1964) On the occurrence and stratigraphic position of Permo-Carboniferous tillites in Saudi Arabia. *Geol. Randsch.* 54: 193-207
- Hussain M (2007) Elemental chemistry as a tool of stratigraphic correlation: A case study involving lower Paleozoic Wajid, Saq, and Qasim formations in Saudi Arabia. *Marine and Petroleum Geology* 24: 91-108
- Hussain M, Babalola LO, Hariri M (2000) Provenance of the Wajid Sandstone, Southeastern Margin of the Arabian Shield: Geochemical and Petrographic Approach. AAPG National Conference, New Orleans, April 16, 1999, New Orleans, USA, Extended Abstracts with Programs: 7 p
- Hussain M, Babalola LO, Hariri MM (2004) Heavy minerals in the Wajid Sandstone from Abha-Khamis Mushayt area, southwestern Arabia: implications on provenance and regional tectonic setting. *GeoArabia* 9: 77-102
- ITALCONSULT (1969): Water and Agricultural Development Surveys for Areas II and III. [unpublished]
- Johnson PR, Stewart ICF (1994) Magnetically inferred basement structure in central Saudi Arabia. *Tectonophysics* 245: 37-52
- Keller M, Lehnert O (2010) Ordovician paleokarst and quartz sand: Evidence of volcanically triggered extreme climates?. *Palaeogeography, Palaeoclimatology, Palaeoecology* 296: 297-390
- Keller M, Hinderer M, Al Ajmi, HF, Rausch, R (2011) Palaeozoic glacial depositional environments of SW Saudi Arabia: process and product. In: Martini IP, French HM, Pérez Alberti A. (eds) *Ice-Marginal and Periglacial Processes and Sediments*. Geological Society, London, Special Publications 354: 129-152
- Kellogg KS, Janjou D, Minoux L, Fourniguet J (1986): Explanatory notes to the Geologic Map of the Wadi Tathlith Quadrangle, sheet 20 G, Kingdom of Saudi Arabia. Ministry of Petroleum and Mineral Resources, Deputy Ministry for Mineral Resources: 27 pp
- Klitzsch EH (1981) Lower Palaeozoic rocks of Libya, Egypt, and Sudan. In: Holland CH (ed) *Lower Palaeozoic of the Middle East, Eastern and Southern Africa, and Antarctica*, Wiley New York, pp 131-163
- Knox RWO'B, Franks SG, Cocker JD (2007) Stratigraphic evolution of heavy mineral provenance signatures in sandstones of the Wajid group (Cambrian to Permian), southwestern Saudi Arabia. *GeoArabia* 12(4):65-95

Kolodner K, Avigard D, McWilliams M, Wooden JL, Weissbrod T, Feinstein S (2006) Provenance of north Gondwana Cambrian-Ordovician sandstone: U-Pb SHRIMP dating of detrital zircons from Israel and Jordan. *Geological Magazine* 143: 367-391

Konert G, Afifi AM, Al-Hajri SA, Droste HJ (2001) Paleozoic Stratigraphy And Hydrocarbon Habitat of the Arabian Plate. *GeoArabia* 6: 407-442

Kruck W, Thiele J (1983) Late Palaeozoic Glacial Deposits In The Yemen Arab. Republic. *Geologisches Jahrbuch*, B46: 3-29

Kumpulainen RA (2009) The Ordovician Glaciation in Eritrea and Ethiopia, NE Africa. In: Hambrey MJ, Christoffersen P, Glasser NF, Hubbard B (eds) *Glacial Sedimentary Processes and Products*, 321-342. DOI: 10.1002/9781444304435.ch18

Le Heron DP, Sutcliffe OE, Bourgig K, Craig J, Visentin C, Whittington RJ (2004) Sedimentary architecture of Upper Ordovician tunnel valleys, Gargaf Arch, Libya: Implications for the genesis of a hydrocarbon reservoir. *GeoArabia*, 9: 137-160

Le Heron DP, Sutcliffe OE, Whittington RJ, Craig J (2005) The origins of glacially related soft-sediment deformation structures in Upper Ordovician glaciogenic rocks: implication for ice sheet dynamics. *Palaeogeography, Palaeoclimatology, Palaeoecology* 218: 75–103

Le Heron DP, Craig J, Etienne JL (2009) Ancient glaciations and hydrocarbon accumulations in North Africa and the Middle East. *Earth Science Reviews* 93: 47–76

Le Heron DP, Armstrong HA, Wilson C, Howard JP, Gindre L (2010) Glaciation and deglaciation of the Libyan Desert: The Late Ordovician Record. *Sedimentary Geology* 223: 100-125

Le Heron DP, Dowdeswell JA (2009) Calculating ice volumes and ice flux to constrain the dimensions of a 440 million year old North African ice sheet. *Quarterly Journal of the Geological Society London* 166: 277-281

Lüning S, Craig J, Loydell DK, Storch P, Fitches B (2000) Lower Silurian 'Hot Shales' in North Africa and Arabia: Regional Distribution and Depositional Model. *Earth-Science Review* 49: 121-200

Lüning S, Shahin YM, Loydell D, Al-Rabi HT, Masri A, Tarawneh B, Kolonic S (2005) Anatomy of a world-class source rock: Distribution and depositional model of in Jordan and implications for hydrocarbon potential. *AAPG Bulletin* 89: 1397-1427

Maizels JK (1991) Origin and evolution of Holocene sandurs in areas of jökulhlaup drainage, south Iceland. In: Maizels JK, Caseldine C (Eds.) *Environmental Change in Iceland: Past and Present*. Kluwer, 267– 300

Maizels JK (1993) Lithofacies variations within sandur deposits: the role of runoff regime, flow dynamics and sediment supply characteristics. *Sedimentary Geology* 85: 299– 325

Maizels JK (1997) Jökulhlaup deposits in proglacial areas. *Quaternary Science Reviews* 16: 793-816

Mángano MG, Buatois LA (2004) Reconstructing early Phanerozoic intertidal ecosystem: ichnology of the Cambrian Campanario Formation in northwest Argentina. In: Webby M, Mángano MG, Buatois LA (eds): *Trace Fossils in Evolutionary Palaeoecology*, *Fossils and Strata* 51: 17–38

Mángano MG, Buatois LA, Aceñolaza GF (1996) Trace fossils and sedimentary facies from an Early Ordovician tide-dominated shelf (Santa Rosita Formation, northwest Argentina): implications for ichnofacies models of shallow marine successions. *Ichnos* 5: 53–88

McBride EF (1963) A classification of common sandstones. *Jour. Sed. Petrology* 33: 664-669

McClure HA (1978) Early Palaeozoic Glaciation in Arabia. *Palaeogeography, Palaeoclimatology, Palaeoecology* 25: 315-326

McClure HA (1980) Permian-Carboniferous Glaciation in the Arabian Peninsula. *Bulletin Geological Society America* 91: 707-712

-
- McClure HA (1984) Late Quaternary Paleoenvironments of the Rub' Al Khali. PhD Thesis, University of London
- McClure, HA, Hussey EM, Kaill IJ (1988) Permian-Carboniferous Glacial Deposits in Southern Saudi Arabia. *Geologisches Jahrbuch B68*: 3-31
- McGillivray JG, Hussein MI (1992) The Paleozoic Petroleum Geology of Central Arabia. *AAPG Bulletin* 76.10: 1473-1490
- Melvin J, Miller MA (2002) Significant new biostratigraphic horizons in the Qusaiba Member of the Silurian Qalibah Formation of central Saudi Arabia, and their sedimentological expression in a sequence stratigraphic context. *GeoArabia* 7: 279-282
- Melvin J, Sprague RA (2006) Advances In Arabian Stratigraphy. Origin And Stratigraphic Architecture Of Glaciogenic Sediments In Permian-lower Carboniferous Unayzah A Sandstones, Eastern Central Saudi Arabia. *Georabia* 11: 105-152
- Melvin J, Sprague RA, Heine CH (2010) From Bergs to Ergs: The Late Paleozoic Gondwanan Glaciation And Its Aftermath In Saudi Arabia. In: López-Gamundí O, Buatois LA (eds) Late Paleozoic Glacial Events And Postglacial Transgressions In Gondwana, *GSA Special Paper* 468: 37-80
- Miller KG, Kominz MA, Browning JV, Wright JD, Mountain GS, Katz ME, Sugarman PJ, Cramer BS, Christie-Blick N, Pekar SF (2005) The Phanerozoic Record of Global Sea-Level Change. *Science* 310: 1293-1298
- Miall AD (1978) Lithofacies Types and Vertical Profile Models in Braided River Deposits. *Can. Soc. Pet. Geol. Mem* 5: 597-604
- Miall AD (1997) *The geology of stratigraphic sequences*, First edn. Springer Berlin
- Miall AD (2010) *The geology of stratigraphic sequences*, 2nd edn. Springer Berlin
- Miall AD (in preparation for Symposium "Strata and Time", Geological Society, London, September 2012) A new uniformitarianism: stratigraphy as just a set of "frozen accidents".
- Monod O, Kozlu H, Ghienne JF, Dean WT, Günay Y, Le Hérisse A, Paris F, Robardet M (2003) Late Ordovician glaciation in southern Turkey. *Terra Nova* 15: 249-257
- Ngole TT (2012) An empirical Gas permeability-water permeability correlation for use in sandstone samples from Saudi Arabia. Scientific training, unpublished report, Institute of Applied Geosciences, TU Darmstadt: 31 p
- Olawale IA (2010) Reservoir characterization of the Paleozoic Wajid sandstone aquifer, Saudi Arabia. Scientific training, unpublished report, Institute of Applied Geosciences, TU Darmstadt: 16 p
- Olawale IA (2010) Reservoir characterization of the Paleozoic Wajid sandstone aquifer, Saudi Arabia. Unpublished Master thesis, Institute of Applied Geosciences, TU Darmstadt: 48 p
- Osemwegie I (2011) Reservoir characterization of the Paleozoic Wajid sandstone aquifer, Saudi Arabia. Scientific training, unpublished report, Institute of Applied Geosciences, TU Darmstadt: 25 p
- Osterloff PL, Al-Harthy A, Penney R (2004) Gharif and Khuff Formations, Subsurface Interior Oman. In: Al-Husseini MI (Ed.) Carboniferous, Permian and Early Triassic Arabian Stratigraphy, *Georabia Special Publication* 3: 83-147
- Paola C, Wiele SM, Reinhart MA (1989) Upper-regime parallel lamination as the result of turbulent sediment transport and low-amplitude bed forms. *Sedimentology* 36: 47-59
- Piotrowski JA (1994) Tunnel-valley formation in northwest Germany – geology, mechanisms of formation and subglacial bed conditions for the Bornhöved tunnel valley. *Sedimentary Geology* 89: 107-141
- Piotrowski JA, Kraus AM (1997) Response of sediment to ice-sheet loading in northwestern Germany: effective stresses and glacier-bed stability. *Journal of Glaciology* 43.145: 495-502

-
- Pollastro, R. M. (2003) Total Petroleum Systems Of The Paleozoic And Jurassic, Greater Ghawar Uplift And Adjoining Provinces Of Central Saudi Arabia And Northern Arabian-Persian Gulf. U.S. Geological Survey, Bulletin, 2202-H
- Powers RW, Ramirez LF, Redmond CD, Elberg EL (1966) Geology of the Arabian Peninsula: sedimentary geology of Saudi Arabia. U.S. Geological Survey Professional Paper 560-D: 147 p
- Prave AR (1991) Depositional and sequence stratigraphic framework of the Lower Cambrian Zabriskie Quartzite: implications for regional correlations and the Early Cambrian paleogeography of the Death Valley region of California and Nevada. Geological Society of America Bulletin 104: 505–515
- Reineck HE, Singh IB (1970) Depositional Sedimentary Environments. Springer Berlin
- Rider, MH (2002) The Geological Interpretation of Well Logs. Second Edition, Rider-French Consulting Ltd
- Ross CA, Ross JRP (1988) Late Paleozoic transgressive-regressive deposition. SEPM Special Publication 42: 227-247
- Ross CA, Ross JRP (1995) North American Ordovician depositional sequences and correlations. In: Cooper JD, Droser ML, Finney SC (eds) Ordovician Odyssey, Pacific section SEPM 77: 309-313
- Russell AJ, Roberts MJ, Fay H, Marren PM, Cassidy NJ, Tweed FS, Harris T (2006) Icelandic jökulhlaup impacts: Implications for ice-sheet hydrology, sediment transfer and geomorphology. Geomorphology 75: 33-64
- Sadler PM (1981) Sedimentation rates and the completeness of stratigraphic sections: Journal of Geology 89: 569-584
- Saltzman MR, Young SA (2005) Long-lived glaciation in the Late Ordovician? Isotopic and sequence-stratigraphic evidence from western Laurentia. Geology 33: 109–112
- Schönrok D (2011) Aquifer Stratigraphy Based on Geophysical Borehole Logs of Paleozoic Sandstones in Southwestern Saudi Arabia. Diploma Thesis, Martin-Luther-Universität Halle-Wittenberg
- Sharland PR, Archer R, Casey DM, Davies RB, Hall SH, Heward AP, Horbury AD, Simmons MD (2001) Arabian Plate Sequence Stratigraphy. Geoarabia Special Publication 2
- Sharland PR, Casey DM, Davies RB, Simmons MD, Sutcliffe OE (2004) Arabian Plate Sequence Stratigraphy – revisions to SP2. GeoArabia 9: 199-214
- Seilacher A (1967) Bathymetry of Trace Fossils: Marine Geology 5: 413-428
- Seilacher A, Lüning S, Martin MA, Klitzsch EH, Khoja A, Craig J (2002) Ichnostratigraphic correlation of Lower Palaeozoic clastics in the Kufra Basin (SE Libya). Lethaia 35: 257-262
- Steinke M, Bramkamp RA, Sandor NJ (1958) Stratigraphic relations of Arabian Jurassic oil. In: Habitat of Oil, AAPG: pp 1294 – 1329
- Stephenson MH, Filatoff J (2000a) Correlation Of Carboniferous-Permian Palynological Assemblages from Oman and Saudi Arabia. In: Al-Hajri S, Owens B (eds), Stratigraphic Palynology Of The Palaeozoic Of Saudi Arabia. Geoarabia Special Publication 1: 168-191
- Stephenson MH, Filatoff F (2000b) Description and correlation of Late Permian palynological assemblages from the Khuff Formation, Saudi Arabia and evidence for the duration of the pre-Khuff hiatus. In: Al-Hajri S, Owens B (eds) Stratigraphic Palynology of the Palaeozoic of Saudi Arabia. GeoArabia Special Publication 1: 192-215
- Stoeser DB, Camp V (1985) Pan- African microplate accretion of the Arabian Shield. Saudi Arabian Deputy Ministry for Mineral Resources, Jiddah. Open file report
- Stride AH, Belderson RH, Kenyon NH, Johnson MA (1982) Offshore tidal deposits: sand sheet and sand bank facies. In: Stride, AH (ed) Offshore Tidal Sands: Processes and Deposits, Chapman & Hall New York, pp 95–125

Stump TE, Van Der Eem JG (1995a): Overview of the Stratigraphy, Depositional Environments and Periods of Deformation of the Wajid Outcrop Belt, Southwestern Saudi Arabia. In: Al-Husseini MI (ed) Geo-94, Middle East Petroleum Geosciences Conference. Gulf Petrolink 1: 867-876

Stump TE, Van Der Eem JG (1995b): The stratigraphy, depositional environments and periods of deformation of the Wajid outcrop belt, southwestern Saudi Arabia. *Journal of African Earth Sciences* 21-3: 421-441

Suter JR (2006) Facies models revisited: clastic shelves. In: Posamentier HW, Walker RG (eds) *Facies Models Revisited*, SEPM Special Publication 84: 339 - 397

Suter JR, Berryhill HL Jr., Penland S (1987) Late Quaternary sea-level fluctuations and depositional sequences, southwest Louisiana continental shelf. In: Nummedal D, Pilkey OH, Howard JD (eds) *Sea-level fluctuation and coastal evolution: Society of Economic Paleontologists and Mineralogists Special Publication 41*: 199-219

Taylor A, Goldring R (1993) Description and analysis of bioturbation and ichnofabric. *Journal of the Geological Society of London* 150: 141-148

Torsvik TH, Cocks RM (2011) The Palaeozoic palaeogeography of central Gondwana. In: Van Hinsbergen DJJ, Buiter SJH, Torsvik TH, Gaina C, Webb SJ (eds) *The Formation and Evolution Of Africa: A Synopsis of 3.8 Ga of Earth History*. Geological Society, London, Special Publications 357: 137-166

Vail PR, Mitchum RM Jr., Todd RG, Widmier JM, Thompson S III, Sangree JB, Bubb JN, Hatlelid WG (1977) Seismic stratigraphy and global changes of sea-level. In: Payton CE (ed) *Seismic stratigraphy - applications to hydrocarbon exploration: American Association of Petroleum Geologists Memoir 26*: 49-212

Vaslet D (1990) Upper Ordovician Glacial Deposits in Saudi Arabia. *Episodes* 13: 147-161

Vaslet D, Al-Muallem MS, Maddah SS, Brasse JM, Fourniguet F, Breton JP, Le Nindre YM (1991) Geologic map of the Ar Riyadh Quadrangle, Sheet 241, Kingdom of Saudi Arabia. Ministry of Petroleum and Mineral Resources, Geoscience Map GM-121, with explanatory notes

Wanas HA, Abdel-Maguid NM (2006) Petrography and geochemistry of the Cambro-Ordovician Wajid Sandstone, southwest Saudi Arabia: Implications for provenance and tectonic setting. *Journal of Asian Earth Sciences* 27: 416-429

Zeeb C, Göckus D, Bons P, Al Ajmi H, Rausch R, Blum P (2011) Fracture flow modelling based on satellite images of the Wajid Sandstone, Saudi Arabia. *Hydrogeology Journal* 18: 1699 – 1712

Annex

Table 6: Detailed lithological logs of Wajid outcrops (see attached CD and/or hardcopy)

	Locality	Formation	File name
WDh-1	Jabal Nafila	Dibsiyah	WDh-1.pdf
Wuh-3	Jabal Juwayl	Juwayl	WUh-3.pdf
WKH-1	Jabal Eqab	Khusayyayn	WKh-1.pdf
WSh-2	Jabal Zaffot	Sanamah	WSh-2.pdf
WSh-3 (WDSK)	Jabal Atheer	Sanamah	WSh-3.pdf
WKH-2	Jabal Majed	Khusayyayn	WKh-2.pdf
WKH-3	Jabal Duhaim	Khusayyayn	WKh-3.pdf
WKH-T-Khusayyayn	Jabal Khusayyayn	Khusayyayn	WKh-t.pdf
WSh-1	Jabal Mashbokah	Sanamah	WSh-1.pdf
WUh-2	Jabal Seab	Juwayl	Wuh-2.pdf
WUh-1	Jabal Bani Ruhayyah	Juwayl	WUh-1.pdf
WUh-4	Jabal Abu Ledam	Juwayl	WUh-4.pdf
WUh-5	Jabal Abood	Khusayyayn/Juwayl	WUh-5.pdf
WUh-6-Blehan	Jabal Blehan	Juwayl	WUh-6.pdf
WKUh	Jabal Fard Al-Ban	Khusayyayn/Juwayl	WKUh.pdf
WUh-7	Jabal Um Lsan	Juwayl	WUh-7.pdf

Table 7: Samples taken for palynological analysis.

Sample	Formation
Bani-2 2	Juwayl
Hima 1	Juwayl
Hima 2	Juwayl
Hima 3	Juwayl
Wuh-1 5	Juwayl
Wuh-1 9	Juwayl
Wuh-1 10	Juwayl
Wuh-4 13	Juwayl
Wuh-6 2	Juwayl
Wuh-5 varves	Juwayl
Ma'aleq	Sanamah
Wkh-T 5	Khusayyayn
Wuh-7 1	Juwayl
Fard Alban(B)	Juwayl
Fard top	Juwayl
Fard C	Juwayl
Fard base	Juwayl
Wdh-1 Silt	Dibsiyah
Wdh-1 Silt layer	Dibsiyah
Wdh-1 Silty	Dibsiyah

Table 8: Sample list with Poroperm data used in this study.

Lab No. Sample ID	Sample Name	MINI-PERMEAMETER			COLUMN-PERMEAMETER	
		X	Y	XY (Average)	Z	Intrinsic permeability (mD)
1	Wuh 4(9-12)	1008,17	687,26	847,71	798	811,05
2	WDSK 18	1720,53	3932,73	2826,64	4400,04	3045,9
3	Wuh 3(1) Juwayl	112,35	18,86	65,61	137,13	200,50
4	K-1-18	2237,2	2794,98	2516,09	3256,7	3387,00
5	Wuh 3(4)	709,57	811,34	760,46	823,37	903,9
6	Fard PUU	0,17	70,19	35,18	52,88	43,5
7	Wuh-3 6b	264,55	348,09	306,32	289,43	150,3
8	WDSK (1)	122,81	28,23	75,52	32,01	34,20
9	Wuh-2-5	4163,89	4802	4448,3	5084	5032,5
10	Fard PUU	3840,4	713,67	2510,03	1139	1065,3
11	WDSK 5b	3879,97	6483,34	5181,66	7613,76	8617,4
12	Wkh-3(1)	725,18	2796,33	1760,73	3080,63	3078,7
13	Wuh-3(3)	5,84	59,81	32,82	17,63	15,3
14	Wuu-1 Juwayl	10186,35	5729,73	7958,05	4768,92	880,55
15	Wkh- T(12)	1033,35	1284,97	1159,16	1603,86	1405,2
16	Uh-2 11b	1061,85	464,07	762,96	1178,08	
17	WDSK-16	3473,1	2317,34	2895,22	1931,72	1605,3
18	Wuh-1(4)	4038,29	3438,44	3738,37	5510,65	5043,4
19	WDh-1 Top	445,74	320,41	383,07	321,82	433
20	Wkh-T-2	5621,68	4210,24	4915,96	3194,85	2374,6
21	wuh-7(1) b lehan	0,04	0,03	0,03	0,05	0,04
22	Wkh-1-11	1561,96	1718,04	1640	3083,86	3402,7
23	Wsh-1-18	641,25	552,32	596,79	486,25	829,7
24	Wkh-T-1	1106,86	1154,38	1129,95	1213,34	1300,5
25	Wkh-3(5)	1652,85	964,68	1308,77	410,11	1100,8
26	Wuh-4-3	1308,88	2030,08	1669,48	273	872,4
27	Wuh-2-9	915,61	1176,52	1046,06	1287,97	1324,5
28	S-1-14b	0,02	0,02	0,02	0,02	0,01
29	S-1-1a	2091,93	2036,14	2064,03	2376,95	832,6
30	Wuh-2-10	1040,91	2470,25	1755,58	2740,31	2342,4
31	Wkh-3-13	2763,76	2360,42	2562,09	2676,21	3021,8
32	WDSK 5	1712,34	2408,05	2060,19	2891,39	3343,7
33	Wuu-2	0,58	114,1	57,34	568,62	468,7
34	WDh-1-9	2191,2	2653,29	2422,24	2773,95	2143,5
35	Wkh-T-1	1911,39	1979,48	1945,43	1668,48	2755,9
36	Wuh-3 (6a)	1192,98	1214,43	1203,71	1148,57	1609,8
37	WS-1-17	4,04	10,72	7,38	4,09	2,9
38	Wuh-2-3	1047,44	562,78	805,11	730,82	1662,2
39	Wuh-2-6	1385,42	1496,12	1440,77	1503,03	2131,7
40	WDSK 17a	664,79	939,89	802,34	1030,8	1340,8

41	Wuh-2-1	3258,27	2321,14	2789,7	2401,51	2017,8
42	S-1-1	2952,95	2286,52	2619,73	2378,44	2069
43	S-2 Top	2063,5	1525,85	1794,67	1804,94	2286,5
44	Wuh 4(5)	2691,96	2059,93	2375,94	2230,64	3173,3
45	S-1-15	109,84	20,31	65,07	30,37	11,5
46	Wuh-1-2	1673,66	1768,1	1720,88	1734,33	2101,8
47	Wuh-2-16	4,36	5,55	4,95	6,85	3,06
48	WKh-T-10	1435,78	3782,76	2609,27	1962,82	3343,7
49	Wkh-3-4	277,79	732,67	505,23	912,33	852,4
50	Overheat (1)	3274,6	3482,28	3378,44	3949,51	4847,5
51	Wkh-T-11	1391,64	1399,73	1395,67	560,51	1110,7
52	WDh-1-52	1402,37	381,4	891,89	468,92	492,1
53	Uh-5-8-23	2743,71	2052,86	2398,29	1951,32	3379,5
54	Wkh-3-3	918,19	1994,32	1456,25	2447,47	2186
55	WDh-1-13	39,61	259,48	149,54	212,62	277,66
56	Wkh-T-3	1685,85	1083,83	1384,84	1124,75	1265,4
57	Wkh-T-6	1894,59	1424,89	1659,74	1647,52	1734,8
58	K-1-4	1703,64	2617,46	2160,55	2628,44	2435,2
59	WDSK 9	1947,11	679,04	1313,08	455	1975,2
60	Wdsk 14	1458	1565,15	1511,57	1530,48	2043,8
61	S-2-2b	1871,13	2007,13	1939,5	2194,92	3223,8
62	WKh-T-8	1669,81	1787,6	1728,71	1613,04	1847,7
63	WUU 17	2532,5	2223,85	2378,17	2115,97	2534,7
64	Wuh-1-1	1602	1806,6	1704,61	1574,8	2321,5
65	WDh-1-7	2490,88	2332,34	2411,61	3802,4	4325,8
66	Wuh-4-2	6444,92	4464,68	5454,8	5214,05	5300,2
67	WDh-1(51)	91,1	626,2	358,65	562,73	634
68	Whk-1-8	2447,86	2740,56	2594,21	2485,1	3100,7
69	Wuh-5-26-31	2131,42	1934,49	2032,95	2032,95	2754,8
70	S-2-2a	1345,11	1367,94	1356,53	394,61	755
71	WD - 78	1007,18	858,31	932,75	1012,37	860,2
72	WD - 1 a	2719,41	1872,62	2296,01	2503,9	4475
73	WD - 03 c)	1071,27	1632,26	1351,77	1263,85	2108,6
74	WD - 03 b)			394	376	1974,8
75	WD - 03 a)			175	111	
76	WD - 02			242	277	1361
77	WD - 05			244	151	1193,2
78	WD - 06 c)			200	246	
79	WD - 06 b)			62	292	238
80	WD - 06 a)			116	202	1743,6
81	WD - 08			177	108	
82	WD - 09			>1000	>1000	5037,2
83	WD - 10			202	>1000	4259,2
84	WD - 11					5680,6
85	WD - 12	1439,32	1596,97	1518,14	993,27	2290
86	WD - 13					

87	WD - 1			>1000	>1000	4475
88	WS - 04	17,53	28,29	22,91	28,49	22,1
89	WS - 05			408	244	
90	WK 1			320	1177	
91	SWJ 3.1					3056,9
92	SWJ 3.2	1453,18	1952,71	1702,95	1401,04	2440
93	SWJ 3.3					
94	WJ 1.1					
95	WJ 1.2			138	280	
96	WJ 1.3			527		
97	WJ 1.4					
98	WJ 2			891	348	
99	WJ 5			1072	1136	
100	WJ 3 (?)					
101	WDh-1	13,21	81,62	47,42	241,21	
102	Fard base	0,03	0,1	0,06	0,04	
103	Fard Top	67,56	321,32	194,44	587,25	
104	Hima 1	0,02	0,02	0,02	0,02	
105	Hima 2	0,03	0,03	0,03	0,01	
106	Hima 3	0,05	0,11	0,08	0,03	
107	Fard base					
108	Fard Top	17,7	52,08	34,89	52,9	
109	Fard base					
110	Fard Top	400,85	1455,64	928,25	793,4	
111	Fard base					
112	Fard Top					
113	Fard base	660	1171,74	915,89	1052,41	
114	Fard Top	1,44	1,47	1,45	4,21	
115	Fard base	0,32	0,09	0,21	72,24	
116	Fard Top					
117	Fard base					
118	Fard Top					
119	Fard base					
120	Fard Top					
121	Fard base					
122	Fard Top	2707,24	2915,06	2811,15	2866,23	
123	Fard base					
124	Fard Top	450,41	796,98	623,7	327,61	
125	PD-5	5,49	0,14	2,81	2,14	
126	PD-2	0,01	0,02	0,01	0,01	
127	PD-3	35,63	0,47	18,05	8,81	
128	PD-4	2,44	0,01	1,22	0,01	
129	Wuh-2-12	0,01	0,1	0,06	0,14	
130	Wuh-2-13					
131	Fard-A	0,28	0,29	0,29	0,3	
132	Fard- B	25,87	155,2	90,54	56,33	

133	Bani Khatma				
134	Wuh-7	0,01	0,03	0,07	0,02
135	Wuh-2-11	556,51	382,14	449,32	423,34
136	PD-1				
137	Wuh-4-6	7667,08	7647,96	7657,52	4753,77
138	Wuh-2-4	805,71	6784,29	3795,03	5191,14
139	U-2-12	38,57	129,77	84,17	134,91
140	Wud-1				
141	Wdh-1-31				

CURRICULUM VITAE, H. AL-AJMI

Contact Information

Surname: Al Ajmi
 Name: Hussain Fahad Hussain
 Address: Riyadh, Kingdom of Saudi Arabia
 Telephone: 00966-14478288 (Home)
 00966-14791802 EXT: 121 (office)
 Mobile: 00966-506662263
 Mobile: 00966-546663922
 Fax: 00966-14792068
 Fax: 00966-12052009
 E-mail: hussain.alajmii@yahoo.com

Personal Data

Date of birth: 14.4.1964
 Place of birth: Riyadh, Saudi Arabia
 Nationality: Saudi
 Marital status: married, 6 children

Current Position

Chief Geologist, Ministry of Water and Electricity, Riyadh, Saudi Arabia
 Full-time PhD student with GTZ, Riyadh office

Educational Background

1980 – 1984	High school, King Abdul Aziz School, Science division, Riyadh
1984 – 1985	Advanced English, Mathematics and Airplane (power plant & fuselage) maintenance courses, Saudi Arabian Airlines Institute (Saudia), Jeddah, Saudi Arabia
1985 – 1989	employee in "Saudia" (Saudi Arabian Airlines) reservation office in Riyadh; self employment in private business
1989 – April 1994	Study of Geology (General Geology, Collage of Science, King Saud University, Saudi Arabia. Reception of BSc.
1995	Three months advanced English course, King Saud University

December 2006:	MSc in Geology, Collage of Science, King Saud University Title of Master thesis: "Geology of Sakaka Area, Northern Saudi Arabia"
March 2013	PhD- In Sedimentology and Stratigraphy from The Technical University of Darmstadt, Germany.

Professional Background

1994 to 2001:	Junior Geologist, Ministry of Agriculture and Water
2001 to 2004:	Junior Geologist, Ministry of Water and Electricity
2004 to 2009 :	Senior Geologist in Ministry of Water and Electricity
2009 – 2013	Chief Geologist in the Ministry of Water and Electricity
Since April 2013	The Chief of The Hydrogeological Consultancy team in The Ministry of Water and Electricity, Saudi Arabia

Professional Experience

- Shallow and deep water well design and supervision (90 m to 2400 m)
- Sedimentological and hydrological studies in the Paleozoic and Mesozoic aquifers in Saudi Arabia
- Geophysical well logging interpretations
- Palynology of Late Middle to Late Paleozoic strata in Saudi Arabia
- Evaluation of ground water aquifer contaminations with sewage water and other contaminants.

Training Courses

- Workshop on "water wells designing and drilling", organized by the Water Resources Development Department, Ministry of Agriculture and Water, Riyadh, 1994.
- Hydrological training course on "Aquifer hydrological parameters calculations", organized by the Water Resources Development Department, Ministry of Agriculture and Water, Riyadh, 1997.
- Advanced course in "The use of isotope and radioactive pollutants in the study of groundwater", organized by Isotopes and Radioactive Pollutants Center, Cairo, Egypt, 1998.
- Workshop on "remote sensing studies", organized by German Foundation for Technical Cooperation, Riyadh (GTZ), 2005.
- Long term training course on "ground water modeling", organized by German Foundation for Technical Cooperation (GTZ), 2006.
- Long term training on "applications of geographical information systems", organized by German Foundation for Technical Cooperation, Riyadh (GTZ), 2007.
- Three weeks mapping course in Spain in 2009.
- 3 days GPR training course in Germany 2009.
- One week rock coring, sampling and hydrological parameters measurements under controlled conditions in Technical University of Darmstadt 2009.

Fellowship, Scientific Visits and Conferences

- Attending all Saudi conferences and seminars in the field of geology since 1995
- Visit to "Desert Research Center", Cairo, Egypt, 1998
- Visit to "Ground water Research Center", Cairo, Egypt, 1998
- Visit to a number of Water Research Centers in Germany, 2006
- 3rd International Conference on Water Resources and Arid Environments and 1st Arab Water Forum, 2008.
- A member in the (**INTERNATIONAL ASSOCIATION OF SEDIMENTOLOGISTS**) (**IAS**).
- An active member in the **SAUDI STRATIGRAPHICAL COMMITTEE**, in **SAUDI GEOLOGICAL SURVEY (SGS)**.

Technical Reports, Publications, Abstracts

- The impact of the tectonic movements of the "Central Arabian Graben system" on mixing water between different aquifers in Wadi Nisah area, southwestern Riyadh, 1997, unpublished report.
- Study of groundwater levels drop in the northern part of the Al-Kharj area, south of Riyadh, 2006, unpublished report.
- Study of Al-Kharj groundwater contamination by treated wastewater, south of Riyadh, 2007- 2008, unpublished report.
- Al-Ajmi, H.; Keller, M.; Hinderer, M.; Rausch, R. (in press): New Insights into the Facies Distribution of the Wajid Sandstone in Its Western Outcrop Area and Implication on Reservoir Properties, Prince Sultan International Water Conference, Riyadh
- Al-Ajmi, H.; Keller, M.; Hinderer, M.; Rausch, R.: Palaeozoic Glacial And Proglacial Depositional Environments On The Arabian Platform I: Ordovician Glaciation (Sanamah Formation, Lower Wajid Group, SW Saudi Arabia), IAS Meeting 2009, Alghero.
- C Philipp Blum and Daniel Bohnsack.; The Role of Outcrop Analogue studies for the Characterization of aquifer properties, ICWRAE 330-336 5-8 December 2010 Riyadh Saudi Arabia.
- Al-Ajmi, H.; Keller, M.; Hinderer, M.; Rausch, R. Advances in Understanding the relation between reservoir properties and facies distribution in the Paleozoic Wajid Sandstone, Saudi Arabia, Springer Advances in the Reserach of Aquatic Environment v2, p 21-28 2011.
- Al-Ajmi, H.; Keller, M.; Hinderer, M.; Sa'ed Al-Duair, J . Hornung, and C. Schuth. Regional Distribution of Properties of the Palaeozoic Wajid Sandstone Group Southwestern Saudi Arabia. AAPG 50586 posted April (2012).
- Keller, M.; Al-Ajmi, H. ; Hinderer, M.; Rausch, R.: Palaeozoic Glacial And Proglacial Depositional Environments On The Arabian Platform II: Permian Glaciation (Juwayl Formation, Upper Wajid Group, SW Saudi Arabia) , IAS Meeting 2009, Alghero
- Hinderer, M.; Keller, M.; Al-Ajmi, H.; Rausch, R.: Tales of two glaciations in the Paleozoic of southwestern Saudi Arabia: Implications for ice shield dynamics and paleogeography of the southwestern Arabian Platform and adjacent areas. Lithosphere Dynamics And Sedimentary Basins: The Arabian Plate And Analogues, Abu Dhabi 2009
- Keller, M.; Hinderer, M.; Al-Ajmi, H.; Rausch, R.: Aspects of Ordovician glacial deposits in southern Saudi Arabia, IGCP 503 Final meeting, Copenhagen 2009.